TU
WIEN

TECHNISCHE
UNIVERSITÄT
WIEN

VIENNA
UNIVERSITY OF
TECHNOLOGY

DISSERTATION

EPR investigations of free radical formation during oxidation of some plant and fungal
tissues and naturally-occurring phenols

ausgeführt zum Zwecke der Erlangung des akademischen Grades eines Doktors der
technischen Wissenschaften unter der Leitung von

Dr. Bernard Goodman und Univ. Doz. Mag. Dr. Thomas Reichenauer
Abteilung für Umweltforschung
ARC Seibersdorf research GmbH

Ao. Univ. Prof. Dipl.-Chem. Dr. Klaus Stolze
Forschungsinstitut für Biochemische Pharmakologie und Molekulare Toxikologie
Veterinärmedizinische Universität Wien

Ao.Univ.Prof. Dipl.-Ing. Dr.techn. Egon-Erwin Rosenberg
E 164-Institut für Chemische Technologien und Analytik
Technische Universität Wien

eingereicht an der Technischen Universität Wien
Fakultät für Technische Chemie

von

Dipl.-Ing. Katharina Franziska Pirker
Matr.Nr. 9725041
Graf Starhemberggasse 38/9
1040 Wien

Wien, am 12.09.2005

TABLE OF CONTENTS

ACKNOWLEDGEMENT

I would like to express my deep gratefulness and appreciation to the following who supported me in one way or the other during the last years:

Dr. Bernard Goodman who receives my special thanks for his support and guidance through my work with a lot of patience. I am grateful for the useful discussions, his criticism and understanding.

Prof. Klaus Stolze for his professional support and help as well as patience regarding the EPR measurements at the University of Veterinary Medicine, Vienna.

Dr. Thomas Reichenauer for his support and encouragement especially with biological questions as well as for his contribution to the general organisation.

Prof. Egon-Erwin Rosenberg from the Vienna University of Technology for his advice and help, especially in analytical questions.

My colleagues and friends from Seibersdorf for their kindness, thoughtfulness, help and support, in particular Christina Naglreiter, Marietta Nagano, Ester Marqués-Alonso and Joachim Dayteg.

My parents, Dieter and Franziska Pirker, my sisters, Theresa and Anna Pirker, and mostly my boyfriend Florian Großlicht for their great understanding and support during this time.

ZUSAMMENFASSUNG

Frisches Obst und Gemüse sind wichtige Bestandteile gesunder Ernährung. Die positive Wirkung ist auf den hohen Anteil an Mineralstoffen, Ballaststoffen, Kohlenhydraten und Antioxidantien zurückzuführen. Antioxidantien sind Moleküle, die in niedriger Konzentration im Vergleich zum oxidierbaren Substrat die Oxidation dieses Substrats signifikant verzögern. Sie reagieren meist mit reaktiven Sauerstoffspezies ($\cdot$OH, H_2O_2, $^1O_2$, $O_2^{-\cdot}$, etc.), was zur Folge hat, dass aus den Antioxidantien Radikale entstehen. Der Mechanismus dieser Reaktion ist von wesentlicher Bedeutung und unter anderem Gegenstand dieser Arbeit, die sich in drei Teile gliedert.

Im ersten Teil wurde die Produktion freier Radikale mittels Elektronenspinresonanz (ESR) Spektroskopie in Pilz- und Pflanzenprodukten (Champignons, Kräuter, Karotten) bestimmt. Dabei wurden die Proben in Gegenwart eines „spin traps" zerrieben. Dieser Vorgang sollte den Kauvorgang beim Essen simulieren. Lokale Unterschiede in der Radikalgenerierung wurde an drei verschiedenen Stellen der Karotte untersucht.

Der zweiten Teil der Arbeit beschäftigte sich mit dem Oxidationsverhalten von vier Polyphenolen (Kämpferol, Luteolin, Carnosolsäure, Rosmarinsäure), die in relevanten Konzentrationen in speziellen Kräutern vorkommen. Die Oxidation erfolgte im alkalischen Medium in Gegenwart von O_2 (Autoxidation) und bei neutralem pH-Wert mit den Enzymsystemen Meerrettich-Peroxidase/H_2O_2 und Xanthin/Xanthin Oxidase sowie mit Hydroxylradikalen (generiert via Fenton Reaktion) und Superoxid Anionen (aus Kaliumsuperoxid).

Analytische Methoden zur quantitativen Bestimmung von Ascorbinsäure, Carotenoiden und Anthocyanen in Pflanzenmaterialien wurden im dritten Teil der Arbeit behandelt.

Karotten und Kräuter zeigten pro-oxidatives Verhalten bei der Verwendung von PBN (N-*tert*-Butyl-α-phenylnitron) und 4-POBN (N-*tert*-Butyl-α-(4-pyridyl)-nitron-N'-oxid) als spin traps. Mit DMPO (5,5-Dimethyl-1-pyrrolin-N-oxid)-Derivaten, TRAZON (1,3,3-Trimethyl-6-azabicyclo[3.2.1]oct-6-en-*N*-oxid) und PEPO (5-Propyloxycarbonyl-5-ethylpyrrolin-1-oxid) als spin traps wurde die Produktion von Kohlenstoff (C)-zentrierten Radikalen nachgewiesen, mit DEPMPO (5-(Diethoxyphosphoryl)-5-methyl-

1-pyrrolin-*N*-oxid) und DPPMPO (5-(Di-n-propoxyphosphoryl)-5-methyl-1-pyrrolin-N-oxid) auch ·OH-Radikale. Die Identifizierung des C-zentrierten Radikals (N-*t*-Butylhydronitroxid) im Champignon erfolgte anhand dieser spin trap Reihe.

Die verschiedenen Bedingungen zur Oxidation der Polyphenole führten zu unterschiedlichen EPR-Spektren, die als Basis für Strukturvorschläge dienten. Obwohl die gewählten Oxidationsformen relativ mild sind, konnten alle gewählten Substanzen oxidiert werden, was deren ausgezeichnete Eigenschaft bestätigt, freie Radikale zu fangen.

Kämpferol und Carnosolsäure änderten nach ihrer Oxidation ihre Grundstruktur. Es ist daher denkbar, dass ihre Metabolite eine entscheidende Rolle als Schutz gegen freie Radikale spielen. Im Gegensatz dazu blieben die Strukturen von Rosmarinsäure und Luteolin erhalten, was darauf hindeutet, dass deren antioxidative Wirkung auf einem Redox-Zyklus basiert.

CHAPTER 1

INTRODUCTION

A diet rich in fresh fruits and vegetables is known to have positive effects on human health, e.g. a decrease in the risk of heart disease and stroke, a control of blood pressure and cholesterol, a prevention of some types of cancer and diverticulitis (an ailment of the intestinal), protection against cataract and macular degeneration. 5 to 9 servings of fruit and vegetables a day are recommended dependent on the calorie intake of the person. A variety of different fruits and vegetables is at least as important as the amount taken. (Harvard School of Public Health, 2004)

The positive effect of such food products is ascribed to their high content of vitamins and minerals, fibre, carbohydrates and phytochemicals. There is some evidence that specific compounds are responsible for the various health impacts, e.g. the carotenoid lycopene in tomatoes. The use of antioxidants as dietary supplements is therefore an increasing field nowadays, although there is no proof that vitamin supplements prevent people of any disease. Some of them, e.g. vitamin C and E, seem not to harm if they are taken in a limited dose, but it is disadvised to take β-carotene supplements. On the other hand, people suffering from specific illnesses or having a lack of the recommended vitamins in their diet, pregnant and nursing women, may benefit and need those vitamins as supplements. (Barrett, 2005)

Plants produce a wide range of antioxidants for different purposes, e.g. secondary metabolites fulfil the role of defence against herbivores, fungi and bacteria, viruses, other plants competing for light, water and nutrients, they act as signal compounds to attract pollinating and seed dispersing animals, support the communication between plants and symbiotic microorganisms and protect against UV-light or other physical stress (Wink, 1999); ascorbic acid is involved in the electron transport chain and is a cofactor of enzymes (Smirnoff, 1996). However, one of the most important tasks of antioxidants in plants is the protection against a surplus production of reactive oxygen species (ROS) which are short-lived and highly reactive compounds. Overproduction of ROS can be initiated by various environmental stress conditions, such as drought,

1

ozone, ultraviolet radiation, and extreme temperatures, as well as being in response to biotic damage caused by fungal or microbial infection. (Smirnoff, 1993)

Free radicals, such as the superoxide radical anion (O_2^-) and hydroxyl radical ($\cdot$OH), non-radical species such as singlet oxygen ($^1O_2$) and hydrogen peroxide (H_2O_2), as well as products from the reaction of these compounds with lipid molecules, such as lipid peroxide (LOO$\cdot$), collectively make up the group of molecules known as ROS. They are found in every living system and have important roles in various biological reactions, e.g. they are formed in the photosynthesis process by the electron transport, they are involved in the generation of natural products by photoxidation (Graf, 1990) or act as regulators against fungi and other threats in plant cells by activating defence genes (Foyer and Noctor, 2001). Increased generation of free radicals may be associated with negative properties such as cell membrane and DNA damage. In a healthy living system antioxidants and free radicals are in balance. A large unbalance between these two groups of molecule is likely to be detrimental and either cause directly or render the organism susceptible to disease. Thus, dependent on their reactivity and concentration, antioxidants can be either beneficial to health or toxic.

Various methods for detection of the ability of samples to scavenge ROS have been established, and a high activity is often considered to be related to a health benefit of the food product (Frankel and Meyer, 2000). It is important, however, to understand the mechanisms of reactions of antioxidants with free radicals since antioxidant molecules are themselves often transformed into free radicals. The antioxidant-derived radical may be reduced back to its original state, a process known as redox-cycling. α-Tocopherol and ascorbic acid (vitamins E and C) are two well-known examples of antioxidant molecules that redox cycle in biological systems.

A direct, definitive and non-destructive method to detect free radicals in both the solid and liquid phase is Electron Paramagnetic Resonance (EPR), also called Electron Spin Resonance (ESR) spectroscopy. For more than half a century, this technique has been used to study the bonding in stable paramagnetic compounds. However, the technique can also be used to detect unstable radical species and a variety of procedures have been developed for this purpose. In the present work, I have used molecules known as spin traps for this purpose. (A spin trap is a diamagnetic molecule that reacts with an

2

unstable free radical to produce a more stable radical species that can be used to determine the identity of the original radical).

The study of free radicals in foods by EPR spectroscopy is still in its infancy, but it is becoming more interesting, especially since it may provide an approach to the prediction of shelf lives of various types of food product (Morello et al., 2002). The status of free radicals and antioxidant molecules in fruits and vegetables changes after harvesting and is affected by both the storage time and conditions. Preparation and processing of fresh food products (e.g. chopping, cooking, etc.) may also have an influence on antioxidant concentrations. (Gil et al., 1999)

The principal aim of the work in this thesis was to gain a better understanding of the free radical chemistry in mechanically damaged plant tissues, which is a normal occurrence during the preparation and consumption of fresh plant food products. This work is divided into three experimental parts.

In the 1st part three different types of plant product (mushroom, herbs and carrots) were used to detect free radical production by EPR during the process of grinding, which was assumed to be equivalent to the physical process of mastication. This was performed in the presence of spin traps, molecules that are able to react with unstable free radicals to form more stable radical adducts. Spatial variations of radical formation were investigated with carrot samples taken from three different positions of the root. (Chapter 2.2.-2.4.)

The 2nd part of this thesis covers the oxidation behaviour of four polyphenolic compounds (kaempferol, luteolin, carnosic acid, and rosmarinic acid), which are important components of the herbs investigated in the previous section. Oxidation conditions included autoxidation in alkaline solution, enzymatic oxidation with horseradish peroxidase/H_2O_2 and xanthine/xanthine oxidase and reactions at pH 7 with the hydroxyl radical and the superoxide radical anion, obtained respectively from the Fenton reaction and potassium superoxide. (Chapter 2.5.)

In addition, three different analytical methods for the quantitative determination of ascorbic acid, carotenoids and anthocyanins were developed and applied to plant tissues in the 3rd part of this thesis. (Chapter 2.1.)

CHAPTER 2

BACKGROUND

2.1. BIOLOGICAL MATERIAL

Various plant products representing different types of botanical tissue (mushrooms – fungi, carrots – plant roots, and herbs – plant leaves) were used, and free radicals generated by cell disruption were detected by EPR spectroscopy. Mushrooms were chosen because of the growing interest in the medicinal properties of fungi, and because previous investigations by Goodman et al. (2002) showed interesting free radical EPR spectra. Carrots are important horticultural crops for central Europe and they also make important contributions to human diets because of their high pro-vitamin A contents. Herbs are used primarily in small amounts to influence the sensory properties of foods. Their culinary properties are mainly derived from their essential oils which contain some bio-active compounds. Each of these foods can be eaten raw, and hence the experiments also can be considered to represent a simulation of the mastication process in the mouth.

The following section gives an overview of the main components in mushrooms, carrots and herbs and their importance as food products.

2.1.1. Mushrooms

The common mushroom with the highest level of production is *Agaricus bisporus*, but there are other mushrooms such as shiitake (*Lentinula edodes*) or straw (*Volvariella volvacea*) which are gaining in popularity due to moderate quantities of good quality protein, dietary fibre, vitamin C, B-group vitamins, and minerals.

In general mushrooms are thought to be good sources of protein. There are limited amounts of sulphur-containing amino acids such as methionine or cystine, and some other essential amino acids, but a large fraction of the protein amino acids exist in free forms. The amounts of lipids in mushrooms are small and the fatty acids are mainly unsaturated. The carbohydrate fraction varies from 3-28 %, but there is also an

5

appreciable amount of fibre (3-32% on a dry weight basis). The main minerals found in mushrooms are phosphorous, potassium, calcium and a very low amount of iron. In contaminated soils mushrooms take up and accumulate cadmium and zinc quite easily. Regarding vitamins, mushrooms contain thiamine (B_1), riboflavin (B_2), niacin (B_3), biotin (H), and ascorbic acid (vitamin C). β-carotene has also been detected, as has ergosterol, which converts to active vitamin D in the presence of ultraviolet irradiation. (Breene, 1990)

An investigation of Cheung et al. (2003) showed that the amount of total phenolic compounds in methanol and water extracts of shiitake and straw mushroom could be correlated with the antioxidative activity, measured with three different methods. Phenolic compounds, therefore, seem to contribute significantly to the antioxidative activity of mushrooms. Also, although it has not been proven, there is evidence that mushrooms have positive health impacts, and medicinal effects attributed to mushrooms include antitumor, antiviral, anticholesterol, and antithrombotic activity. (Breene, 1990)

2.1.2. Herbs

The word herb refers to "non woody seed-producing plants that die down on the end of the growing season" in botanical nomenclature, "vegetable products to improve flavour or aroma of food and beverages" in the culinary arts, and "medicinal plants used to treat diseases" in botanical medicine (Pietta et al., 2003).

From the nutritional point of view, herbs have low fat contents. An investigation of Achinewhu et al. (1995) showed a variation of crude protein from 4.6 to 22.1 %, of fat from 7.5 to 36.0 % and of total carbohydrate from 34.6 to 71.9 % for different spices and herbs harvested in Nigeria. The main minerals are potassium and calcium, but herbs contain also phosphorus, magnesium, sodium, iron and zinc. In general, the carotenoid content (pro-vitamin A) is high in leaves. Other vitamins detected include Vitamin B_1, B_2, B_6, E, C, and folic acid (B_9). (www.nutrition.at)

Various medicinal properties are attributed to active phytochemicals, such as flavonoids, terpenoids, lignans, sulfides, polyphenolics, carotenoids, coumarins, saponins, plant sterols, curcumins, and phthalides. The flavours of herbs and spices are

6

derived from the aromatic components in their essential oils and oleoresins. (Craig, 1999)

Many herbs are commonly used as medicinal plants (Tyler, 1994; Anon, 1994). They have been suggested to play important roles in stabilizing blood pressure and cholesterol levels and hence decrease the risk of cardiovascular disease (Walker, 1996). There is also evidence that several herbs help to sustain the immune system, e.g. *Echinacea* (purple coneflower) or licorice. Some herbs have been reported to show anticancer activity, e.g. members of the *Labiatae* family (basil, mints, oregano, rosemary, sage, and thyme), the *Zingiberaceae* family (tumeric and ginger), the *Umbelliferae* family (anise, caraway, celery, chervil, cilantro, coriander, cumin, dill, fennel, and parsley), licorice root, green tea, flax, and tarragon. (Craig, 1999) The activities of a number of herbal medicines are considered to be derived from their general antioxidant properties e.g. *Gingko biloba* L. (Tyler, 1994); *Silybum marianum* L. (milk thistle) (Leng-Peschlow, 1991). Since almost all the flavonoid classes (flavonols, flavones, their dihydroderivatives, isoflavones, catechins, flavanolignans, and anthocyanins) are present in herbs, the activity has been specifically associated with phenolic compounds e.g. *Melissa officinalis* L. (Koch-Heitzmann et al., 1988); *Thymus vulgaris* L. (List, 1973); members of the *Labiatae* family (Madsen et al., 1996), which would also be expected to function as antioxidants.

Small quantities of herbs are able to change the sensory properties of a food dish, thus indicating that herb-derived substances are involved in chemical reactions with other food components. Apart from the sensory effect herb extracts are also used in the food industry to retard lipid peroxidation. Herbor 025®, a rosemary extract, was investigated as antioxidant in ham, meat dumplings, dried oats, roasted hazelnuts, dehydrated salmon and fried oriental noodles. Another extract from mixed aromatic spices called Spice Cocktail Provencal, showed stabilizing effects of animal fats and frozen fish products. (Aruoma et al., 1996)

2.1.3. Carrots

Carrots are one of the most important vegetables in the world. Their main nutrients are carbohydrates, their contents of proteins and fats being much lower. Their high fibre

contents are considered to be beneficial to health. Potassium is the main mineral, along with sodium, calcium, phosphor, magnesium, and iron. Carrots contain high contents of β-carotene (9.6 mg/100g fresh weight), which functions as pro-vitamin A in humans. Other vitamins detected in carrots include vitamin E, K, B_1, B_2, B_6, C, niacin (B_3), pantothenic acid (B_5), biotin (H), and folic acid (B_9). The amount of vitamin C in 100 g carrot is around 7 mg. Carotenoids and monoterpenes are major secondary metabolites. (Carlsson, 2000)

2.2. ANTIOXIDANT COMPOUNDS

'An antioxidant is any substance that, when present at low concentrations compared to those of an oxidisable substrate, significantly delays or prevents oxidation of that substrate.' The term oxidisable substrate covers 'everything found in foods and in living tissues including proteins, lipids, carbohydrates and DNA'. (Halliwell et al., 1995) Antioxidants can either inhibit generation of reactive oxygen species (ROS) or directly scavenge them, forming radicals on their own. They may also cause an increase of the levels of endogenous antioxidant defences, e.g. by initiating increased generation of SOD or catalase. (Halliwell et al., 1995)

Antioxidants are often products of secondary metabolism (Fig. 2.1.). They can be both hydrophilic and lipophilic and are stored in specific compartments in plants (Fig. 2.2.). The biosynthesis of flavonoids, anthocyanins, ascorbic acid, carotenoids and special phenols, which were subject of this thesis, are described in this section together with their reported functions in plants and humans.

2.2.1. Flavonoids and Anthocyanins

More than 4000 naturally occurring flavonoids have been detected. Flavonoids can be divided into 2 major sub-classes, the anthocyanins and anthoxantins. Anthocyanins are water-soluble plant pigments which are concentrated in the vacuoles of epidermal or subepidermal cells and almost exclusively in the form of glycosides. They are highly coloured and can be seen as the red, blue and purple colours of flower petals, fruits, roots and leaves. Anthoxantins are either colourless or coloured white to yellow. They are stored in the vacuole when they are hydrophilic and in epidermal glandular cells, on plant surfaces, or are exuded from plant roots when they have lipophilic properties (Fig. 2.2.). Flavonols, flavanols, flavones, flavans, isoflavones, and isoflavans belong to the anthoxantin class. (Aviram and Fuhrman, 2003)

The structure of flavonoids is given in Fig. 2.3. The oxygen in the C-ring is positively charged in anthocyanidins which distinguishes this group from other flavonoids. The glycosidic linkage is at the OH-groups of carbon 3 (and/or 5) which stabilises the molecule. Possible sugars are glucose, galactose, arabinose, and rhamnose which also

exist in di- and trisaccharides. Dependent on the amount and positions of hydroxyl groups in flavonoids (usually on carbon 3, 5, 7, 3', 4', and 5') the antioxidant activity varies. For the most effective radical scavenging the structure should contain an o-dihydroxy structure in the B ring, a 2,3 double bond in conjugation with a 4-oxo function in the C ring and OH-groups in position 3 and 5 with the 4-oxo function. (Rice-Evans et al., 1996)

Biosynthesis

The majority of flavonoids are formed from phenylalanine, a product of the shikimic acid pathway, by the phenylpropanoid pathway (Fig. 2.4.). Phenylalanine is transformed to cinnamate by phenylalanine ammonia-lyase (PAL). Hydroxylation of cinnamate catalysed by the enzyme cinnamate 4-hydroxylase leads to the formation of 4-coumarate which reacts further to 4-coumaroyl-CoA with the enzyme 4-coumarate:CoA ligase.

Three molecules of malonyl-CoA (generated from reaction of acetyl-CoA with ATP and one hydrogencarbonate anion) react with 4-coumaroyl-CoA with the help of chalcone synthase. Chalcone can now be transformed into flavanone from which the flavones and flavanonole as well as over some steps the anthocyanins can be formed. (Petersen et al., 1999; Seigler, 1998)

If plants receive more light, more photosynthetic activity leads to more acetyl-CoA formation which increases the flavonoid biosynthesis and plants gain brighter colours. (Wikipedia, 2005)

Biochemistry and health effect

The health effect of flavonoids is mainly ascribed to their antioxidative properties by electron donation and metal-chelating properties. This is structurally supported by a catechol group in ring B, the planarity of the molecule, the presence of a double bond between C2 and 3 in conjugation with a carbonyl group on C4 and an OH group on C3 in ring C (Schroeter and Spencer, 2003; van Acker et al., 1996; Rice-Evans et al., 1996). There are some positive effects described such as slowing down the coagulation of

10

blood, a reduction of the aggregation of platelets, an influence on visual process, a protection of the vessels, inhibition of LDL oxidation, anti-inflammatory, anti-allergic, antischemic, immunomodulatory, and anti-tumoral activities. That could be an explanation for reduced coronary thrombosis with increased flavonoid intake. Investigations have also shown inhibitory effects of flavonoids to enzymes, e.g. lipoxygenases, cyclooxygenases, mono-oxygenases, xanthine oxidase, mitochondrial succinoxidase, reduced nicotinamide-adenine dinucleotide (NADH) oxidase, phopholipase A_2, topoisomerases, and protein kinases. (Pietta et al., 2003)

There is some evidence from epidemiological studies and investigations *in vivo* and in cell culture systems that flavonoids are potential neuroprotective agents. The *in vivo* effect which is often explained as a hydrogen-donating system may be not the dominating process due to measurements of plasma and tissue concentrations of flavonoids and metabolites. It is rather supposed that the bioactivity *in vivo* is related to the ability of flavonoids to modulate protein functions, intracellular cell signalling, and receptor activities by interacting with ATP-binding sites and benzodiazepine-binding areas. (Schroeter and Spencer, 2003)

Beside all the positive effects described for flavonoids there are also studies showing cytotoxic and pro-oxidant effects in cell systems which are mainly concentration dependent (high micromolar to low millimolar). Since the results are based on *in vitro* experiments, caution has to be taken with any conclusions to *in vivo* situations. (Spencer et al., 2003; Cao et al., 1997)

Anthocyanins are allowed to be taken as food supplements. There is no general *quantum satis* or acceptable daily intake (ADI) determined for such molecules. Intakes of kaempferol and luteolin are still the subject of testing.
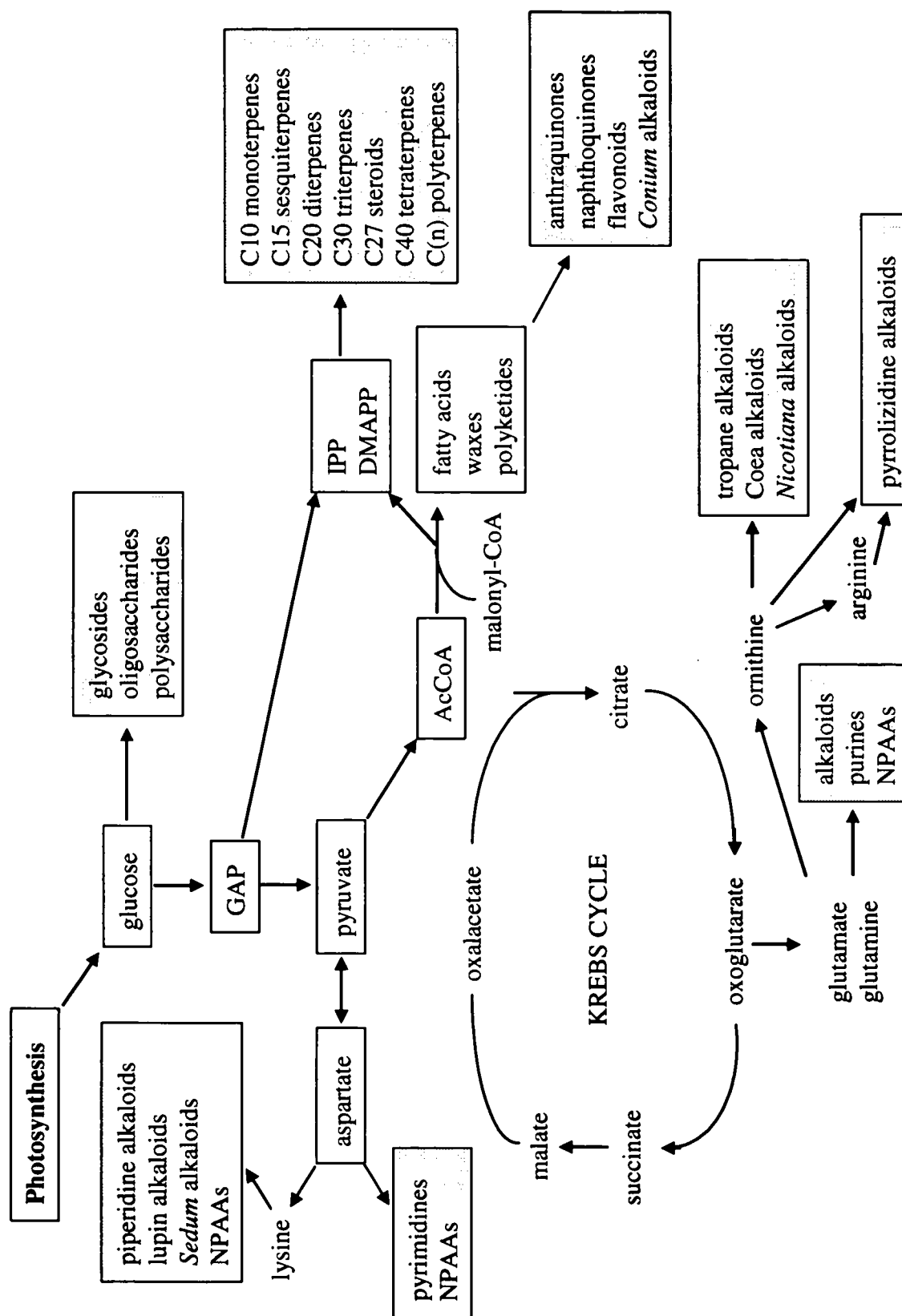
Fig. 2.1. Different secondary metabolites and their main pathways. Abbreviations: IPP, isopentenyl diphosphate; DMAPP, dimethyl allyl diphosphate; GAP, glyceraldehyde-3-phosphate; NPAAs, nonprotein amino acids; AcCoA, acetyl coenzyme A. (Wink, 1999)
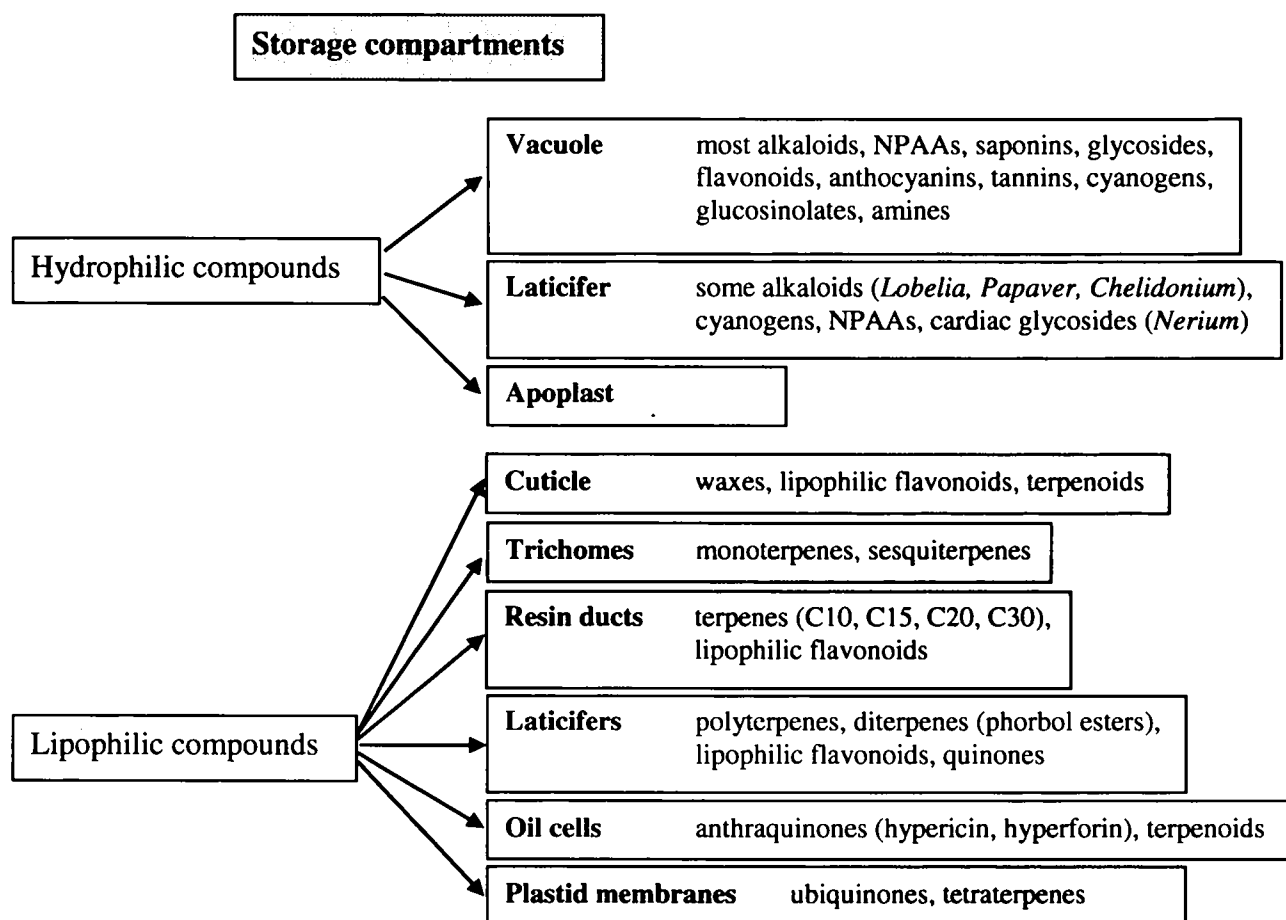
Storage compartments

| Vacuole | most alkaloids, NPAAs, saponins, glycosides, flavonoids, anthocyanins, tannins, cyanogens, glucosinolates, amines |

Hydrophilic compounds

| Laticifer | some alkaloids (*Lobelia, Papaver, Chelidonium*), cyanogens, NPAAs, cardiac glycosides (*Nerium*) |

| Apoplast | |

| Cuticle | waxes, lipophilic flavonoids, terpenoids |

| Trichomes | monoterpenes, sesquiterpenes |

| Resin ducts | terpenes (C10, C15, C20, C30), lipophilic flavonoids |

Lipophilic compounds

| Laticifers | polyterpenes, diterpenes (phorbol esters), lipophilic flavonoids, quinones |

| Oil cells | anthraquinones (hypericin, hyperforin), terpenoids |

| Plastid membranes | ubiquinones, tetraterpenes |

Fig. 2.2. Hydrophilic and lipophilic compounds and their storage compartments. (Wink, 1999)
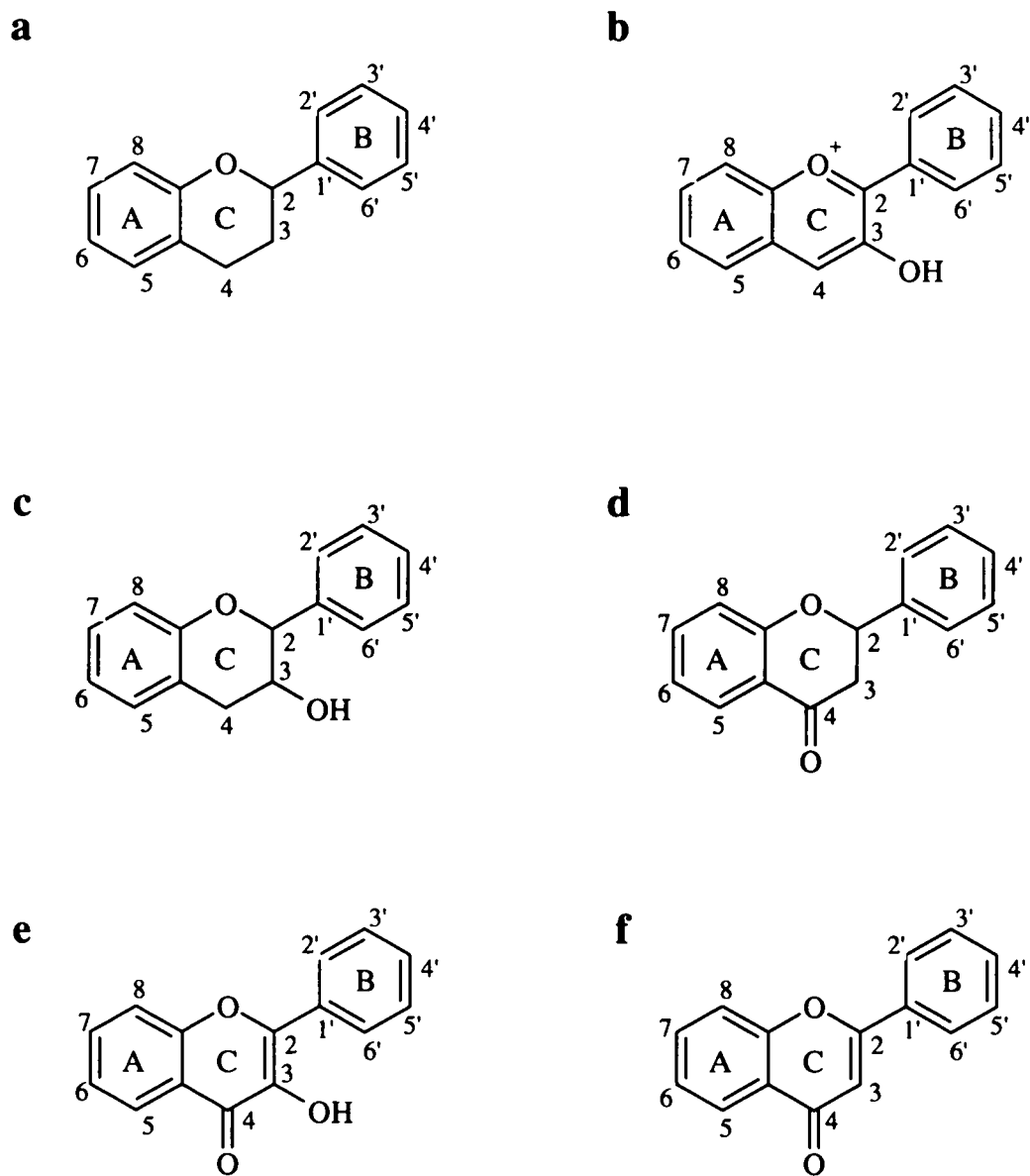
Fig. 2.3. Basic structure of (a) flavonoids. Subclasses are (b) anthocyanidins, (c) flavan-3-ol, (d) flavanone, (e) flavon-3-ol, (f) flavone.
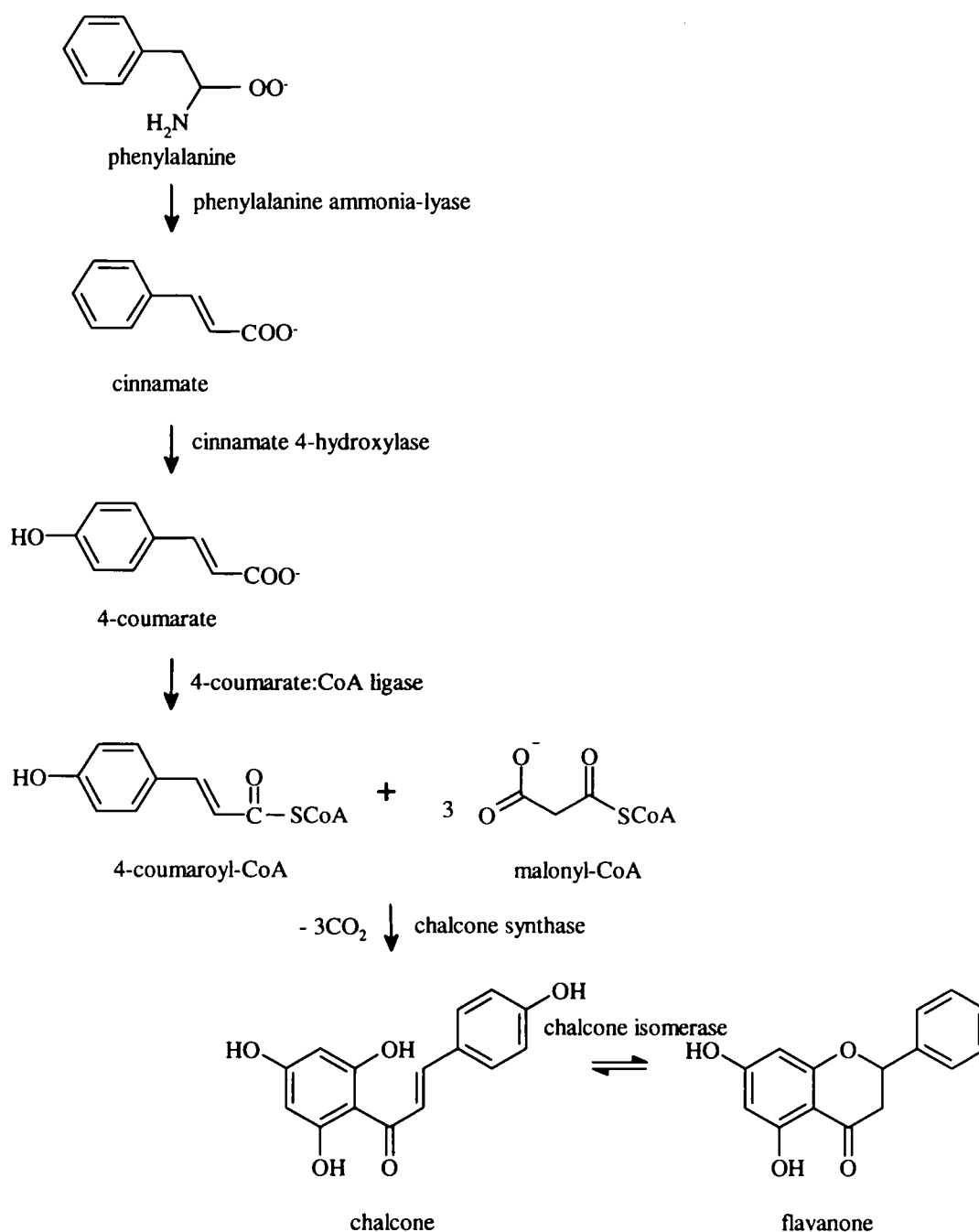
Fig. 2.4. Biosynthetic pathway of flavonoids.

2.2.2. Ascorbic Acid

The antioxidant ascorbic acid plays an important role in all biological systems. Since it is a small water-soluble molecule it is found in the majority of the cell compartments in plants – in cytosol, chloroplasts, vacuoles, mitochondria and cell walls (Smirnoff, 1996). Humans and some animal species are not able to synthesise it because they lack

15

the last enzyme of the biosynthetic pathway, so they have to ingest ascorbic acid. The main sources are plants and milk which is the only animal product containing a significant amount of ascorbic acid (1-5 mg per 100 g). Fresh fruits and vegetables (especially citrus fruits, tomatoes, green peppers, broccoli, and spinach), baked potatoes and leafy vegetables are good sources. (Davies et al., 1991; Brody, 1999)

The reducing ability of ascorbic acid is derived from the ene-diol group between carbons 2 and 3. One electron oxidation leads to the formation of the monodehydroascorbate (MDA) radical, which disproportionates to ascorbic acid and dehydroascorbic acid (DHA) (Fig. 2.5.a). After oxidation of ascorbic acid (Pastore et al., 2001), investigations by LC/MS in acidic (pH 2) aqueous solution showed that DHA has a hydrated bicyclic hemiketal structure. This structure was also suggested by Smirnoff (1996), and another illustration of the disproportional reaction is shown in Fig. 2.5.b. DHA is unstable at pH > 7. Under normal conditions the reduced form is preferred, and this accounts for about 90 % of the ascorbate pool. Two enzymes are responsible for the reduction of DHA to ascorbic acid, the monodehydroascorbate reductase using NAD(P)H as reductant, and the dehydroascorbate reductase using glutathione as reductant (ascorbate-glutathione cycle or Halliwell-Foyer-Asada cycle). (Smirnoff, 1996)
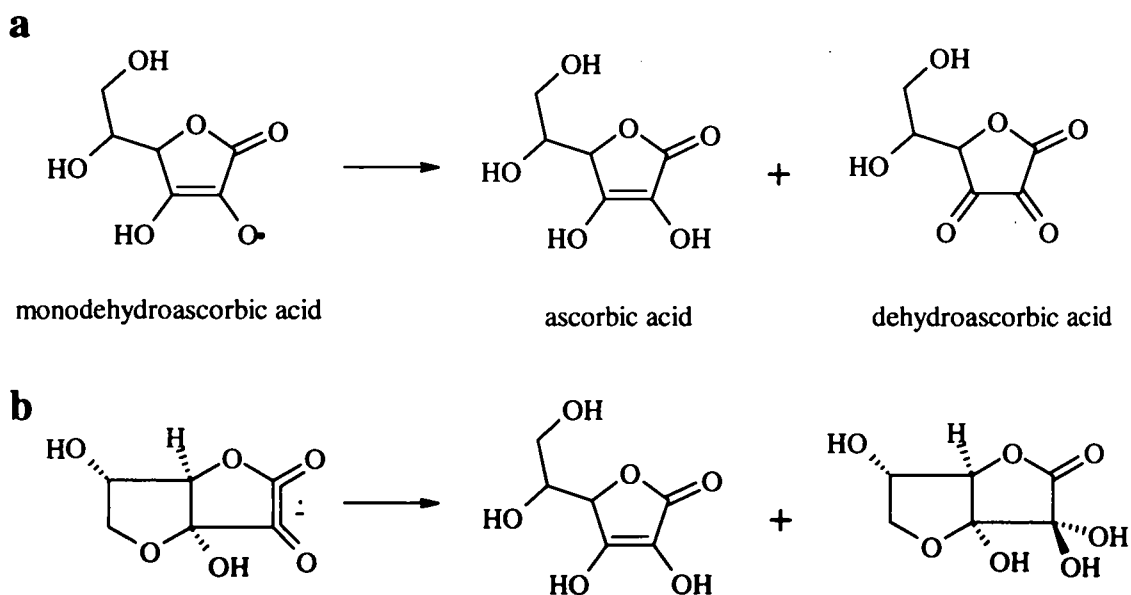
a

monodehydroascorbic acid   ascorbic acid   dehydroascorbic acid

b

Fig. 2.5. Disproportionation of the ascorbate radical, (a) conventional illustration (Brody, 1999), (b) different illustration (Smirnoff, 1996).

Biosynthesis

Ascorbic acid is thought to be synthesised in plants by the so-called "Smirnoff-Wheeler" pathway (Fig. 2.6.), which is probably the main pathway. (Barata-Soares et al., 2004; Wheeler et al., 1998) The immediate precursor of ascorbic acid is L-galactono-1,4-lactone, which is formed from D-glucose via phosphorylated sugars and nucleotide-linked sugars.

Biochemistry and health effects

Four biochemical functions of ascorbic acid are described in plants. It is an antioxidant that is able to remove ROS directly, and also indirectly by the regenerating of α-tocopherol after its reaction with ROS. Vitamin E and C interact synergistically. Secondly it is a cofactor for a range of enzymes. It is involved in electron transport, and can function both as an electron donor and acceptor. Ascorbic acid is also the initial product of the oxalate and tartrate synthesis. It is responsible for the reduction of ferric iron (Fe^{3+}) to ferrous iron (Fe^{2+}), which is the active form in enzymes for catalytic activity. It is involved in cell wall metabolism and expansion, as well as in cell division. (Smirnoff, 1996; Davies et al., 1991)

An important role for ascorbic acid for humans is in the formation of collagen. A deficiency of vitamin C which is quoted as ≤ 0.1 mg/100 ml plasma, leads to scurvy, the first signs of the illness being visible after *c.* 1 month. Since ascorbic acid reduces Fe^{3+} to Fe^{2+} which is more easily taken up, it helps to protect against anaemia. (Brody, 1999; Davies et al., 1991) Vitamin C is an important blood antioxidant, reacting with ROS, regenerating α-tocopherol after its reaction with free radicals, and hence protecting low-density lipoprotein (LDL) from oxidation. Alul et al. (2003) also reported a protection of ascorbate against LDL oxidation by a pro-oxidant combination of homocysteine and iron. Similar results were obtained by Suh et al. (2003) who found that ascorbate didn't act as a pro-oxidant in a system of redox-active iron or copper, H_2O_2 and human plasma. Its behaviour was that of an antioxidant rather than a pro-oxidant, which would enhance lipid peroxidation.
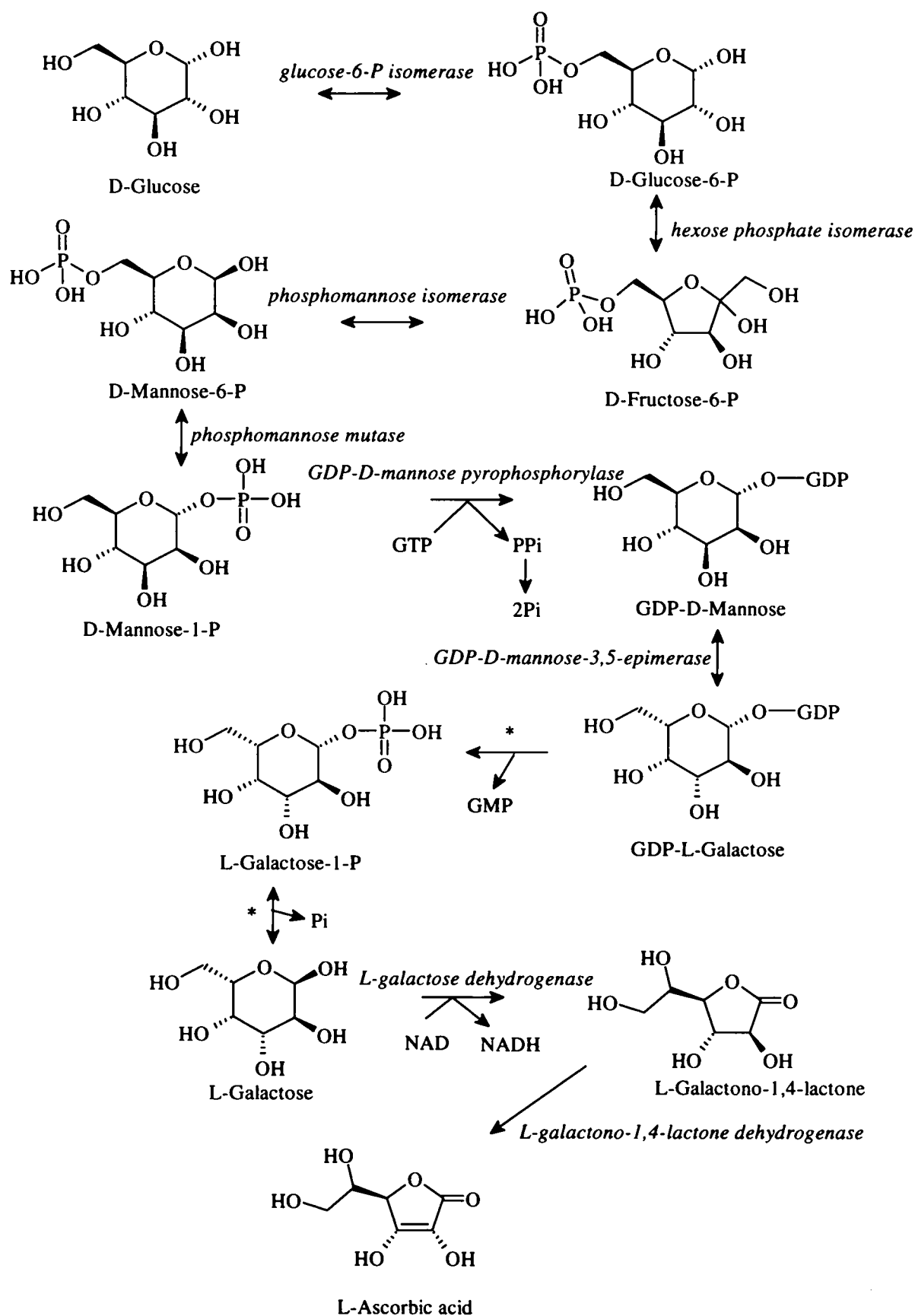
Fig. 2.6. Biosynthesis of ascorbic acid. *speculative steps, GDP-guanosine 5'-diphosphate, GTP-guanosine 5'-triphosphate, GMP-guanosine 5'-monophosphate, PPi-pyrophosphate (Wheeler et al., 1998; Barata-Soares et al.,2004)

18

A recommended daily dietary allowance (RDA) is suggested to be ≥ 60 mg daily. (Higdon, 2004; Gesundheitsratgeber)

2.2.3. Carotenoids

The name 'carotene' is derived from the Latin name for carrots – *Daucus carota*. In addition to carrots, carotenoids which are fat-soluble, are also found in many flowers (e.g. sunflower, marigold) where they are responsible for the yellow-orange colour, and in fruits (e.g. tomato, orange) where they have orange-red colours. The highest amounts of carotenoids can be found in photosynthetic tissues of plants and algae, where they are normally masked by the green of chlorophyll, but are visible after degradation of chlorophyll, e.g. in autumn.

The structure of carotenoids is characterised by the C_{40} isoprenoid skeleton which is modified by cyclisation, substitution, elimination, addition, and rearrangement leading to more than 600 different naturally occurring structures (Britton et al. 1995, 1998; Goodwin and Britton 1988; Brody 1999). The structures of the main carotenoids from a leaf extract (which were detected by HPLC in the present work) are shown in Fig. 2.7.

Biosynthesis

The biosynthesis of carotenoids (Fig. 2.8.) starts with the isoprenoid or terpenoid pathway. All isoprenoid compounds are generated from the C_5-isoprene unit given as isopentenyl disphosphate (IDP) which isomerises to dimethylallyl disphosphate (DMADP). IDP and DMADP react to produce geranyl diphosphate (GDP) by condensation, a reaction which is catalysed by the enzyme prenyl transferase. Addition of two further IDP molecules leads initially to the formation of farnesyl diphosphate (FDP) with the help of prenyl transferase, and then geranylgeranyl diphosphate (GGDP), the latter reaction being catalysed by GGDP synthase. Two molecules of GGDP condense to form phytoene in the presence of the enzyme phytoene synthase. Phytoene is the C_{40}-carotenoid skeleton, and conjugated structures are then formed by desaturation. Monocyclic and dicyclic carotenoid skeletons with a six-membered ring at one or both ends are produced by an isomerisation or rearrangement of an acyclic end group.

Biochemistry and health effects

Carotenoids fulfil two main functions in plants – colouration and photoprotection. Humans and animals are attracted by bright colours of fruits and vegetables. In the photosynthetic system, carotenoids function as protection against photosensitised oxidation by quenching the excitation energy of the chlorophyll triplet state after it has absorbed a photon and by scavenging singlet oxygen. Xanthophylls, such as neoxanthin, violaxanthin, antheraxanthin, zeaxanthin, function as light-harvesting pigments. They pass on the excitation energy to chlorophyll by electron transfer. Carotenoids are also indicators of stress which can be seen by the zeaxanthin-violaxanthin xanthophyll cycle.

For humans carotenoids have their most important role as pro-vitamin A which is converted into vitamin A (retinol) in the body. It is an essential molecule in the visual process. Large deficiencies of vitamin A lead to xerophthalmia, blindness and premature death. Vitamin A also maintains growth and reproductive efficiency as well as epithelial tissues, and prevents their keratinisation. In animal experiments, there is some evidence that carotenoids protect against cancer, heart disease and AIDS. As lipid-soluble antioxidants carotenoids have been investigated as protectants against lipid oxidation processes initiated by free radicals.

The RDA value of vitamin A (retinol) is set with 0.8 mg per day in Europe. 2.0 mg of β-carotene (dissolved in some oil and swallowed) are equivalent to 1.0 mg of retinol. (Gesundheitsratgeber; Brody, 1999)
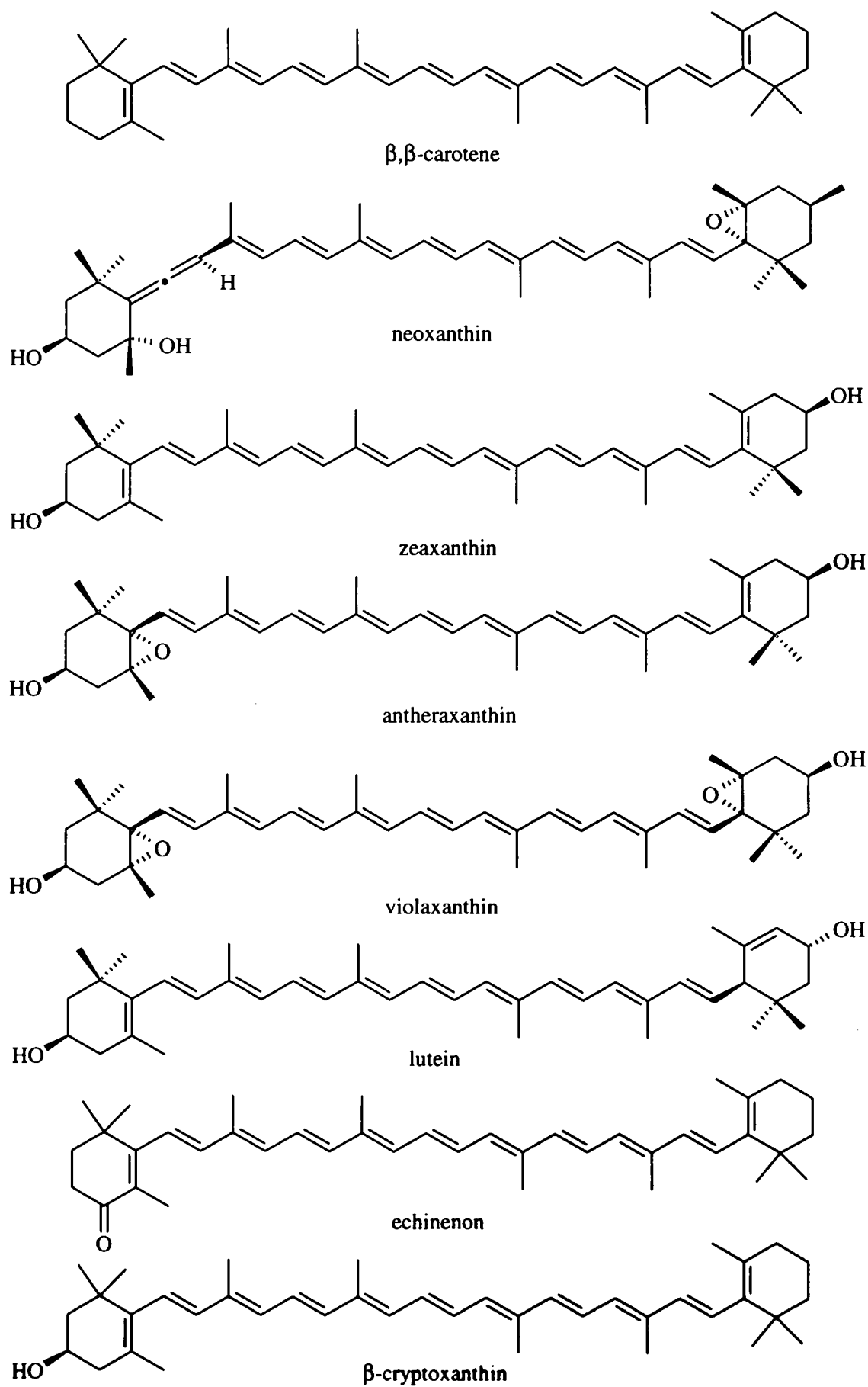
β,β-carotene

neoxanthin

zeaxanthin

antheraxanthin

violaxanthin

lutein

echinenon

β-cryptoxanthin

Fig. 2.7. Structures of carotenoids detected by HPLC analysis.

21

IDP:DMADP isomerase

IDP   DMADP

condensation, prenyl transferase

geranyl diphosphate (C$_{10}$)

+ IDP, prenyl transferase

farnesyl diphosphate (C$_{15}$)

+ IDP, GGDP synthase

geranylgeranyl diphosphate (C$_{20}$)

x2, phytoene synthase

phytoene
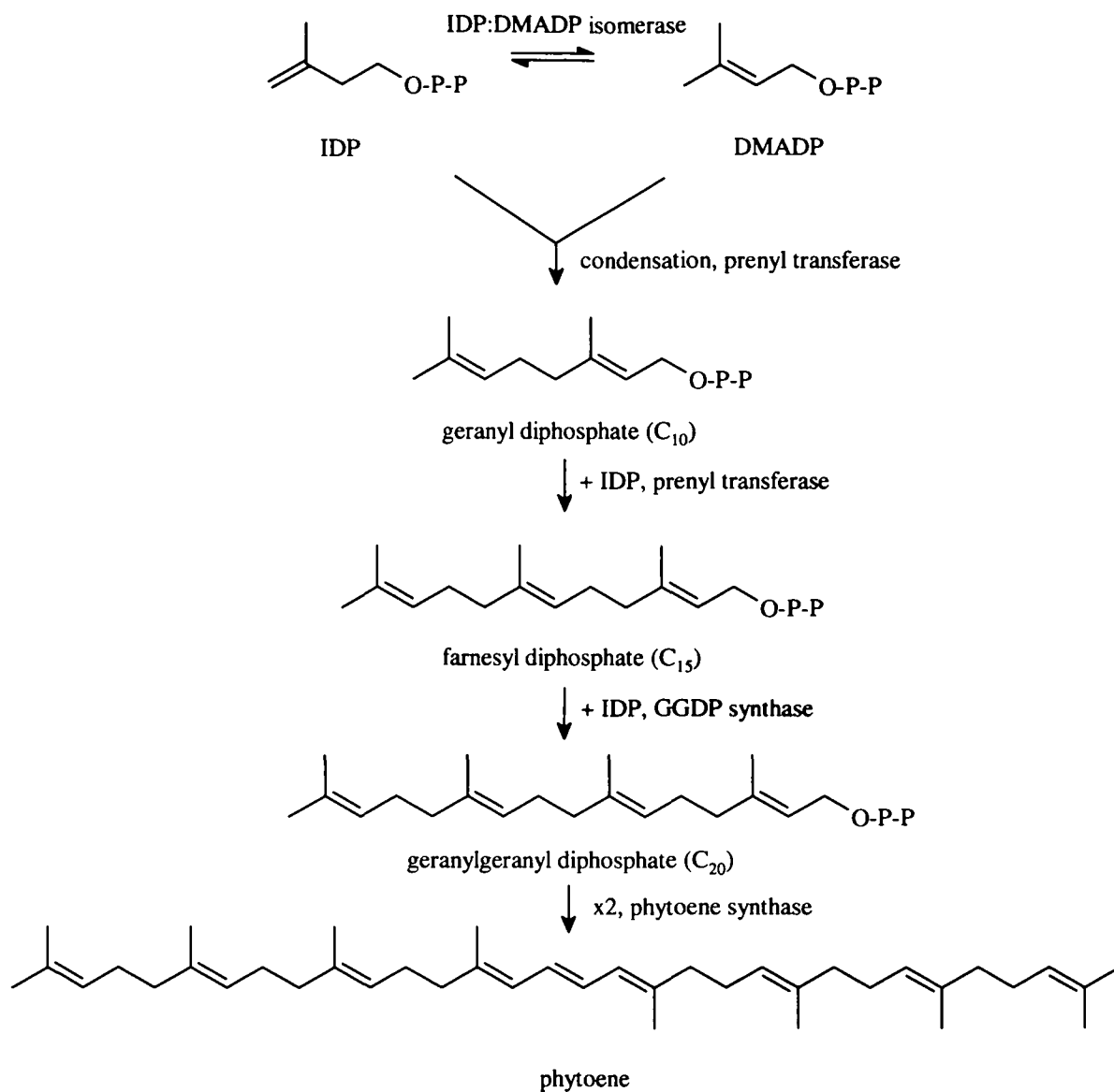
Fig. 2.8. Biosynthesis of carotenoids.

2.2.4. Rosmarinic Acid (RA) and Carnosic Acid (CA)

RA is a water-soluble ester of caffeic acid and 3,4-dihydroxyphenyllactate (Fig. 2.9.a). It is mainly found in the family of *Lamiaceae* and is extracted from rosemary, where it is stored in the vacuole of the plant cell.

CA, a lipophilic abietane diterpene (Fig. 2.9.b), is a main antioxidant in the herbs sage and rosemary. The concentration of CA in rosemary leaves is 100 times higher than α-

tocopherol and 35 times higher than β-carotene. (Munné-Bosch and Alegre, 2001) It is easily oxidised and is a precursor of several related diterpenes, e.g. carnosol, rosmanol. The antioxidant ability comes from the catechol structure on carbons 11 and 12. Unlike α-tocopherol, CA is not regenerated after it has been oxidised (González et al., 1995).

At a subcellular level, CA was only found in chloroplasts where it is synthesised (Munné-Bosch and Alegre, 2001). The highest concentrations of CA are therefore found in leaves of rosemary, with lower levels in flowers and stems, whereas RA is concentrated mainly in flowers. The seasonal variations of RA in leaves are similar to those of CA and are at a maximum before flowering. Only low concentrations of these two compounds are detected in roots of rosemary (del Bano et al., 2003)
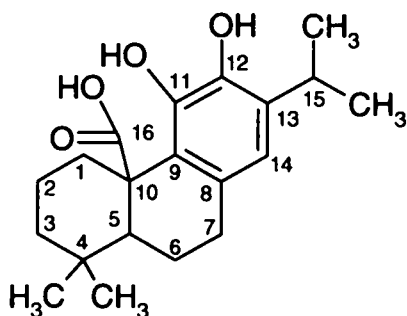
a
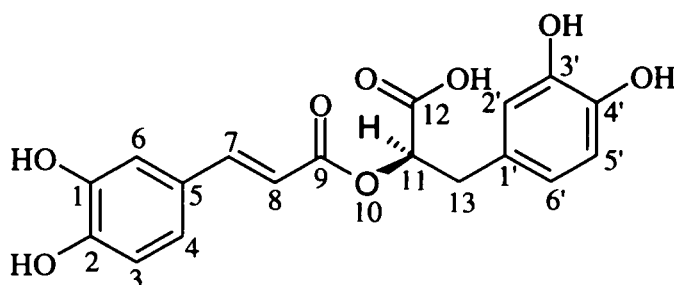
b

Fig. 2.9. Structure of (a) rosmarinic acid and (b) carnosic acid.

Biosynthesis of rosmarinic acid

The biosynthesis of rosmarinic acid starts from the amino acids phenylalanine and tyrosine and proceeds in two parallel pathways (Fig. 2.10.). The intermediates 4-

coumaroyl-CoA and 4-hydroxyphenyllactate are esterified to 4-coumaroyl-4'-hydroxyphenyllactate, the former involving the release of CoA, and catalysed by the enzyme RA synthase. RA is then formed by hydroxylation over two further steps which are initiated by two membrane-bound hydroxylases regulating the hydroxylation on position 3 and 3' on the aromatic rings. (Berger, 2001)

Biosynthesis of carnosic acid

Carnosic acid is synthesised in plastids in four stages. The first step is the formation of isopentenyl disphosphate (IPP) which is produced via the non-mevalonate 1-deoxy-D-xylulose-5-phosphate (DOXP) pathway (Fig. 2.11.) (Lichtenthaler, 1999). The second step is the condensation of IPP with three further basic C_5 units to build geranylgeranyl diphosphate (GGPP, C_{20}). The last stage includes internal addition to form copalyl pyrophosphate which is the substrate for carnosic acid (Fig. 2.12.). (McGarvey and Croteau, 1995; Munné-Bosch and Alegre, 2001; Gershenzon and Kreis, 1999)

Biochemistry and health effects of rosmarinic and carnosic acid

In plants RA most likely protects against attack by fungi and bacteria. It may also deter eating enemies. It has high antioxidant ability due to the two catechol groups in the structure and can be oxidised to o-quinones which are able to bind to peptides and inactivate them. Since RA is stored in vacuoles and therefore separated from oxidases, oxidation occurs only when the membranes are destroyed which support the theory of protection. (Berger, 2001)

RA has been reported to have antioxidant, antiviral, antibacterial, antitumor, antihepatitis, antimutagenicity, anti-allergic, anticarcinogenicity and anti-inflammatory properties. It inhibits HIV-1 and blood clotting. (Berger, 2001; Bors et al, 2004; Cao et al., 2005; Milić and Milić, 1998; Ito et al., 1998)
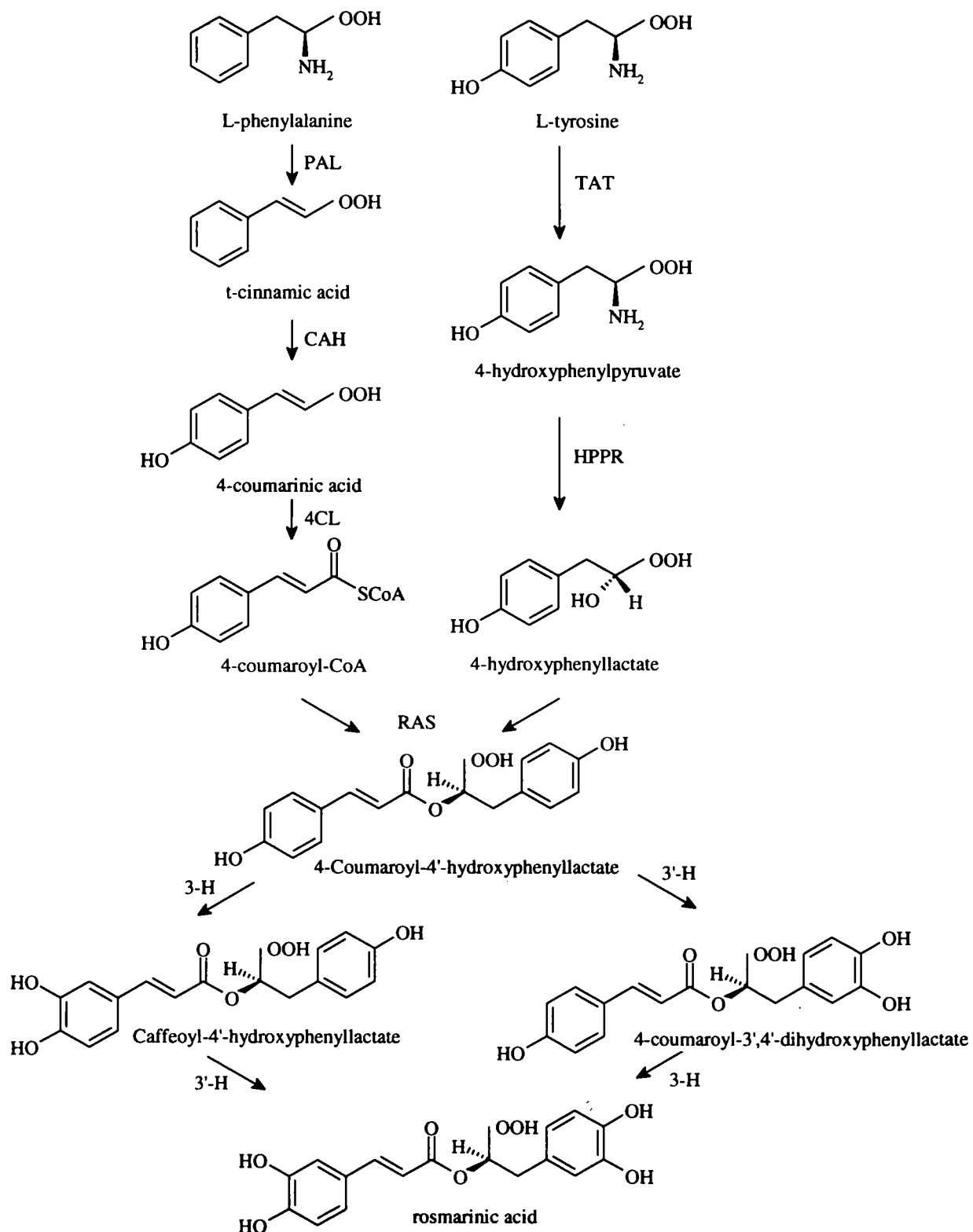
Fig. 2.10. Biosynthesis of RA. (enzymes: PAL=phenylalanine ammonium-lyase, CAH=cinnamic acid 4-hydroxylase, 4CL=4-coumarat:CoA ligase, TAT=tyrosine aminotransferase, HPPR=hydroxyphenylpyruvat reductase, RAS=RA synthase)
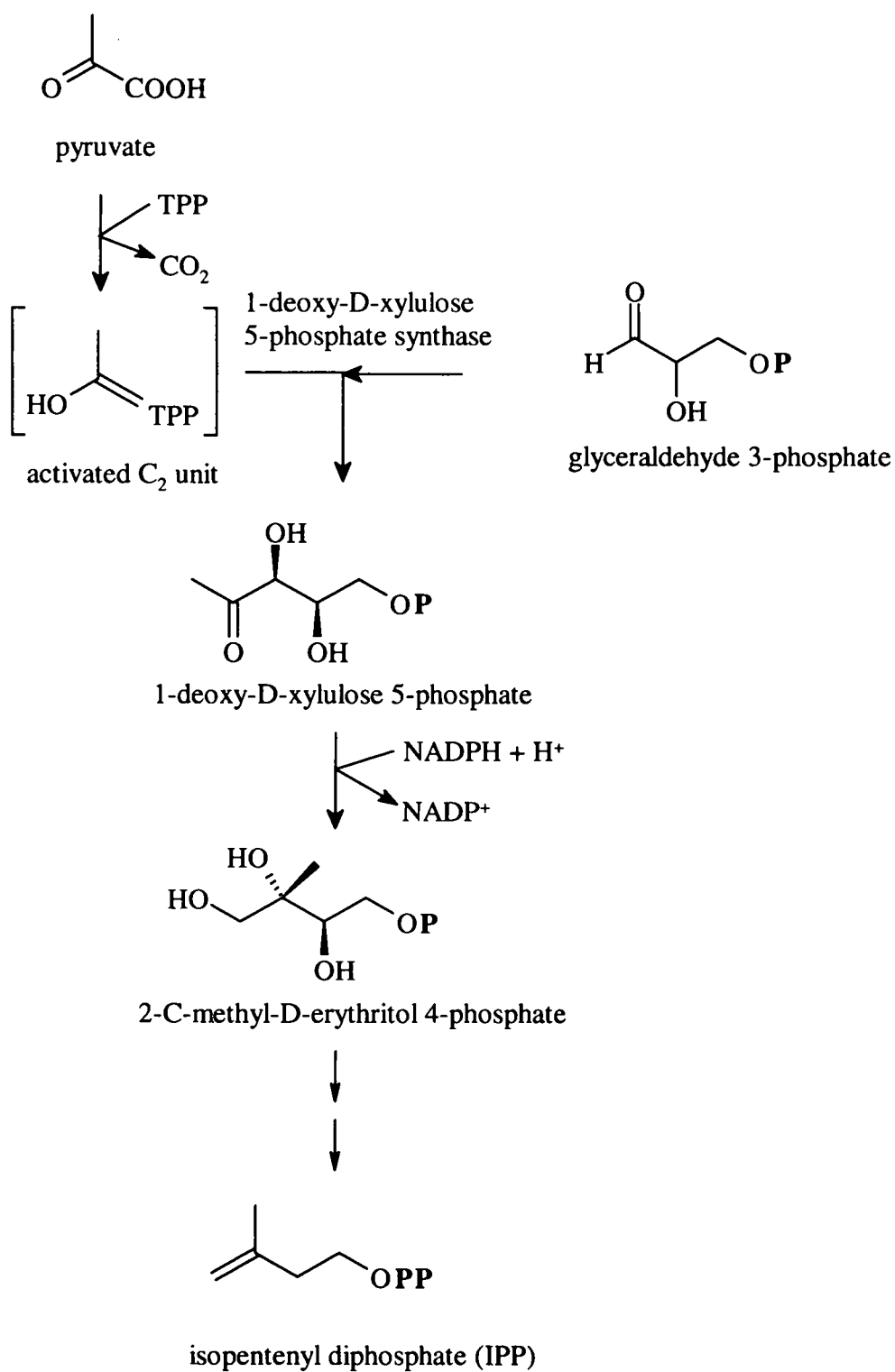
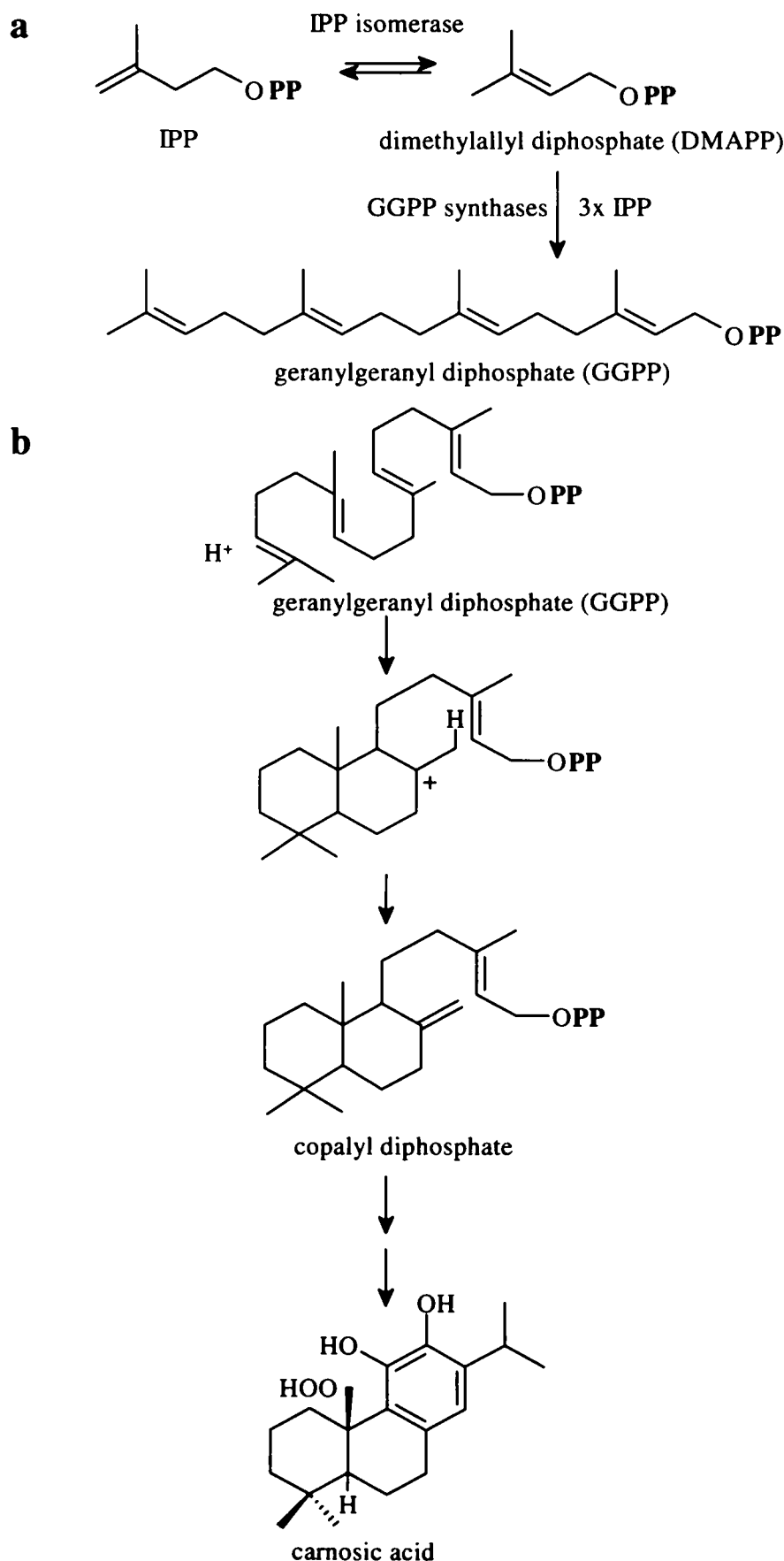Fig. 2.11. Formation of IPP by the 1-deoxy-D-xylulose-5-phosphate pathway (TPP - thiamine pyrophosphate).

a

IPP isomerase

IPP

dimethylallyl diphosphate (DMAPP)

GGPP synthases | 3x IPP

geranylgeranyl diphosphate (GGPP)

b

H⁺

geranylgeranyl diphosphate (GGPP)

copalyl diphosphate

carnosic acid

Fig. 2.12. (a) Formation of GGPP, (b) proposed pathway for the last stage of the CA biosynthesis. (Gershenzon and Kreis, 1999)

27

CA functions as an antioxidant in chloroplasts together with its oxidation products rosmanol and isorosmanol. (Munné-Bosch and Alegre, 2001). CA and carnosol, its oxidation product, are good protectors of biological systems against oxidative stress, including lipid peroxidation and superoxide anion generation. (Haraguchi et al., 1995) They inhibit ·OH generation by the Fenton reaction through their ability to chelate iron, and are also effective scavengers of peroxyl radicals (Aruoma et al., 1992).

Carnosic acid has antifungal, antitumoral, antimutagenic, antiviral, antiproliferative activities and is also able to inhibit nitric oxide formation. (Gigante et al., 2003)

Rosemary plants exposed to drought and high light stress increase their concentration of highly oxidised abietane diterpenes and show a decrease of CA. This indicates the antioxidant behaviour of CA, which is unable to regenerate, and is the substrate for isorosmanol and dimethyl isorosmanol. (Munné-Bosch et al., 1999) A further investigation of drought stress with rosemary, sage and lemon balm showed a functional interdependence between the low molecular weight antioxidants CA, ascorbic acid and α-tocopherol. Whereas CA concentrations in rosemary and sage leaves decreased with increasing stress by forming oxidised diterpenes, lemon balm leaves showed an increase in ascorbic acid and α-tocopherol levels with stress; rosemary and sage on the other hand had constant levels of ascorbic acid. (Munné-Bosch and Alegre, 2003) CA and RA also showed both synergistically antioxidative effects with other molecules, e.g. lycopene (Fuhrman et al., 2000).

Rosemary extracts have high antioxidant activity and are used as anti-inflammatory and antimicrobial agents in medicine. The active compounds in lipid extracts are CA and carnosol, whereas RA is the main antioxidant in aqueous extracts. (del Bano et al., 2003)

A study with T98G Human glioblastoma cells and rosemary extract showed that especially CA enhanced the synthesis of nerve growth factor, an important protein for the growth and functional maintenance of nerve tissue. This effect is most likely due to the catechol group in the structure (Kosaka and Yokoi, 2003).

2.3. CHARACTERISATION OF ANTIOXIDANT STATUS

The characterisation of antioxidants is based on different methods with different objectives. Most approaches detect the ability of antioxidants to scavenge free radicals, e.g. the TEAC (Trolox equivalent antioxidant activity) assay (Rice-Evans et al., 1996), ORAC (oxygen radical absorbance capacity) assay (Cao et al., 1997) or the DPPH radical (1,1-diphenyl-2-picryl-hydrazyl) assay (Sánchez-Moreno et al., 1998). Another assay which was originally established for detection of the ferric reducing ability of plasma (FRAP) (Benzie et al., 1996), is now also used to measure the reducing ability of food samples. (Frankel and Meyer, 2000)

All of these assays deliver general information about specific radical scavenging ability of the sample but they all suffer from providing information on the biological target which should be protected. Contrasting results from different methods using the same molecules show that the activity is strongly dependent on the test system and on the substrate. 'There cannot be a short-cut approach to determining the activity of antioxidants'. (Frankel and Meyer, 2000) Furthermore it is recommended to determine the antioxidant activity under various conditions of oxidation, to use several methods to detect different products of oxidation and the systems should be related to real systems (e.g. food and biological reactions).

It is presumed that the amounts of antioxidants are correlated with their activities. Hence the philosophy is often that increasing the amounts of antioxidants in food should provide improved protection against "free radical attack" in cells. There are different analytical methods to determine the amount of certain antioxidants in plants and food. The application of three analytical methods on different plant tissues for quantitation of antioxidants was one aim of this work. A photometric assay was used to determine the amount of anthocyanins, a fluorometric approach was chosen to detect ascorbic acid and an HPLC method was taken to separate carotenoids and detect their amount in certain plant tissues. These analytical methods are discussed below. (Kellner et al., 2004; Otto, 2000; Skoog and Leary, 1992)

A photometric detection is commonly used in quantitative (trace) analysis of metals, drugs, body fluids, and food. The advantages are the sensitivity (down to 10^{-7} M), high

selectivity, good reproducibility and accuracy (relative uncertainties of 1 to 3 %) and ease of operation. The limit of detection is dependent on the extinction coefficient. In our case, cyanidin-3-glucoside – the standard for anthocyanins - has an extinction coefficient of 28033 L $mol^{-1}cm^{-1}$ (Wrolstad, 1982) which leads to a minimum detection of $3.5 \cdot 10^{-7}$ M at an extinction of 0.01 according to the Lambert-Beer Law. Applications for qualitative analysis are limited because the number of absorption maxima and minima is relatively small. The information obtained from UV/VIS spectroscopy can support identification of the molecular structure with the help of wavelength assignment tables, although there are now more informative techniques available, e.g. NMR spectroscopy. Nevertheless, UV/VIS spectroscopy is a cheap and useful tool in combination with HPLC.

Fluorescence techniques are used for determination of inorganic and organic substances. The concentration-intensity dependency of fluorescence spectra is more complicated than with UV/VIS spectra. Fluorescence yield has also to be considered. In contrast to absorption techniques, fluorescence is directly proportional to the intensity of the excitation energy and the dynamic concentration range can cover three decades (10^{-7} – 10^{-4} M). Fluorescence techniques are extremely sensitive (ppb range). However, the number of fluorescent substances is limited and the precision and accuracy is usually poorer than those of spectrophotometric methods.

There are some points which have to be considered with the fluorometric detection of ascorbic acid. The reaction of dehydroascorbic acid with o-phenylenediamine is time dependent and detection is made after 35 minutes reaction time. Hence there will always be a small range of fluorescence deviation due to the time-consuming handling of more than one sample per run. The sensitivity of the measurement can be improved by increasing the PMT (photomultiplier tube) voltage, but this also leads to a higher noise level. Therefore a compromise has to be found to reach the ideal signal-to-noise ratio. A calibration curve at a fixed PMT voltage covers a certain concentration range. The sample points should be in that range of linearity. In our case the standard addition curve was carried out from 5 to 40 µg/ml ascorbic acid plus 2 g pepper (see Chapter 3.1.2.) using a PMT setting of 700.

HPLC is a technique that is used for both qualitative and quantitative analysis. It has a good sensitivity, is adaptable to accurate quantitative determinations, is able to separate non-volatile species or thermally labile ones, and has a widespread applicability to substances of interest such as amino acids, proteins, nucleic acids. The reproducibility of retention times is less accurate than the wavelength precision in spectroscopy, but using standards for comparison provides useful information about the absence or presence of a substance. For quantitative analysis the peak height or area is taken. Both have disadvantages, e.g. the peak height is problematic in the case of alterations in the peak form, determination of the peak area is critical in case of peak broadening or very narrow peaks because of locating the exact positions for the beginning and the end of the peak. The separation and the quantitative yield can be maximised by choosing the right column temperature, flow rate, volume of injection, columns, and mobile phase. An analysis by HPLC is much more time consuming than detection by a fluorometer or photometer. However, HPLC analysis allows the analysis of several compounds in one run in contrast to fluorescence or absorption spectroscopy. In the case of carotenoids the flow rate was chosen to be 1 ml/min. For applications to carotenoids, one has to bear in mind that the technique has some limitations. The columns used are PEEK with an upper pressure limit of 300 bar. Therefore the flow rate is limited. Any loss of sample during the preparation is compensated by using an internal standard in the extract. An external standard which is run before each set of samples is used to compensate any daily variations of the instrument. The peaks do not show a typical Gaussian form, which makes evaluation of peak area difficult, especially when there are overlapping peaks. Sometimes an error from manual integration, e.g. in the case of overlapping peaks, cannot be avoided, but it can be minimized if integration is always carried out in the same manner by the same person. The detector is a DAD (diode array detector). The carotenoids are measured at a fixed wavelength of 450 nm, which is not the absorption maximum for all detected molecules. Hence a small error has to be expected due to absorbance measurements beside the peak maximum.

The most time consuming part which introduces the largest variability, is the preparation of the sample. Frozen material is normally used with these methods and the weighing of frozen powder has to be done as accurately as possible. There is a point when no liquid nitrogen is evaporated any more and no water is condensed. This is the

right time to read the weight. From my experience the biggest deviations of results come from the inhomogeneity of the sample powder and weighing errors.

2.4. CHARACTERISATION OF FREE RADICAL STATUS

Reactive oxygen species (ROS) may be either compounds with free radical character containing at least one unpaired electron, e.g. triplet (ground) state oxygen ($^3O_2$), hydroxyl ($\cdot OH$), superoxide anion (O_2^-), peroxy and alkoxy (RO_2^- and RO^-) radicals, or non-radicals such as singlet oxygen ($^1O_2$) and hydrogen peroxide (H_2O_2). They play essential roles in biochemical pathways, food degradation and in disease. Their generation is associated with processes such as senescence and pathogen attack, but they may also be a consequence of extreme environmental conditions, e.g. high or low temperature, herbicides, air pollutants, UV irradiation, nutrient deficiencies, toxic metals. (Smirnoff, 1993) Three biochemical systems, which are used in this work to oxidise phenolic compounds, are described in more detail.

O_2^- is generated in nearly all aerobic cells and can cross membranes through a specific 'channel', whereas $\cdot OH$ which is formed in different parts of the cell, cannot diffuse away from its site of formation since it reacts with virtually every component it meets. Xanthine oxidase which occurs in milk, liver and jejunum, catalyses the transformation of xanthine to uric acid generating O_2^- (Equ. 2.1.; Terada et al., 1990).
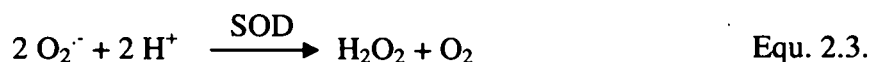

xanthine

uric acid

Equ. 2.1.
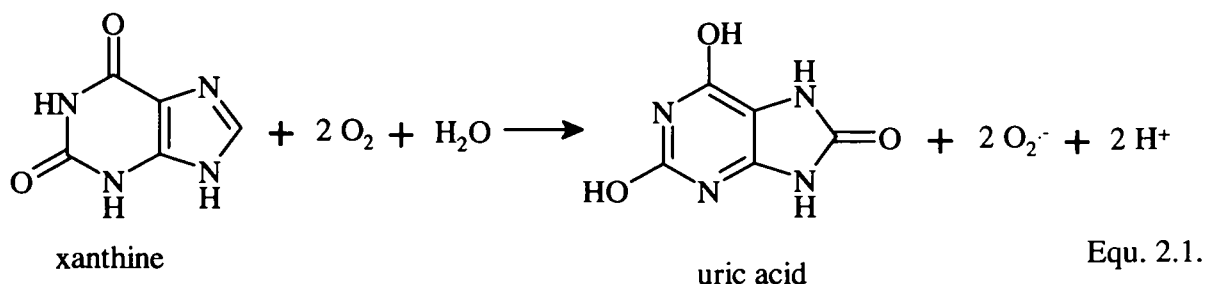
A main route for $\cdot OH$ generation is via the Fenton reaction (Equ. 2.2.) where H_2O_2 oxidises ferrous (Fe^{2+}) ion to ferric (Fe^{3+}) ion. Since the presence of H_2O_2 and a small amount of Fe^{2+} is normal *in vivo*, the Fenton reaction is common. The $\cdot OH$ radical reacts in three ways: by abstraction of a hydrogen atom to form H_2O, addition to another structure, e.g. aromatic rings, and acceptance of an electron, e.g. from the chlorine ion. (Halliwell and Gutteridge, 1984)

$$Fe^{2+} + H_2O_2 \longrightarrow Fe^{3+} + \cdot OH + OH^- \qquad\qquad \text{Equ. 2.2.}$$
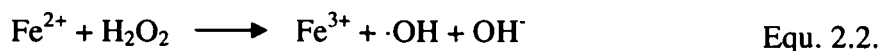
The system horseradish peroxidase (HRP) and H_2O_2 is an alternative for oxidising phenolic compounds. Fig. 2.13. shows a generalised reaction scheme for heme peroxidases and catalases (Jakopitsch et al., 2005). HRP, a ferric protoporphyrin IX, which is bound ionically or covalently to cell-wall polymers and is localized in the apoplastic space, reacts with H_2O_2 to form three compounds. Compound I (a ferryl porphyrin π-cation radical or a ferryl protein radical) is generated by oxidation of the native enzyme with one H_2O_2-molecule. It can either react directly back to the ferric enzyme by another H_2O_2 or indirectly via compound II (a ferryl species or protein radical) by two one-electron reductions in the presence of an one-electron donor (e.g. phenolic compounds). Addition of $O_2^{\cdot-}$ then generates the so-called compound III (a ferrous-dioxy/ferric-superoxide complex). A physiologically relevant way for its formation is reaction of the enzyme with $O_2^{\cdot-}$ produced by the oxidative cycle with a suitable substrate such as NADH (Chen and Schopfer, 1999). Compound III is also formed from compound II with an excess of H_2O_2 or from the ferrous heme protein by dioxygen binding.

The formation of $\cdot OH$ radicals is also related to superoxide anion production in the cell. Superoxide anion radicals dismutate to H_2O_2 and O_2 in the presence of superoxide dismutase (SOD) (Equ. 2.3.). The so-called Haber-Weiss reaction (Equ. 2.4.) of superoxide and H_2O_2 leads then to $\cdot OH$ radical generation. (Smirnoff, 1993)

$$2\,O_2^{\cdot-} + 2\,H^+ \xrightarrow{\text{SOD}} H_2O_2 + O_2 \qquad\qquad \text{Equ. 2.3.}$$

$$O_2^{\cdot-} + H_2O_2 \longrightarrow \cdot OH + OH^- + O_2 \qquad\qquad \text{Equ. 2.4.}$$

Free radicals can be detected by various biochemical methods, e.g. detection of superoxide anion radicals by reduction of cytochrome c (Green and Hill, 1984), detection of OH-radicals by a fluorimetric detection of the hydroxylation of benzoate or by a photometric detection of the degradation of deoxyribose (Chen and Schopfer, 1999). All these biochemical methods are indirect determinations of the radicals, where the sample matrix has to be treated and hence changed in a special way before

detection. Since radicals are often highly reactive compounds, the actual status in the samples may not be reproducible any more. Such methods have to be taken with care and under consideration of possible errors in the results.
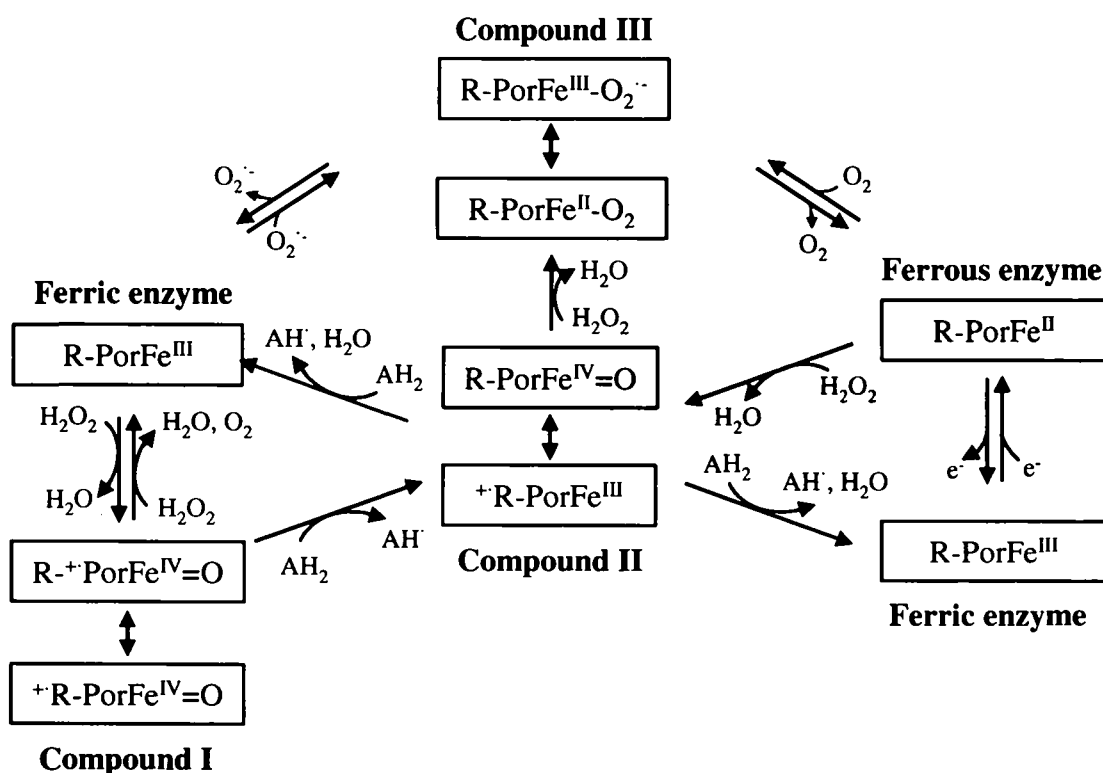

Fig. 2.13. Reaction scheme of heme peroxidases and catalases. (Jakopitsch et al., 2005). (AH_2 – one-electron donor)

2.4.1. EPR Spectroscopy

Electron paramagnetic resonance (EPR) or electron spin resonance (ESR) spectroscopy is a non-invasive method for the detection of paramagnetic molecules, such as free radicals and many transition-metal ions (Bolton, 1972). The physical condition of the sample can be solid or liquid in the form of crystals, powders, solutions or frozen solutions. Although it is limited to special molecules it can be a useful tool for certain questions. The theoretical information about EPR presented in this section was taken

from the 2003 lectures of Prof. Vana (Vienna University of Technology), and from Goodman & Raynor, 1970, Bolton, 1972, and Poole, 1997.

Principles of EPR

The principles of EPR can be described by quantum-mechanical theory. An electron is a charged particle in motion and creates a magnetic moment which is described by the spin quantum number m_s, (this has the values of $\pm 1/2$). In the absence of a magnetic field the energies of the spin states are equal. Applying an external field leads to separation of energies and a change in population of the energy states according to the Boltzmann statistics. This energy separation is called the electronic Zeeman effect (Fig. 2.14.). The energetically more favourable state has the electron magnetic moment parallel to the external field. The energy states are equal to $g\mu_B B_o m_s$ where g is the g-value or g-factor, a specific constant typical of the molecule containing the unpaired electron, μ_B is the Bohr magneton ($9.27 \cdot 10^{-24}$ J/T), B_o the external magnetic field, and m_s the electron spin quantum number ($\pm 1/2$). The energy separation (ΔE) grows with an increasing magnetic field. Transitions between the electron spin energy levels can be induced by the absorption of electromagnetic radication when the energy of the photons $h\nu$ is equal to ΔE (Equ. 2.5., where h is the Planck's constant ($6.62607 \cdot 10^{-24}$ Js) and ν is the microwave frequency).

$$\Delta E = g\mu_B B_o = h\upsilon \qquad \text{Equ. 2.5.}$$

Spectrometers operate in various microwave frequency bands, L (~1 GHz)-, S (3 GHz)-, X (9 GHz)-, K (24 GHz)-, Q (34 GHz)- and W (90 GHz)-band, though X-band is the most commonly used one.
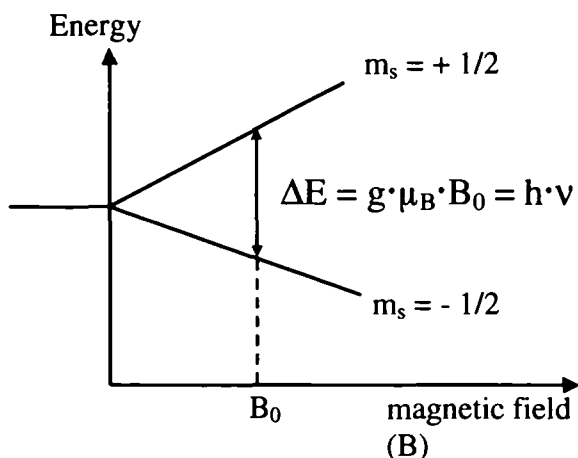
Fig. 2.14. The electronic Zeeman effect including the resonance conditions. (Poole, 1997)

EPR spectra

EPR spectra are obtained by measuring the absorption of the microwave energy at the resonance conditions in Fig. 2.14. Normally the magnetic field is scanned while the frequency is fixed and spectra are obtained as the first derivative of the absorption curve (Fig. 2.15.). Resolution of overlapping peaks can be improved by recording the second derivatives. An EPR spectrum is characterised by the g-value, the line width and shape, the signal intensity, the hyperfine splitting and the anisotropy.

g-value

The g-value is the proportionality constant of Equ. 2.5. and is equal to $71.44775 \cdot v/B_0$, where v is in GHz and B_0 is in T. For a free electron $g = 2.0023$. The g-values of different molecules differ from that of the free electron because of the interaction of the electron spin and orbital angular momenta, which leads to a shift in the resonance energy (<2.0023 if coupling is with empty orbital(s), >2.0023 if coupling is with filled orbitals). g-values of solid samples are often anisotropic, which means they are dependent on the direction of the orbital containing the unpaired electron relative to the applied magnetic field, whereas in fluid solutions the anisotropic effect is generally averaged by rapid molecular tumbling.
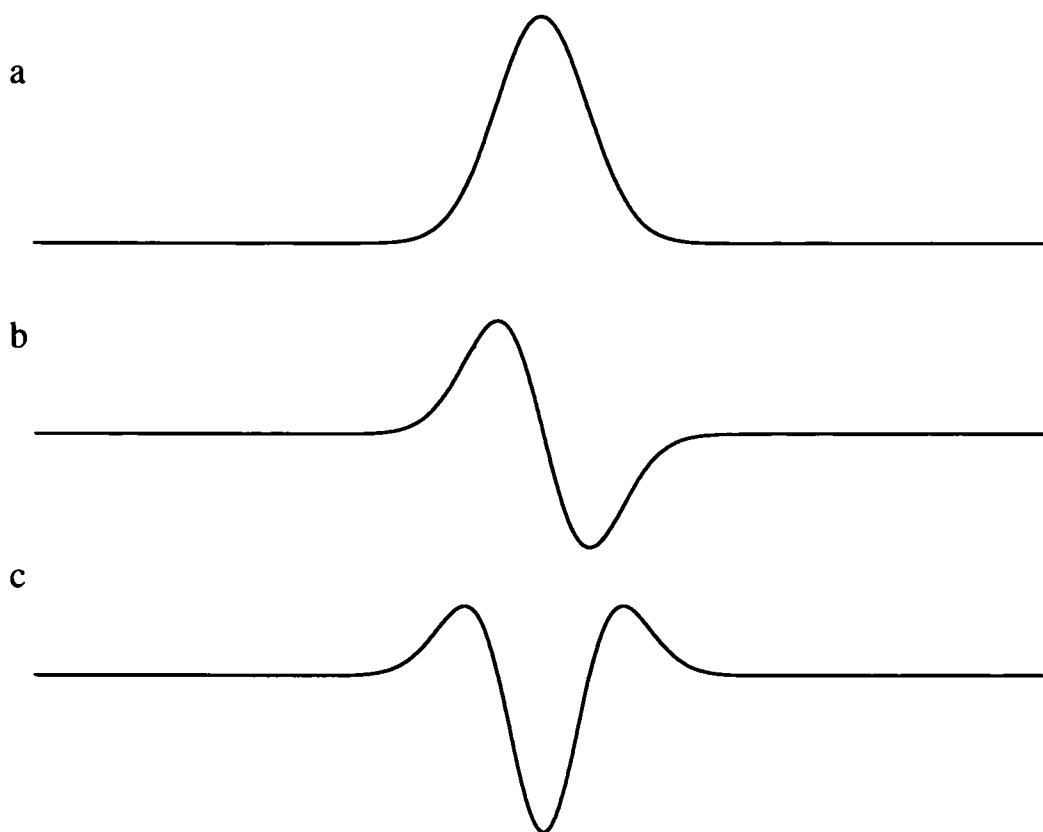
37

Fig. 2.15. EPR-spectra shown as absorption peak (a), the first derivative (b) and the second derivative of the absorption peak (c).

Relaxation, line width and shape

The resonance situation leads to two opposing processes in the molecule. On one hand the microwave field tries to equalise the difference in the population density, whereas relaxation processes try to restore the Boltzmann distribution. The latter consist of 2 separate processes – spin-lattice-relaxation and spin-spin-relaxation.

In a conventional EPR experiment, spin-lattice-relaxation is responsible for maintaining a constant absorption signal since the interaction between the electron spin and the lattice re-establishes the Boltzmann distribution. Without this interaction the electron spin energy levels would rapidly become equally populated; then no further microwave energy could be absorbed, the lines become broader and the transition becomes saturated. On the other hand a broader absorption line also occurs when the relaxation

time is too short, which can be explained by the Heisenberg uncertainty principle - a short relaxation time (T_1) leads to a broader energy state ($\Delta v = 1/T_1$). The interaction between the spin and the lattice occurs through two processes – the direct and the Raman process. The direct process involves the exchange of a complete quantum v_0 with a lattice vibration, the Raman process takes place over a two-photon transition, where an additional photon v_1 is absorbed first to the available energy state and another one v_2 is then emitted. The difference between v_1 and v_2 is the initial frequency v_0. This process occurs only when enough photons are available which is the case at high temperatures, whereas the direct process dominates at very low temperatures. The relaxation time is determined as the time from saturation to the recovery of the thermal equilibrium.

The spin-spin-interaction occurs between the spins of unpaired electrons. The movement of the spin in the external magnetic field can be considered as a magnetic dipole having a fixed component in the direction of the magnetic field; this produces an additional field at a neighbouring unpaired electron, resulting in a shift in the total field and hence a shift in its energy levels. This interaction is usually seen in the spectrum as line broadening. Additionally the broadening of the absorption takes place for electrons in neighbourhood which have the same Larmor frequency (equal to the same g-value) since the oscillating field induces transitions in the adjacent electron leading to a decrease of the normal life time.

A normal dipole-dipole interaction leads to a Gaussian line shape. Interactions between spin and lattice or motional averaging effects will narrow the lines – exchange narrowing - resulting in a Lorentzian shape. The line width represents the energy distribution within the energy levels and the interaction of the unpaired electron with its environment. If hyperfine splitting constants or the separation of different components in a sample are smaller than the line width, the absorption line will broaden.

Signal intensity

Double integration of the first derivative provides the signal intensity which is proportional to the number of unpaired electrons as long as saturation is avoided. Quantification of radical amounts is not very accurate due to the instability of most of

the radicals and their high reaction rate. However, there are semiquantitative methods using standards like DPPH or Mn which are run at the same time as the samples.

Hyperfine splitting

In addition to the external magnetic field, nuclei with non-zero spins such as ^{1}H (I=1/2), ^{14}N (I=1), ^{13}C (I=1/2) create additional magnetic fields which interact with the unpaired electron and cause a splitting of the energy levels into $2I + 1$ components. This leads to a splitting of the peaks in the EPR spectrum which is called the hyperfine splitting. The change of the nuclear spin quantum number m_I is much slower than the one of the electron spin quantum number m_s, therefore m_I is fixed during an electronic transition and two possible transitions are allowed according to the selection rules of $m_s = \pm 1$ and $m_I = 0$ (Fig. 2.16.). A typical hydrogen atom spectrum where two peaks of equal intensity are visible is given below the energy diagram. The distance between the peaks is called the hyperfine splitting described by the hyperfine coupling constant, a (which is usually quoted in mT or gauss). There is a direct proportionality between the hyperfine splitting and the product of the magnetic moment μ_N of the nucleus and the fractional occupancy of the molecular orbital containing the unpaired electron.

The interaction of the unpaired electron can be with more than one nucleus of the same type, e.g. with hydrogen atoms from a CH-, CH_2- or CH_3-group resulting in an intensity relation according to Fig. 2.17. Interactions with different type of nuclei lead to spectra showing the strong interaction with one type of nucleus leading to $(2J_1+1)$-splittings and all these lines are further split due to the weaker interactions with the other nucleus into $(2J_2+1)$-splittings. No overlapping sets of hyperfine splitting lines occur if the weaker interaction is very small compared to the strong one.
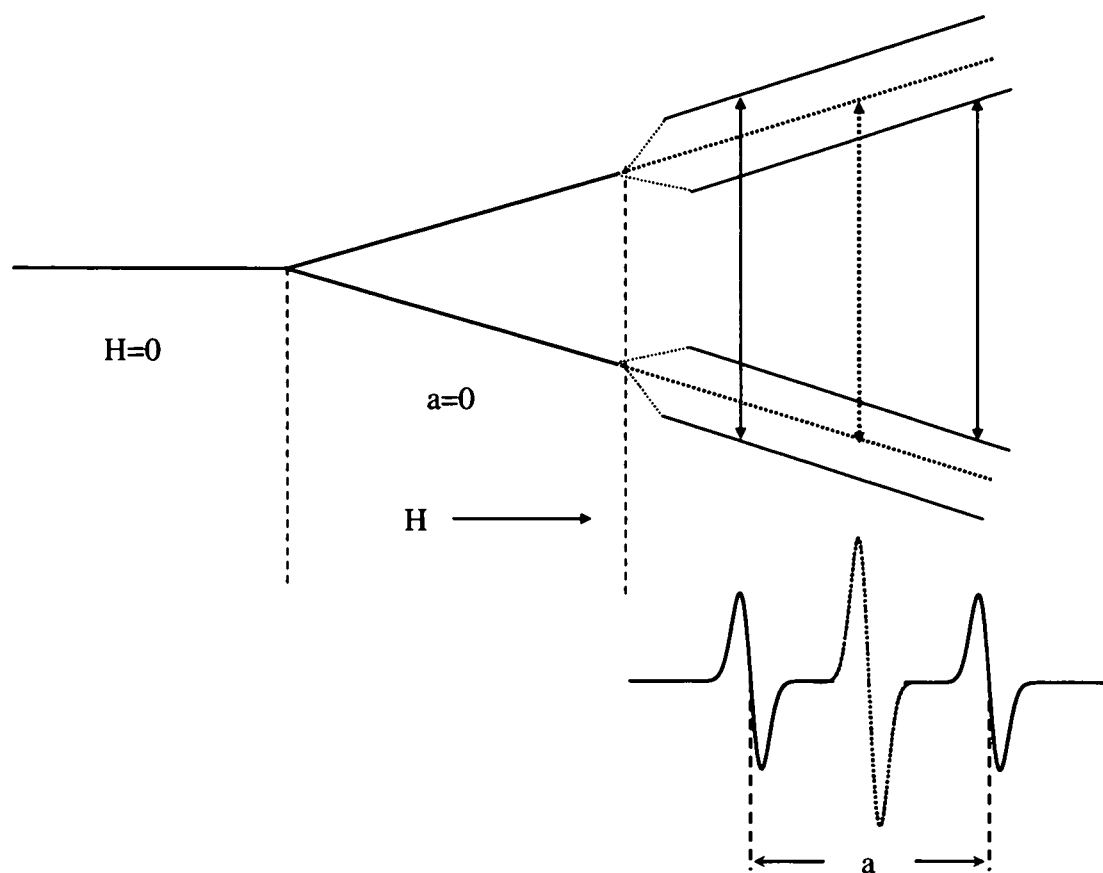
Fig. 2.16. Separation of the energy levels dependent on the magnetic field shown in the hydrogen atom. The dotted transition indicates the situation where a would be zero. (Bolton, 1972)

I=1/2   n=1   1   1

         2   1   2   1

         3   1   3   3   1

         4   1   4   6   4   1

         5 1   5   10   10   5   1

                         ...

Fig. 2.17. Intensity ratio of peaks coming from n equal proton couplings (Goodman, 1970).

Anisotropy

The hyperfine splitting due to the interaction of the electron with the nucleus is dependent on the type of orbital in which it occurs, e.g. s, p or d. If the electron is in an s orbital, the hyperfine coupling constant will be large due to the high electron density at the nucleus and independent of direction since s orbitals are symmetrical (isotropic hyperfine splitting). Anisotropic hyperfine splitting occurs when the electron is in a p or d orbital. In this case there is no electron density at the nucleus, the interaction which is based on two magnetic dipoles, is small and dependent on the direction (resolved in x, y, and z) of the orbital relative to the applied magnetic field and to the separation of the dipoles. The magnitude of this hyperfine coupling is zero when it is integrated over all directions. However, a small isotropic hyperfine splitting is usually observed as a result of polarisation of filled s-orbitals by the unpaired electron(s). (see e.g. Goodman and Raynor, 1970) Hybridisation of s, p, and d orbitals leads to a combination of isotropic and anisotropic couplings.

There is also a dependency of the hyperfine splitting on the physical state of the sample. Any solid matrix including frozen solutions will show the sum of isotropic and anisotropic interactions whereas with fluid solutions only the isotropic coupling will be observed due to the fact that anisotropic coupling is averaged to zero. In the case of large biochemical molecules in fluid systems, the tumbling frequency of the molecule may be lower than the resonance frequency leading to an anisotropic spectrum similar to that associated with a solid state molecule. This situation is also often observed when spin traps are used and large molecules are trapped leading to line width/height variations in the spectrum.

Saturation

The Boltzmann equation (Equ. 2.6.) describes the number of electrons in the ground (N_{gd}) and excited states (N_{ex}), where ΔE is $2g\mu_B B$. Resonance can only be observed if N_{ex} is different to N_{gd}. Any change in the occupation of the two levels is given by Equ. 2.7.

$$\frac{N_{gd}}{N_{ex}} = e^{-\frac{\Delta E}{kT}}$$

Equ. 2.6.

k ... Boltzmann constant ($1.380622 \cdot 10^{-23}$ J/K)

T ... temperature of the system

$$\frac{dN_{ex}}{dt} = N_{gd} \cdot W_{gd-ex} - N_{ex} \cdot W_{ex-gd}$$

Equ. 2.7.

W_{gd-ex} ... probability for the electron transition from the ground to the excited state

W_{ex-gd} ... probability for the electron transition from the excited to the ground state

Saturation occurs when N_{ex} approaches N_{gd}. When $N_{ex} = N_{gd}$ an electron is emitted for every one absorbed. Then an increase in the microwave power has no influence on the signal intensity. At low temperature saturation occurs relatively easy. A typical saturation curve is given in Fig. 2.18.
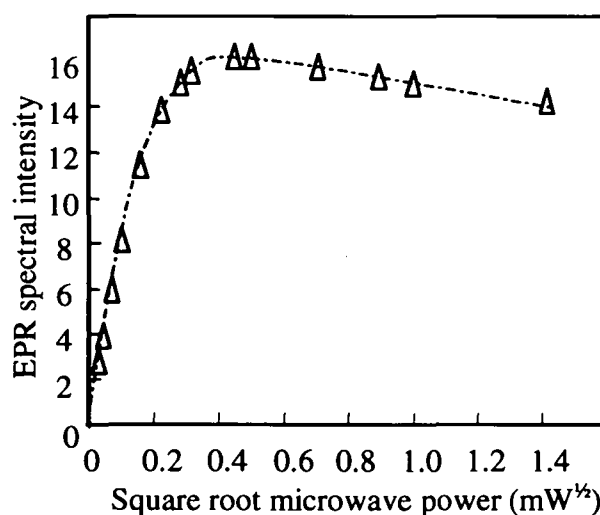
Fig. 2.18. Typical saturation curve of DPPH at 77 K.

EPR-spectrometer

An EPR-spectrometer consists of a homogeneous magnetic field, a microwave source, a microwave conductor, a microwave resonator, a detector, an amplifier, and a regulating system. A diagram of a typical EPR-spectrometer is given in Fig. 2.19.
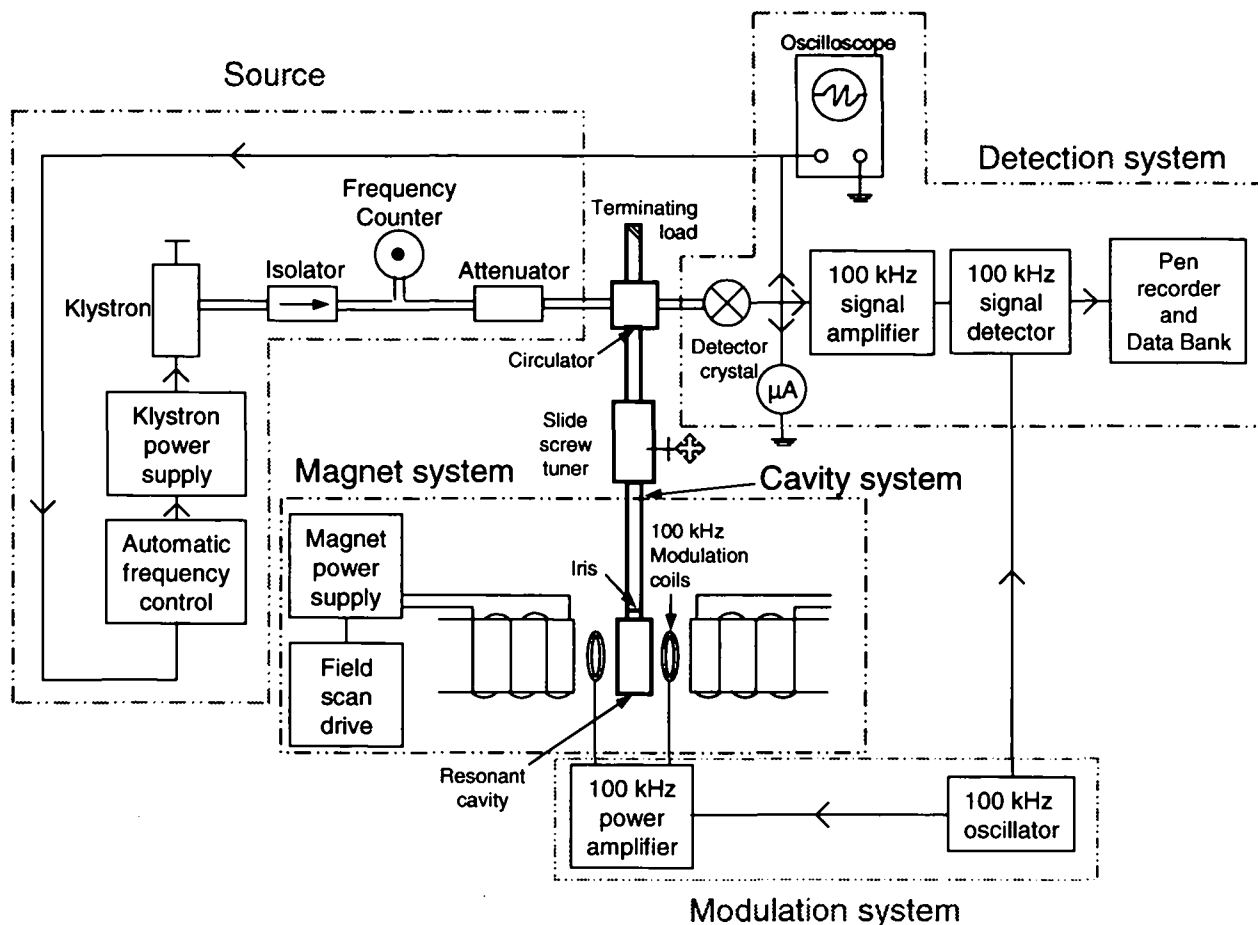
Fig. 2.19. Diagram of a typical X-band EPR spectrometer. (Bolton, 1972)

The magnetic field is produced by an electromagnet. The production of microwaves in the EPR spectrometer we used (Bruker ESP 300E, Bruker Biospin, Rheinstetten, Germany) is made by klystrons but many instruments nowadays use Gunn diodes as microwave sources. Transmission of the radiation from the source to the resonator as well as to the detector occurs with wavelength conductors. The resonator (cavity) is the part of the microwave conductor where interaction with the sample occurs and where a standing wavelength is produced. Silicium-Diodes are used for detecting the microwave signal.

Principle of measurement

The microwave bridge is the core of the spectrometer and the connection between the microwave source and the detector. To receive high signal-to-noise ratios and baseline

stability, the magnetic field is modulated at low frequency. Therefore the microwave signal is also modulated with the same frequency and the resulting spectrum is obtained as a 1st derivative of the absorption. In the present work, the best value of the modulation frequency to compromise noise and resolution was 100 kHz.

Variable parameters

Some parameters have to be chosen and set independent of the sample before the EPR spectrum can be recorded. The optimum microwave power varies a lot with the temperature at which the spectrum is recorded, e.g. frozen samples get saturated very easy; therefore the power needed is low (about 0.1 mW), freeze-dried biological samples can be recorded at room temperature with 1 mW, whereas good spectra can be obtained with spin-trapped samples using 10 or 20 mW microwave power (Pirker, 2002). The choice of the modulation amplitude is a compromise between the signal height and peak resolution. With decreasing modulation amplitude, resolution is improved, but the peak height is decreased. Another parameter is the receiver gain. It should be chosen to be big enough to obtain a good signal considering that an increasing receiver gain also increases the noise level. The speed of recording one spectrum can be regulated by the conversion time whereas the time constants filter out the noise by slowing down the response time of the spectrometer. The centre field and the sweep width of a spectrum are two other parameters which are adjusted to the sample conditions.

All simulations of EPR spectra were carried out using the program SimFonia from Bruker.

2.4.2. Spin Traps

The generation of unstable short-lived free radicals in a system can be detected by using molecules called spin traps. The technique was first demonstrated in the late 1960s (Janzen, 1984). Spin traps are diamagnetic compounds that react with radicals to produce new long-lived radicals which are stable enough to be detected by EPR. Qualitative information can be obtained from the parameters of the spectrum. An unknown trapped compound can be classified as belonging to a specific group of radicals, e.g. carbon-centred, oxygen-centred, or sulphur-centred, as a result of its EPR parameters (The older literature was collected in the N.I.E.H.S. spin trap database, but this has not been maintained in recent years). Since solvent effects can have major effects on the hyperfine splitting of the spin adduct, the solvent used in the experiment has to be clearly stated. (Buettner, 1987) The most commonly used spin traps are nitrones and nitroso compounds. In this work some derivates of dimethyl-1-pyrroline *N*-oxide (DMPO) such as 5-(diethoxyphosphoryl)-5-methyl-1-pyrroline *N*-oxide (DEPMPO), 5-(di-n-butoxyphosphoryl)-5-methyl-1-pyrroline N-oxide (DBPMPO), 5-(bis-(2-ethylhexyloxy)phosphoryl)-5-methyl-1-pyrroline N-oxide (DEHPMPO), and 5-(di-n-propoxyphosphoryl)-5-methyl-1-pyrroline N-oxide (DPPMPO) were used as well as the spin traps phenyl-*N*-*t*-butylnitrone (PBN), α-(4-pyridyl-1-oxide)-*N*-*t*-butylnitrone (4-POBN), 5-propyloxycarbonyl-5-ethylpyrroline-1-oxide (PEPO), and 1,3,3-trimethyl-6-azabicyclo[3.2.1]oct-6-ene-*N*-oxide (TRAZON). Their structures are given in Fig. 2.20. The radical attack takes place at the unsaturated α-carbon atom next to the nitrogen atom producing an adduct called nitroxide radical. The unpaired electron is delocalised over the molecular orbital which is the reason for the stability of the radical. All spin traps except PBN and 4-POBN were synthesised at the Research Institute of Biochemical Pharmacology and Molecular Toxicology at the University of Veterinary Medicine, Vienna.

The DMPO derivates have been used extensively with biological systems (see e.g. Buettner, 1987). However, DMPO is unable to discriminate between the superoxide radical anions and the hydroxyl radicals. This problem has been overcome with various phosphorylated derivates, which are suitable for studying the generation of superoxide radical anions and peroxyl as well as hydroxyl radicals (Fréjaville et al., 1995). The traps used were designed to probe selectively either the aqueous or lipid phase of the samples.

46

DEPMPO is very hydrophilic. Increasing the size of the organic chain on the phosphoryl group increases the lipophilicity of the spin trap. The EPR spectra of the phosphorylated derivatives of DMPO consist of two doublets from interaction of the unpaired electron with nuclear spins of the isotopes ^{31}P and ^{1}H (both having $I = \frac{1}{2}$) and a triplet from the interaction with the spin ^{14}N ($I = 1$), giving a total of 12 peaks if the hyperfine splitting constants of ^{31}P, ^{1}H, and ^{14}N are not equal (Fig. 2.21.). The synthesis of DMPO derivates is given in Scheme 1 (Stolze et al., 2000).

PEPO is a highly hydrophilic spin trap, which has been reported to form exceptionally stable superoxide adducts (half-life c. 20 minutes, Stolze et al., 2003). Spectra are simpler than with the phosphorylated spin traps described in the previous paragraph, and consist of at least 6 peaks with just one ^{1}H and ^{14}N nucleus contributing to the resonance (Fig. 2.22.). The synthesis (Stolze et al., 2003) is described in Scheme 2.

The final spin trap synthesised at the University of Veterinary Medicine, Vienna, was the bicyclic nitrone, TRAZON, which forms relatively stable adducts with lipid alkoxyl radicals (Stolze et al., 2002). The spectra are often quite complex, since both exo and endo adducts can be formed and each of these has hyperfine structure from up to five ^{1}H atoms in addition to the ^{14}N (Fig. 2.23.). TRAZON is more lipophilic than DMPO, making it a good spin trap for detecting lipid-derived radicals. It is interesting that alkoxyl radicals with short chain lengths produce different spectra than alkoxyl radical adducts with long chain lengths. The synthesis of TRAZON (Sankuratri and Janzen, 1996) is given in Scheme 3.

Typical spectra of PBN and 4-POBN are given in Fig. 2.24. The spin adducts are stable and the spectra are easy to interpret. They consist of 6 peaks, one triplet from the nitrogen (^{14}N) interaction which is further split into doublets from the hydrogen (^{1}H) coupling. PBN is lipophilic whereas 4-POBN is hydrophilic. Both spin traps are prone to hydrolysis in aqueous solution, forming aldehyde and a hydroxylamine which is promoted at lower pH. Hydrolysis followed by air oxidation produces 4-POBN-OH which is identical to the spin adduct of 4-POBN and ·OH radical. (Janzen, 1984)
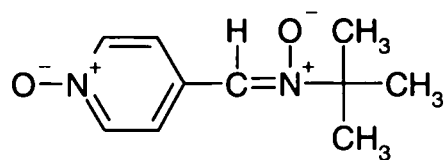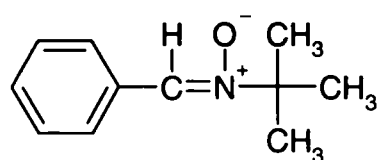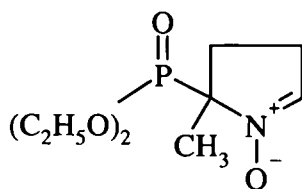
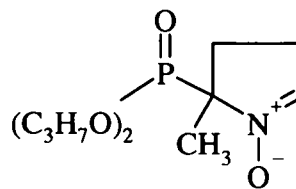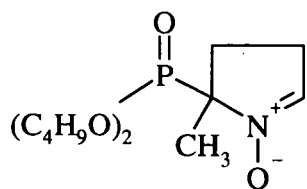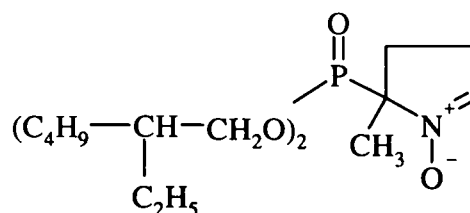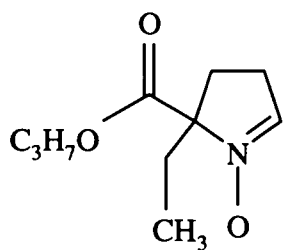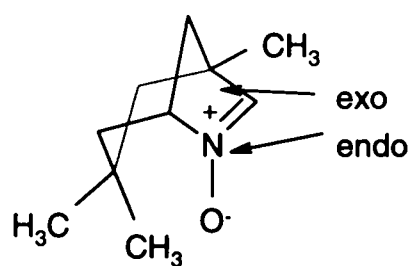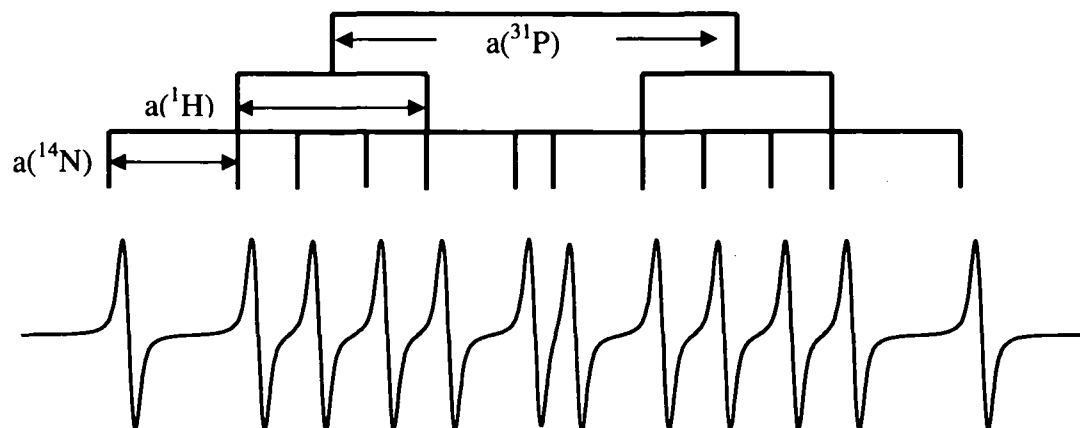Fig. 2.20. Structures of spin traps used in this work.
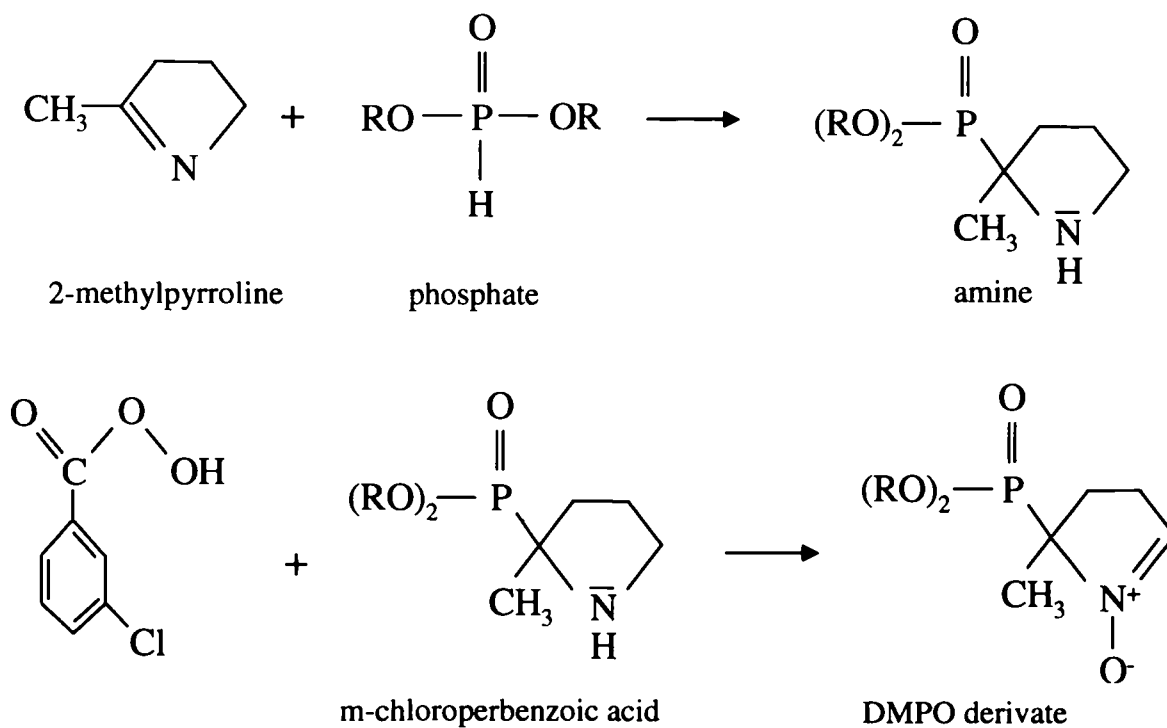
Fig. 2.21. EPR spectrum from a simulation of a typical carbon-centred radical adduct with DPPMPO. The splittings are described by the stick diagram.

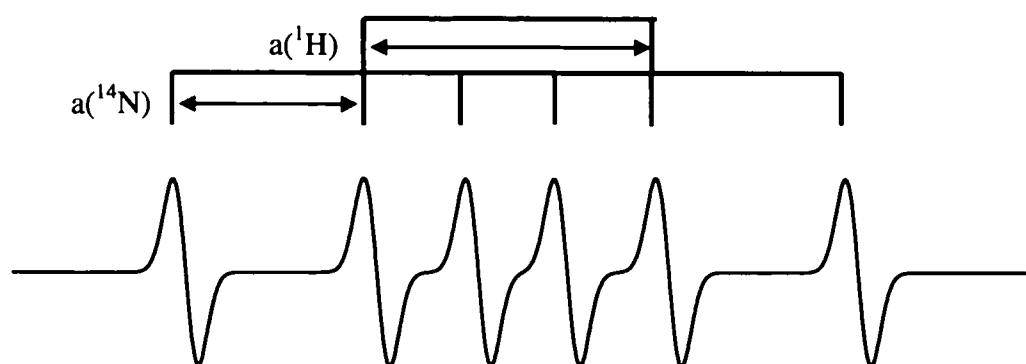Scheme 1. Synthesis of DMPO derivates.

Fig. 2.22. EPR spectrum from a simulation of a radical trapped by PEPO. The splittings are described by the stick diagram.

Fig. 2.23. EPR spectrum from a simulation of a radical trapped by TRAZON. The splittings are described by the stick diagram.

Scheme 2. Synthesis of PEPO.

1,3,3-Trimethyl-6-azabicyclo[3.2.1]octane

1,3,3-trimethyl-6-azabicyclo[3.2.1]oct-6-ene-*N*-oxide
(TRAZON)

Scheme 3. Synthesis of TRAZON.

Fig. 2.24. EPR spectrum from a simulation of a radical trapped by PBN. The splittings are described by the stick diagram.
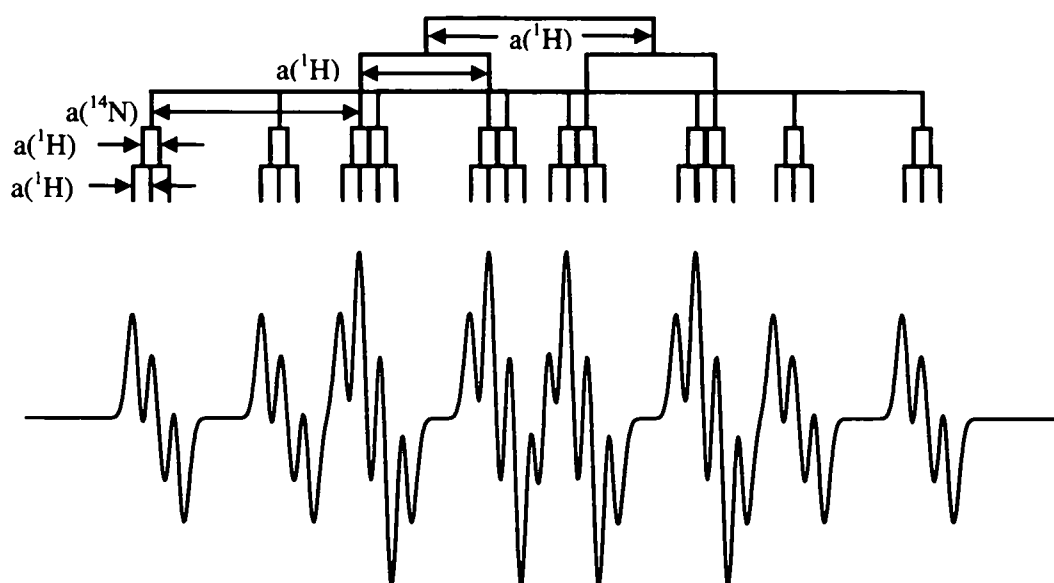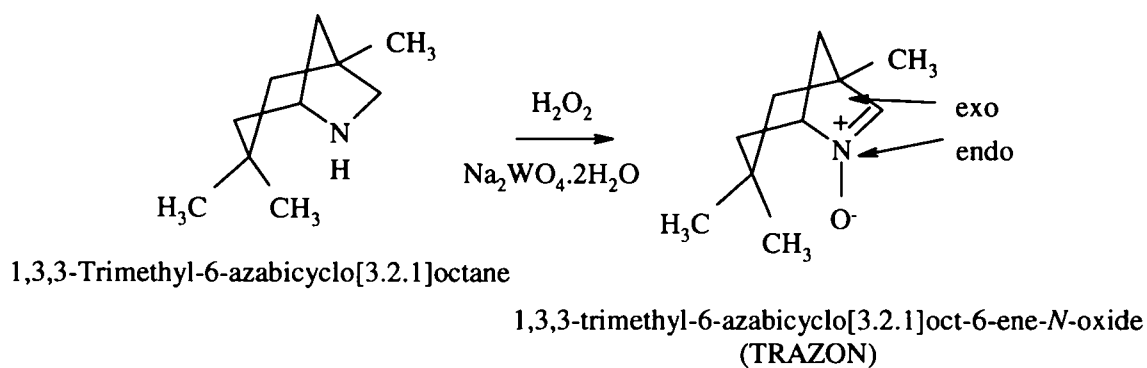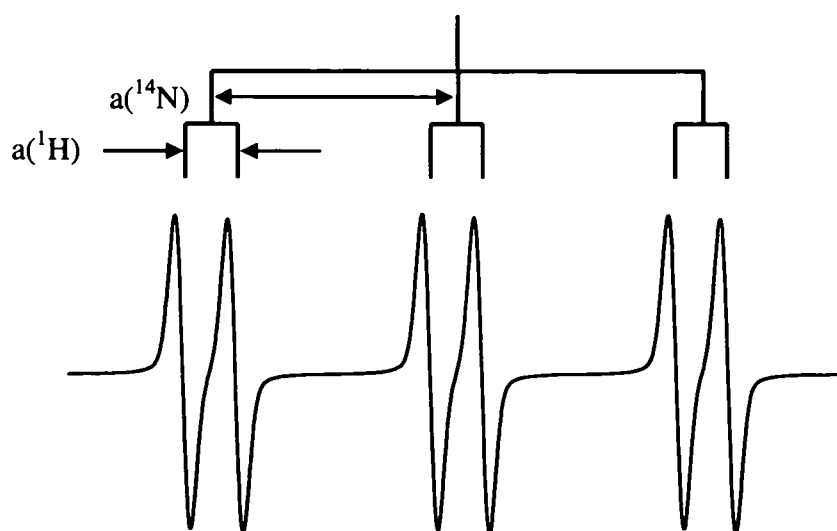
CHAPTER 3

EXPERIMENTS

3.1. ANALYTICAL METHODS

3.1.1. Detection of Anthocyanins

Quantitative determination of anthocyanins can be performed using the pH-differential method (Wrolstad, 1982), where photometric absorbance is measured at two different pH values (pH 1 and pH 4.5). At the lower pH (pH 1-3), the anthocyanins are red coloured, the keto groups are protonated and the absorbance has its maximum. Deprotonation occurs with increasing pH (pH 4-6) accompanied by an absorbance decrease and colour lightening. At pH 7-8 the colour changes to violet and blue, and finally to yellow when the pH > 8. The structural changes with pH are shown in Fig. 3.1. This pH dependency is used in the pH-differential approach to determine anthocyanin concentrations. The corrected absorbance, A, is given by the following equation:

$$A = (A_{max} \ [at \ 512 \ nm, \ pH \ 1] - A \ [at \ 700 \ nm, \ pH \ 1]) - $$
$$(A_{max} \ [at \ 512 \ nm, \ pH \ 4.5] - A \ [at \ 700 \ nm, \ pH \ 4.5])$$

Equ. 3.1.

The concentration, c, is then calculated using the Lambert-Beer Law and the molar extinction coefficient, ε, of cyanidin-3-glucoside:

$$c = A \cdot F \cdot d^{-1} \cdot \varepsilon^{-1}$$

Equ. 3.2.

where F is a dilution factor and d is the layer thickness of the cuvette.

quinonoidal base: blue
pH = 7

flavylium cation (oxonium form): orange to purple
pH = 1

-H+

-H+, +H$_2$O

chalcone: colorless
pH = 4.5

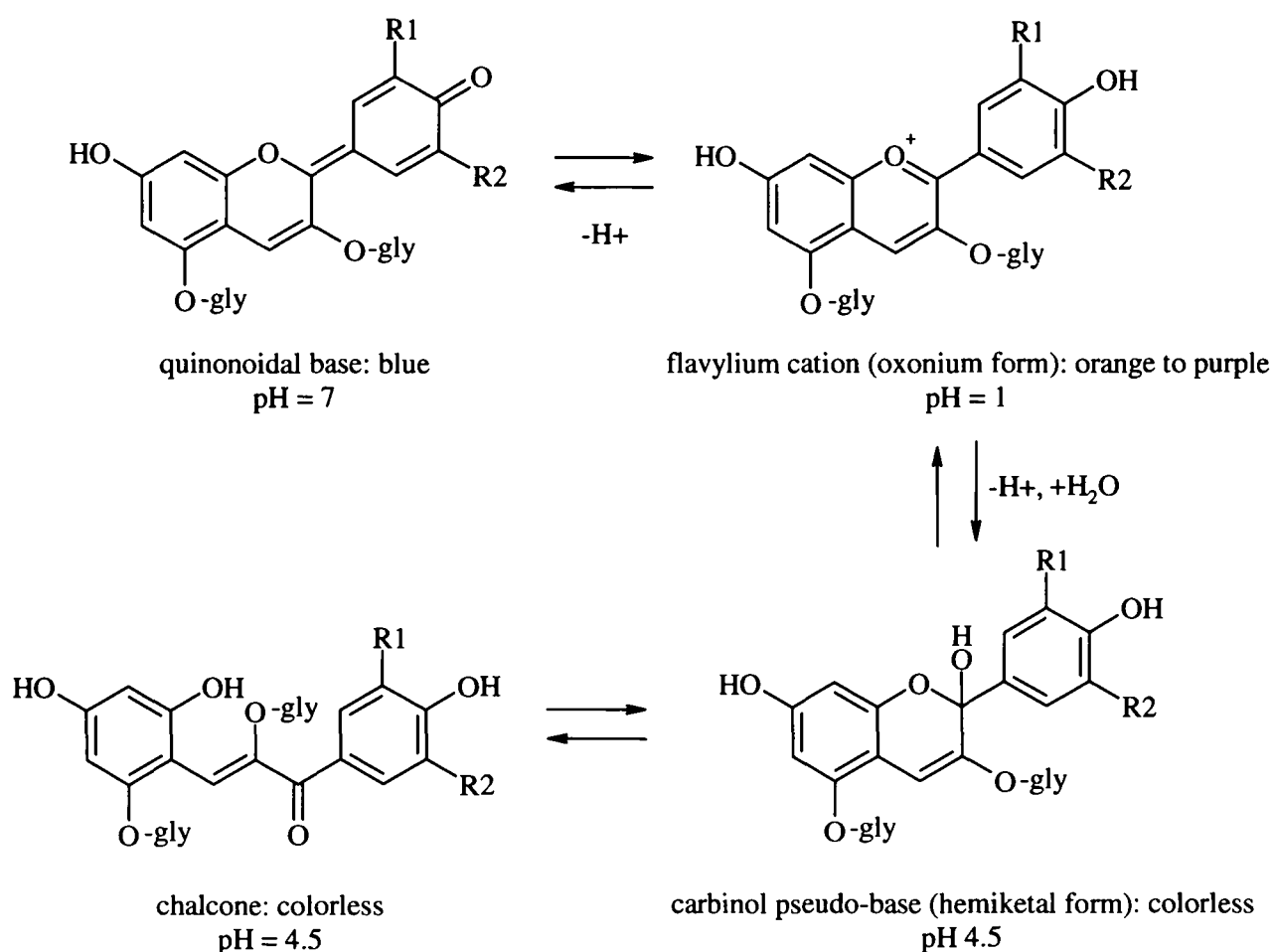carbinol pseudo-base (hemiketal form): colorless
pH 4.5

Fig. 3.1. Structural dependency of the pH in anthocyanins. (Giusti and Wrolstad, 2001)

Materials and sample preparation

A citrate-phosphate-buffer was first prepared with three different pH-values – pH 1, 4.5, and 7. The calibration curve was then produced from measurements of the standard cyanidin-3-glucoside (2100 μmol/L; 1 mg/ml) in MeOH/1% HCl as solvent. For the photometric measurement 1 ml of the buffer (pH 1 or pH 4.5) was transferred to the sample cuvette and a known amount of the standard solution (between 5 and 20 μl) added. Pure buffer at pH 7 was used as blank. Absorption maxima at 512 nm and 700 nm were taken using a Beckman DU 640 photometer and a calibration curve of c versus A was constructed (Fig. 3.2.). This curve shows a linear relationship between c and A

over the concentration range of 7-35 $\mu mol/l$ and extrapolates to a small absorbance (0.05) at $c = 0$.

For determination of anthocyanin levels in experimental samples, 1 ml buffer (pH 1 or pH 4.5) was transferred to the sample cuvette and mixed with 50 μl sample extract (*e.g.* 0.5 g frozen strawberry in 1 ml MeOH/1 % HCl) or with 50 μl sample extract plus a known amount of the standard stock solution (in our case 3, 5, 7.5, 9, 10, 12.5, or 15 μl) to consider any matrix effect of the sample solution. The absorbance at 512 nm or 700 nm was measured and curves of c versus A constructed as described above (Fig. 3.3.), where c is the concentration of the standard. The concentration of anthocyanins in the experimental sample was then equal to the difference in values of x when $y = 0$.

At pH 4.5 and higher concentrations of anthocyanins, the reaction (visible as colour lightening) is relatively slow, and takes up to 1 – 2 min. for completion; the measurement was therefore allowed adequate time for sample equilibration. Also the samples were pipetted directly into the solutions, otherwise some methanol could have been lost by evaporation. In addition, all methanol solutions were kept on ice and additionally the anthocyanin solutions were stored in the dark to prevent any degradation.

The standard addition method is considerably more time consuming than the conventional approach where the concentration in the experimental sample is read directly from the standard calibration curve using the experimental absorbance. However, I found that the extinction coefficient of the standard is dependent on the composition of the solution. Thus until this dependence is fully understood, the more laborious method described here is necessary.
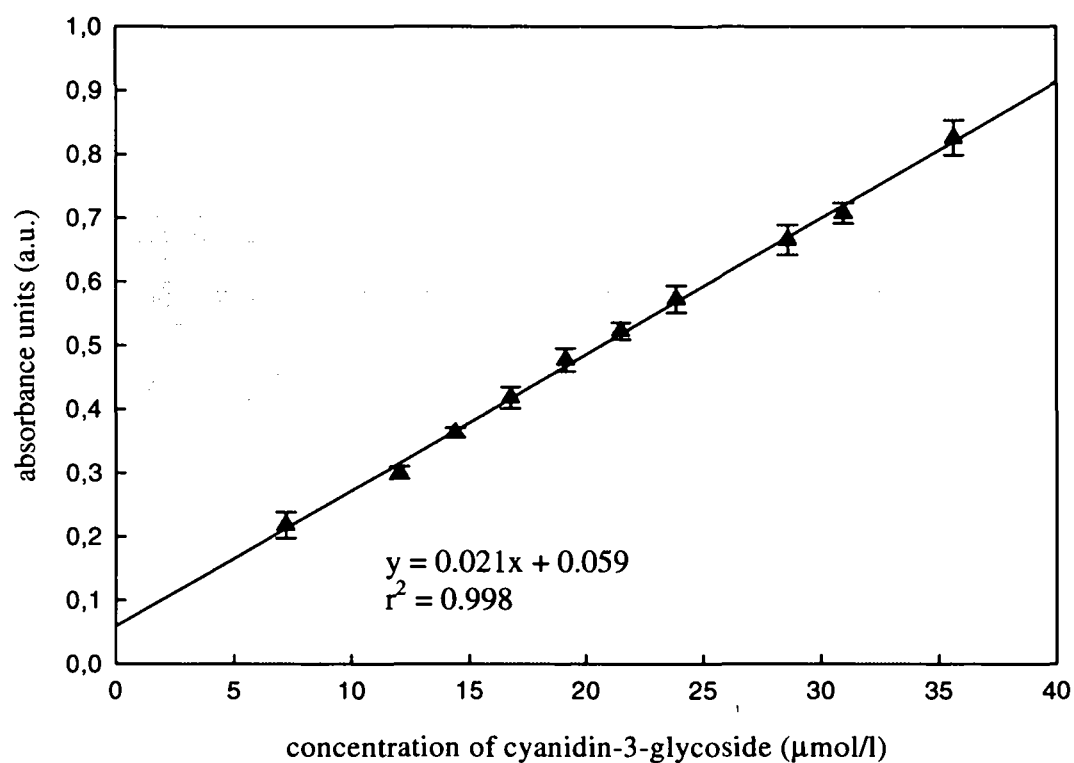
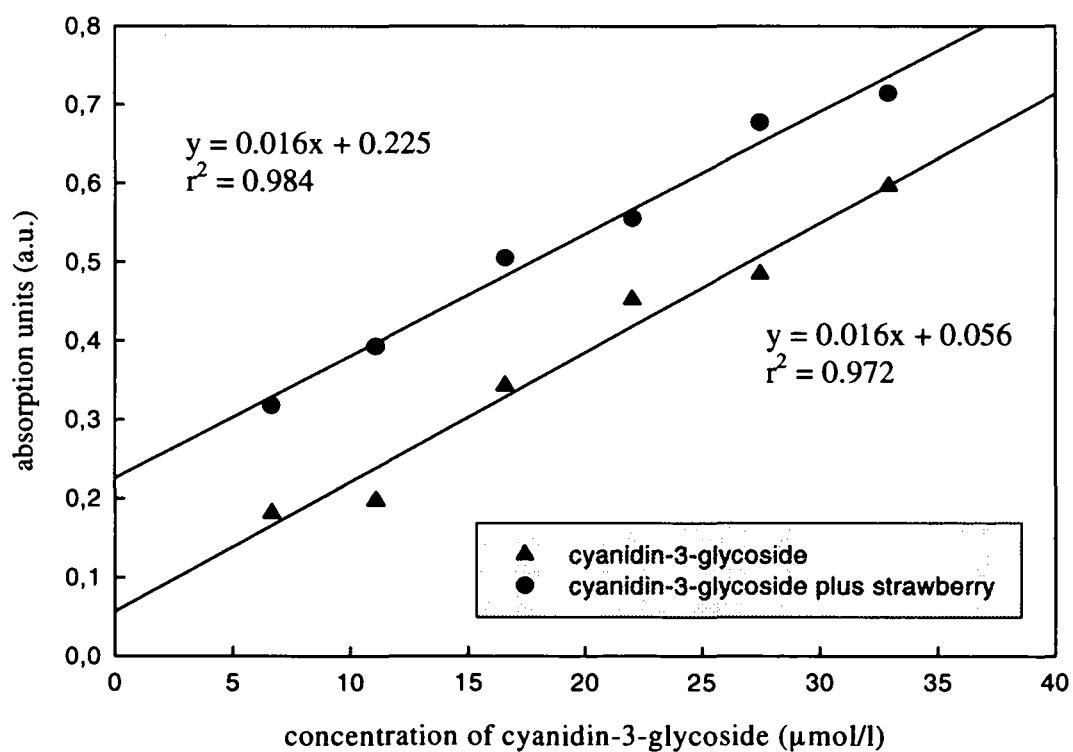Fig. 3.2. Calibration curve of cyanidin-3-glycoside. (error bars: SD for n=3)

Fig. 3.3. Standard addition curve using cyanidin-3-glycoside and frozen strawberry powder.

56

3.1.2. Detection of Ascorbic Acid

Fluorometric determination of ascorbic acid is based on the oxidation of ascorbic acid to dehydroascorbic acid in the presence of activated charcoal. Dehydroascorbic acid binds to o-phenylenediamine generating the fluorescent quinoxaline derivative (Fig. 3.4.).
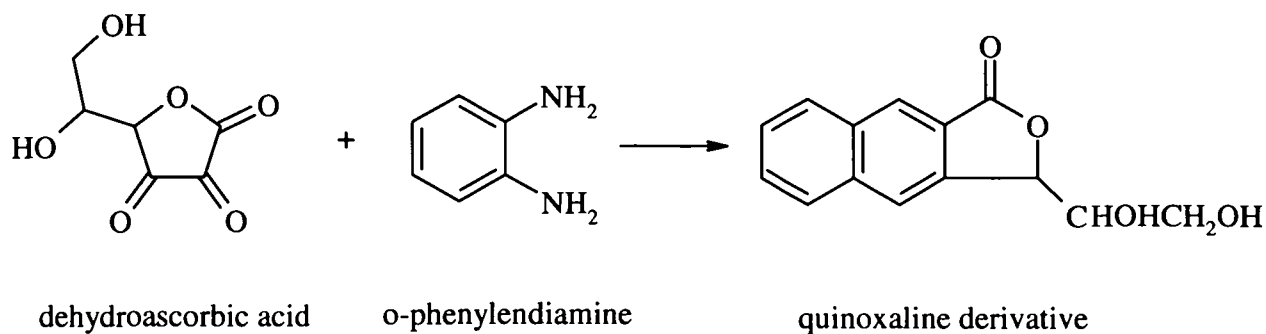

dehydroascorbic acid   o-phenylendiamine   quinoxaline derivative

Fig. 3.4. Conversion of dehydroascorbic acid with o-phenylendiamine.

This approach was used to determine ascorbic acid in pepper fruits.

Reagents

Metaphosphoric acid-acetic acid: 15 g HPO_3 pellets were dissolved in 40 ml acetic acid and ~200 ml distilled water and then diluted to 500 ml with distilled water. The pH was controlled and set to pH 1.4. Since HPO_3 slowly changes to H_3PO_4, the solution was stored in a refrigerator where it remained stable for 7-10 days. It functioned as the extraction solvent.

L-Ascorbic acid standard solution: A stock solution of 1 mg/ml was made by weighing 50 mg ascorbic acid, transferring it into a 50 ml volume flask, and then diluting it with the extraction solvent immediately before use. From this stock solution all the other concentrations were made.

o-Phenylenediamine solution: 20 mg o-phenylenediamine-2HCl was dissolved in 100 ml distilled water immediately before use.

Sodium acetate solution: 500 g NaOAc·3H$_2$O was dissolved in distilled water and diluted to 1 l.

Boric acid-sodium acetate solution: 3 g H$_3$BO$_3$ was dissolved in 100 ml NaOAc solution. The solution was prepared fresh every day.

Acid-washed Norit: The activated charcoal was already acid-washed when purchased.

Sample preparation and measurement

Frozen pepper samples (77 K) were ground in a coffee blender. The necessary quantity of the pulverized sample was then transferred into an Erlenmeyer flask. 50 ml of extraction solvent was added and the solution was placed in an ultrasonic bath for 3 minutes. The suspension was then filtered under vacuum. The filtrate was transferred into a 250 ml Erlenmeyer flask and 1 g acid-washed Norit was added. After shaking for approximately 2 minutes, the solution was filtered. The first few ml were discarded. For the sample blank solution, 5 ml of the filtrate were transferred into a 100 ml volume flask containing 5 ml H$_3$BO$_3$-NaOAc solution, which inhibits the later reaction of dehydroascorbic acid with o-phenylendiamine. The mixture was allowed to stand on a shaker for 15 minutes, during which time the sample solution was prepared by transferring 5 ml of the filtrate into a 100 ml volumetric flask containing 5 ml NaOAc solution. The solution was diluted to volume with distilled water. 1 ml of the sample solution was transferred into the fluorescence cuvette, designated as sample cuvette. After 15 minutes the blank solution was diluted to volume with distilled water. 1 ml of this solution was transferred into a cuvette, designated as blank cuvette. The cuvettes were placed in a light protecting polystyrene box covered with aluminium foil. With the addition of 2.5 ml of o-phenylenediamine solution into each cuvette the reaction was timed with a stop-watch for 35 minutes, during which time the cuvettes were standing at room temperature proctected from light.

After exactly 35 minutes the cuvettes were placed in the fluorometer (SAFAS FLEX-XENIUS) and the fluorescence emission spectra of sample and blank solutions were recorded   at

$\lambda = 426$ nm using an excitation wavelength of $\lambda = 350$ nm. A typical excitation and emission spectrum of ascorbic acid is given in Fig. 3.5.

Determination of the amount of pepper to use in each measurement

The decision on the amount of pepper to be used for each measurement was based on a calibration curve at a middle voltage of PMT (photomultiplier tube) 700 determined with 1, 2, 3, 4, and 5 g of a homogeneous ground pepper sample. Each point was measured once (Fig. 3.6.). 2 g of pepper gave an instrument reading of around 17 which is in the optimum range for the detector; this is also an amount of powder, which can be filtered quickly after extraction.
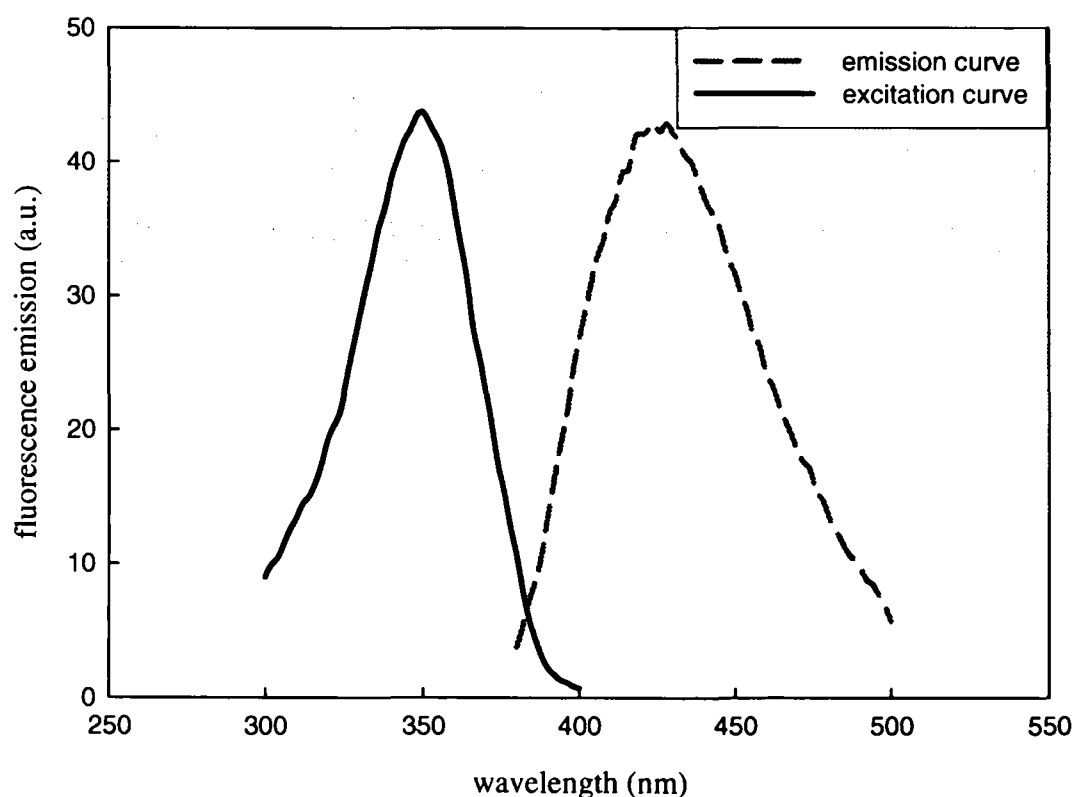
Fig. 3.5. Fluorescence emission and excitation curves for the ascorbic acid quinoxaline derivative.

59

Investigation of matrix effects

To check if there is any matrix effect with pepper fruits, two calibration curves were measured, one was an ascorbic acid calibration and one was based on ascorbic acid plus 2 g of pepper. Parallel curves would mean no matrix effect, whereas different slopes indicate an influence of the matrix. The calibration range was taken from 0 to 40 μg/ml ascorbic acid, since 40 μg/ml AA are *c.* 20 fluorescence units which is roughly double the initial value from 2 g pepper. Intervals of 5 μg/ml were chosen, resulting in 9 calibration points for the pepper curve. With most samples, each point was measured three times at a middle voltage of 700 of the PMT (Fig. 3.7.).

Discussion

According to the calibration curve from Fig. 3.6., 2 g pepper were sufficient for these analyses, since the fluorescence emission was in a good range for the detector. Therefore the influence of any matrix effects was checked only with 2 g of frozen homogenized pepper powder at a PMT voltage of 700. All points on the calibration curve of the pure standard ascorbic acid were measured three times, but because of limited amounts of some samples, some points in the standard addition curve were only measured twice. Fig. 3.7. shows that the slopes of the two curves are not the same and there is thus an appreciable matrix effect in these samples. The slope of the standard addition curve is flatter than the calibration curve for pure ascorbic acid, which means that some amount of added ascorbic acid was consumed or not detected. Thus the ascorbic acid concentration of any unknown pepper sample should be calculated using the standard addition curve and not with the calibration curve of pure ascorbic acid.

During the experiment, the most critical step was weighing the frozen powder into the flask. The weight was taken after the sample had lost all the liquid nitrogen and before it adsorbed water from the atmosphere. Deviations from this procedure would lead to incorrect weights and potentially large errors in the final result. For this experiment the concentration of ascorbic acid in the pepper sample, calculated from the negative intercept on the x-axis of Fig. 3.7., was 66.8 μg/ml. After multiplying this by 50 for the extraction volume (50 ml m-HPO_3) and dividing by 2 for the sample mass (2 g of the frozen powder were used), the ascorbic acid content was 167 mg/100 g (frozen tissue).
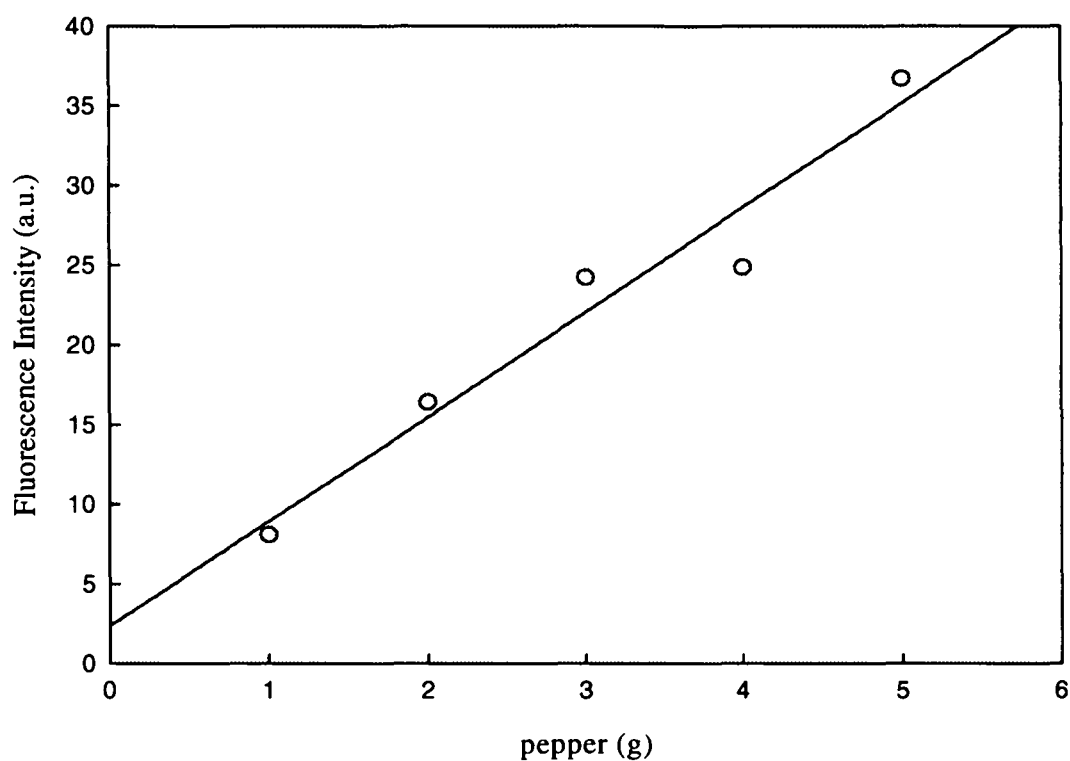
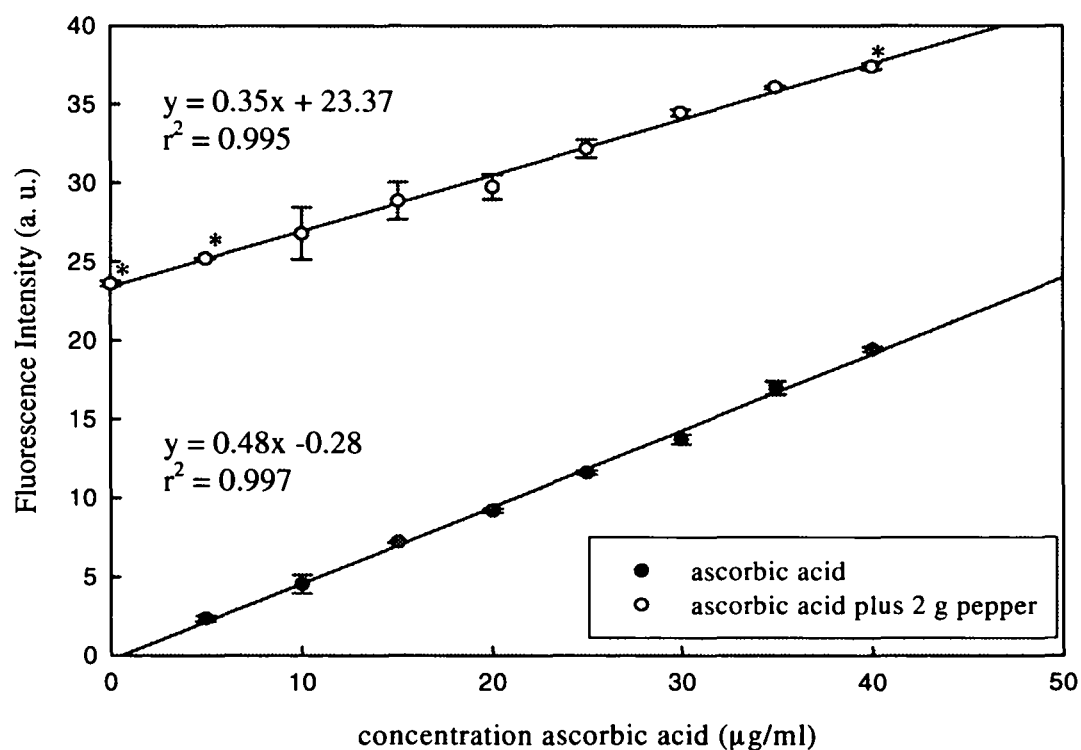Fig. 3.6. Calibration curve for different amounts of pepper.

Fig. 3.7. Calibration curve for ascorbic acid and standard addition curve for ascorbic acid with 2 g pepper. All points were measured three times except for those marked * which were measured twice.

61

3.1.3. Detection of Carotenoids

Determination of carotenoids in the herb lemon balm was performed using the HPLC method of Hart and Scott (1995).

Reagents

Extraction medium: Tetrahydrofuran (THF) and methanol (MeOH) were mixed 1:1.

Mobile phase: The mobile phase consisted of acetonitrile (MeCN):methanol (MeOH): dichloromethane (DCM) 75:20:5 v/v/v, with 0.1 % butylated hydroxytoluene (BHT) as an antioxidant and 0.05 % triethylamine (TEA), which helps to desorb the carotenoids from the column. The methanol contained 0.05 M ammonium acetate.

Carotenoid standard solutions

Lutein, α-carotene and β-carotene were stored in a mixture of chloroform and hexane (1:9 v/v). Zeaxanthin was dissolved in chloroform. Chlorophyll a and b were kept in acetone. Stock solutions of violaxanthin and antherxanthin were dissolved in a mixture of hexane and THF (1:1.22 v/v). Echinenone and β-cryptoxanthin were dissolved and stored in a mixture of chloroform and hexane (1:1 v/v). All solvents contained 0.1 % butylated hydroxytoluene (BHT) and were stored in air-tight screw-topped brown bottles under nitrogen at -18 °C.

Preparation of the individual working solutions

The stock solutions were brought to room temperature and filtered through a 0.45 μm polyvinylidene fluoride (PVDF) syringe filter. Using nitrogen gas an aliquot of the filtered solution was evaporated and dissolved in the mobile phase to reach a concentration of approximately 1 μg/ml. To keep a check on the performance of the HPLC-system, daily measurements were made using a mixed standard from the individual filtered stock solutions of the carotenoids.

Determination of the concentration of the working solutions

Accurate concentrations of the working solutions were measured by photometric absorbance. An aliquot of the filtered stock solution was evaporated under nitrogen, and diluted with the appropriate solvent (Table 3.1.) to produce an absorbance of approximately 0.5 AU. Concentrations were calculated using the appropriate extinction coefficients (Scott et al., 1996) of the carotenoids (Table 3.1.) and the Lambert-Beer Law. The concentrations of the filtered stock solutions are presented in Table 3.2.

Table 3.1. Absorbance maxima and physical parameters of the used carotenoid standards.

standard	solvent	λ_{max} (nm)	$E^{1\%}_{1cm}$	M.Wt. (g/mol)
Antheraxanthin	EtOH	446	2240	585
β-carotene	hexane	450	2560	537
β-cryptoxanthin	hexane	450	2460	553
chlorophyll a	EtOH	665	840	894
chlorophyll b	EtOH	649	518	907
Echinenone	hexane	457	2195	552
Lutein	EtOH	445	2550	569
Violaxanthin	EtOH	441	2425	601
Zeaxanthin	EtOH	452	2480	569

Table 3.2. Concentration and purity of filtered stock solutions.

standard	conc. of filtered stock solution (µg/µl)	purity (%)	corr. concentration of filtered solution (µg/µl)
Antheraxanthin	0.062	90.8	0.056
β-carotene	0.088	92.1	0.081
β-cryptoxanthin	0.298	94.7	0.282
chlorophyll a	0.307	92.1	0.283
chlorophyll b	0.503	84.3	0.424
Echinenone	0.253	97.6	0.247
Lutein	0.033	95.1	0.031
Violaxanthin	0.107	87.4	0.094
Zeaxanthin	0.373	94.8	0.354

Purity of the working solutions

The purity of the prepared working solutions was determined by the peak area of the carotenoids as a percentage of the total area of the chromatogram. The concentrations of the working solutions were then corrected accordingly (Table 3.2.).

Calibration curves of the carotenoids

Individual calibration curves were made from each carotenoid standard (Fig. 3.8. and 3.9.). The linearity of the calibration curves was confirmed for concentrations in the range of 0.05 μg/ml to 5 μg/ml.

Calculation of the carotenoid concentration

Determination of the carotenoid concentration (μg/ml) was based on the calculation of response factors relative to β-cryptoxanthin (Table 3.3.). Each batch of samples was accompanied by a measurement of a working solution of β-cryptoxanthin (B). Relative response factors (RF) were calculated according to Equ 3.3. The low response factor of chlorophyll a (Table 3.3.) is due to the low absorbance of this substance at 450 nm.

$$RF = \frac{Peak\ area\ of\ carotenoid\ working\ solution\ at\ 1\mu g\,/\,ml}{Peak\ area\ of\ working\ solution\ of\ B\ at\ 1\mu g\,/\,ml}$$

Equ. 3.3.

The carotenoid concentration in samples was determined following Equ. 3.4. and 3.5.

Table 3.3. Relative response factors of the used carotenoids related to β-cryptoxanthin and based on the peak areas of 1 μg/ml.

standard	Peak area of 1 μg/ml working solution	Relative response factors (RF)
Antheraxanthin	627.14	0.777
β-carotene	762.08	0.944
β-cryptoxanthin	807.39	1.000
chlorophyll a	70.75	0.088
chlorophyll b	318.47	0.394
Echinenone	534.70	0.662
Lutein	761.80	0.944
Violaxanthin	623.17	0.772
Zeaxanthin	656.11	0.813

concentration of carotenoid A ($\mu g / ml$ of extract)=

$$\frac{\text{area of peak A of diluted extract}}{\text{area of B at 1 } \mu g / ml} \div RF(A) \cdot \text{dilution of extract} \cdot \frac{100}{\% rec \ int \ std}$$

Equ. 3.4.

concentration of carotenoid A ($\mu g / 100g$)=

$$\frac{\text{concentration of carotenoid A} (\mu g / ml \text{ of extract})}{\text{concentration of herb sample in extract} (g / ml)} \cdot 100$$

Equ. 3.5.

Internal standard

Echinenone was used as an internal standard to estimate any loss of carotenoids during the extraction procedure. β-apo-8'-carotenal, the common internal standard, was not used because it co-elutes with chlorophyll b, whereas echinenone can be separated from the chlorophyll peaks.
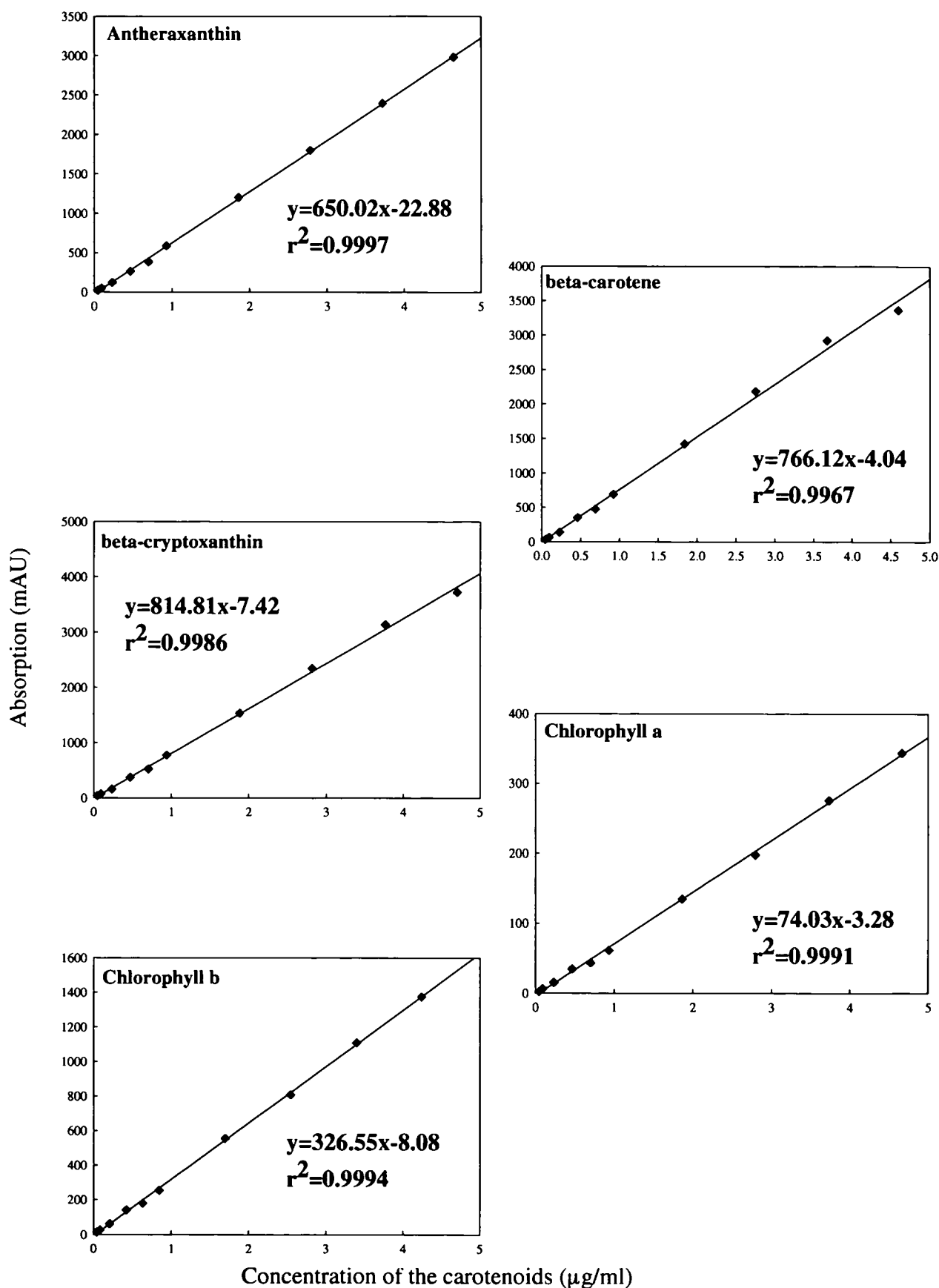
Fig. 3.8. Calibration curves of the carotenoids antheraxanthin, β-carotene, β-cryptoxanthin, chlorophyll a and chlorophyll b.
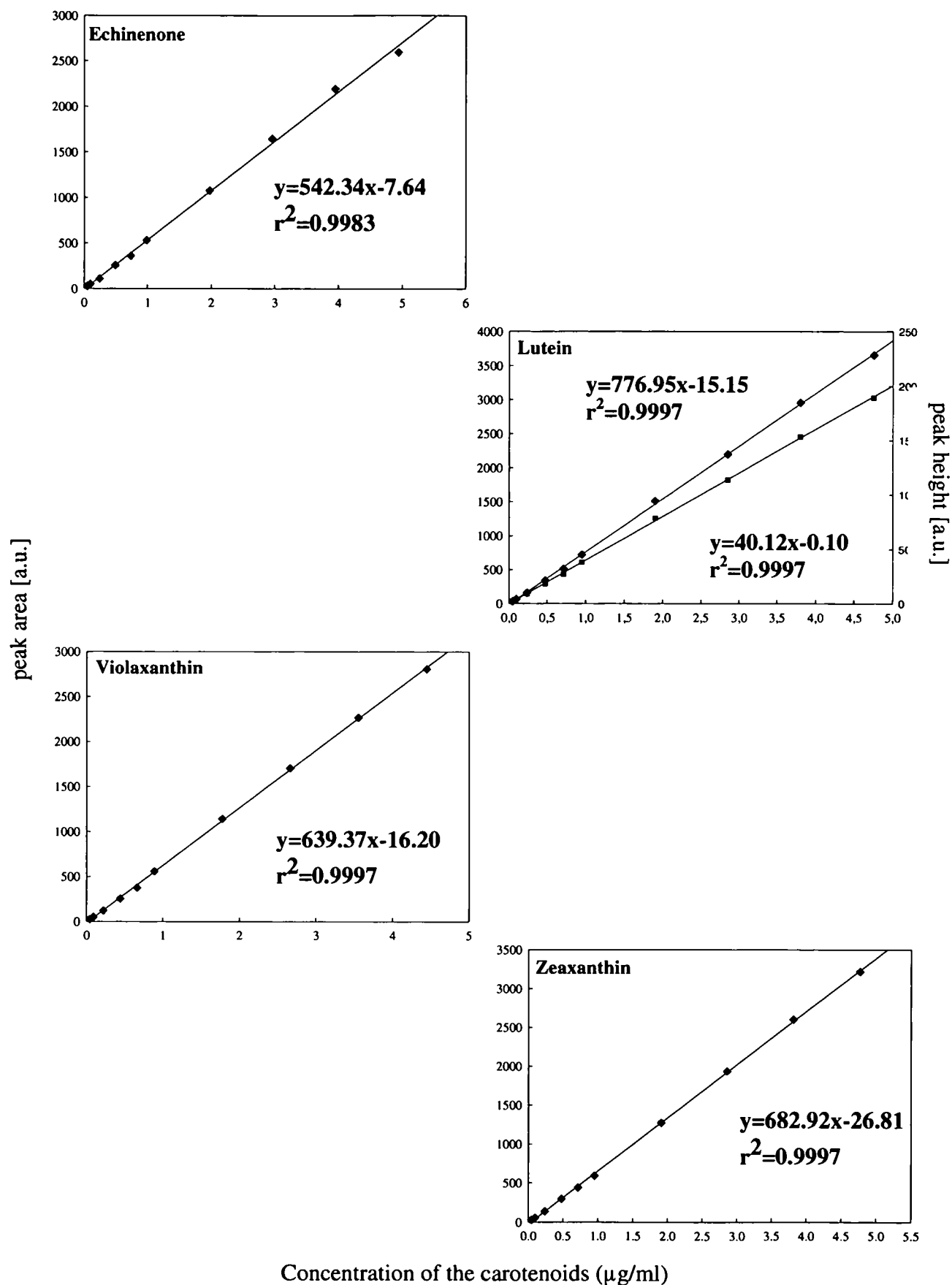
Fig. 3.9. Calibration curves of the carotenoids echinenone, lutein (including peak height calibration), violaxanthin, and zeaxanthin.

Sample preparation and extraction

Intact leaves of lemon balm were frozen to 77 K in liquid nitrogen immediately after harvest. Shortly before measurement the frozen leaves were homogenised under liquid nitrogen in a coffee blender. 1 g of the powder was transferred into a conical flask together with 0.5 g solid magnesium carbonate to neutralize any organic acids. 50 ml of the extraction solvent (THF:MeOH=1:1 v/v) and the internal standard were added. The sample solution was then placed in an ultrasonic bath for about 2 minutes, after which the suspension was filtered through a glass fibre pad in a Buchner funnel under vacuum. The filter cake was transferred back into the Erlenmeyer flask together with the filter pad for a second extraction with another 50 ml extraction solvent. After filtration the flask was washed with 25 ml extraction solvent and the washing was filtered. Another 25 ml extraction solvent were used to wash the filter cake. All the filtrates were combined (150 ml) and transferred to a 500 ml separating funnel to remove any water. 50 ml of petroleum ether (PE) and 25 ml of a 10% sodium chloride solution (to avoid the formation of emulsions) were added. After careful shaking the lower THF/MeOH/aqueous phase was drawn off and the upper PE phase was collected in a 250 ml evaporating flask. The THF/MeOH/aqueous phase was extracted two more times with 50 ml PE. The combined PE phases were evaporated at 35°C in a rotary evaporator to near dryness. The residue was redissolved in approximately 20 ml PE in an ultrasonic bath, transferred into a 25 ml evaporating flask, and again evaporated to just dryness. 1 ml DCM was added to redissolve the residue in an ultrasonic bath. The solution was filtered through a 0.45 μm syringe filter holder and an aliquot of it was diluted appropriately (e.g. 20 times) with the mobile phase.

HPLC separation

A system of three columns was used on an Agilent 1100 instrument. The first column – 10 x 4.6 mm long - was filled with 5 μm Vydac 201TP54. The second pre-column – 100 x 4.6 mm long – was filled with 5 μm Spherisorb ODS2 and the third column (analytical column) – 250 x 4.6 mm long - was filled again with Vydac material. The measurement is based on an isocratic separation using one solvent as the mobile phase. The different polarities of the columns helps to separate oxygenated carotenoids from

those consisting only of hydrocarbons. 40 μl sample solution were injected per run with a flow rate of 1.0 ml/min. The peaks were monitored at 450 nm.

Results and Discussion of the lemon balm extract

The lemon balm extract analysed by the HPLC included the carotenoids violaxanthin, antheraxanthin, lutein, zeaxanthin, chlorophyll a and b, and β-carotene. According to the literature (Britton, 1995) the first peak (retention time of 8.4 min.) is due to neoxanthin, where the absorption maximum is at 438 nm. Since we did not have this standard, neoxanthin was not included in the calibration. Fig. 3.10. shows the chromatogram of the HPLC separation. The retention times and concentrations calculated by Equ. 3.4. and 3.5. are summarized in Table 3.4. including the peak areas of the standard β-cryptoxanthin and the internal standard echinenone.

$$\text{concentration of carotenoid A } [\mu g/ml \text{ extract}] = \frac{\begin{array}{c}\textit{area of peak A of}\\\textit{diluted extract}\end{array}}{781 \textit{ at 1 } \mu g/ml} \div RF(A) \cdot 20 \cdot \frac{100}{93.5}$$

$$\text{concentration of carotenoid A } [\mu g/100g] = \frac{\begin{array}{c}\textit{concentration of carotenoid A}\\(\mu g \,/\, ml \textit{ of extract})\end{array}}{1.27 \,(g \,/\, ml)} \cdot 100$$

In the HPLC chromatogram the peaks of lutein and zeaxanthin are not separated since the intensity of the zeaxanthin peak is too low for the generation of a valley between the two peaks. As a consequence the concentrations were calculated by deconvoluting this peak assuming that the shape of the lutein peak was the same as that obtained from pure lutein with 5.23 μg/ml. The resulting peak area of lutein calculated over the regression line was 4048, which were subtracted from the total area of lutein and zeaxanthin (4831) to give a peak area of 782 for zeaxanthin.
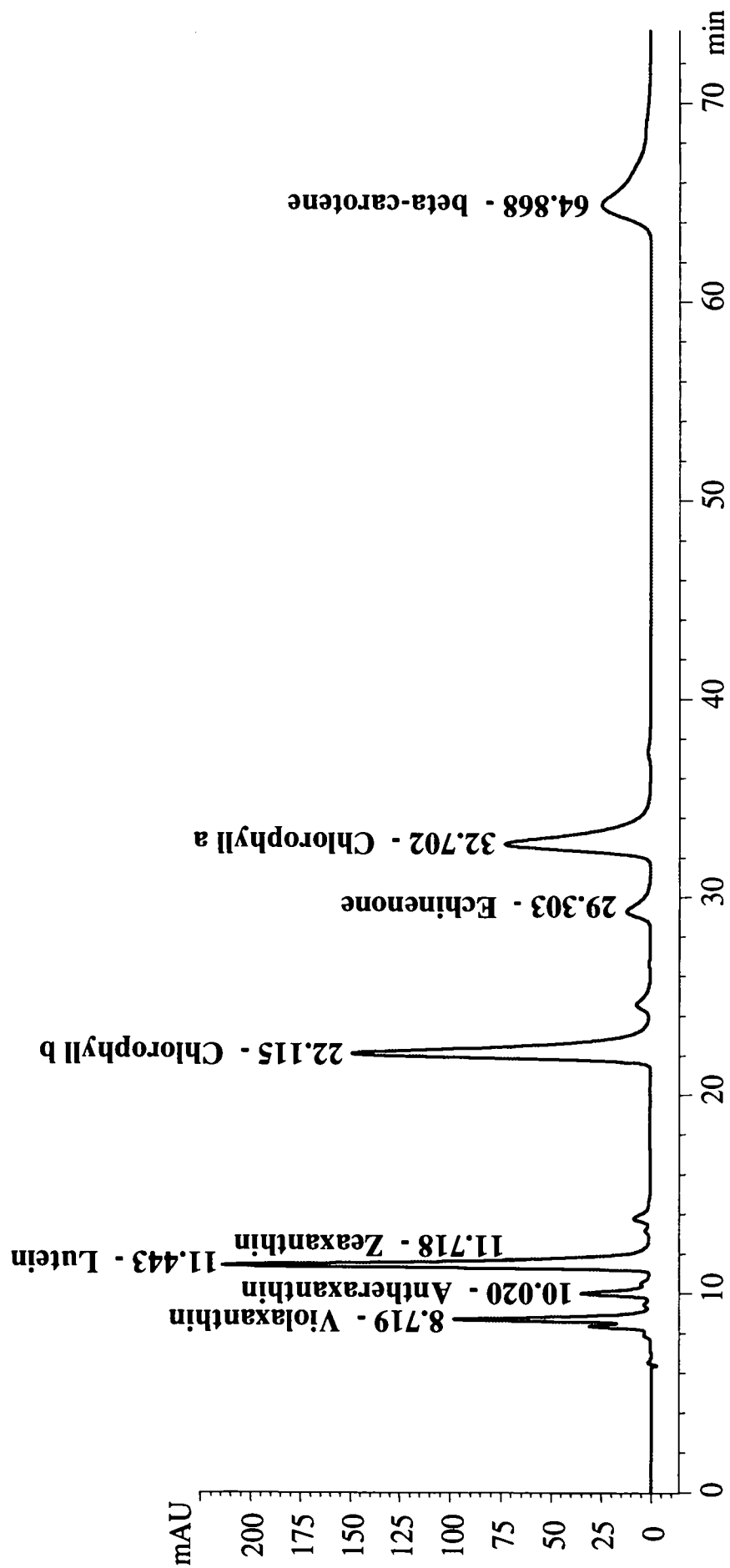
Fig. 3.10. HPLC-chromatogram of a lemon balm extract.

The peak area of β-cryptoxanthin for 1 μg/ml was calculated from the stock solution with a concentration of 0.94 μg/ml which was injected into the HPLC directly before the injection of the lemon balm extract. The peak area (771.1) from 0.94 μg/ml was calculated back to the area of 1 μg/ml using the regression line equation.

For determination of the recovery of the internal standard 100 μl (0.247 μg/μl) of the stock solution of echinenone were added to the sample powder together with the extraction medium. The concentration of echinenone in the diluted extraction should have been 1.24 μg/ml. From the peak area of echinenone (624) in the HPLC chromatogram, the final concentration of the standard was determined as 1.16 μg/ml. The recovery of echinenone for this extraction procedure was thus 93.5 %.

The concentration of the herb sample in the extract was 1.27 g/ml, since 1.27 g of the frozen lemon balm powder were weighed into the Erlenmeyer flask, and after evaporation, 1 ml of DCM was added as the extraction volume. Before injection into the HPLC the extract was diluted 20-fold to reach a carotenoid concentration within the linear range of the calibration curves.

The final concentrations of the carotenoids (Table 3.4.) are given in μg/100 g frozen material.

Table 3.4. Summary of the carotenoid results from a lemon balm extract.

standard	retention time (min.)	peak area	conc. of carotenoid A (μg/ml extract)	conc. of carotenoid A (μg/100g frozen material)
Violaxanthin	8.7	1581	56.09	4417
Antheraxanthin	10.0	620	21.85	1720
Lutein	11.4	4048	117.45	9248
Zeaxanthin	11.7	782	26.34	2074
chlorophyll b	22.1	5770	401.09	31582
β-cryptoxanthin	27.0	810	-	-
Echinenone	29.3	624	-	-
chlorophyll a	32.7	4394	1368.00	107717
β-carotene	64.9	3668	106.42	8380

These results are comparable with carotenoid data from dill, determined by Murkovic et al. (2000). They found that the sum of lutein and zeaxanthin was 13820 ± 3810 $\mu g/100g$ and β-carotene was 5450 ± 1190 $\mu g/100g$ dill. The ratio of chlorophyll a:b is normally around 3 (Steer, 2005); in the present investigation of lemon balm, the ratio was 3.4.

3.2. MUSHROOMS

The principal objective of this study was to investigate free radical processes that are initiated in mushrooms by cell disruption. This experiment aimed to simulate eating plant products in an uncooked state (see also Chapter 3.3. and Chapter 3.4.). Several spin traps were used to detect short-lived radicals which were produced during maceration of *Agaricus* mushroom. Four of the spin traps chosen are related to dimethyl-1-pyrroline *N*-oxide (DMPO), which has been used extensively with biological systems (see e.g. Buettner, 1987). The traps used were designed with substituents of various polarity to probe selectively either the aqueous or lipid phase of the samples.

Material

Cultivated mushrooms (*Agaricus bisporus*) were purchased from a local supermarket and stored in a refrigerator at 4°C until they were studied (1-2 days from purchase). 4-POBN was purchased from the Sigma Chemical Company and stored in the solid form in a cold room (at *c*. -15°C) for approximately 2 years prior to use. EPR spectra of solutions of this 4-POBN sample did not show the presence of any signal that could have resulted from reactions of the spin trap during storage. Other spin traps, namely 5-(diethoxyphosphoryl)-5-methyl-1-pyrroline-*N*-oxide (DEPMPO), 5-(di-n-butoxyphosphoryl)-5-methyl-1-pyrroline N-oxide (DBPMPO), 5-(bis-(2-ethylhexyloxy)phosphoryl)-5-methyl-1-pyrroline N-oxide (DEHPMPO), 5-(di-n-propoxyphosphoryl)-5-methyl-1-pyrroline N-oxide (DPPMPO), 5-propoxy-carbonyl-5-ethylpyrroline-1-oxide (PEPO) and 1,3,3-trimethyl-6-azabicyclo[3.2.1]oct-6-ene-*N*-oxide (TRAZON) were synthesised at the Institute of Applied Botany in Vienna according to previously published methods (Sankuratri, 1996; Stolze et al., 2000 and 2003). Solutions of these spin traps were made up in distilled water.

Experimental setup

The experiment was carried out by first peeling the mushroom, then cutting a thin slice (c. 2 mm) from the middle part of the mushroom and placed in a mortar. This was then crushed gently together with the spin trap solution (279 mM DEPMPO, 288 mM

DBPMPO, 2-3 M DEHPMPO, 360 mM DPPMPO, 960 mM PEPO, and 2-3 M TRAZON). The mixture was centrifuged for 3 min. (13000 rpm, 4 °C) and 500 µl of the supernatant were transferred into cryotubes and immediately frozen to 77 K. DEPMPO was used for an additional experiment in which the mixture was allowed to stand 30 min. at room temperature before cooling down to liquid nitrogen. Before the EPR-measurement the frozen liquid was thawed in a warm water bath (c. 40 °C) and immediately transferred into the flat cell. For the experiment with 4-POBN, a small quantity of the spin trap (c. 1 mg) was taken and mixed in a mortar together with 500 µl distilled water and a thin slice of the mushroom. After gentle grinding, the mixture was filtered through a disposable syringe filter holder (Fa. Sartorius, 0.45 µm) and transferred into the flat cell. The same procedure was carried out in a glove bag under argon to investigate the influence of oxygen on the reaction. The recorded spectra are single scans in 1024 points taking about 84 s. A microwave power of 20 mW, modulation frequency of 100 kHz, modulation amplitude of 0.0681 mT and a sweep width of 12 or 14 mT were used.

EPR-spectra

Typical EPR-spectra of mushrooms with different spin traps are given in the Figures 3.11. – 3.19., and the hyperfine splitting parameters derived from them are summarised in Table 3.5. The sextet of the 4-POBN adduct (Fig. 3.11.a) results from interaction of the unpaired electron of the trapped radical with the ^1H (I=1/2) on the α-carbon of the spin trap leading to a doublet which is further split into triplets by coupling with ^{14}N (I=1) of the nitroxide group. Recording the spectrum with high instrumental gain (Fig. 3.11.c) resolved weak satellite peaks from three different ^{13}C (I=1/2, natural abundance 1.108%) splittings. These come from the t-butyl group, the three methyl groups and the α-carbon atom (Goodman et al., 2002). Each peak of the sextet is separately split into a doublet by interaction with one ^{13}C atom. Two additional peaks correspond to half of the spectrum from molecules with the ^{15}N isotope (I=1/2, natural abundance 0.365%), the other peaks being obscured by the main spectrum.
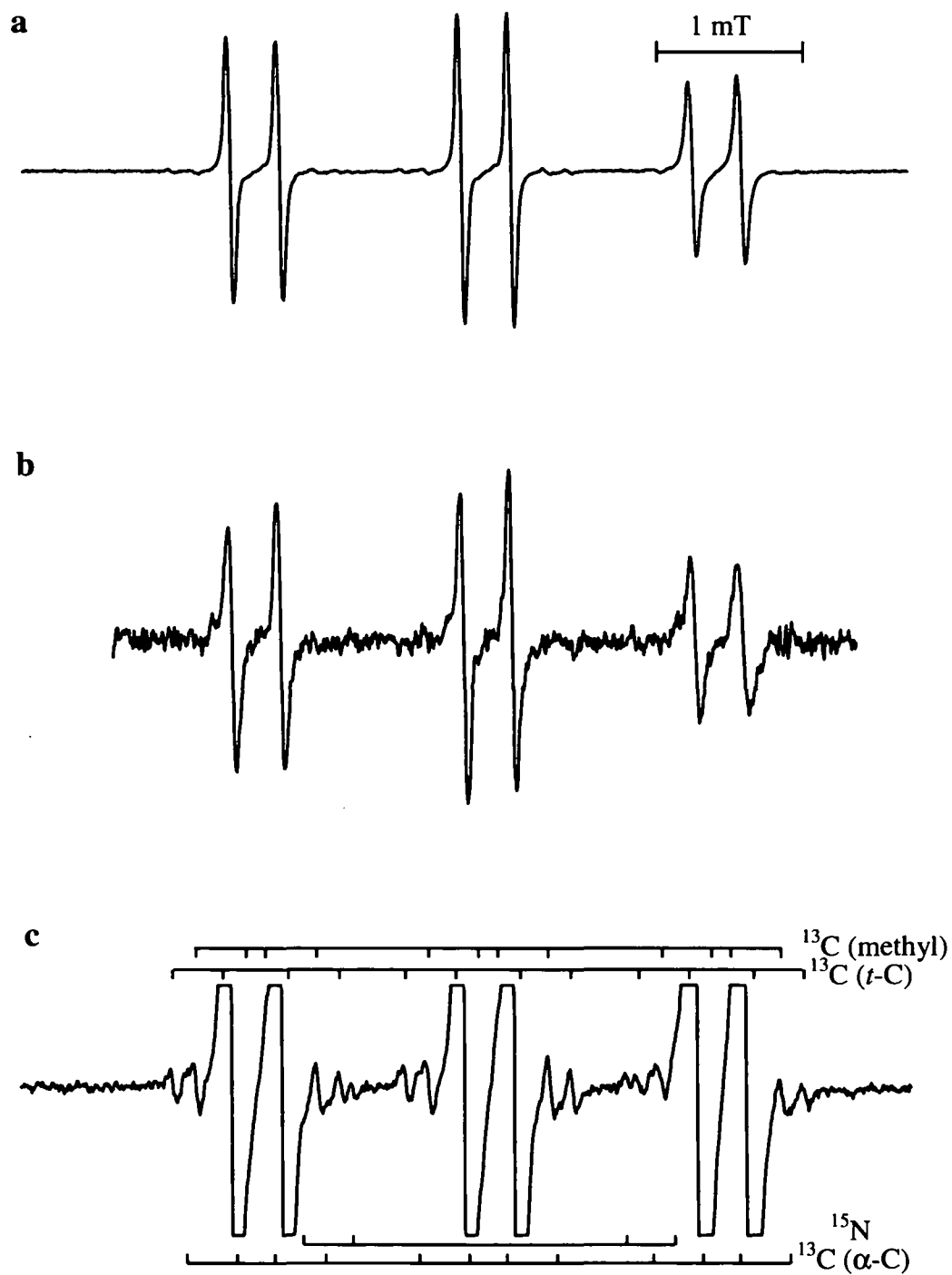
Fig. 3.11. EPR spectrum of (a) the C-centred radical from mushroom trapped by 4-POBN, (b) 4-(hydroxymethyl) phenyl radical adduct of 4-POBN, (c) spectrum from (a) measured with a high instrumental gain. Spectral interpretation is shown by the "stick" diagram.

75

$a(^{31}P)=4.45$ mT

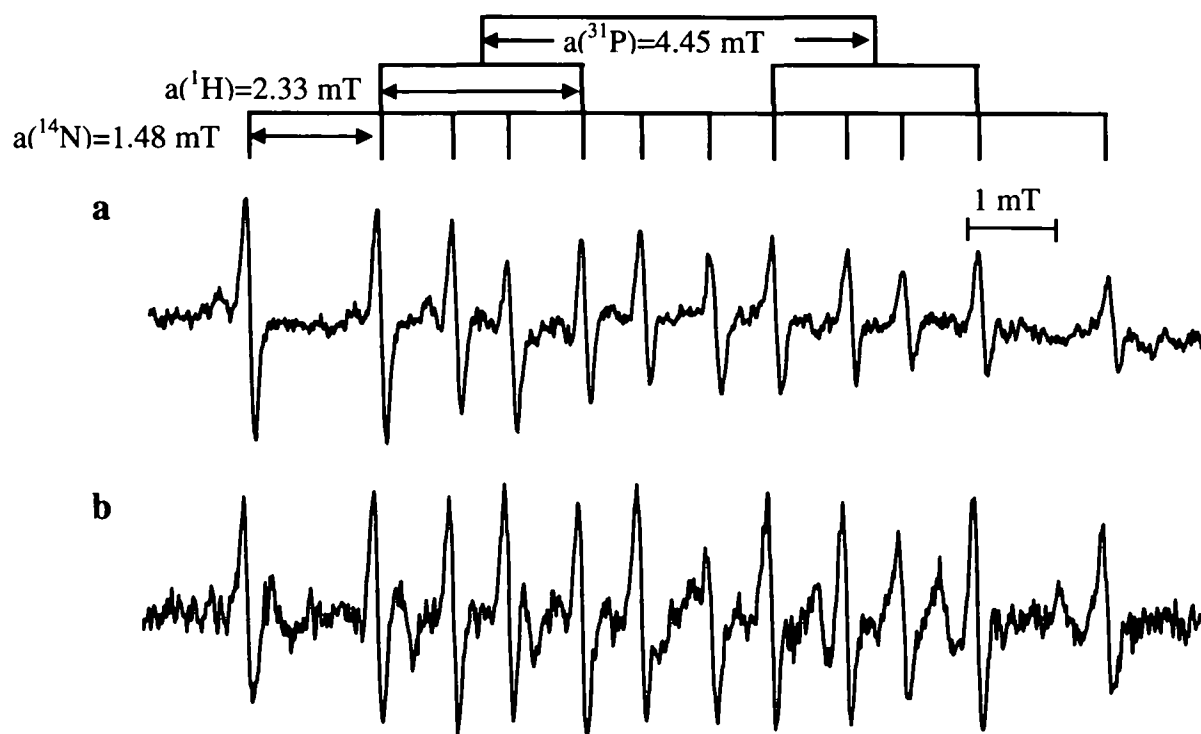$a(^1H)=2.33$ mT

$a(^{14}N)=1.48$ mT

1 mT

a

b

Fig. 3.12. EPR spectrum of (a) the C-centred radical from mushroom trapped by DEPMPO, (b) 4-(hydroxymethyl) phenyl radical adduct of DEPMPO. Spectral interpretation is shown by the "stick" diagram.

$a(^{31}P)=4.724$ mT

$a(^1H)=1.3$ mT

$a(^{14}N)=1.4$ mT

1 mT

a

b

Fig. 3.13. EPR spectrum of (a) the ·OH radical from mushroom after oxidation with Fe(CN)₆ trapped by DEPMPO, (b) simulation of the spectrum (a). Spectral interpretation is shown by the "stick" diagram.

$a(^{31}P)=4.512$ mT

$a(^1H)=2.324$ mT

$a(^{14}N)=1.478$ mT

1 mT

a

b

Fig. 3.14. EPR spectrum of (a) the C-centred radical from mushroom trapped by DBPMPO, (b) simulation of spectrum (a). Spectral interpretation is shown by the "stick" diagram.

$a(^1H)=2.3$ mT

$a(^{14}N)=1.5$ mT

$a(^1H)=0.15$ mT

1 mT

a

b

Fig. 3.15 EPR spectrum of (a) the C-centred radical from mushroom trapped by PEPO, (b) 4-(hydroxymethyl) phenyl radical adduct of PEPO. Spectral interpretation is shown by the "stick" diagram.
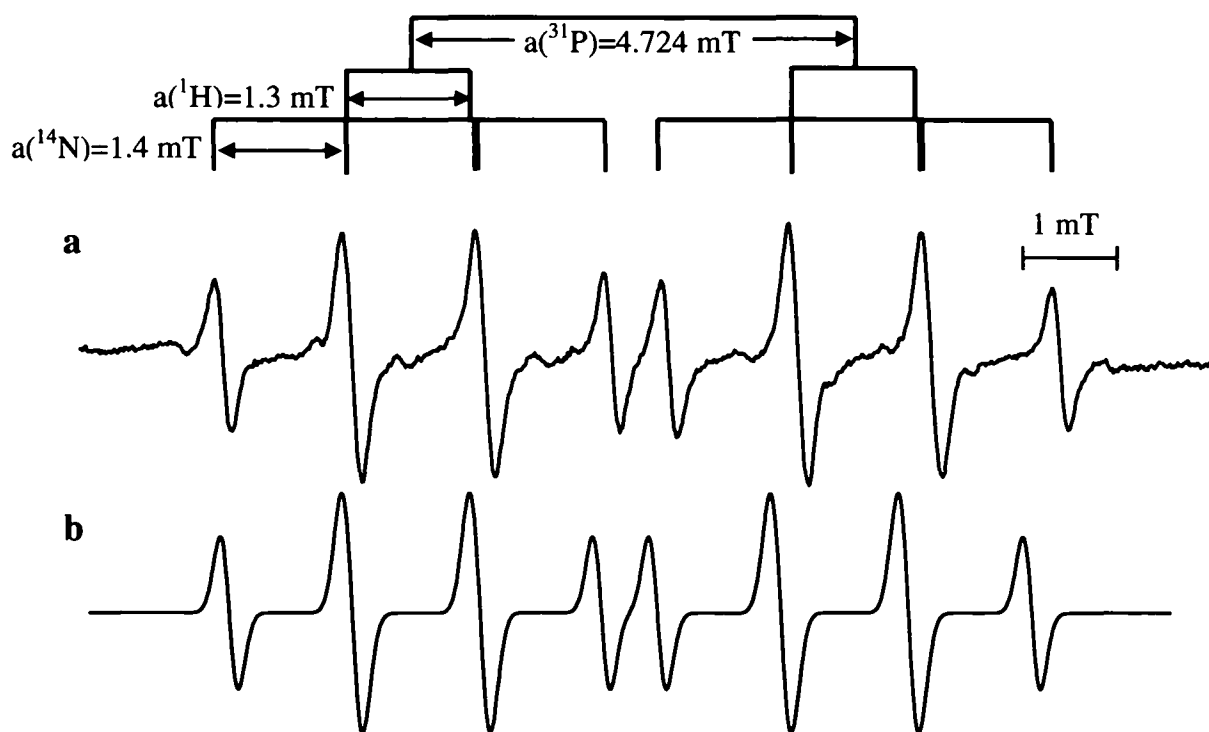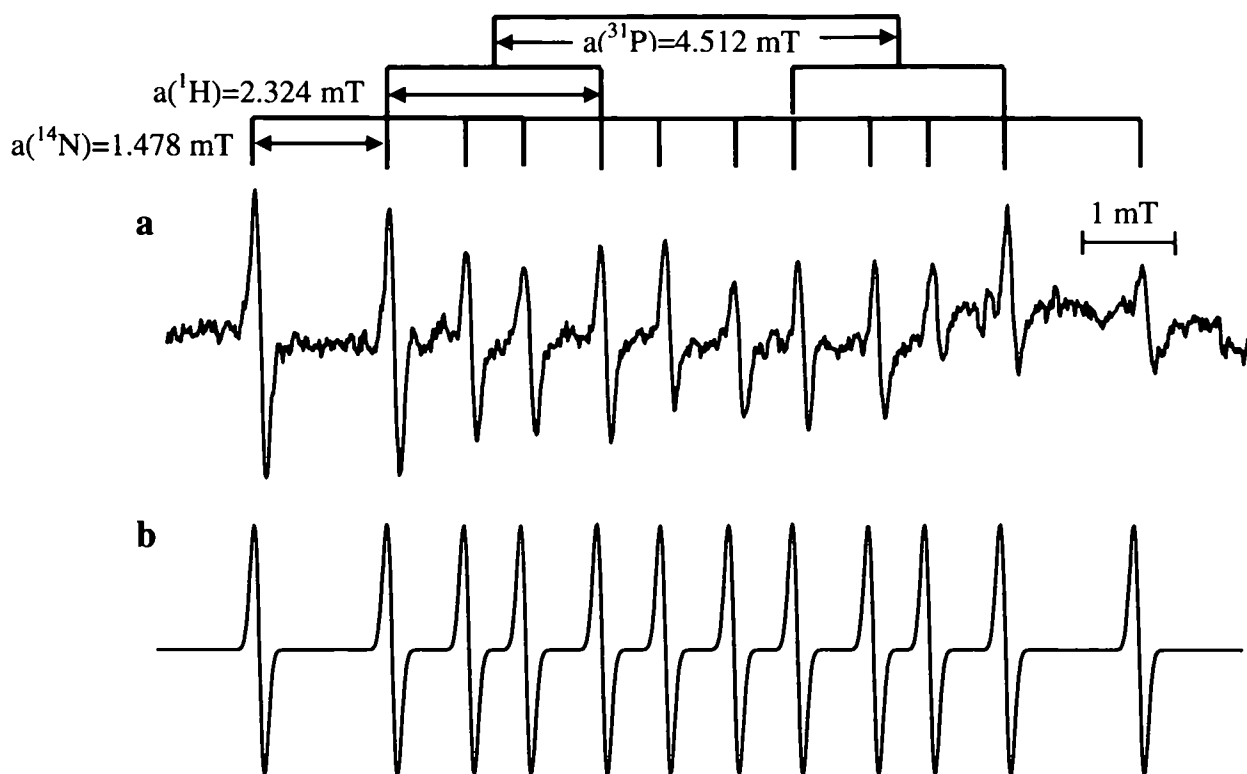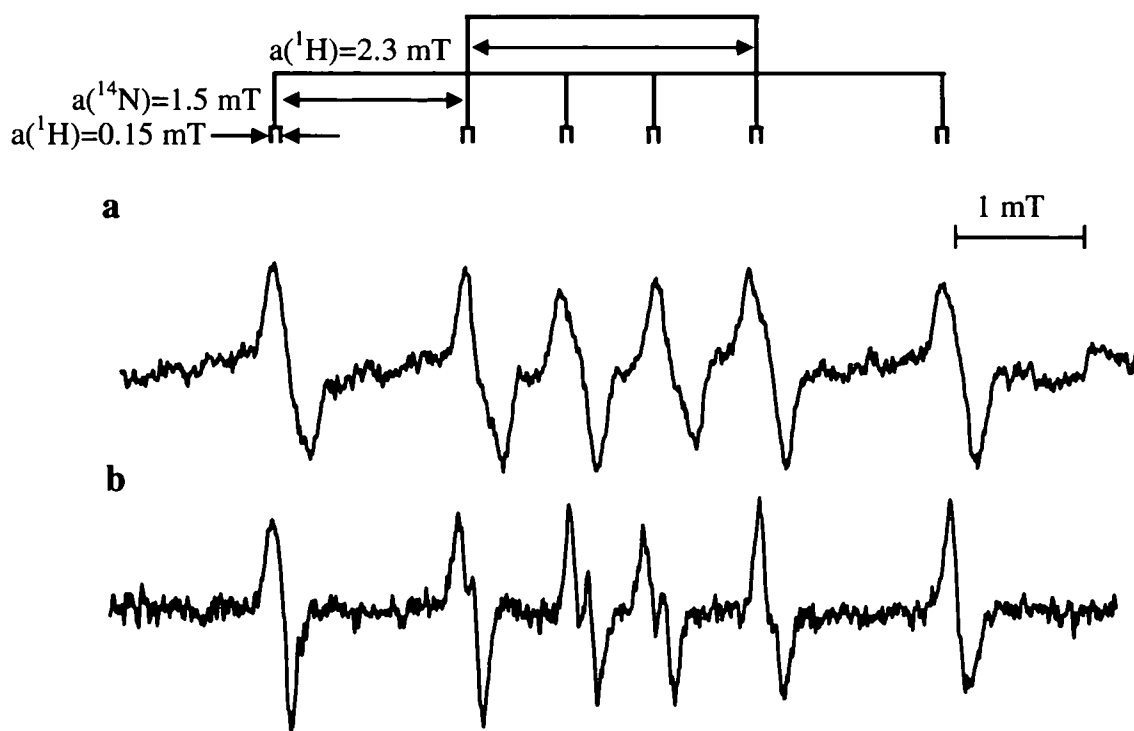
Fig. 3.16. EPR spectrum of (a) the 1st C-centred radical from mushroom trapped by DPPMPO, (b) simulation of spectrum (a). Spectral interpretation is shown by the "stick" diagram.

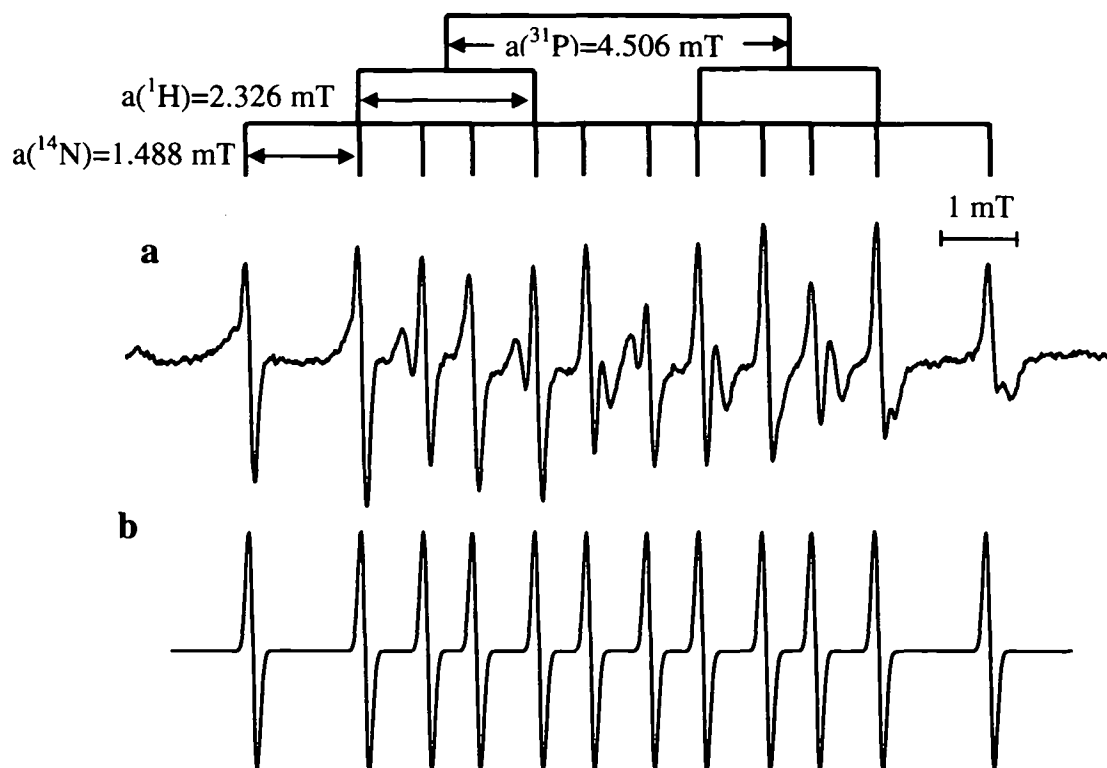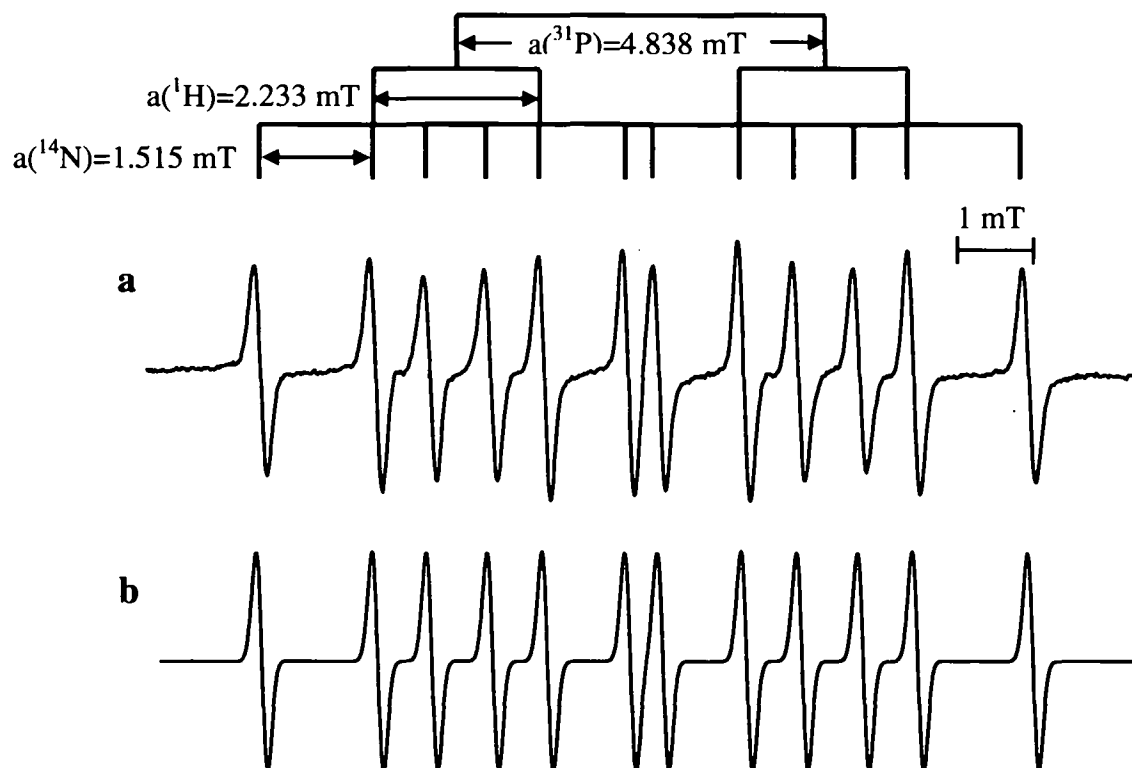Fig. 3.17. EPR spectrum of (a) the 2nd C-centred radical from mushroom trapped by DPPMPO, (b) simulation of spectrum (a). Spectral interpretation is shown by the "stick" diagram.
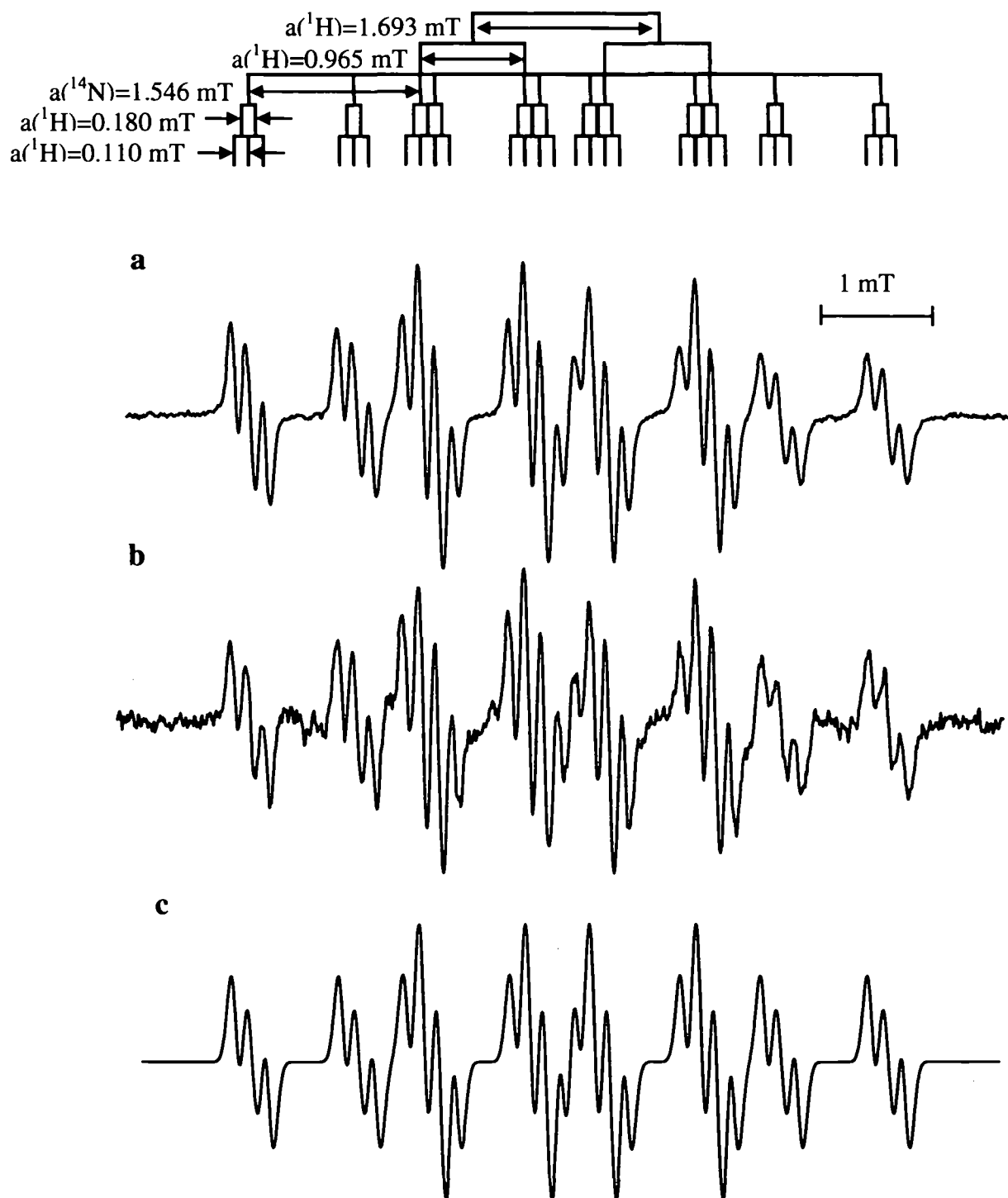
Fig. 3.18. EPR spectrum of (a) the C-centred radical from mushroom trapped by TRAZON, (b) 4-(hydroxymethyl) phenyl radical adduct of TRAZON, (c) simulation of (a). Spectral interpretation is shown by the "stick" diagram.
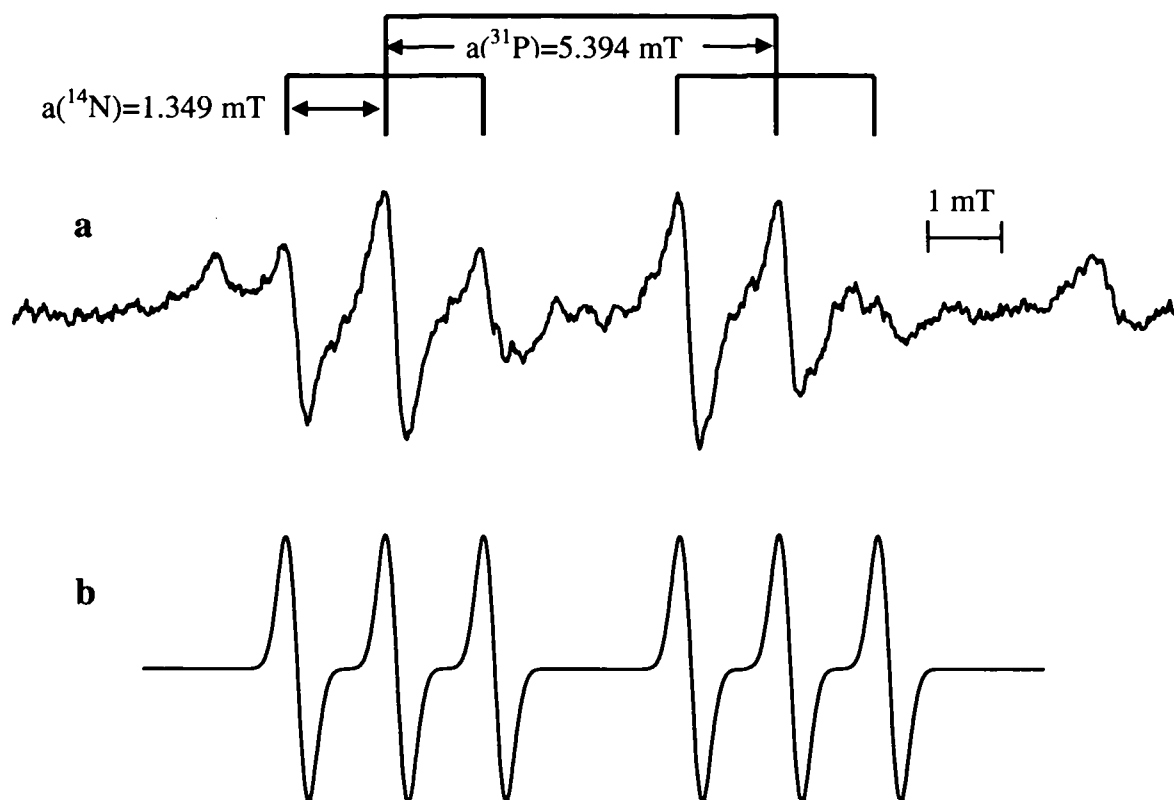
Fig. 3.19. EPR spectrum of (a) the C-centred radical from mushroom trapped by DEHPMPO, (b) best fit for spectrum (a) obtained by simulation. Spectral interpretation is shown by the "stick" diagram.

Spectra recorded with 4-POBN after preparation under inert atmosphere were identical to the samples prepared under ambient atmosphere but with intensity reduced to c. 2%. This could be explained by the presence of small amounts of oxygen which were not removed from the glove bag or which were trapped in the mushroom cells. An identical spectrum was obtained on reaction of 4-POBN with the 4-(hydroxymethyl) phenyl radical (Fig. 3.11.b).

With DEPMPO, hyperfine splittings arise from interaction of the unpaired electron with ^{31}P (I=1/2), ^{1}H(I=1/2) and ^{14}N(I=1) nuclei (Fig. 3.12.a), leading to 12 peaks in the spectrum. The $a(^{31}P)$ value in this spectrum is appreciably smaller than that reported for carbon centred adducts (Fréjaville et al., 1995), but identical to that of the 4-(hydroxymethyl) phenyl radical adduct (Fig. 3.12.b). The adduct was not stable and the EPR signal decayed within a few minutes. Identical results were observed from the samples that were allowed to stand at RT for half an hour before being frozen in liquid

nitrogen. Assuming that oxygen is involved in the formation of the radical, a steady state concentration at RT between production and decaying of the radical could be an explanation for this result, the decay of the EPR-signal in the spectrometer resulting from consumption of oxygen in the flat cell. Addition of potassium ferricyanide after the signal decayed led to a regeneration of the signal. After this signal decayed, however, the spin trap adduct of the ·OH-radical was formed (Fig. 3.13.). The ·OH radical adduct is characterised by 8 peaks because the ^{1}H, and ^{14}N splittings are similar.

The result obtained with DBPMPO (Fig. 3.14.) is similar to that from DEPMPO, the adduct had limited stability and the a(^{31}P) value was appreciably smaller than that reported for aliphatic carbon centred adducts (Stolze et al., 2000).

The spectrum with PEPO showed 6 peaks (Fig. 3.15.a), but on the basis of the spectrum of the 4-(hydroxymethyl) phenyl radical adduct (Fig. 3.15.b), there is probably an unresolved splitting from a 2nd proton.

DPPMPO produced spectra that consisted of a mixture of components (Fig. 3.16.). Since their relative intensities changed over time deconvolution of the spectra was possible. The first (unstable) product (Fig. 3.16.) consisted of 12 peaks and had parameters similar to the adduct with DEPMPO; thus it probably corresponds to the 4-(hydroxymethyl) phenyl radical. The 2nd component (Fig. 3.17.), which was more stable, also had 12 peaks. Its parameters were virtually identical to those reported for aliphatic carbon-centred radicals (Stolze et al., 2000). Therefore two different types of carbon-centred radical could be detected with this spin trap.

Spectra from Trazon adducts are more complex (Fig. 3.18.). Two inequivalent molecules can be formed by radical addition to the α-C, and each of these can show hyperfine structure from up to 5 inequivalent protons in addition to the ^{14}N nucleus. The present spectrum of 28 peaks from mushroom is due to interaction of the unpaired electron with the ^{14}N and four ^{1}H nuclei.

DEHPMPO and mushroom generated spectra of completely different shape from those observed in all of the other spin trap experiment (Fig. 3.19.). The variation in linewidths is typical of that seen in samples with restricted motion. Stolze et al. (2000) reported

that the spectrum of alkoxyl adducts of DEHPMPO are also broad. Furthermore, the ^{1}H splitting appears to be missing from the spectrum. Hence the spectrum consists just of a ^{31}P and a ^{14}N splitting. There are additional peaks that do not obviously fit with the others.

Table. 3.5. Summary of hyperfine splitting parameters observed with different spin traps.

spin trap	system	a(^{31}P)[1] (mT)	a(^{1}H)[1] (mT)	a(^{14}N)[1] (mT)	ΔBpp[2] (mT)	g-value[1]
DEPMPO	mushroom	4.50	2.33	1.48		2.0057
	4-(hydroxymethyl) phenyl radical	4.50	2.33	1.48	0.1	2.0056
4-POBN	mushroom		0.33	1.56		2.0058
	4-(hydroxymethyl) phenyl radical		0.32	1.56	0.05	2.0057
	POBN· radical		0.145, 0.05	1.49, 0.18		
	coriander, elder, chives		0.26	1.57		
PEPO	mushroom		2.30	1.50		2.0057
	4-(hydroxymethyl) phenyl radical		2.30, 0.129	1.52	0.15	2.0056
TRAZON	mushroom		1.69, 0.97, 0.18, 0.11	1.55		2.0056
	4-(hydroxymethyl) phenyl radical		1.70, 0.97, 0.18, 0.11	1.55	0.1	2.0055
DEHPMPO	Mushroom	5.39		1.35		
	4-(hydroxymethyl) phenyl radical	5.48		1.39		

[1]Hyperfine splittings were confirmed by simulation and are accurate to $c.$ 0.01 mT. Errors associated with the g-values are $c.$ ± 0.0003 (estimated by variability in the centre field correction from repeated measurements with DPPH).

[2]ΔBpp is the field separations of the peaks and troughs of the 1st derivative spectra (from simulations using Gaussian shape).

Synthesis of the 4-(hydroxymethyl)phenyl radical

4-(hydroxymethyl)benzene diazonium salts are found in appreciable amounts in mushroom and the 4-(hydroxymethyl)phenyl radical can be produced from it. Its structure is given in Fig. 3.20.
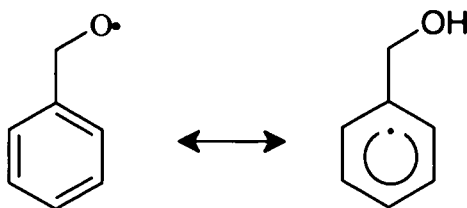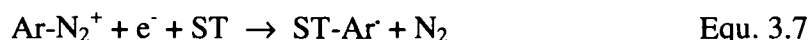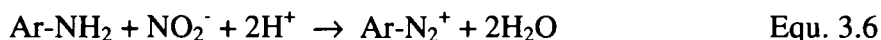
Fig. 3.20. Structure of 4-(hydroxymethyl)phenyl radical.

The synthesis of the radical was carried out by the following reactions (Equ. 3.6. and 3.7.):

$$Ar-NH_2 + NO_2^- + 2H^+ \rightarrow Ar-N_2^+ + 2H_2O \qquad \text{Equ. 3.6}$$

$$Ar-N_2^+ + e^- + ST \rightarrow ST-Ar^{\cdot} + N_2 \qquad \text{Equ. 3.7}$$

1 mol of the primary amine was dissolved in 2.5 mol hydrochloric acid, placed in an ice-salt-mixture, and an equivalent amount of a 2.5 mol/l sodium nitrite solution was then added slowly under agitation. 50 μl of this diazo-solution were transferred to an Eppendorf tube along with 50 μl of spin trap (ST) solution (0.1 mol/l for 4-POBN, c. 15 mmol/l for DEPMPO, PEPO, and TRAZON, 2 mol/l for DEHPMPO). After 30 sec, 400 μl phosphate buffer was added and the mixture was transferred to a flat cell for measurement of its EPR spectrum. Since spectra with mushroom and the spin traps DBPMPO and DPPMPO gave similar parameters to the one from DEPMPO, these spin traps were not investigated further with the synthesised radical.

Additional experiments were carried out under inert atmosphere in a glove bag filled with argon to examine the influence of oxygen. Two approaches were tried, both using degassed solutions of the amine, $NaNO_2$, spin trap, buffer and water, and differing only in the way the spin trap solution was mixed with the diazonium salt. In the 1st method the preparation procedure was identical to that for the preparation in air, except that all operations were carried out in a glove bag filled with argon. In the 2nd method the solutions were made up in a test tube bubbled with nitrogen gas, and the final solution was pumped directly into a flow cell located in the EPR spectrometer. This latter method decreased appreciably the time delay between mixing the spin trap and radical solutions and recording the EPR spectrum.

Identity of the radical formed in mushroom

In their original work, Hiramoto et al. (1995) reported EPR spectral parameters for DMPO, PBN and 3,5-dibromo-4-nitrosobenzene sulfonate (DBNBS) adducts of the 4-(hydroxymethyl)phenyl radical. This radical is readily formed from the 4-hydroxymethyl benzene diazonium salt, which in turn is formed by enzymatic hydrolysis of agaritine, a major component of *Agaricus bisporus*, (Levenberg, 1962; Ross et al., 1982). Previous experiments (Goodman et al., 2002) showed that the EPR spectral parameters for PBN and 4-POBN adducts from mushrooms were similar to those from the synthetic radical. These current measurements using the spin traps 4-POBN, DEPMPO, DEHPMPO, PEPO and TRAZON support this conclusion.

In the spectrum of the DEPMPO adduct of the synthetic 4-(hydroxymethyl)phenyl radical, the hydroxyl-radical adduct of DEPMPO, with the parameters $a(^{31}P)=4.72$ mT, $a(^{1}H)\sim a(^{14}N)=1.38$ mT, was visible at the beginning of the experiment, but its intensity decreased rapidly. The generation of this radical was not observed after preparation under inert atmosphere. In contrast, the carbon-centred radical adduct was stable for at least 20 minutes. Reaction of the spin traps with the synthesised radical under inert atmospheres (nitrogen or argon) gave the same results as those seen in air.

Discussion

There is some evidence that mushrooms have medicinal effects such as antitumor, antiviral, anticholesterol, and antithrombotic properties (Breene, 1990). Phenolic compounds may contribute to these observations since such molecules in certain mushroom varieties were correlated with the antioxidative activity of methanol/water extracts of these mushroom samples (Cheung et al., 2003).

The EPR results from the measurements with *Agaricus* mushrooms indicate the trapping of a carbon-centred radical, which is most likely the 4-(hydroxymethyl)phenyl radical. Our results show conclusively that the 4-POBN radical adduct requires O_2 for its formation, and that the adduct with DEPMPO is unstable in the absence of O_2. The stability of the 4-(hydroxymethyl)phenyl radical adducts with DEPMPO indicates that

the instability of the signal in mushroom extracts is not the result of an inherent instability of the radical adduct, and may, therefore, be the result of reaction with radical scavengers in the mushroom. Such behaviour has been observed with coffee (instant), which has the ability to rapidly scavenge radical adducts of DEPMPO, but forms stable adducts with 4-POBN (Pascual et al., 2002). The apparent stability of the mushroom adduct with DEPMPO when the sample was allowed to stand in air before it was frozen to 77 K is then in reality a steady state situation, in which the rates of adduct formation and decomposition are balanced due to enough surrounding oxygen.

For the 4-(hydroxymethyl)phenyl radical adducts of 4-POBN the present experiments measured values for the ^{13}C hyperfine coupling constants from the tertiary- and methyl-carbons of the t-butyl group, as well as from the α-carbon adjacent to the nitroxide group. Such values are potentially informative for the characterisation of adducts formed with unknown radicals, but at present there is no library to show the level of variability of ^{13}C coupling constants for 4-POBN adducts of different types of known radicals. This investigation has also derived spectral parameters for adducts of 4-(hydroxymethyl)phenyl radicals with the spin traps DEPMPO, DEHPMPO, PEPO and TRAZON, whose adducts with such radicals had not previously been reported.

3.3. HERBS

This investigation focussed on the detection of unstable radical species in several herbs using the spin trap 4-POBN. It was performed with the objective of simulating the mastication process in order to address the question as to whether a free radical burst occurs when biologically viable tissue is eaten.

Materials and Sample preparation

Fresh samples were either harvested from the herb garden of my mother, immediately frozen to 77 K, and maintained at that temperature until they were studied, or purchased from a local vegetable market on the day of study. These latter samples were kept at room temperature. In addition, commercial samples of freeze-dried herbs (marketed by the Kotanyi Company, Wolkersdorf, Austria) were purchased pre-packaged from local suppliers. Full details of the specimens studied are presented in Table 3.6.

One or two leaves (dependent on size) were crushed gently with a small quantity of 4-POBN (*c.* 1 mg) and distilled water (500 μl), filtered through a disposable syringe filter holder (Fa. Sartorius, 0.45 μm), and the solution transferred to a flat cell for recording the EPR spectrum. Measurements with a sample of thyme in which the spin trap was added separately to fresh and frozen leaves showed that there were no qualitative differences between the results from the two preparation procedures.

Another experiment was carried out with sage which was bought in a small pot at a local market. Leaves were harvested at various times of the day to investigate the influence of sunlight intensity. Based on this investigation sage, which was grown in a herb plot at the ARC Seibersdorf (Picture 3.1.) under controlled, stress free conditions, was harvested 7 times over a 24 hour period. The leaves were cut directly into aluminium bags, immediately frozen in liquid nitrogen and stored at 77 K until they were measured by EPR as described above.

Table 3.6. Full details of herb samples investigated.

Common name	Latin name	Physical form investigated		
		fresh	frozen	freeze-dried
Basil	*Ocimum basilicum*	x		
Bay	*Laurus nobilis*		x	
Celery	*Apium graveolens*		x	
Chives	*Allium schoenoprasum*	x	x	x
Coriander	*Coriandrum sativum*	x		
Dead nettle (red)	*Lamium maculatum*		x	
Dead nettle (white)	*Lamium album*		x	
Elder	*Sambucus nigra*		x	
Ivy	*Hedera helix*		x	
Lavender	*Lavendula angustifolia*		x	
Lemon balm	*Melissa officinalis*		x	
Lovage	*Levisticum officinalis*		x	x
Marjoram	*Origanum majorana*		x	x
Mint	*Mentha piperita*	x	x	
Oregano	*Origanum vulgare*			x
Parsley	*Petroselinum sativum*	x	x	x
Parsley crimpy	*Petroselinum crispum*	x	x	
Rosemary	*Rosmarinus officinalis*	x	x	x
Sage	*Salvia officinalis*	x	x	
Stinging-nettle	*Urtica dioica*		x	
Tarragon	*Artemisia dracunculus*		x	
Thyme	*Thymus vulgaris*	x	x	x

EPR spectral measurements and processing

All spectra were acquired with a microwave power of 20 mW and 100 kHz modulation frequency. A modulation amplitude of 0.1 mT was used for most spectra, but smaller values ($\geq$0.03 mT) were used with selected samples to check for the possible presence of small hyperfine splittings. Additionally, larger modulations ($\leq$0.16 mT) were used on occasions when the spectra were very weak.
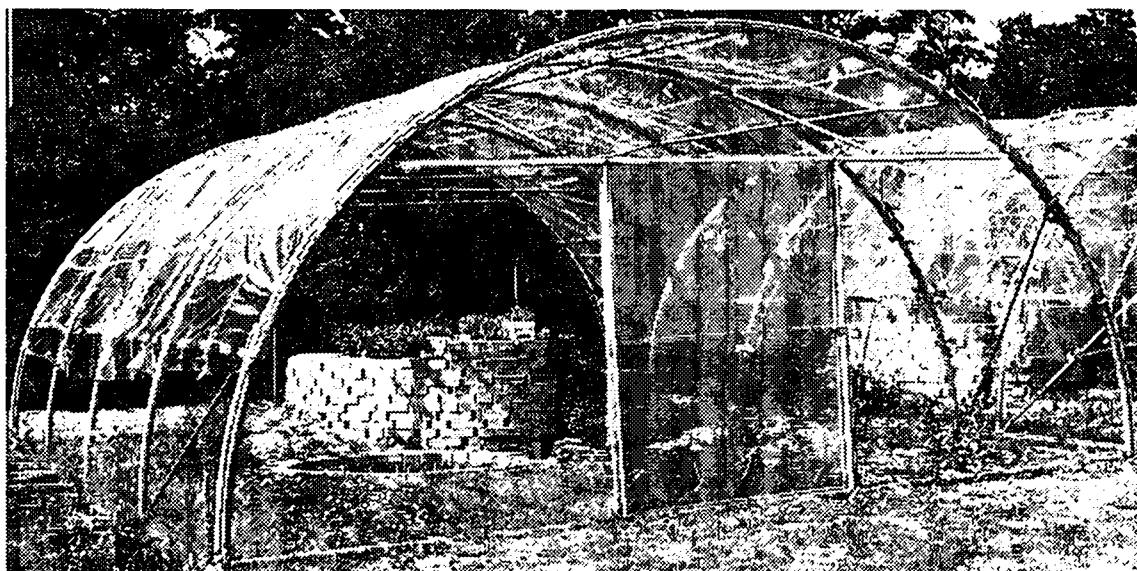
Picture 3.1. Herb plot at ARC Seibersdorf research GmbH.

Results and Discussion

In the absence of any spin trap the EPR spectra from the herb samples were dominated by a sextet signal from Mn (II). In the presence of 4-POBN three fundamentally different free radical EPR spectra, consisting of doublet, sextet or dodecet signals, were obtained from different herb samples. These signals are similar to those observed in a study of macerated vegetables (Goodman et al., 2002), where the doublet had $a(^1H)$ = 0.18 mT, the sextet had $a(^{14}N)$ = 1.59 mT, $a(^1H)$ = 0.32 mT and the dodecet could be fitted with three hyperfine splittings, $a(^{14}N)$ = 1.493 mT, $a(^{14}N)$ = 0.182 mT, $a(^1H)$ = 0.145 mT. These spectra are assigned respectively to the (monodehydro)ascorbate radical (Laroff et al., 1972), a carbon-centred radical adduct of 4-POBN (Buettner, 1987) and the 4-POBN adduct of the 4-POBN· radical (McCormick et al., 1995).

In the samples studied, the ascorbate radical was seen with parsley, bay, white dead nettle and lovage, although the spectrum from lovage also contained the sextet component (Fig. 3.21. and Fig. 3.22.). The ascorbate radical is produced by the (1-electron) oxidation of ascorbic acid (Equ. 3.8.).
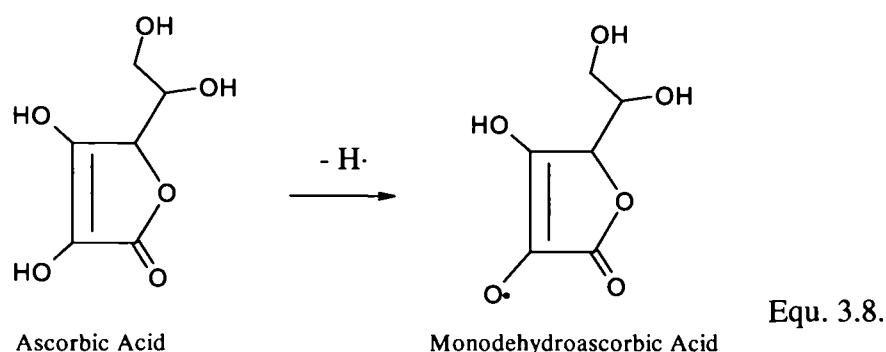
OH

HO

HO

OH

O

O

Ascorbic Acid

- H·

OH

HO

OH

O·

O

O

Monodehydroascorbic Acid

Equ. 3.8.

However, the same signal was observed when the sample preparation was carried out in an inert atmosphere, indicating that the oxidation agent was derived exclusively from the plant tissue. Different methods of sample preparation were investigated with parsley, but no qualitative differences in the spectra were observed between fresh, frozen, and freeze-dried samples. The similarity of these results is somewhat surprising since the drying of plant tissues generally leads to a major reduction in their ascorbic acid contents (Food Standards Agency, 2002), and we have shown previously (Pirker et al., 2002) that the freeze-drying process involves substantial free radical activity. It might have been expected, therefore, that the sextet signal would have been seen in the freeze-dried sample, since the formation of radical adducts of the spin trap becomes more important as ascorbic acid levels drop (Muckenschnabel et al., 2003). However, parsley is generally very rich in ascorbic acid (Food Standards Agency, 2002) and the present results suggest that appreciable quantities of this antioxidant remain in the freeze-dried sample.

In addition to lovage, the sextet signal was also observed with coriander leaves, elder fruits and freeze-dried chives. Fig. 3.23. shows a typical sextet signal obtained with the herb coriander where different linewidths as a result of incomplete averaging of the anisotropy are visible in the spectrum. The wide range of tissue types that exhibit this signal suggests that it results from a general reaction of physically damaged tissue. However, the same spectrum was observed when sample preparation was performed under an inert atmosphere, indicating that O_2 was not involved in the reactions leading to the formation of the radical adduct. Indeed, with red dead nettle leaves the sextet spectrum was observed when sample preparation was performed under argon, but the

dodecet spectrum (see below) was obtained when the sample was prepared in air. No signal was observed with fresh and frozen samples of chives, but this could be because it was below the detection limit.

The dodecet spectrum was observed with samples of basil, celery, red dead nettle, ivy, lavender, lemon balm, marjoram, mint, rosemary, sage, stinging nettle, tarragon and thyme (Fig. 3.24.a); it has been shown by McCormick et al. (1995) to correspond to the 4-POBN adduct of the 4-POBN· radical, which is formed by oxidation of the spin trap. The EPR spectrum, illustrated for stinging nettle (Fig. 3.24.a), can be interpreted in terms of two triplets from interaction of the unpaired electron with two nitrogen nuclei and one doublet from interaction with the hydrogen nucleus. However, at low modulation amplitude, additional hyperfine structure was observed (Fig. 3.24.b), analogous to that reported by Glidewell et al. (1994) for lettuce macerated in the presence of 4-POBN. This spectrum can be simulated (Fig. 3.24.c) by two triplets from ^{14}N and two doublets from ^{1}H. Similar spectra were also observed in previous experiments (Goodman et al., 2002) with samples of carrot hypocotyl rootstock and lettuce leaf, and with >50% of the herb samples studied in the present work. Its generation indicates that the ability to oxidize the spin trap is a property that is common to many plant tissues. This reaction was shown to require O_2, as mentioned in the previous paragraph for red dead nettle leaves, but the fact that the dodecet signal was not universally observed in all aerobically-prepared samples suggests that this is not a direct reaction. Thus it seems likely that specific plant components are oxidized when tissues are broken down in air and that product(s) of this reaction are sufficiently powerful oxidant(s) to oxidise the spin trap.

$a(^1H) = 0.18$ mT

0.1 mT
H
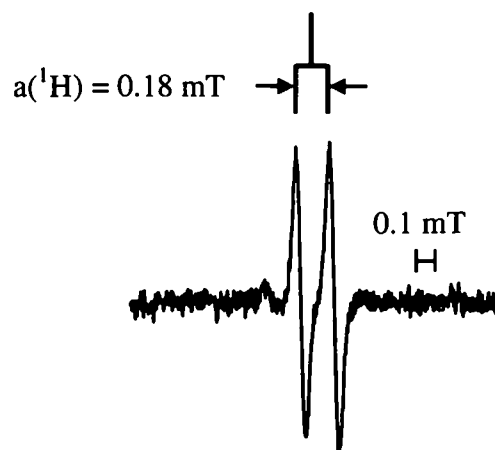
Fig. 3.21. Ascorbate radical detected in the herb parsley. Spectral interpretation is shown by the stick diagram.

$a(^{14}N) = 1.59$ mT

$a(^1H) = 0.32$ mT

1 mT
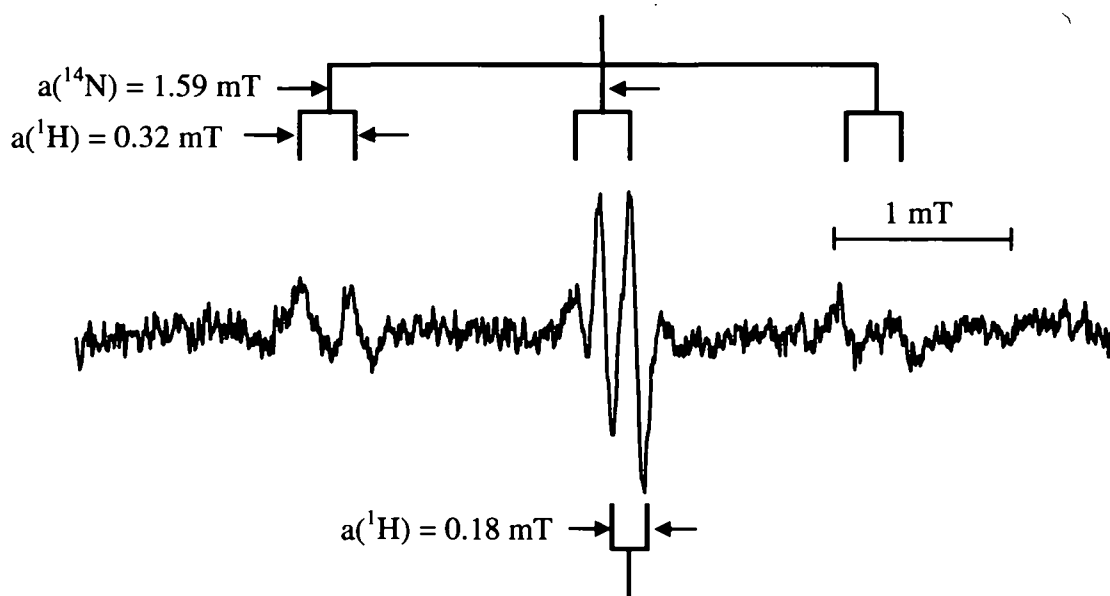
$a(^1H) = 0.18$ mT

Fig. 3.22. Ascorbate radical and a carbon-centred radical trapped by 4-POBN in the herb lovage. Spectral interpretation is shown by the stick diagram.

$a(^{14}N) = 1.56$ mT

$a(^{1}H) = 0.247$ mT

a

1 mT

b
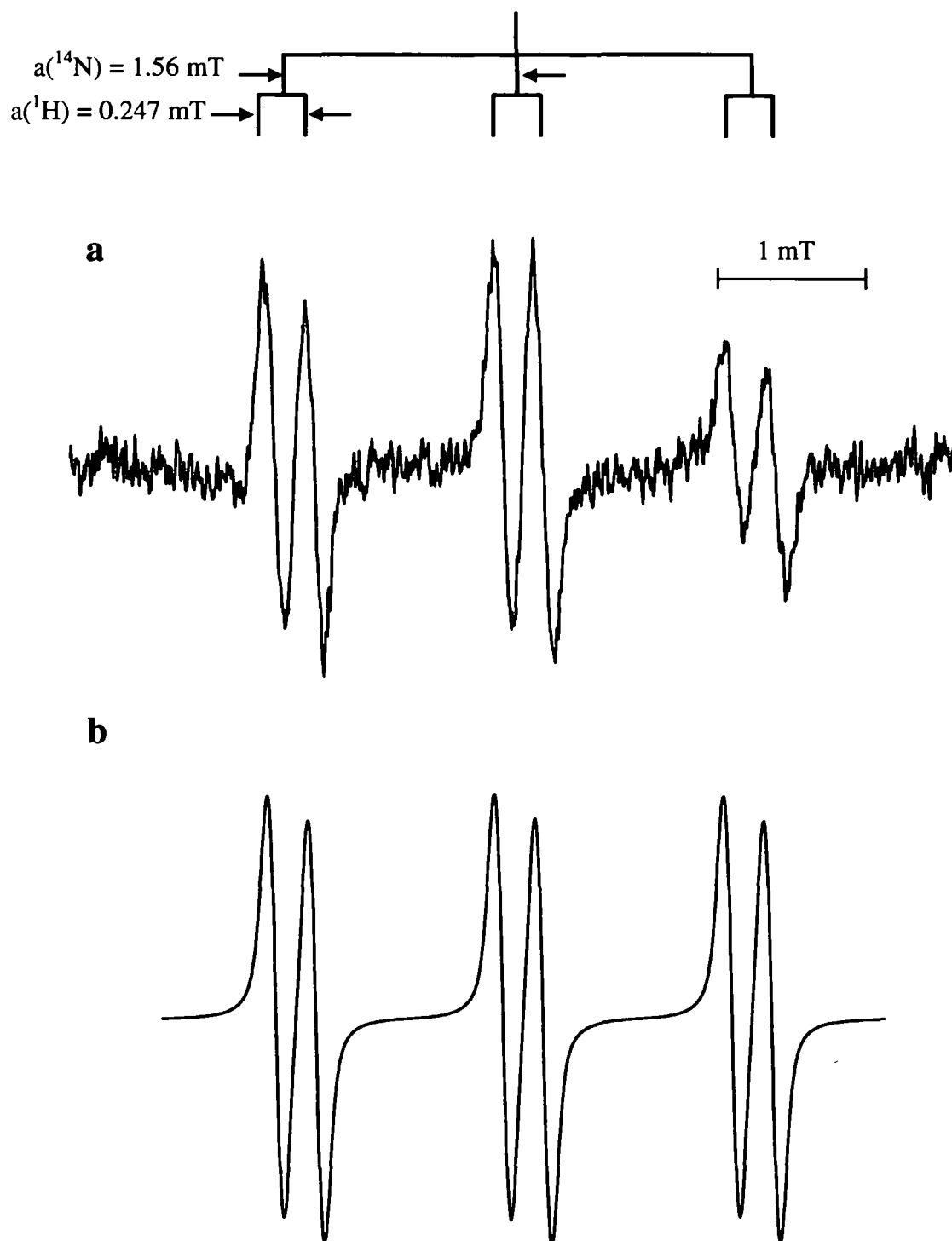
Fig. 3.23. (a) Carbon centred radical trapped by 4-POBN in the herb coriander, (b) simulation of (a). Spectral interpretation is shown by the stick diagram.

$a(^{14}N)=1.493$ mT

$a(^{14}N)=0.182$ mT ⟶

$a(^1H)= 0.145$ mT ⟶

1 mT

a

b

c

Fig. 3.24. EPR spectrum of 4-POBN· radical from stinging nettle trapped by 4-POBN, (a) experimental spectrum using 0.1 mT modulation amplitude, (b) experimental spectrum using 0.04 mT modulation amplitude, (c) simulation of (b). Spectral interpretation is shown by the stick diagram (which does not include the small ^1H splitting of 0.05 mT).

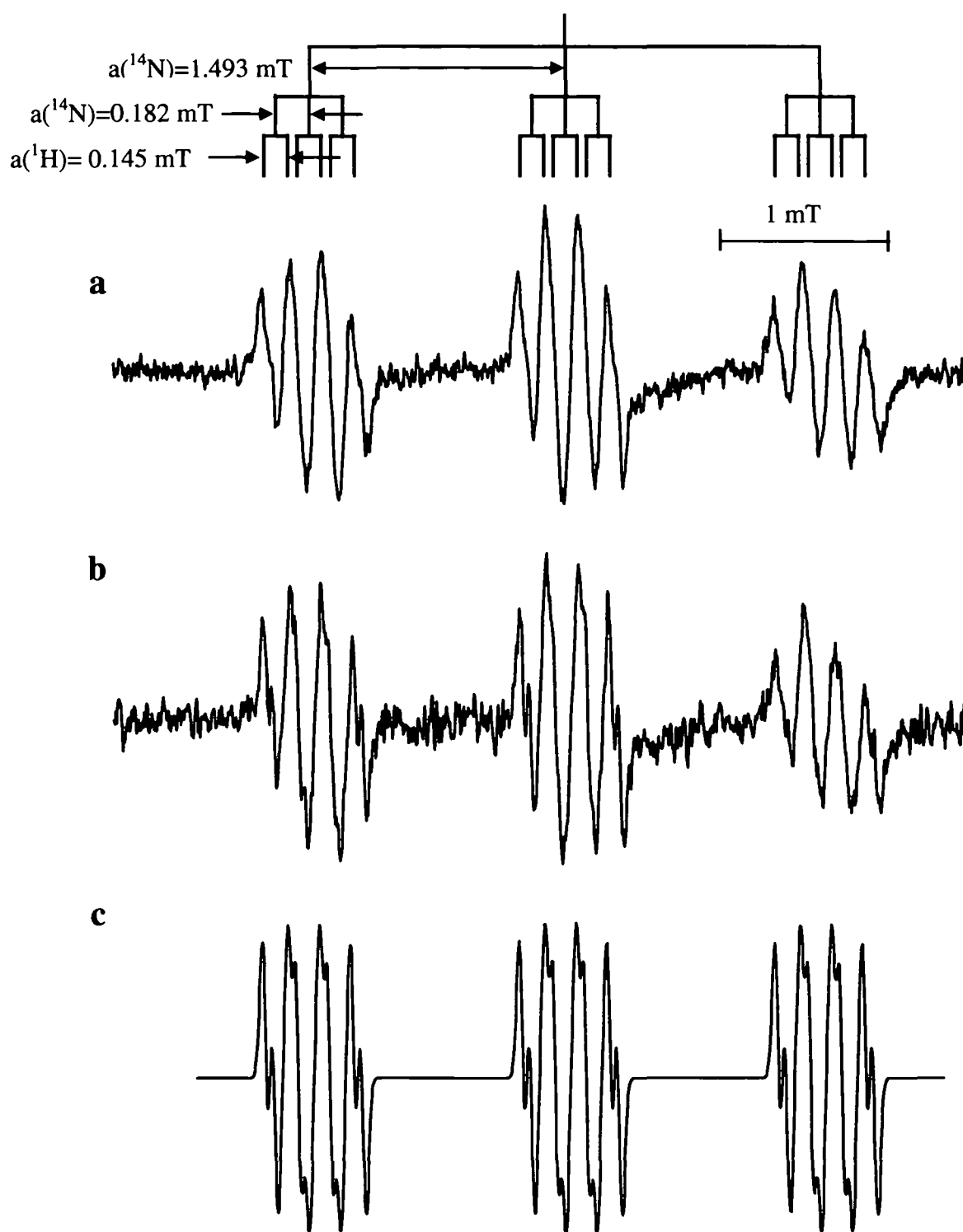We also observed in experiments with stinging nettle that the ability to generate the dodecet signal diminished with increased storage time, even at low temperature. Measurements made at the beginning of the experiment (about three days after the harvest), produced a strong dodecet signal, whereas a much weaker signal was obtained after the sample had been stored for three weeks in liquid nitrogen (but with a few minutes exposure to ambient temperature). It would appear, therefore, that a component of this oxidation pathway in stinging nettle has limited stability after the sample has been harvested, although the observation of the dodecet spectrum from the reaction of 4-POBN with freeze-dried samples of marjoram, thyme and rosemary indicates that this is not a general characteristic.

An additional experiment with sage and 4-POBN showed an influence of either the sunlight intensity or the time of day with two different EPR spectra, the sextet or the dodecet, being observed. Initial measurements seemed to support involvement of sunshine in the generation of the dodecet signal, since the sextet signal became visible after moving the plants into the shade. A problem with this conclusion is inconsistency in the plant behaviour. Another investigation was performed in which sage, that was grown outside in a herb garden, was harvested regularly over a 24-hour period. Unfortunately this experiment did not provide a definitive answer since ~50 % of the samples showed the sextet signal and the other 50 % of the samples were dominated by the dodecet signal. There was no general relationship between time or sunlight intensity and the nature of the EPR signal. Thus different leaves exhibited fundamentally different properties, even though they were carefully chosen replicates.

There was no influence of atmosphere on the formation of the sextet signal with the coriander samples in contrast to the observations with *Agaricus* mushrooms (see Chapter 3.2.). There are, therefore, fundamental differences in the processes for carbon-centred radical formation in these two types of food products, and the radical trapped from the plant tissues would appear to be formed directly as a result of physical damage to the tissue. It might be possible that the coriander samples contained sufficient quantities of O_2 for oxidation to occur in the inert atmosphere since they were photosynthetic tissue. However, in the experiments with red dead nettle the sextet signal was only observed in an inert atmosphere, thus indicating that O_2 is not required for its formation in these plant tissues.

EPR spectra from the herb thyme, which contains large quantities of the phenols thymol and carvacrol were very weak and inconsistent with the formation of a carbon-centred radical adduct of 4-POBN, even though both carvacrol and thymol readily generate radicals in simple chemical systems (Deighton et al., 1993 and 1994). Indeed, the reaction between 4-POBN and the plant tissue extract resulted in oxidation of the spin trap, again indicating that the chemical processes occurring on physical damage to the plant tissue are distinctly different from those of potentially-reactive components.

Oxidation of the spin trap occurred on reaction of 4-POBN with >50 % of the various types of herb samples studied in the present work (Table 3.6.), whereas the expected radical adduct spectra were only seen with three plant species (coriander, elder and chives). It appears that physical damage to the tissues of many herb samples results in the initiation of powerful oxidation reactions. Such reactions may, therefore, be fundamental to the generation of flavour-active compounds in foods in which such herbal products are incorporated, and may also have a role in the medicinal properties of these plants. This observation is in contrast to the common assumption that health benefits from plant tissues are due to their high contents of antioxidants which reduce the formation of free radicals and other ROS (e.g. Madsen et al., 1996; Parejo et al., 2002). Since changes in the signal vary between dodecet and sextet within one plant and within one day, it was not possible to obtain further information about the mechanisms that lead to generation of the dodecet signal from these experiments.

In parsley, which is known to be rich in ascorbic acid (Food Standards Agency, 2002), no reaction was observed with 4-POBN, and instead the spectrum of the ascorbate radical was generated. Similar spectra have also been reported for cabbage leaf, carrot hypocotyls root stock, celery stalk, cress shoots, cucumber fruit and parsley leaf (Goodman et al., 2002), and for fruits of pepper (*Capsicum annuum*) and leaves of French bean (*Phaseolus vulgaris*) (Muckenschnabel et al., 2001 and 2003). The fact that ascorbate radical formation (investigated in parsley, but there is no reason to suspect that this is not a general effect) was independent of O_2 suggests that the ability of ascorbic acid to inhibit carbon-centred free radical generation exists under anaerobic as well as aerobic conditions, an observation which could at least in part explain the health benefits of Vitamin C rich foods.

In the present experiments, lovage was the only sample which produced simultaneously the signals from the ascorbate radical and the carbon-centred radical adduct of 4-POBN. Although Muckenschnabel et al. (2001) observed a gradual transition between the two types of spectrum with distance from the edge of soft rot lesions in leaves of *Phaseolus vulgaris* and fruits of *Capsicum annuum*, other investigations (Goodman et al., 2002) showed that it was rare to see signals from both of these radicals in the same food sample. It would appear, therefore, that this happens only in samples with appreciable quantities of ascorbic acid and that ascorbic acid may have a fundamental role in inhibiting the formation of carbon-centred radical when the tissue is damaged.

Conclusion

Oxidative processes are important in free radical generation in many of the herbs, and in >50 % of the samples product(s) were formed which were able to oxidise the spin trap 4-POBN. Although such foods are generally promoted for their antioxidant properties, this observation of widespread pro-oxidant activity in plant tissues (that are traditionally consumed in uncooked forms) is not surprising, because prooxidative enzymes such as oxidases and peroxidases (Vamos-Vigyazo, 1981) are present in the uncooked state. Since the influence of the cooking process is, very complex (it affects not only enzymatic activities but also the level and bioavailability of many food components), it was not investigated in the present studies. However, the observation of pro-oxidant activity in many plant food products suggests that it may be necessary to rethink our ideas on antioxidants in foods. Nevertheless, a specific role for the antioxidant ascorbic acid was also observed in these experiments, since it inhibited the formation of carbon-centred free radicals. This inhibition was independent of oxygen, consistent with the ability of this molecule to function as a food preservative and beneficial dietary component. The observations of this herb investigation formed the basis for further experiments with individual compounds from herbs under different oxidation conditions (see Chapter 3.5.) in order to obtain more information about the mechanisms of such reactions.

3.4. CARROTS

<u>Free radical formation in carrots investigated with different spin traps</u>

Carrot samples were investigated with three substituted derivatives of dimethyl-1-pyrroline N-oxide (DMPO) and 5-propoxy-carbonyl-5-ethylpyrroline-1-oxide (PEPO) to receive qualitative information about the radicals generated during cell disruption. These measurements build on the early work of Goodman et al. (2002), who used a limited number of spin traps in their investigations and reported qualitative variation in the results from different specimens.

Materials and sample preparation

Carrots were bought from a supermarket one or two days before sample preparation. Aqueous stock solutions of the spin traps (279 mM DEPMPO, 360 mM DPPMPO, 288 mM DBPMPO, and 960 mM PEPO) were provided by the Research Institute of Biochemical Pharmacology and Molecular Toxicology at the University of Veterinary Medicine, Vienna.

For investigations with two spin traps – DEPMPO, DPPMPO (~300 mM) - thin slices of fresh carrot were crushed in a mortar together with the spin trap. The mixture was then centrifuged for 3 minutes (13000 rpm, 4 °C), after which 500 µl of the supernatant were transferred into cryo tubes and stored in liquid nitrogen. DEPMPO was also diluted with 20 mM phosphate buffer (pH 7) containing a 0.5 mM iron chelator (EDTA). The suspension was filtered through a disposable syringe filter holder (Fa. Sartorius, 0.45 µm), the filtrate was transferred into the flat cell and the EPR spectrum measured immediately.

The spin traps PEPO and DBPMPO were used with carrot juice - carrot and distilled water mixed in a blender. 300 µl of the carrot juice were mixed with 300 µl of the spin trap solution and centrifuged for 3 minutes (13000 rpm, 4 °C); the supernatant was transferred into cryo tubes and stored at liquid nitrogen. Immediately prior to running the EPR spectra, the frozen samples were thawed in a water bath (hot water, ~40 °C) and transferred to a flat cell as quickly as possible. Spectra were recorded as single

scans, taking 84 s in 1024 points using 100 kHz modulation frequency. A microwave power of 20 mW, modulation amplitude of 0.0681 mT and a sweep width of 12 or 14 mT were used.

Results

The EPR spectra obtained with carrots and the different spin traps are shown in Fig. 3.25. – 3.27. and their measured hyperfine parameters in Table 3.7., along with selected values from the literature. The spectrum with DEPMPO as spin trap in Fig. 3.25.a corresponds to a hydroxyl radical adduct, but with an additional peak near the centre of the spectrum. The separation between this peak and the one immediately up-field from it is c. 1.8 gauss. It could, therefore, correspond to one half of a doublet from the monodehydroascorbate radical ($a(^1H)$ = 1.8 gauss) (Buettner and Jurkewicz, 1993), with the other half being obscured by the OH-radical adduct signal.

Fig. 3.26.a shows the spectrum of carrot mixed with DPPMPO. It consists of a mixture of components that were relatively stable. The parameters obtained by simulating the deconvoluted components are consistent with a mixture of hydroxyl and carbon-centred radical adducts (Fig. 3.26.c and d). In Fig. 3.26.b the two simulated components are added together (the height of the ·OH radical adduct multiplied by 0.58). When this is compared with the original spectrum, it can be that there is a third component in Fig. 3.26.a.

When the experiment with DEPMPO was repeated in the presence of an iron chelator (EDTA) at pH 7, the carbon-centred radical dominated the spectrum (Fig. 3.25.c), and the contribution from the hydroxyl radical adduct was much lower than in Fig. 3.25.a, indicating that formation of the hydroxyl radical was inhibited.

Mixing carrot juice with the spin trap PEPO resulted in a sextet spectrum with $a(^1H)$=2.3 mT, $a(^{14}N)$=1.5 mT) (Fig. 3.27.a), which is virtually identical to that obtained with mushrooms (Fig. 3.15.a), whereas no signal was obtained with DBPMPO.

Discussion

The generation of free radicals in carrots was investigated with different spin traps during cell disruption. Although the experimental procedure was similar to that used with mushrooms (see Chapter 3.2.), the results in most cases were quite different. With both DEPMPO and DPPMPO, spectra were seen which corresponded to a mixture of hydroxyl and carbon-centred radical adducts. As was reported by Goodman et al. (2002), the carbon-centred radical adduct with DEPMPO was less stable than the hydroxyl radical adduct. However, the spectrum obtained with DEPMPO was also accompanied by an additional peak which probably corresponds to one half of the spectrum from the monodehydroascorbate radical.

When EDTA was added to the sample along with DEPMPO, the contribution of the hydroxyl radical to the spectrum was decreased appreciably. Since EDTA is frequently used to hold Fe(III) in solution in model Fenton reaction systems, the above result suggests that it might interfere with a reactant that is a precursor of the Fenton reaction, and possibly inhibits the formation of H_2O_2 by the superoxide dismutase enzyme.

Although similar spectra were obtained with PEPO and both macerated mushroom and carrot juice, this does not necessarily mean that the identity of the radical adduct was the same for both samples, although it does suggest that the trapped radical is carbon-centred. It should be noted that the ^{14}N and ^{1}H hyperfine splittings obtained with DEPMPO were similar for mushroom and carrot samples, but the different ^{31}P values indicated that the adducts were derived from different types of radicals.

Since reasonable spectral intensity was observed in these measurements, additional experiments were undertaken to investigate the effects of age and sampling position on the free radical behaviour of carrots (see next section).
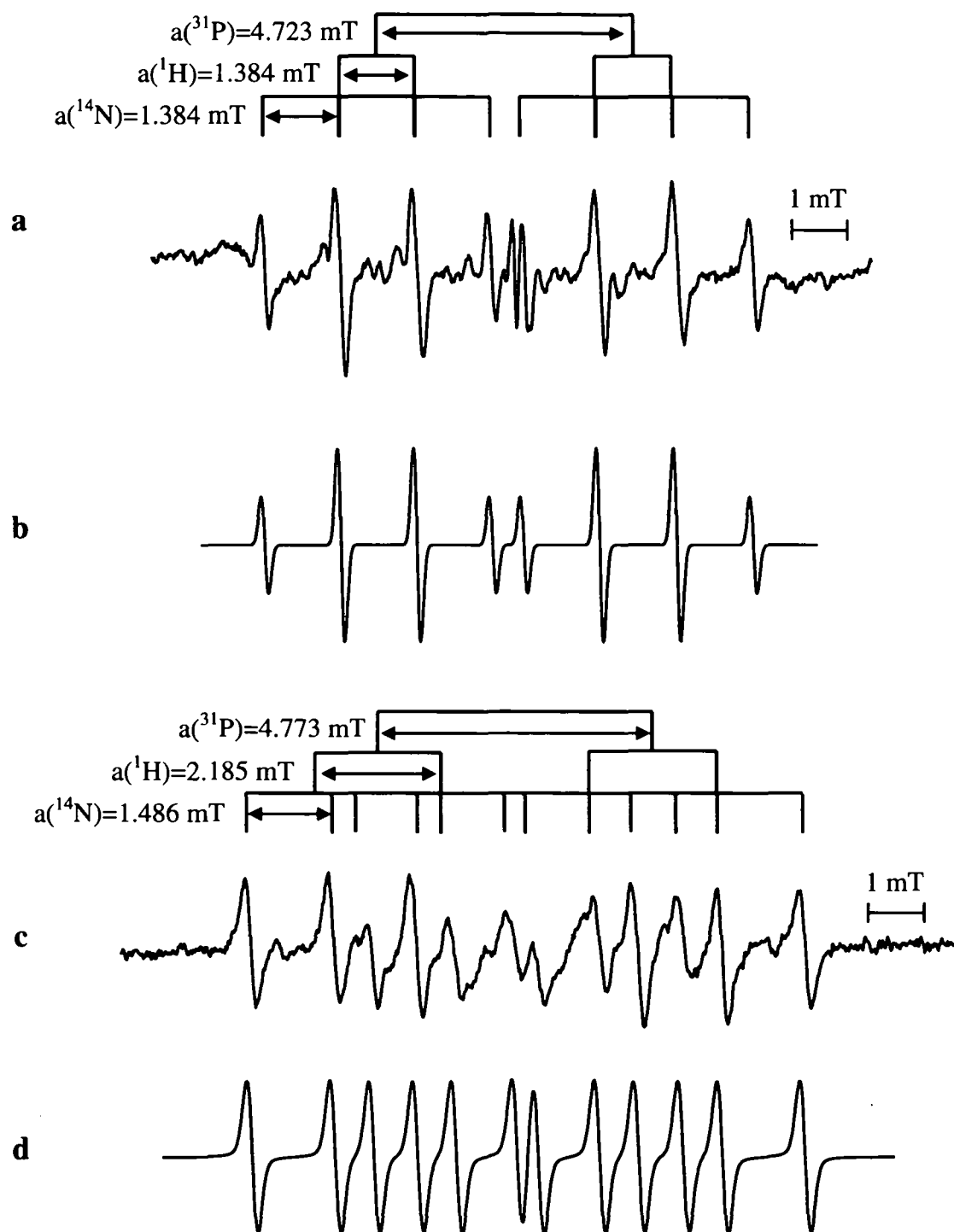
Fig. 3.25. EPR spectrum of (a) a hydroxyl radical from carrot trapped by DEPMPO, (b) simulation of spectrum (a), (c) spectrum received from carrot and DEPMPO in the presence of buffer and EDTA, (d) simulation of a carbon-centred radical. Spectral interpretation is shown by the "stick" diagram.

Table 3.7. Summary of hyperfine splitting parameters compared with literature data.

| Adduct	System	$a(^{31}P)$ (mT)	$a(^1H)$ (mT)	$a(^{14}N)$ (mT)
N-(t-butyl)aminoxyl	Dikalov et al. (1999)		1.393	1.461
4-POBN· radical	McCormick et al. (1995)		0.180	1.49, 0.185
	Carrot (present paper)		0.145, 0.050	1.490, 0.180
PBN-COCH₃ '	NIEHS database (1998)		0.330	1.590
PBN-C	Carrot (present paper)		0.328	1.590
DEPMPO-OH	Fréjaville et al (1995)	4.780	1.300	1.400
	Carrot (present paper)	4.723	1.384	1.384
DPPMPO-OH	Stolze et al (2000)	4.695	1.320	1.400
	Carrot (present paper)	4.680	1.382	1.382
DEPMPO-C	Fréjaville et al (1995)	4.810	2.230	1.500
	Carrot (present paper)	4.773	2.185	1.486
DPPMPO-C	Stolze et al (2000)	4.848	2.218	1.512
	Carrot (present paper)	4.780	2.223	1.515
PEPO-OH	Stolze et al (2003)		1.594, 0.063	1.400
			1.201, 0.078	1.387
PEPO-OOH	Stolze et al (2003)		1.160, 0.903	1.321, 1.321
PEPO-C	carrot juice (present paper)		2.300	1.500
PEPO-C(LOOH)	(unpublished results)		2.349	1.503
PEPO-CH₂OH	(unpublished results)		2.150, 0.087	1.474
PEPO-CH₃	(unpublished results)		2.417	1.508
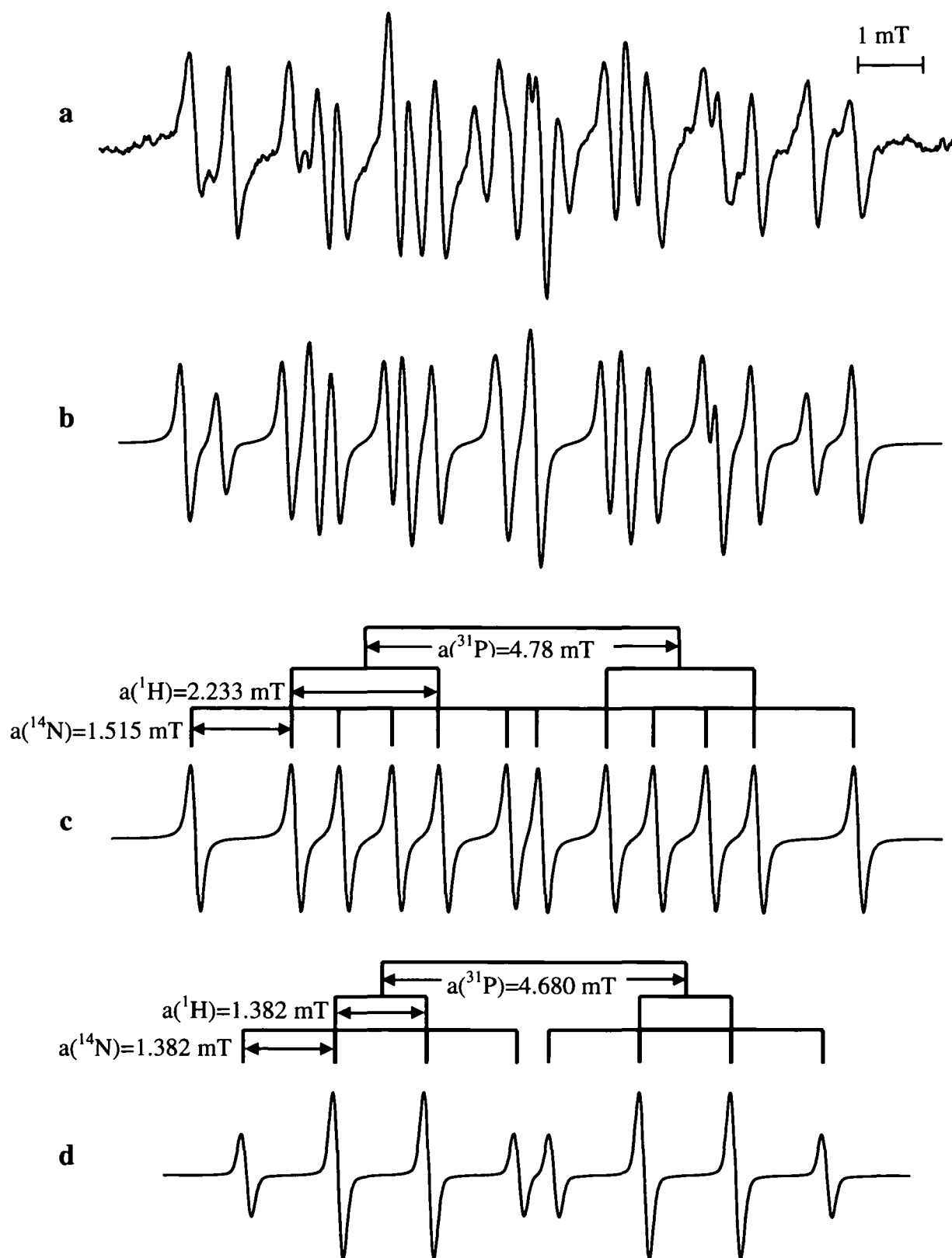
Fig. 3.26. EPR spectra from carrot and DPPMPO. (a) experimental spectrum, (b) simulation of a carbon-centred radical combined with a hydroxyl-radical, (c) simulation of the carbon-centred radical adduct, (d) simulation of the hydroxyl-radical adduct. Spectral interpretation is shown by the "stick" diagrams.
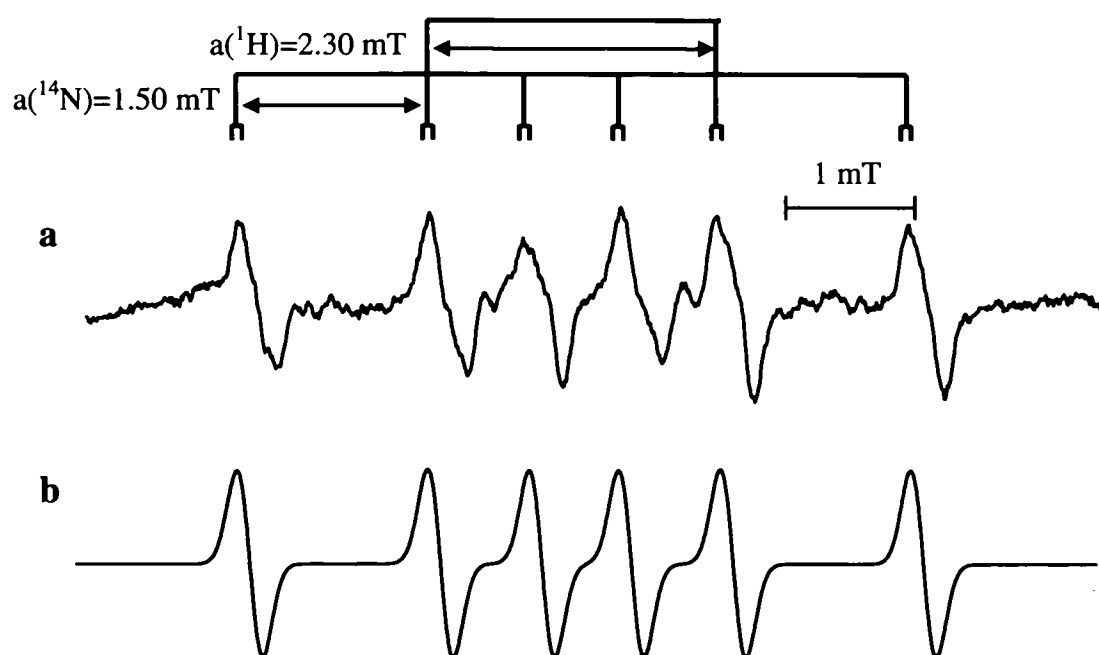
Fig. 3.27. EPR spectrum of (a) a radical in carrot trapped by PEPO, (b) simulation of the spectrum (a). Spectral interpretation is shown by the "stick" diagram.

Free radical formation in carrots investigated at different positions and growth stages of the root

This investigation involved the study of one variety of carrot (*Daucus carota cv.* Maestro) grown under stress free conditions. The level of carotenoids was measured along with free radicals. The influence of maturity on the composition of pigments and free radical generation was determined with samples harvested at three different growth stages.

Material and sample preparation

Carrot seeds (*cv. Maestro*) were sown in two 15-liter pots. The pots were covered with plastic until the plants were *c.* 2 cm high. During germination the pots were watered from above only. Later a self-irrigating system was used. Each pot was placed on a bucket filled with water, and wicks were used to connect the water bucket with the pot. Three harvests (49, 55 and 83 days after sewing) were carried out, representing three different developmental stages of the carrots. Thin slices of each carrot sample were taken from the top, the centre, and the tip of the root (Fig. 3.28.). They were immediately frozen to 77 K and stored in liquid nitrogen until analysis.
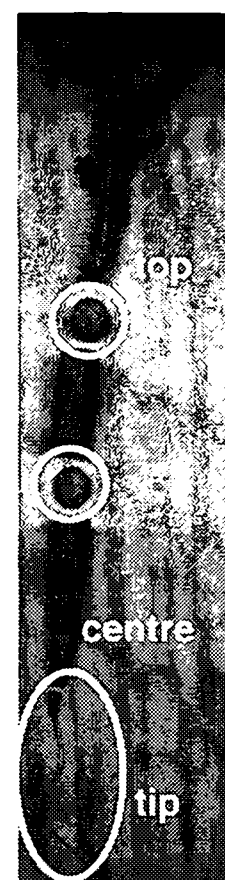

Fig. 3.28. Carrot samples (yellow marked) taken from each root.

Analysis

EPR-analyses with the carrot tissues were carried out using two different spin traps – one more lipophilic, phenyl-*N-t*-butylnitrone (PBN), and one more hydrophilic, α-(4-pyridyl-1-oxide)-*N-t*-butylnitrone (4-POBN), to detect short-lived radicals when cells were disrupted. The 4-POBN solution was made with water, the PBN solution was prepared with a 10 % ethanol solution.

Frozen carrot samples were ground under liquid nitrogen until a homogenous powder was obtained. A small quantity of the powder (one small spoon) was gently mixed with 800μl of the spin trap solution (164 mM) in a second mortar. The suspension was filtered through a disposable syringe filter holder (Fa. Sartorius, 0.45 μm), and the filtrate was transferred into the flat cell and measured immediately. The recorded spectra consist of 10 added scans, each taking about 42 s, in 1024 points using 100 kHz modulation frequency. A microwave power of 20 mW, modulation amplitude of 0.16 mT and a sweep width of 6 mT were used. The spectra were baseline corrected and filtered for quantifying the results. The first peak, doublet or quartet was integrated.

The carotenoids lutein, α-carotene and β-carotene were determined and quantified by HPLC using the method of Scott et al. (1995) (see Chapter 3.1). The HPLC analysis was carried out at the TU Graz, Department of Food Chemistry and Technology.

EPR-Results

The EPR spectra with PBN (Fig. 3.29.) contained a mixture of 2 components, a sextet and a quartet which are assigned respectively to an adduct of the spin trap and a breakdown product of PBN. Parameters for the sextet (a(^{1}H)=0.328 mT and a(^{14}N)=1.59 mT) correspond to a carbon-centred radical adduct (N.I.E.H.S. Spin-Trap DataBase). The quartet with a(^{14}N)=a(^{1}H)=1.43 mT corresponds to the N-t-butyl hydronitroxide radical, which is formed via a radical induced fragmentation of the spin trap (Britigan et al., 1990; Chamulitrat et al., 1993; Atamna et al., 2000). With the sextet component, line broadening is visible at the high field end of the spectrum. This is consistent with incomplete averaging of the spectral anisotropy (see Chapter 2 – page 41), because the tumbling motion of the radical is not at the rapid limit. This in turn suggests that the size of the trapped radical is not very small.
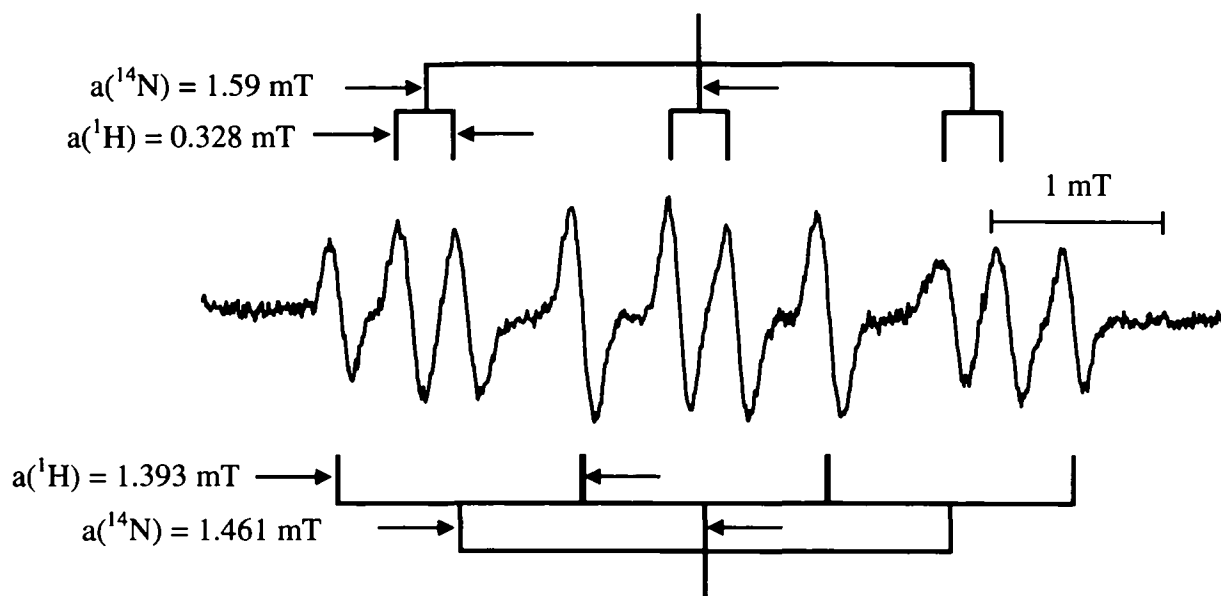
Fig. 3.29. A typical EPR spectrum of a carrot sample, using the spin trap PBN. It consists of the sextet and the quartet. Interpretation is shown by the stick diagrams.

The intensity of the sextet signal with PBN varied with the position in the carrot root from which the sample was taken (Fig. 3.30.). The highest signal came from the centre of the root and the lowest signal from the tip. The state of maturity of the carrot had little or no influence on the signal intensity.

Variations in the intensity of the N-t-butyl hydronitroxide radical signal were also dependent on the position of the sample in the carrot root and were the opposite to those of the sextet. This signal was lowest in samples taken from the centre of the carrot (Fig. 3.31.). It also decreased progressively with increasing maturity of the carrot.
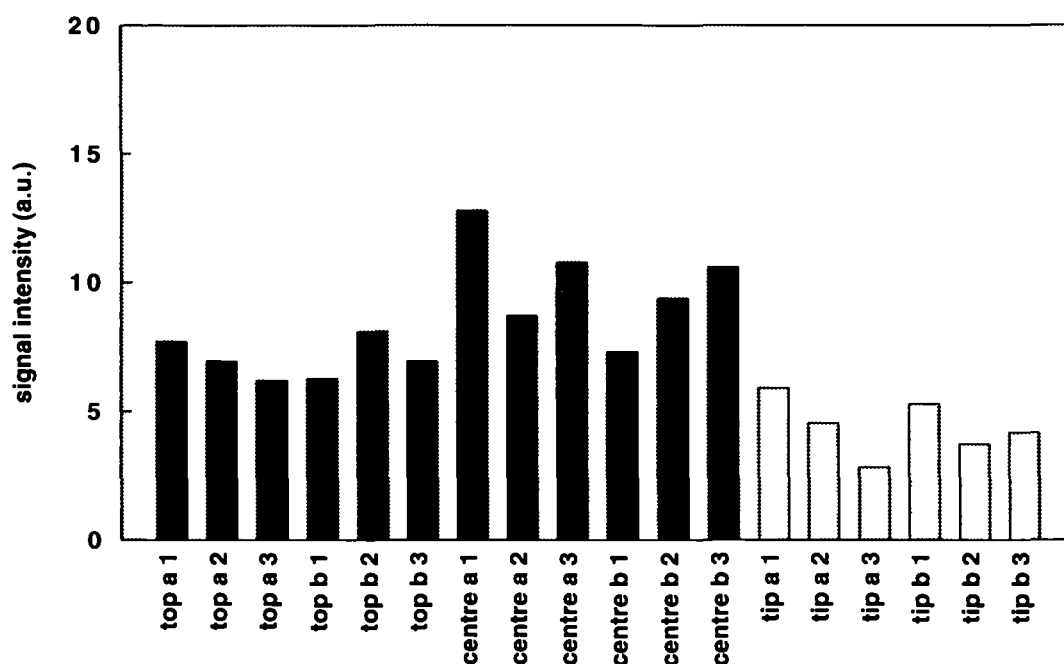
Fig. 3.30. Signal intensity of the carbon-centred radical trapped with PBN in relation to the position and maturity of the carrot. a, b are two replicates of the carrots. top, centre, tip are the position of the carrot where the samples were taken. 1, 2, 3 are the 1st, 2nd and 3rd harvests.
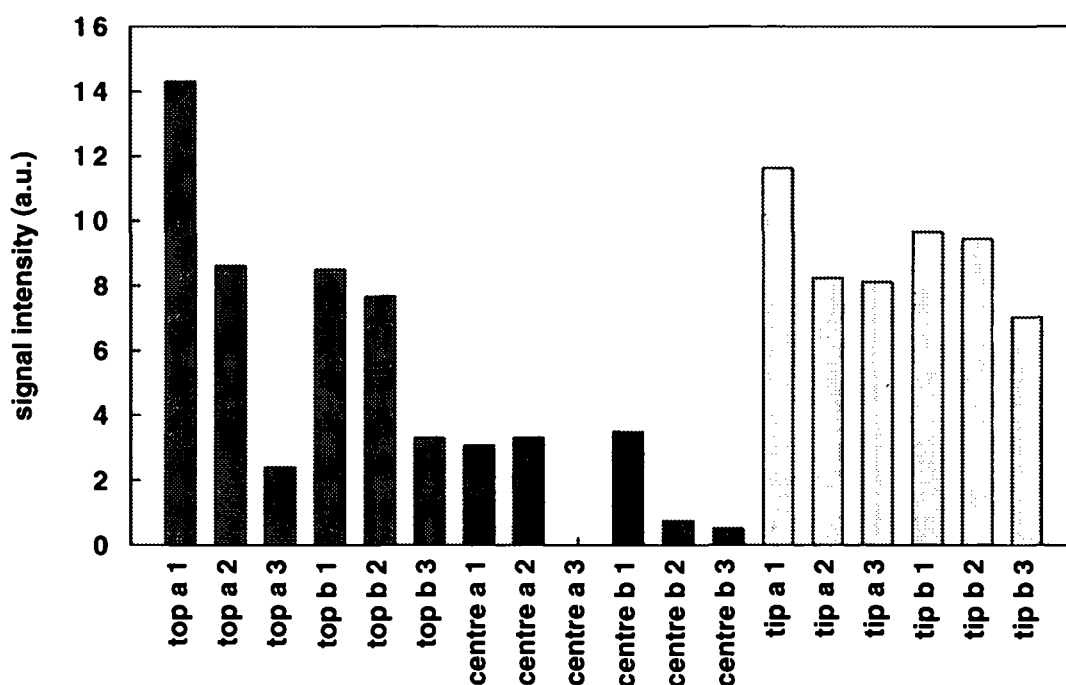

Fig. 3.31. Signal intensity of the N-t-butyl hydronitroxide radical in relation to the position and to the maturity of the carrot. a, b are two replicates of the carrots. top, centre, tip are the position of the carrot where the samples were taken. 1, 2, 3 are the 1st, 2nd and 3rd harvests.

EPR spectra from the reaction of the spin trap 4-POBN with the carrot samples also showed two different signals (Fig. 3.32.). One signal consists of twelve peaks – a triplet of quartets from the 4-POBN adduct of its oxidised product 4-POBN·. This signal contains two nitrogen splittings ($a(^{14}N)$ = 1.493 and 0.182 mT) and one hydrogen splitting ($a(^1H)$ = 0.145 mT). The second EPR-signal corresponds to the N-t-butyl hydronitroxide radical, as was seen with PBN.

$a(^{14}N) = 1.493$ mT

$a(^{14}N) = 0.182$ mT

$a(^1H) = 0.145$ mT

1 mT

$a(^1H) = 1.393$ mT
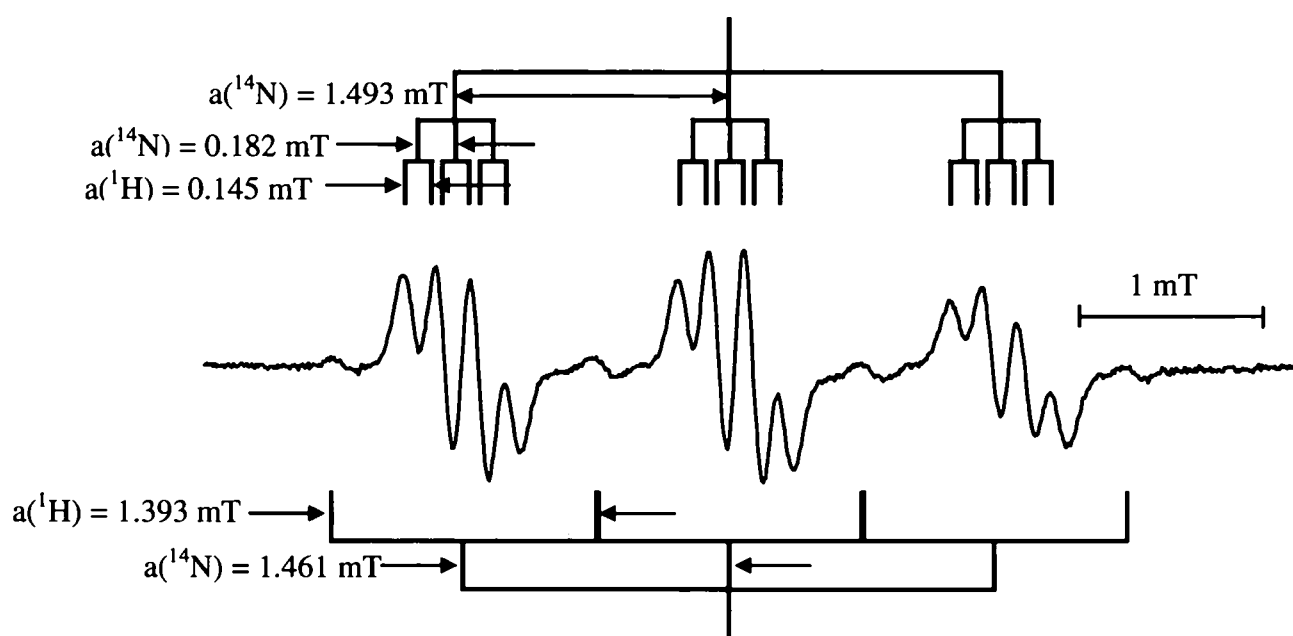
$a(^{14}N) = 1.461$ mT

Fig. 3.32. Typical EPR spectrum of a carrot sample using 4-POBN as spin trap. It consists of the oxidation product and the breakdown product. Interpretation is shown by the stick diagram.

Some replicates showed a relation between the intensity of the oxidation product and the position of the carrot where the samples were taken. The highest intensity within one replicate and harvest was from the tip of the carrot root (Fig. 3.33.). The lowest signal intensity came from the centre of the carrot. There was no correlation between the EPR signal and the maturity of the carrot.
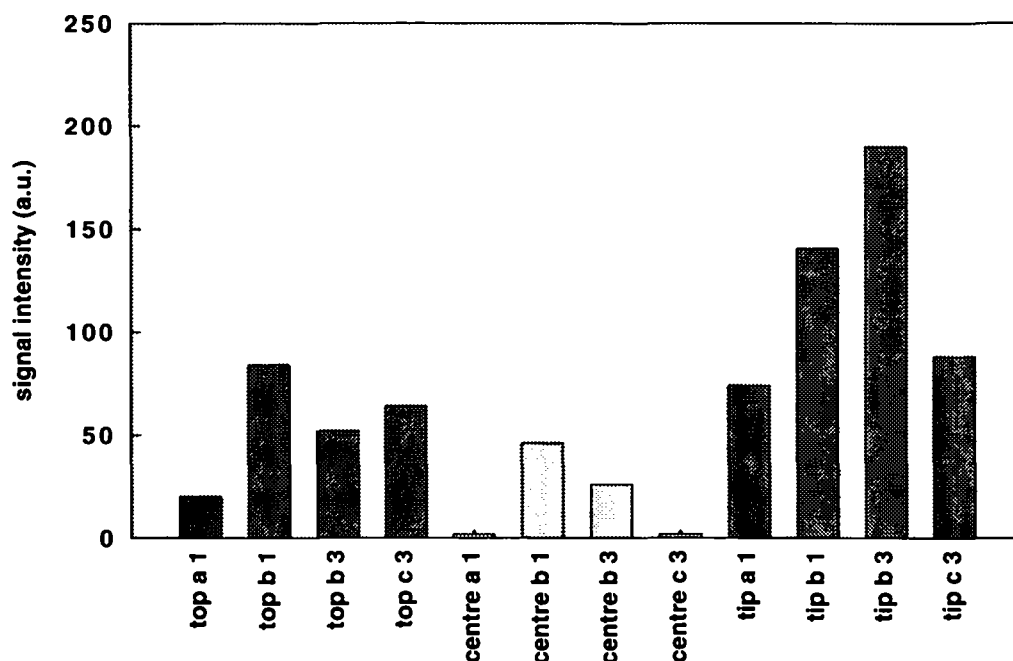
Fig. 3.33. Signal intensity of the oxidation product from 4-POBN in relation to the position and to the maturity of the carrot. c, d are two replicates of the carrots. top, centre, tip are the position of the carrot where the samples were taken. 1 and 3 are the 1st and 3rd harvests.

HPLC Results

The carotenoids lutein, α- and β-carotene could be separated and identified by HPLC analysis. The results of some replicates showed an increasing amount of α- and β-carotene between the 2nd and 3rd harvests in both the top and centre of the carrot (Fig. 3.34.). Slightly lower amounts of α- and β-carotene were found in the centre of the carrot than in the top.

Lutein levels were highest in the tops and lowest in the tips of carrots (Fig. 3.35.), the values from the tops and tips being normalised to those from the centre in this figure. It can be seen that deviations from the centre values decreased with maturity for the tops, but increased for the tips. Since the amount of material in one root tip sample was insufficient for the analyses, these were performed with a mixture of three replicates taken from each harvest.
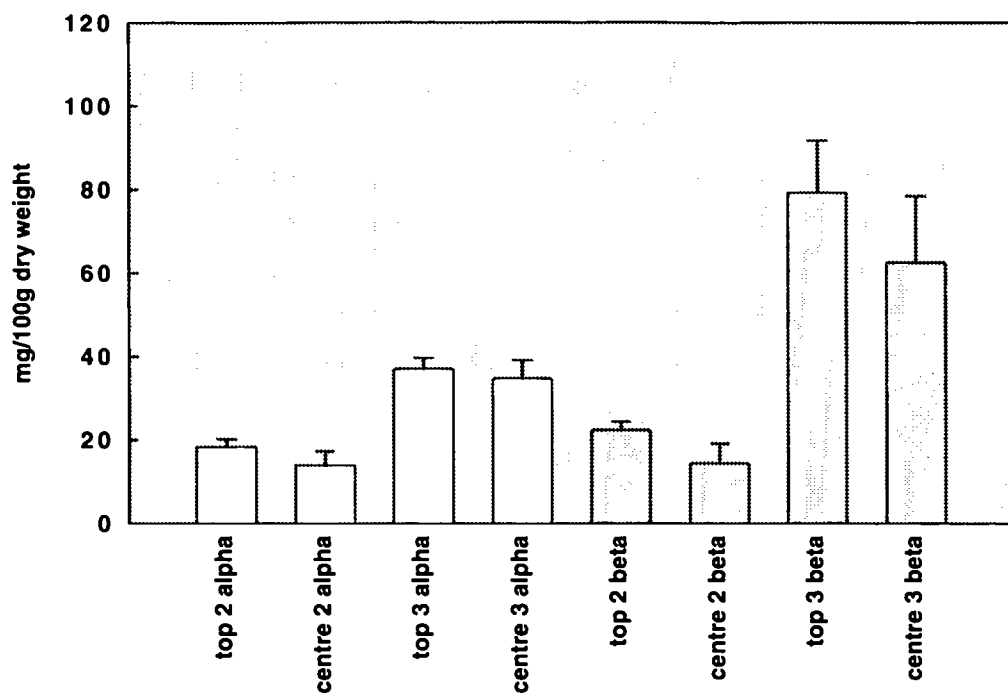
Fig. 3.34. Amounts of α- and β-carotene in relation to the position and maturity of the carrot. alpha, beta stand for α- and β-carotene, top and centre for the carrot position from which the samples were taken. 2, 3 are the 2nd and 3rd harvest.

Fig. 3.35. Amount of Lutein for samples taken from the top and the tip of the carrot root normalised to the values from the centre. a, b, c are three replicates, mix stands for a mixture of all three replicates. 1, 2, 3 are the 1st, 2nd and 3rd harvest.

Discussion

The investigation of carrot samples taken from three different positions of the root, mixed with two spin traps - PBN and 4-POBN - showed t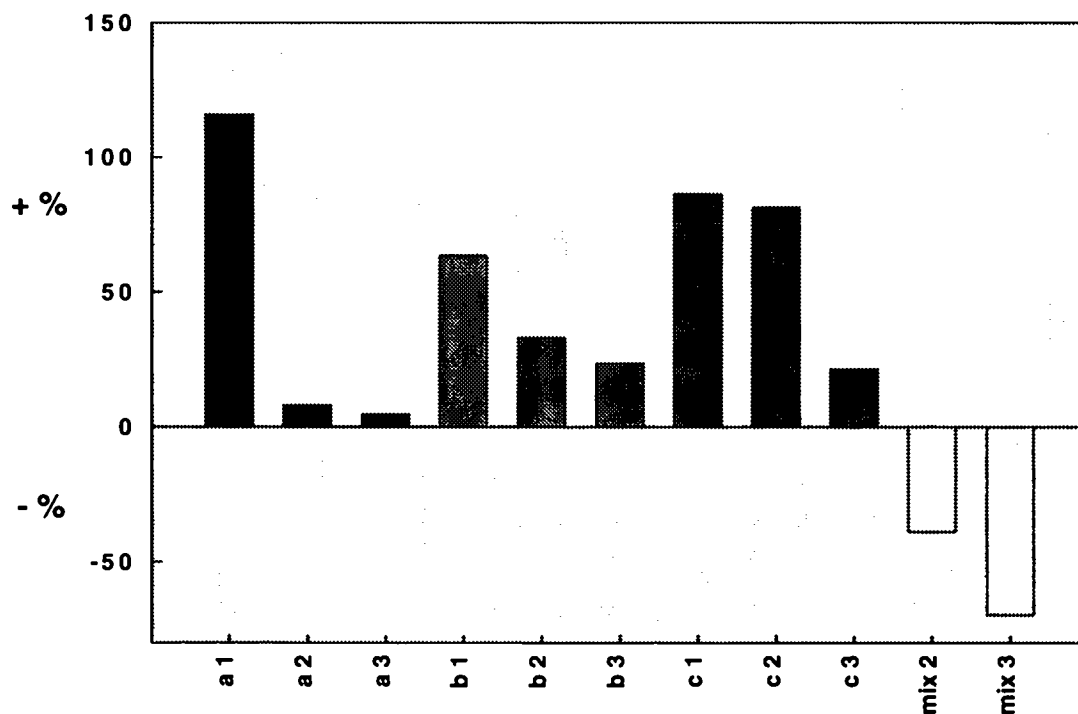wo different EPR signals for each of the spin traps. One of the components, the N-t-butyl hydronitroxide, was common to the reactions with both spin traps and must derive either from a fragmentation of the spin traps (Atamna et al., 2000; Britigan et al., 1990; Chamulitrat et al., 1993) or from an impurity in the spin traps (Dikalov et al., 1999). Decomposition of PBN yields benzaldehyde and N-t-butyl hydroxylamine (Fig. 3.36.), and the latter would also be expected to be a fragmentation product of 4-POBN. According to Dikalov et al. (1999) the N-t-butyl hydronitroxide radical is formed by metal catalysed oxidation of N-(t-butyl)hydroxylamine which is an impurity of the Sigma product PBN. The most relevant metal in carrot tissue is in this case iron with ~2.1 mg/100g (Carlsson, 2000), which catalyses the Fenton reaction. Consequently, ·OH radicals are formed which then react with N-t-butyl hydroxylamines forming N-t-butyl hydronitroxide.
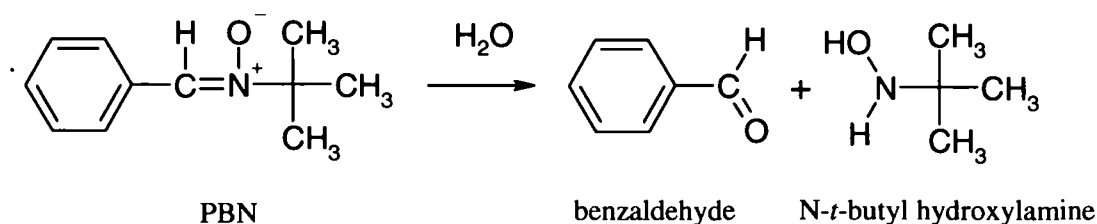
Fig. 3.36. Decomposition pathway for the spin trap PBN.

A short lived carbon-centred radical was trapped by PBN, but not by 4-POBN. It is possible that this radical could be responsible for oxidising 4-POBN to give the 4-POBN· radical which is then trapped by the spin trap itself. This radical was already described in the investigations with herbs (Pirker et al., 2004), lettuce and carrots (Glidewell et al., 1996; Goodman et al., 2002).

Some replicates showed a relation between the intensities of the various EPR signals and the position in the carrot from which the samples were taken. The carbon-centred

radical was mainly generated with tissue from the centre of the root whereas the N-*t*-butyl hydronitroxide radical and 4-POBN oxidation products were most intense in spectra with tissue from the tips. However, the fact that signals from the carbon-centred radical adduct with PBN and the oxidation product of 4-POBN show different intensity relationships with respect to the position of the tissue in the root, suggests that they do not have a common source as was suggested in the previous paragraph. It seems more likely that the 4-POBN˙ and N-*t*-butyl hydronitroxide radicals could have a common precursor, because of the similarities in their distribution profiles within the carrot root, and especially because of their predominance in the root tips. The tip is the youngest part of the carrot root, and has the highest growth potential. The hydroxyl radical has been shown to play an important role in root elongation in maize (*Zea mays*) seedlings by facilitating cell wall loosening in the growing zone (Liszkay et al., 2004; Schopfer et al., 2002; Schopfer, 2001). These authors did not distinguish between the possibilities of ˙OH being generated by Fenton chemistry or from peroxidases in the presence of NADH and H_2O_2. It would appear, therefore that ˙OH radicals could be involved in the generation of the 4-POBN˙ and N-*t*-butyl hydronitroxide radicals. Because of their instability, ˙OH adducts with PBN and 4-POBN were not observed. It should be recalled, however, that these were the major species detected with DEPMPO and related spin traps.

It seems from the current experiments that the hydroxyl radical is also important in the growth zone in carrot hypocotyl root stock, and it may be of general importance in plant root development. The higher level of hydroxyl radical generation at the tips compared to the other tissues in the carrot could also be the explanation for its higher oxidation potential. Furthermore, the fact that the highest levels of carbon-centred radical adduct formation (with PBN) were observed in tissues with the lowest levels of hydroxyl radical generation suggests that formation of (much of) the carbon-centred radicals is independent of hydroxyl radicals.

There was a tendency (visible in some but not all replicates) for there to be slightly higher amounts of α- and β-carotene in the tops of the root than in the centres. A similar observation was also made with lutein, which in addition was lowest in the tips. Deviations from the centre values decreased in the tops and increased in the tips with maturity of the plant root. In a mature carrot there is less difference in size and shape

112

between top and centre of the root, which could be an explanation for the similar amounts of lutein in these two parts of mature carrots.

Combining the results from the HPLC and EPR measurements could lead to the conclusion that the carotenoids inhibit free radical formation in the tissue from the centre and top of the carrots. In contrast, there are lower levels of these antioxidants in the tips, because hydroxyl radical activity is essential for growth.
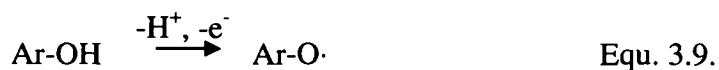
3.5. PHENOLIC COMPOUNDS

Individual plant components, such as rosmarinic acid (phenol), carnosic acid (phenolic diterpene), luteolin (flavone), and kaempferol (flavonol), were chosen for investigations under five different oxidation conditions. Autoxidation using an alkaline (pH 13), aerated solution, was used to produce initial information on the oxidised components. In addition, three enzymatic systems representing different oxidising agents were used at pH 7. Horseradish peroxidase and hydrogen peroxide (HRP/H_2O_2) has been reported to form three complexes with high oxidation potential (Chen and Schopfer, 1999; George, 1953); xanthine and xanthine oxidase (X/XO) generate superoxide anion radicals (McCord and Fridovich, 1969; Terada et al., 1990); and the Fenton reaction system generates hydroxyl radicals. O_2^- was also generated directly from potassium superoxide. Stock solutions in pure DMSO (1 mM) were prepared for each phenolic compound.

Experimental setup

Autoxidation

Autoxidation proceeds by deprotonation and electron abstraction producing radicals (Equ. 3.9.). Two different experimental setups were used in order to investigate the influence of the amount of oxygen as well as of the relative concentrations of NaOH and the phenol.

$$Ar\text{-}OH \xrightarrow{-H^+,-e^-} Ar\text{-}O\cdot \qquad\qquad Equ.\ 3.9.$$

In the first procedure (Proc. 1), 200 µl of a 0.1 M sodium hydroxide solution were transferred into a flat cell, then 200 µl of the phenolic solution were added. The reaction between the phenolic compound and the alkali was immediately visible as a strong yellow band at the interface of the two liquid phases. Diffusion of the molecules resulted in a more or less homogeneous final solution in the flat cell. After addition of the phenolic solution, the flat cell was immediately placed in the spectrometer and the spectrum recorded within one minute. In this procedure the amount of oxygen is limited to that dissolved in the solutions and the head space in the flat cell. The second

procedure (Proc. 2) was carried out in an Eppendorf tube to test the influence of a higher oxygen concentration. 200 μl of the NaOH-solution and 200 μl of the phenolic solution were transferred into an Eppendorf tube and mixed with a Vortex mixer for a few seconds. The mixed solution had an intensive yellow colour and since the oxidation is an exothermic process the tube walls got warm very quickly. The oxidised solution was transferred into a flat cell within a few seconds and placed immediately into the spectrometer for recording the spectrum. The amount of oxygen available for reaction in this experiment (Proc. 2) was expected to be much higher than in the first set up (Proc. 1).

The dependence of relative concentrations of NaOH and phenolic compound was tested using Proc. 2 by thoroughly mixing the two solutions in an Eppendorf tube. The two stock solutions were combined in different amounts; 1:1, 1.67:1 and 3:1 volume ratios of phenolic compound:NaOH solutions.

HRP/H₂O₂

Concentrations of solutions for the system HRP/H_2O_2 were similar to that published by Miura et al. (2003). 200 μl of a potassium phosphate buffer (pH 7) were mixed in an Eppendorf tube together with 50 μl of $ZnCl_2$ (10 mM), 50 μl HRP (12.5 μM), and 5 μl H_2O_2 (100 μM). All solutions were made with distilled water. 200 μl of the mixed solution were transferred into the flat cell and 200 μl of the phenolic stock solution were added. The flat cell was placed in the spectrometer and the spectrum recorded within 1 minute.

Xanthine/Xanthine oxidase

The system X/XO was used to generate superoxide anion radicals. The experiment was carried out with 200 μl of a potassium phosphate buffer (pH 7) mixed for a few seconds together with 20 μl of xanthine solution (657 μM) and 5 μl of xanthine oxidase (8 μl/ml, 22 unit/ml). All individual solutions were prepared with distilled water. 200 μl of the mixed solution were transferred into the flat cell and 200 μl of the phenolic stock solution were added. The flat cell was placed in the spectrometer and the spectrum recorded within 1 minute.

Fenton reaction system

Hydroxyl radicals are generated in the Fenton system by the reaction of H_2O_2 with Fe(II); ascorbic acid is added to ensure redox cycling of the iron. The reaction concentrations were taken from the PhD thesis of Pascual (2000). 200 µl of a potassium phosphate buffer (pH 7) were placed in an Eppendorf tube. 20 µl ascorbic acid (20 mM), 5 µl $FeCl_3 \cdot 6H_2O$ (10 mM), 5 µl EDTA (25 mM), and 5 µl H_2O_2 (100 µM) were added and the solution was mixed for a few seconds using a Vortex mixer. To avoid competitive reactions of the phenolic compound with ascorbic acid, the system was also tested without ascorbic acid. Distilled water was used for preparation of the individual solutions. 200 µl of the mixed solution were transferred into the flat cell and 200 µl of the phenolic stock solution were placed on top of that. The cell was immediately placed into the spectrometer and the EPR spectrum recorded immediately after tuning.

Potassium superoxide

The reaction of superoxide radical anions with phenolic compounds was also investigated using potassium superoxide. For this purpose 40 µl of the phenolic solution (10 mM) where mixed in an Eppendorf tube with 60 µl of distilled H_2O in the case of luteolin and RA and with 160 µl DMSO in the case of kaempferol and CA. The solution was added to *c*. 0.5 mg KO_2 and the reaction was stopped after approx. 5 sec. by adding 300 µl (in the case of luteolin and RA) resp. 200 µl (in the case of kaempferol and CA) of buffer (pH 6.9) containing 5 µl catalase (1 mg/ml) and 10 µl SOD (2 mg/ml). The solution was then transferred into a flat cell which was placed in the spectrometer and the spectrum was recorded within 1 minute.

After fixing the flat cell in the cavity, the spectrometer was always tuned manually to minimise the time between the commencement of the reaction and recording the spectrum.

3.5.1. Kaempferol

Kaempferol is a compound of the flavonol group. Its structure is given in Fig. 3.37. It consists of two aromatic rings and one heterocyclic ring with four hydroxyl groups on the positions 3, 5, 7, and 4'. Ring C contains also a keto group. The main reaction centre where oxidation occurs is thought to be the hydroxyl group on the B-ring.
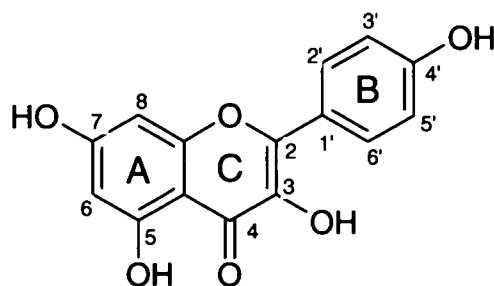

Fig. 3.37. Structure of kaempferol.

Autoxidation

Autoxidation of kaempferol led to five different EPR signals which could be separated and simulated. Other weak signals, which were partially hidden behind these main peaks, could not be isolated. The experiment using Proc. 1 gave mainly a spectrum of five peaks (Fig. 3.37.), whereas with Proc. 2 seven peaks (Fig. 3.38.) were visible in the spectrum. The seven peak spectrum was also eventually observed with Proc. 1 after the intensity of the five peak spectrum decreased. Fig. 3.39. shows the spectra at different times after mixing the solutions, the last one being recorded 8 minutes after the first. Additional peaks, which were unstable and disappeared after one minute, are visible between the 1st and the 2nd as well as between the 4th and 5th peak of the quintet, but the complete signal from this/these radical/s could not be resolved.

With the majority of the measurements using Proc. 1, two quintets with similar parameters were visible. In an attempt to slow down the reaction kinetics and therefore to allow a better observation of the spectral changes, solutions cooled to 0°C were also investigated. Fig. 3.40. shows time sequence spectra obtained from two cooled kaempferol solutions. One solution was one week old (Fig. 3.40.a-c), the other solution

was prepared fresh on the day of measurement (Fig. 3.40.d-f). Both experiments showed two similar quintets with slightly different g-values and intensities. One quintet signal was less stable than the other and its intensity decreased faster (Figs. 3.40b, c and 3.40.e, f). The relative intensities ratio of the two components was slightly different in the two solutions. Interpretation of the spectra in terms of two quintets with slightly different g-values was confirmed by simulation of Fig. 3.40.b and 3.40.e (Fig. 3.41.). The splitting in the upper part of the peaks was simulated with a lower intensity of the left of the two quintets whereas the splitting in the lower part of the peaks was obtained with a lower intensity of the right quintet. An explanation for this observation could be the use of an organic medium (DMSO solution) in the upper phase containing the flavonoid and a water based medium (NaOH solution) in the lower phase. At the interface of these two phases in the flat cell the radical was formed in both phases. Since the g-value as well as the stability of the signal is dependent on the solvent, the shift of the two observed quintets can be explained by the simultaneous formation of this radical in both phases.

The intensity of the quintet signal decreased with time. Flushing air through the flat cell using a syringe reoxidised the flavonoid, but this time the seven peak spectrum appeared immediately. Obviously, the amount of oxygen influences the radical chemistry of the flavonoid.

In another experiment only 100 μl of NaOH were transferred into the flat cell and 300 μl of the kaempferol stock solution was added on top of it. The quintet signal was obtained after flushing a few millilitres of air through the flat cell to mix the two solutions, but it was much more stable (>24 min.) than in the original measurement using 200 μl NaOH and 200 μl kaempferol.

Autoxidation of kaempferol carried out by Proc. 2 resulted in the 7 peak spectrum when the volume ratio of the two solutions was 1:1 = kaempferol:NaOH. The influence of the ratio of the two solutions was tested by changing it into 1.67:1 and 3:1 (kaempferol:NaOH), i.e. increasing the concentration of kaempferol in the mixed solution. This change led to different signals in the EPR spectrum. The spectrum obtained with a 1.67:1 kaempferol to NaOH ratio showed the 7 peak spectrum with additional structure after the quintet signal decreased (Fig. 3.42.). Since the spectrum

was more complex than the original 7 peak spectrum, a 2nd derivative of the radical compound was recorded (Fig. 3.42.c) in order to improve resolution of the overlapping peaks.

A 3:1 ratio kaempferol:NaOH gave a spectrum with at least three components (Fig. 3.43.). The first spectrum (Fig. 3.43.a) consisted of at least two components – the quintet and a signal containing 13 peaks (compound 2). Approximately 5 minutes later the quintet had disappeared and a mixture of two signals was visible, including the 13 peak spectrum (Fig. 3.43.b). After another c. 21 minutes compound 2 had almost disappeared and a spectrum of 8 peaks (compound 3) with nearly equal intensity (Fig. 3.43.c) was observed. The simulation of compound 3 is shown in Fig. 3.43.d. The simulation of Fig. 3.43.b is based on the spectrum of compound 2 after subtracting a simulation of compound 3 (Fig. 3.44.a), since this component was already present in the spectrum.

By using deuterated buffer, it was shown that no exchangeable protons contributed to the hyperfine splittings.

When kaempferide, a compound where the hydroxyl group on ring B is replaced by a methoxy-group (Fig. 3.45.), was used instead of kaempferol for the autoxidation experiments no spectrum was detected. The assumption of ring B as the oxidation site was sustained by this investigation.
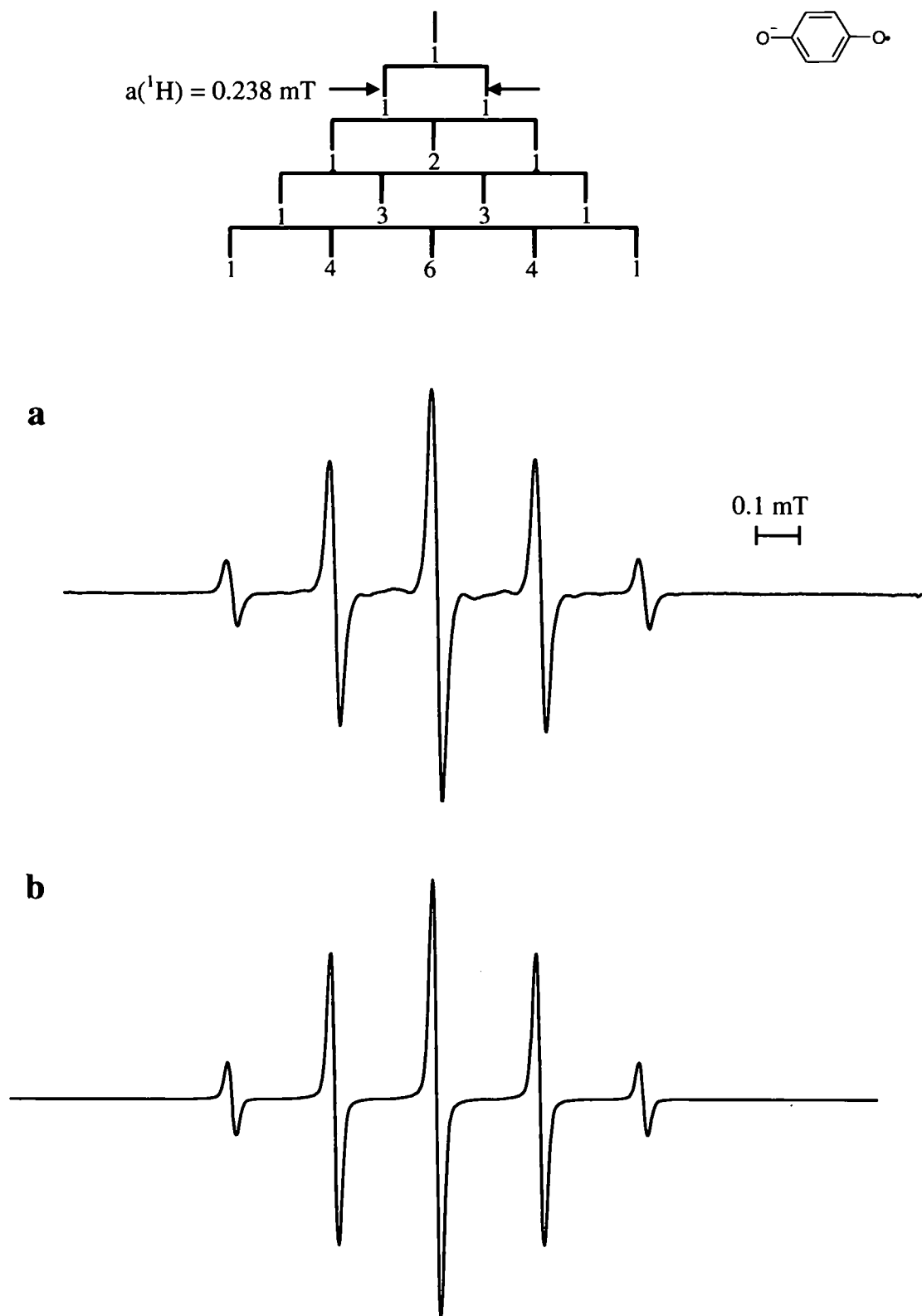
Fig. 3.37. EPR spectrum of kaempferol obtained by autoxidation using Proc. 1. Spectral interpretation is shown by the stick diagram. (MA 0.048 mT, 1 scan)

$a(^1H) = 0.088$ mT

```
              1
            1   1
          1   2   1
        1   3   3   1
      1   4   6   4   1
    1   5  10  10   5   1
  1   6  15  20  15   6   1
1   7  21  35  35  21   7   1
1   8  28  56  70  56  28   8   1
```
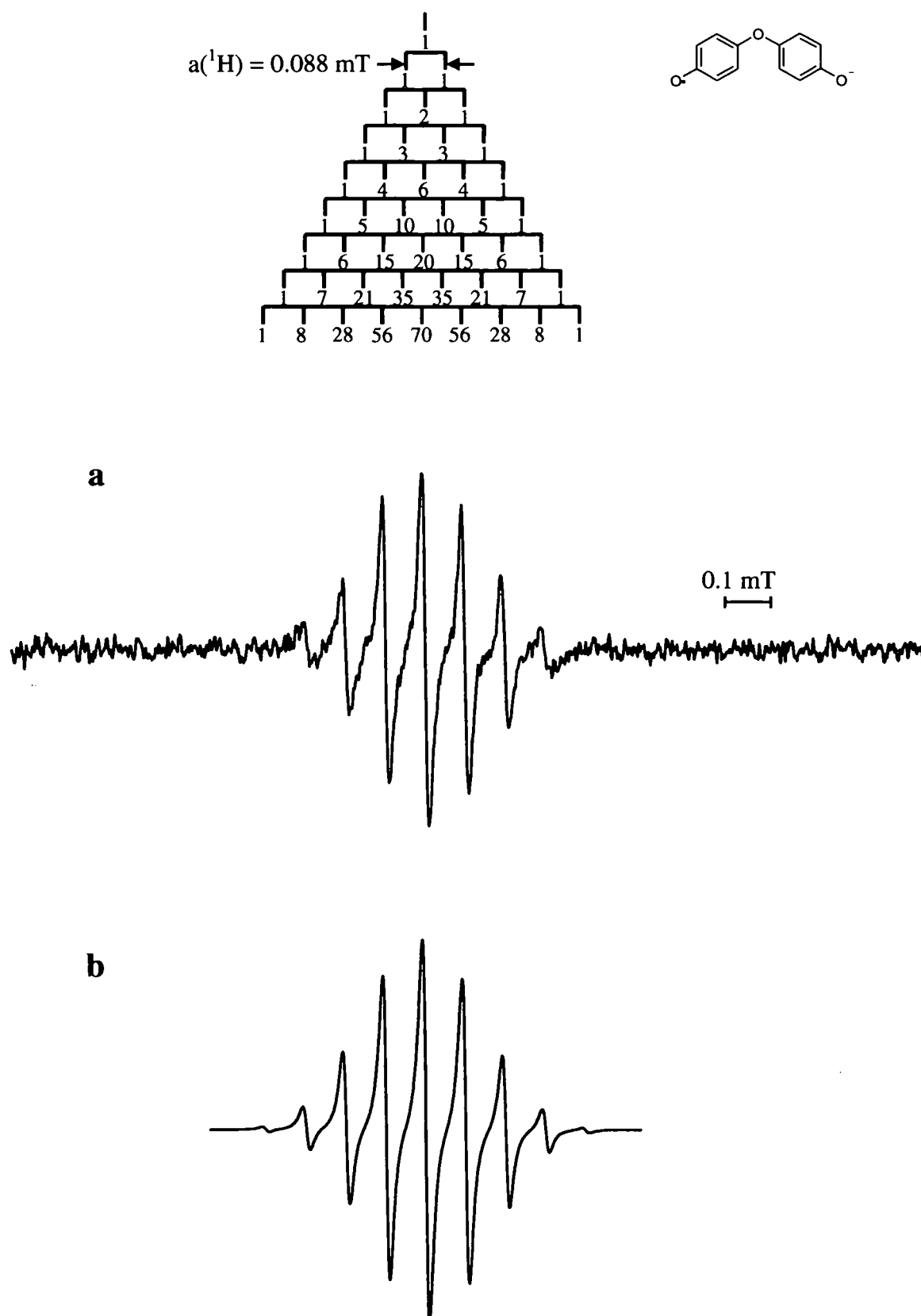
0.1 mT

a

b

Fig. 3.38. EPR spectrum of kaempferol obtained by autoxidation using Proc. 2 with a kaempferol:NaOH ratio of 1:1. Spectral interpretation is shown by the stick diagram. (MA 0.01 mT, 10 scans)

121
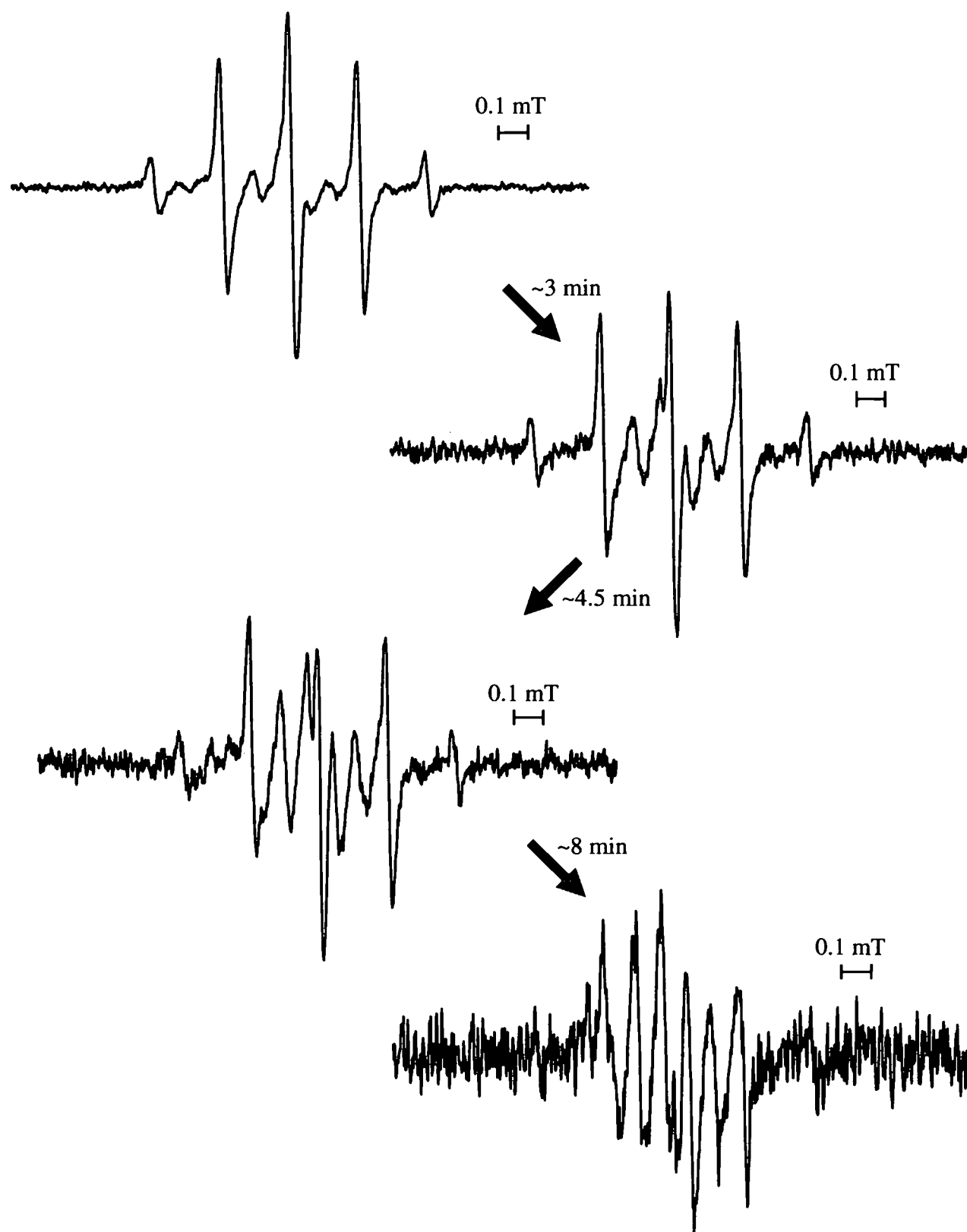
Fig. 3.39. Kinetic measurement of the autoxidation of kaempferol (Proc. 1). (MA 0.038 mT, 1 scan) The times indicate the elapsed period after the 1st spectrum was recorded.

122
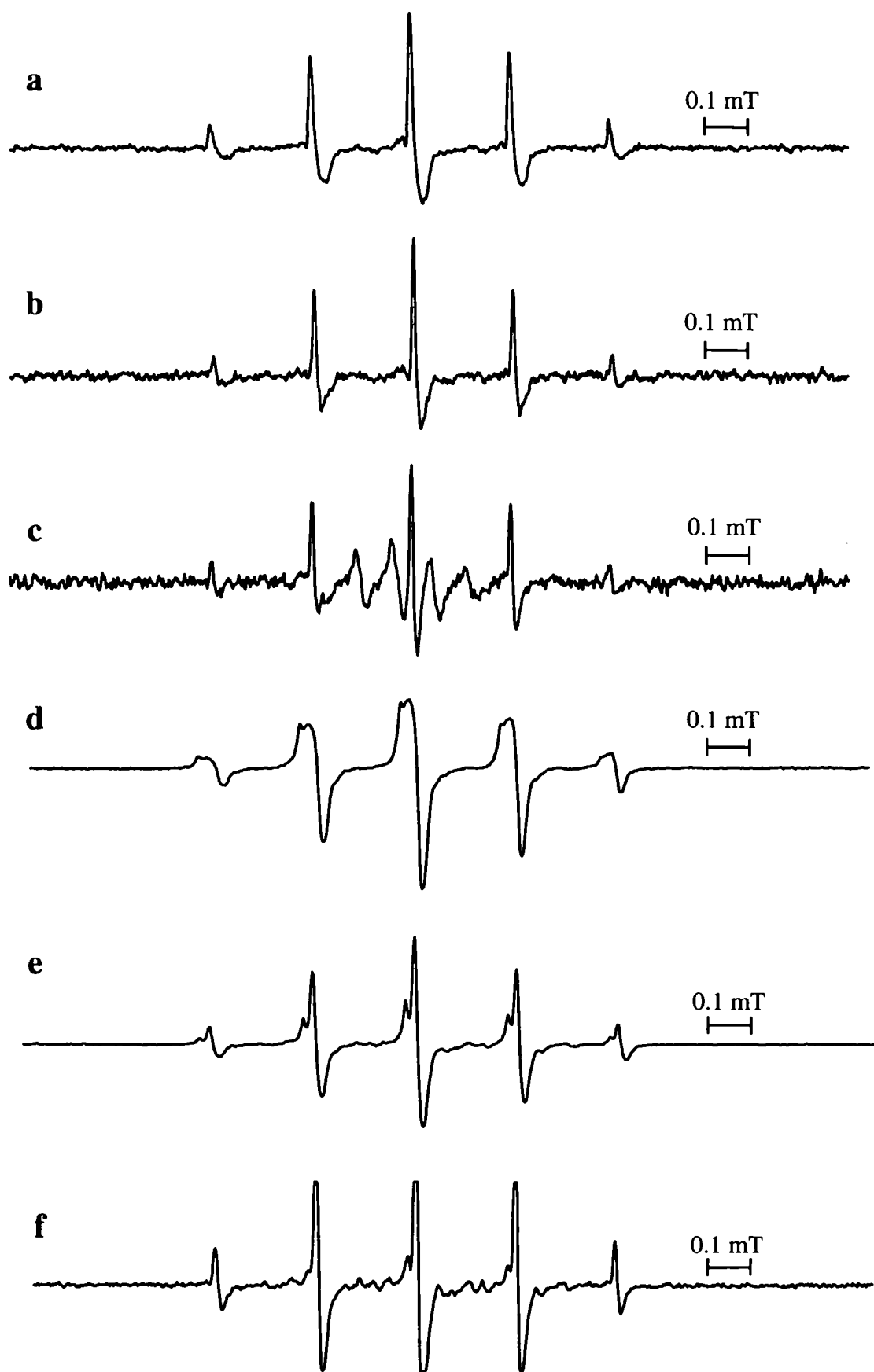
Fig. 3.40. Autoxidation of kaempferol solutions at 0 °C. (a)-(c) one week old solution of kaempferol (MA 0.03 mT), (c) was recorded 15 min. after (a), (d)-(f) freshly prepared solution of kaempferol (MA 0.01 mT), (f) was recorded 41 min. after (d).

123
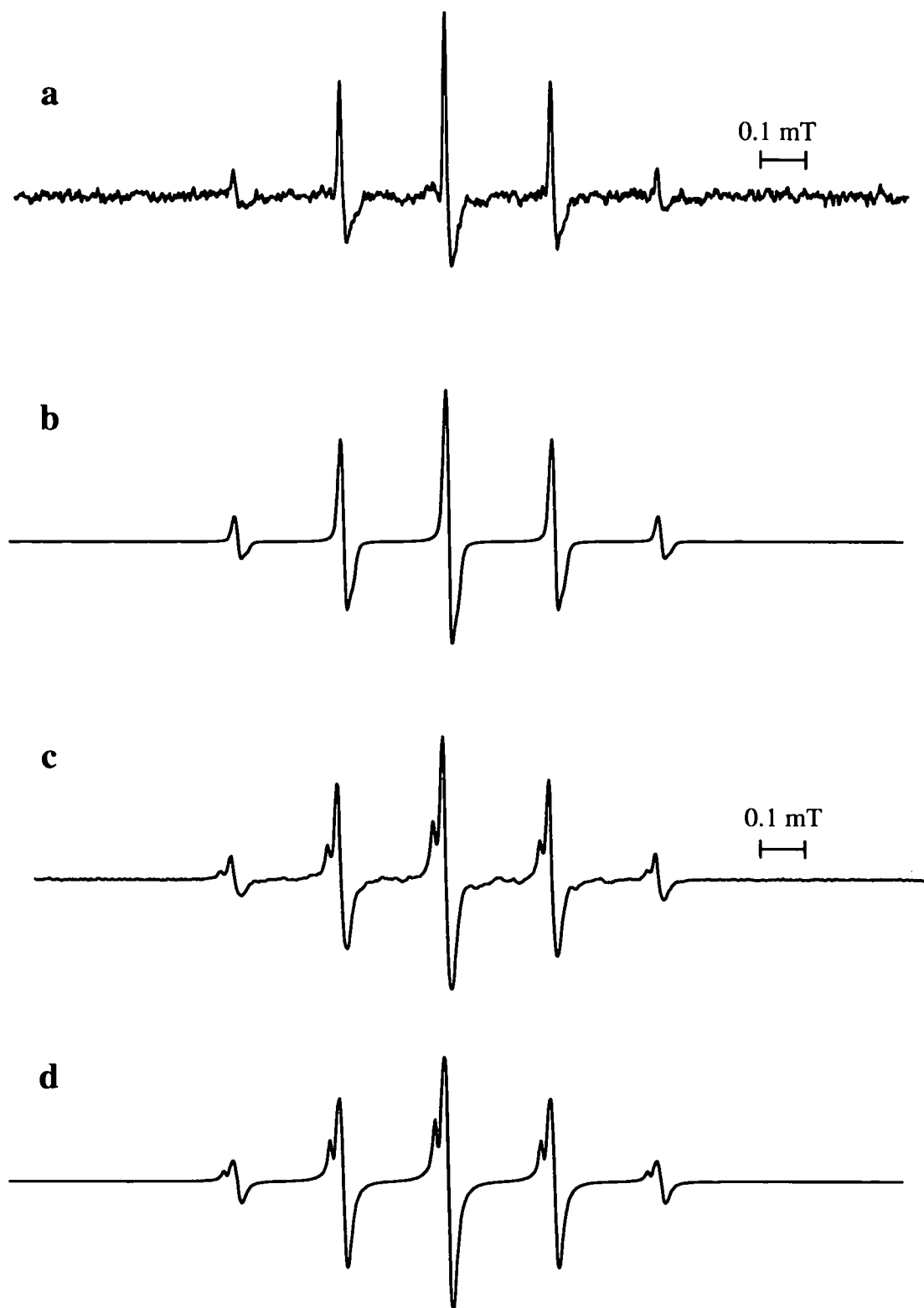
Fig. 3.41. Experimental spectra and simulations from autoxidised kaempferol (Proc. 1). (a) one week old solution of kaempferol, (b) simulation of (a), height ratio of the two compounds 1:0.2, (c) freshly prepared kaempferol solution and (d) simulation of (c), height ratio of the two compounds 1:0.27.
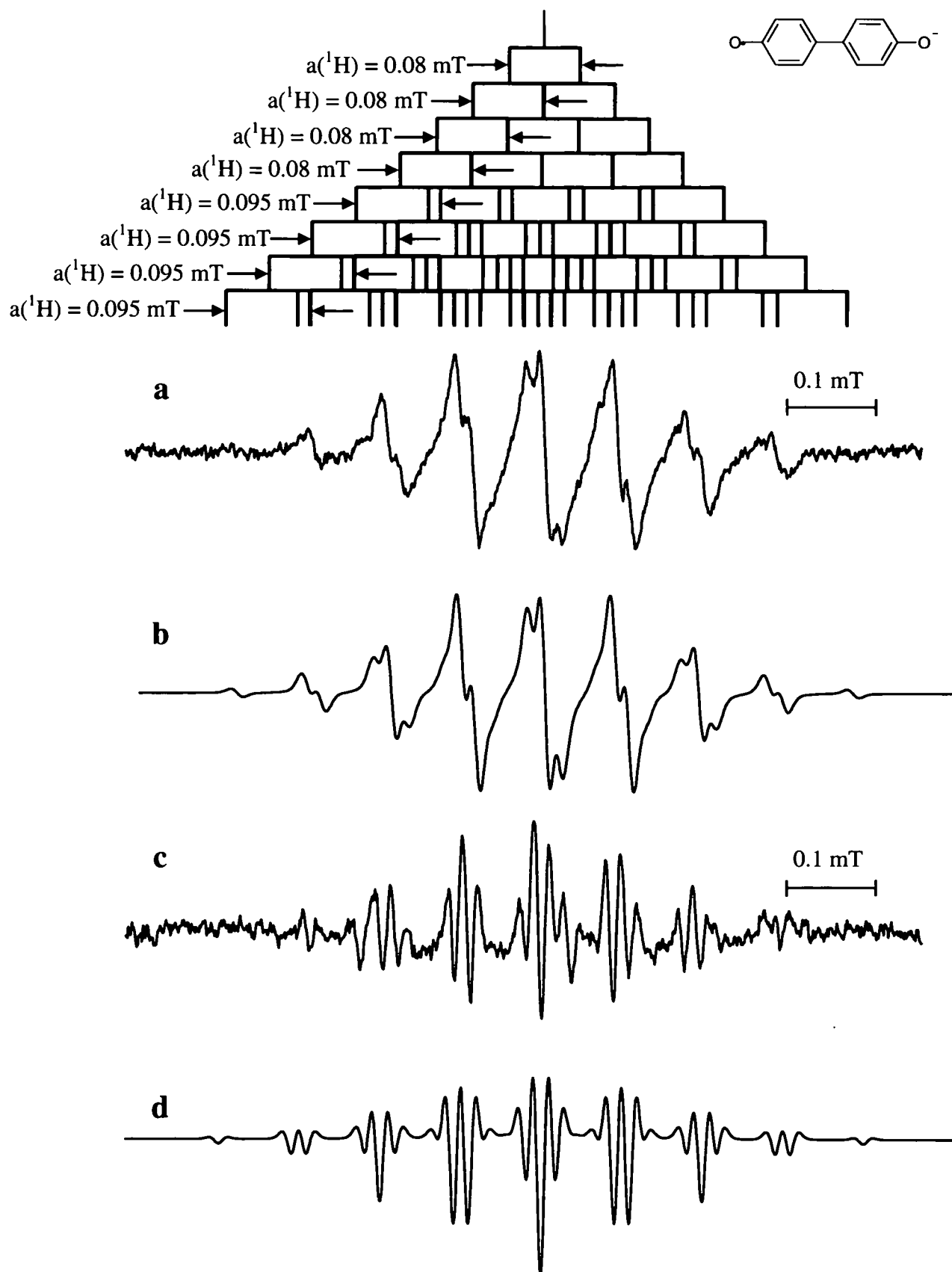
Fig. 3.42. Autoxidation (Proc. 2) of kaempferol using a ratio of kaempferol:NaOH=1.67:1. (a) experimental spectrum, (b) simulation of (a), (c) 2nd derivative of autoxidised kaempferol, (d) simulation of (c). Spectral interpretation is shown by the stick diagram. (MA 0.01 mT, 10 resp. 11 scans)
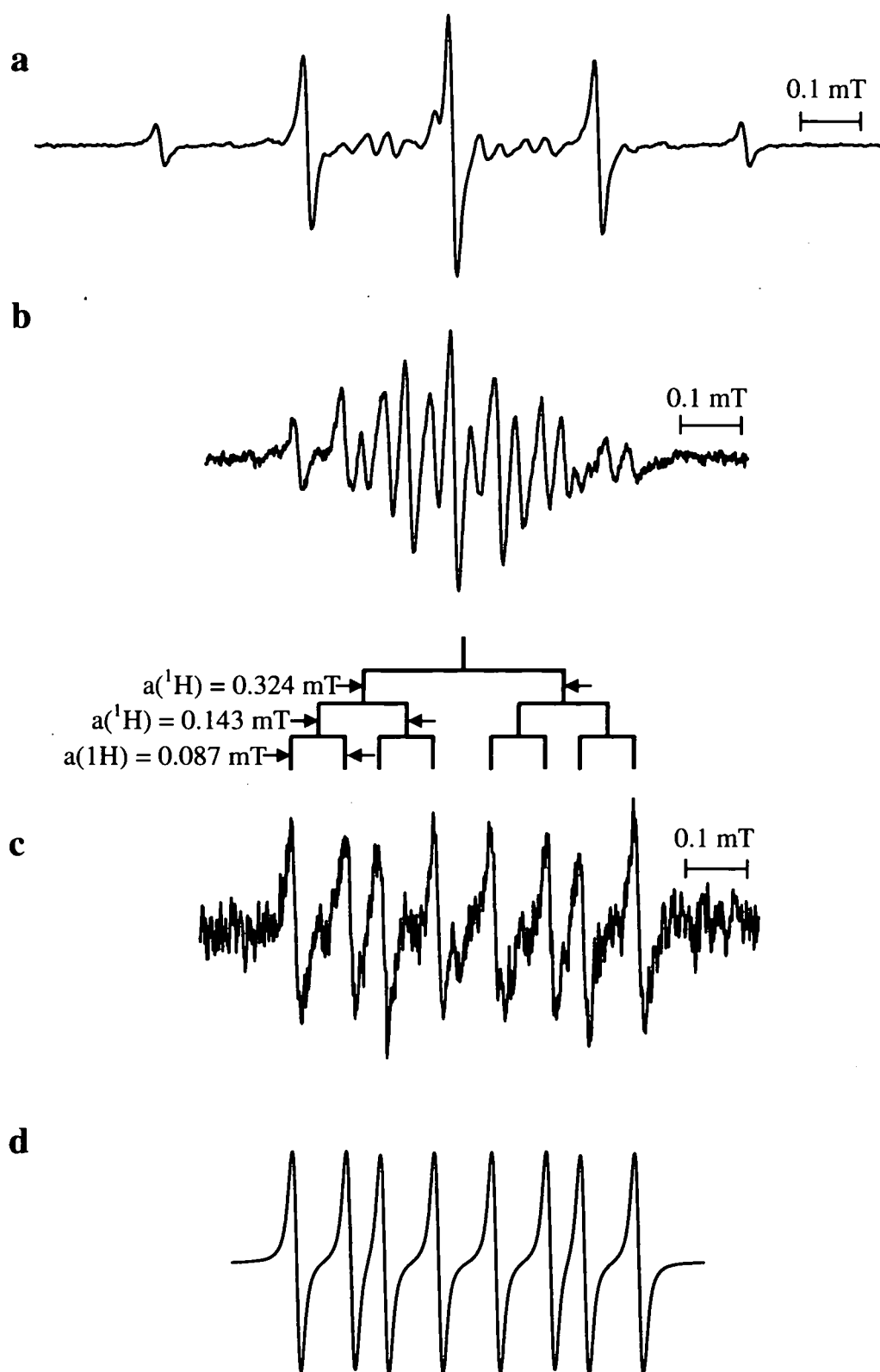
Fig. 3.43. Autoxidation (Proc. 2) of kaempferol using a ratio of kaempferol:NaOH=3:1. (a) first recorded spectrum (3 scans), (b) EPR spectrum obtained 5 min. after the first spectrum, (c) EPR spectrum obtained 21 min. after the first spectrum, (d) simulation of (c). Spectral interpretation of (d) is shown by the stick diagram. (MA 0.01 mT, 10 scans)

$a(^1H) = 0.108$ mT→

$a(^1H) = 0.108$ mT→

$a(^1H) = 0.075$ mT→

$a(^1H) = 0.075$ mT→

$a(^1H) = 0.075$ mT→

$a(^1H) = 0.075$ mT→

a

0.1 mT

b

Fig. 3.44. (a) EPR spectrum of Fig. 3.43.b after subtracting the contribution from compound 3 using the simulated spectrum Fig. 3.43.d, (b) simulation of (a). Spectral interpretation is shown by stick diagram.
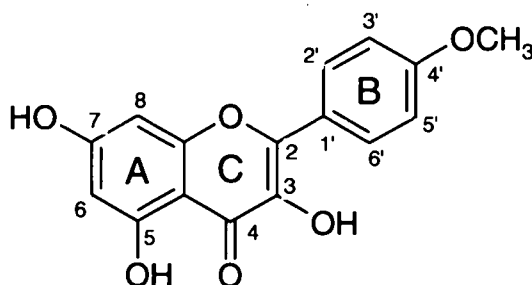
Fig. 3.45. Structure of kaempferide.

Oxidation with potassium superoxide

The use of potassium superoxide in a buffer of pH 7 to oxidise kaempferol resulted in the same quintet spectrum (Fig. 3.46.) as that in Fig. 3.37. A few minor components are also visible in this spectrum.
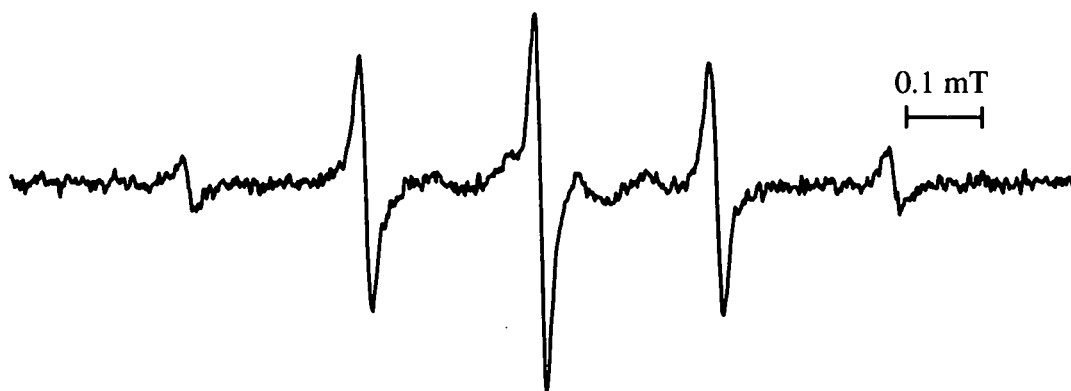
Fig. 3.46. EPR spectrum obtained by oxidation of kaempferol with potassium superoxide. (MA 0.01 mT, 1 scan)
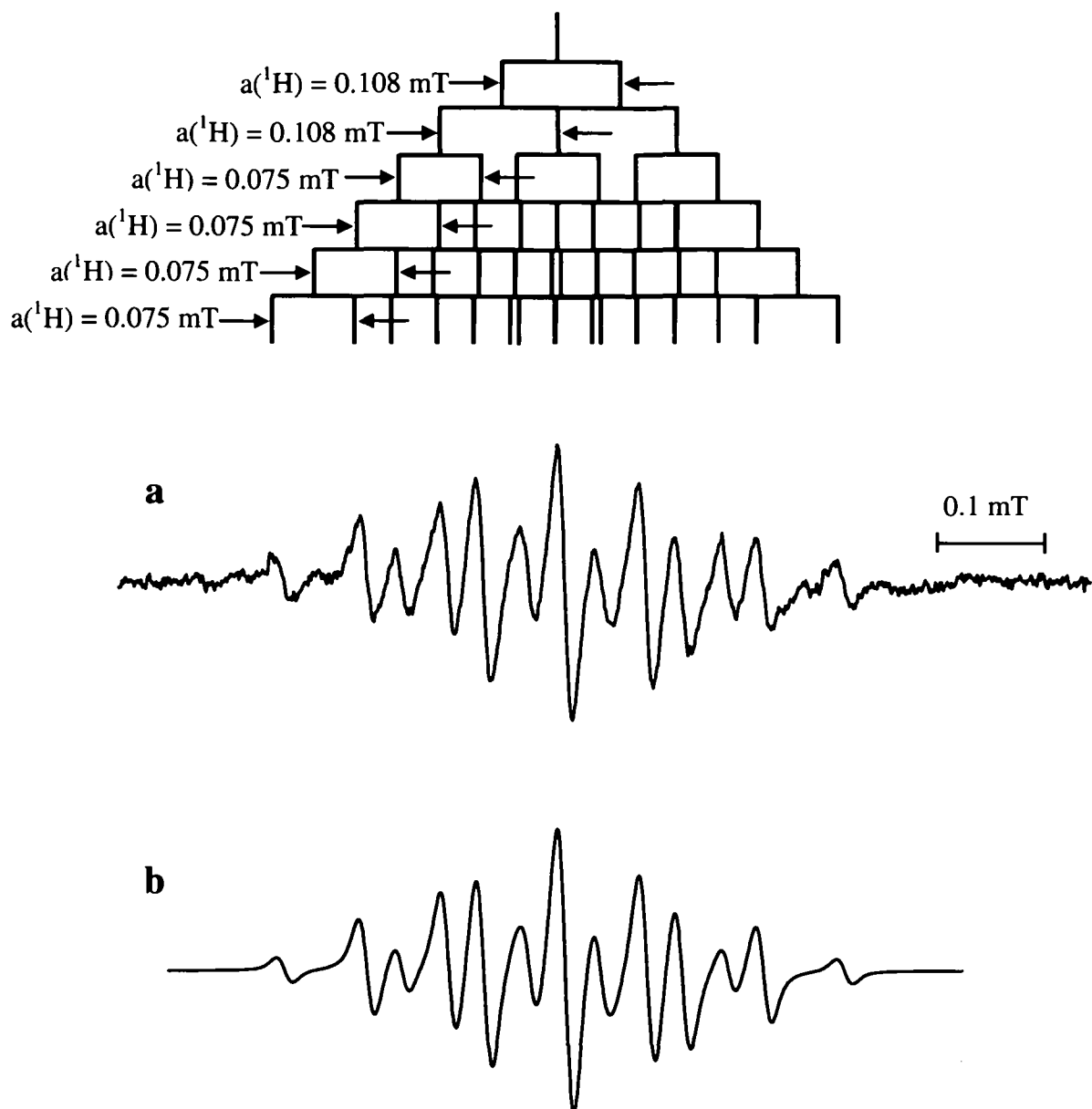
Enzymatic systems: HRP/H₂O₂, X/XO, and Fenton reaction system

Three different enzymatic systems were used to oxidise kaempferol at pH 7. Although the oxidising agent is completely different with these systems (HRP/H_2O_2 forms a ferryl heme complex, X/XO generates superoxide anion radicals, and the Fenton system produces hydroxyl radicals) the same 6-peak spectrum was obtained in all three cases (Fig. 3.47.). These results show again that there is no high oxidation potential necessary to oxidise kaempferol. The spectra could be simulated with five proton couplings around 0.1 mT (Fig. 3.48.).
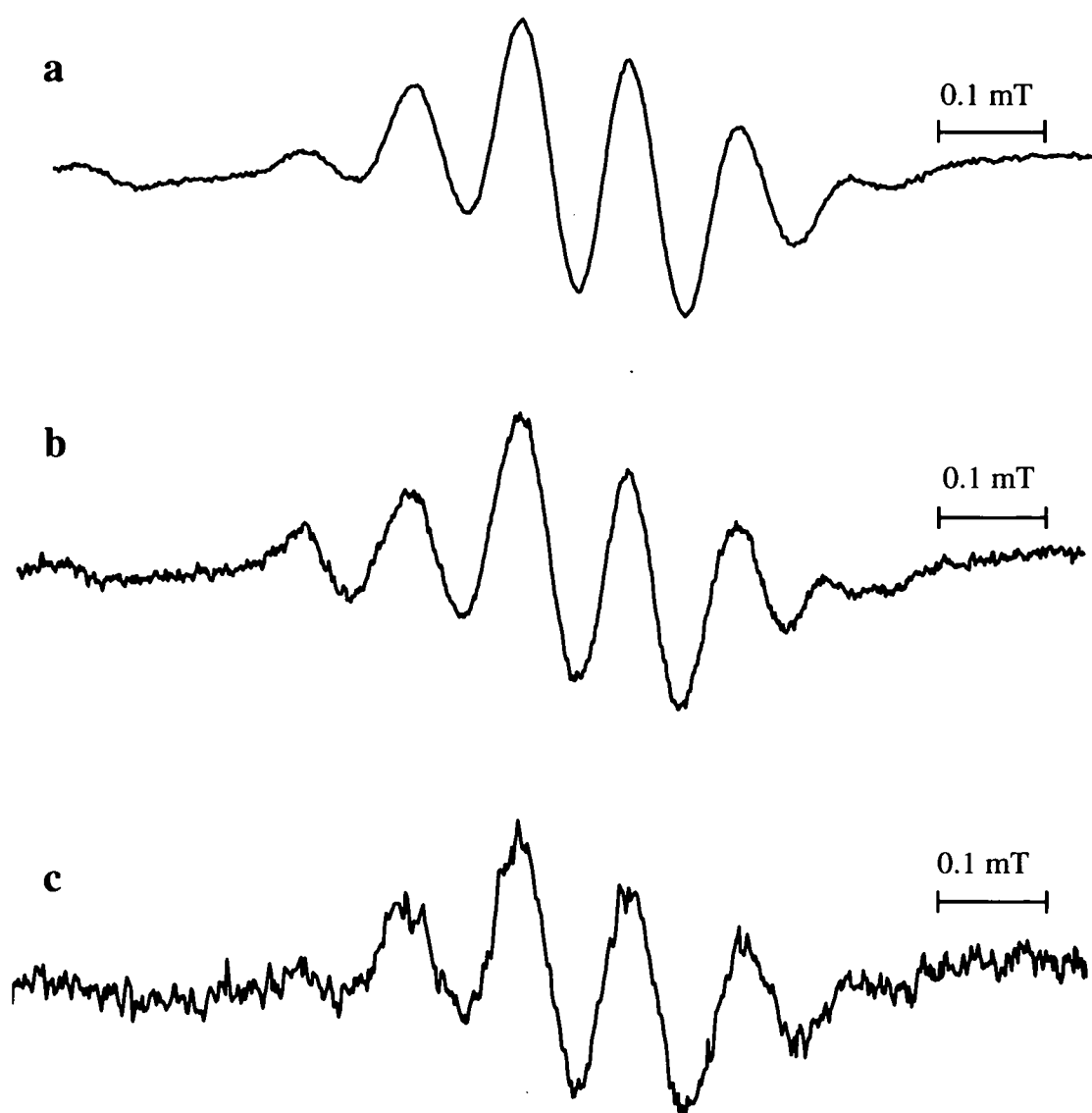
Fig. 3.47. EPR spectrum from kaempferol after reaction with the systems (a) X/XO (0.08 mT, 10 scans), (b) HRP/H_2O_2 (0.05 mT, 20 scans) and (c) Fenton reaction system (0.1 mT, 20 scans).

a(^{1}H) = 0.115 mT⟶

a(^{1}H) = 0.115 mT⟶

a(^{1}H) = 0.103 mT ⟶

a(^{1}H) = 0.087 mT ⟶

a(^{1}H) = 0.087 mT⟶

a

0.1 mT

b

Fig. 3.48. EPR spectrum from kaempferol after reaction with the system X/XO. (a) experimental spectrum, (b) simulation of (a). Spectral interpretation is shown by the stick diagrams.

Structural suggestions

The initial signal in most of the spectra was a quintet, which was identical to that reported by Kuhnle et al. (1969) and assigned 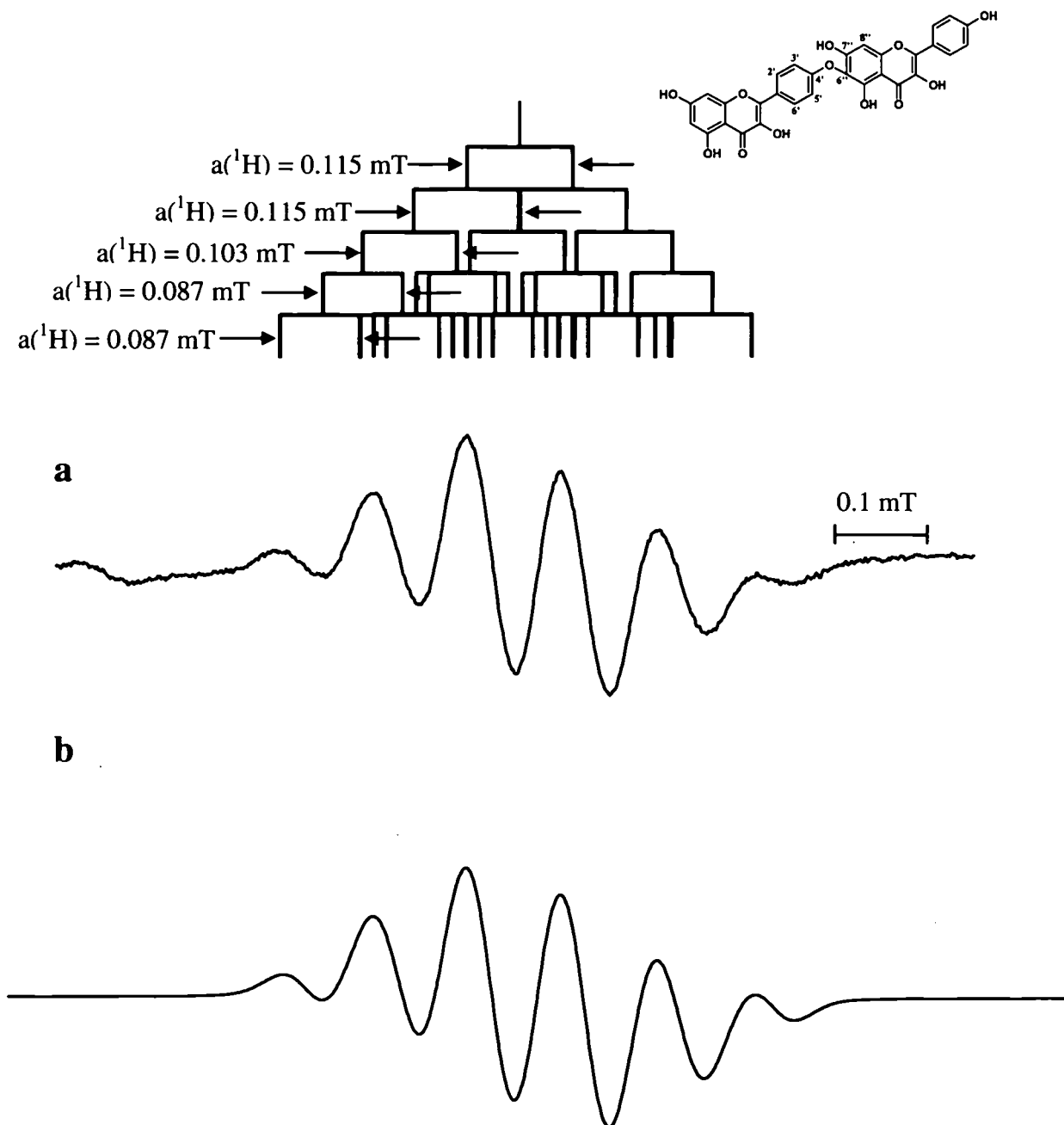to the *p*-benzosemiquinone radical (Fig. 3.49.). An investigation from van Acker et al. (1996) of the half peak oxidation potential of kaempferol in the pH range between 2 and 13 showed that no further release of protons occurred at pH > 9. Thus no protons are involved in oxidation reactions at pH > 9. According to their spin distribution calculations, the spin density in the kaempferol radical is mainly in ring B and remains at the oxygen from which the proton was removed.

Fig. 3.49. Structure of p-benzosemiquinone.

Thus, if autoxidation results in the formation of a phenoxyl derivative on ring B as suggested by van Acker et al (1996), the rapid appearance of the EPR signal from *p*-benzosemiquinone indicates that it is unstable and fragmentation occurs at the 2-1' bond (Fig. 3.50.). Water addition to the double bond is a likely first step after oxidation of ring B. This 2,3-dihydroxyflavanone has been reported by Schröder and Barz (1979). Miller and Schreier (1985) also detected 2,2-dihydroxy-1-(2,4,6-trihydroxyphenyl)-3-(4-hydroxyphenyl)-1,3-propandione, an oxidation product in which ring A is opened. 4-hydroxybenzoic acid and 2,4,6-trihydroxybenzoic acid are two further products of the oxidation reaction of kaempferol with HRP/H_2O_2 (Miller and Schreier, 1985). 4-hydroxybenzoic acid is not very stable in alkaline solution and probably degrades to phenol and CO_2. The intermediate phenoxyl radical is also unstable. Neta et al. (1974) reported the formation of p-hydroquinone from phenoxyl radicals (Fig. 3.51.). Two phenoxyl radicals disproportionate to a phenoxide ion (anion) and a cation of the phenol. In the presence of hydroxyl ions or water, addition of OH groups to the phenol structure is possible at the ortho and para positions to the oxygen. Since the reaction takes place in an alkaline aerated solution, oxidation of hydroquinone occurs very easily

with formation of a benzosemiquinone radical. In the present experiments, formation of the p-benzosemiquinone (Fig. 3.49.) was observed but not o-benzosemiquinone.

The 7 peak spectrum, which was observed after the p-benzosemiquinone radical, could be best simulated by 8 equivalent protons. This radical, therefore, corresponds (most likely) to a dimeric structure where the unpaired electron interacts equally with 8 protons. A possible structure is based on two aromatic rings connected with either an ether bridge or a simple carbon-carbon bond. The original quintet signal, which was always the first signal detected in the spectrum, indicates the presence of semiquinone radicals, and hence quinones, as well as phenoxyl radicals in the solution. It is probable that the short-lived phenoxyl radical reacts with the quinone or semiquinone generating a radical dimer, or a non-radical dimer which is then oxidised to a radical. Based on the equivalence of the eight protons, a most likely structure is suggested in Fig. 3.52.a; two aromatic rings connected by an ether bridge with the unpaired electron delocalised over the whole structure.

To test this interpretation, a solution of phenol with a trace of hydroquinone was oxidised according to Proc. 2. Its spectrum was identical to the 7 peak spectrum from kaempferol. The same signal was also observed after oxidation of a pure phenol solution but the intensity was much lower than from the solution containing a trace of hydroquinone. Thus the hydroquinone is probably part of the radical reaction.

Different ratios of kaempferol and NaOH solution gave different EPR spectra. A slight increase in the kaempferol to NaOH ratio (1.67:1) gave a spectrum with 2 sets of 4 equivalent protons, although their average hyperfine splitting was similar to that of the previous 7-peak spectrum from equivalent 8 protons. It is probable that this signal is also a dimeric radical and may correspond to Fig. 3.52.b, which would be expected to show two sets of four equivalent protons.
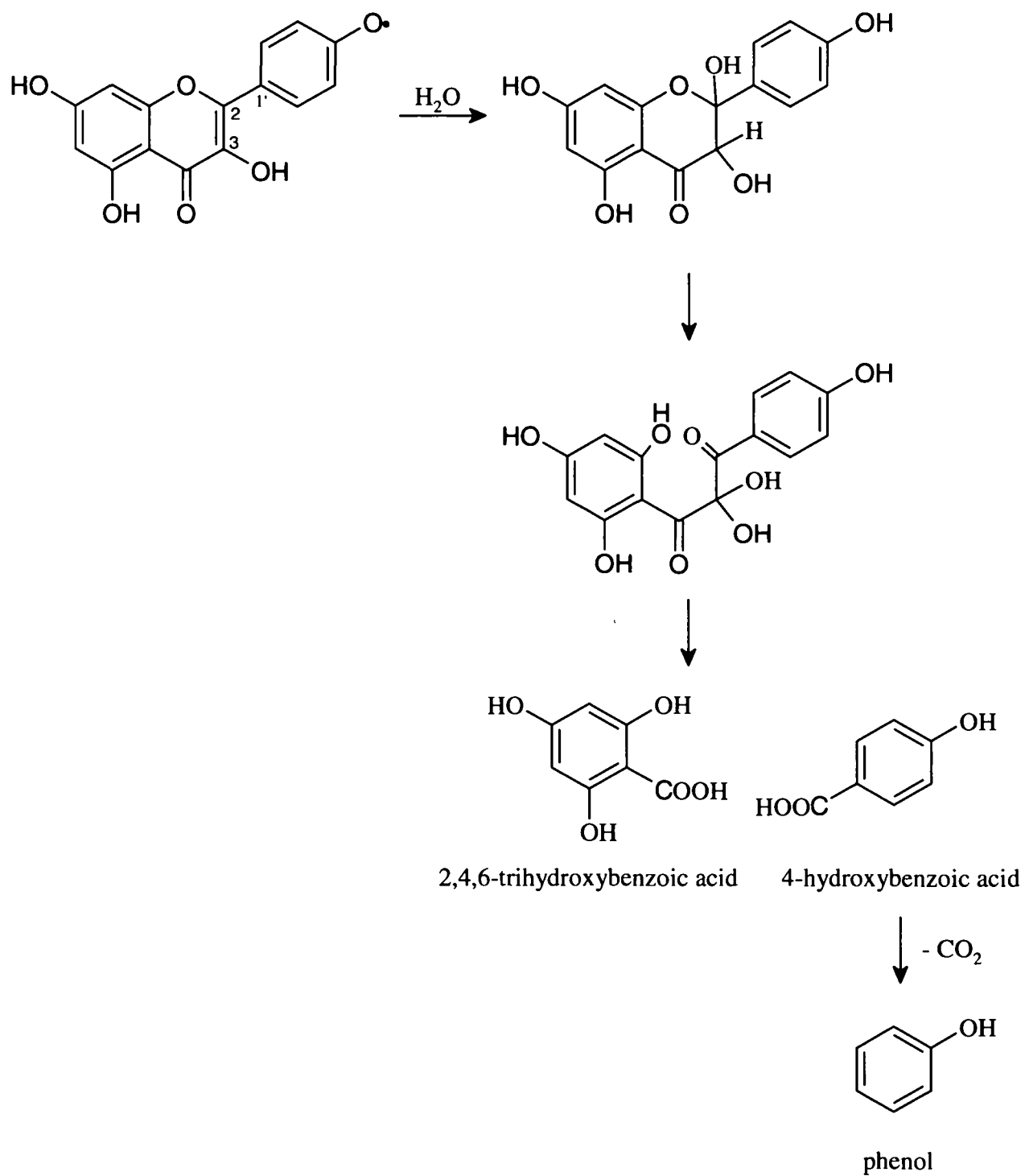
Fig. 3.50. Proposed reaction pathway for the oxidation and disproportionation of kaempferol.
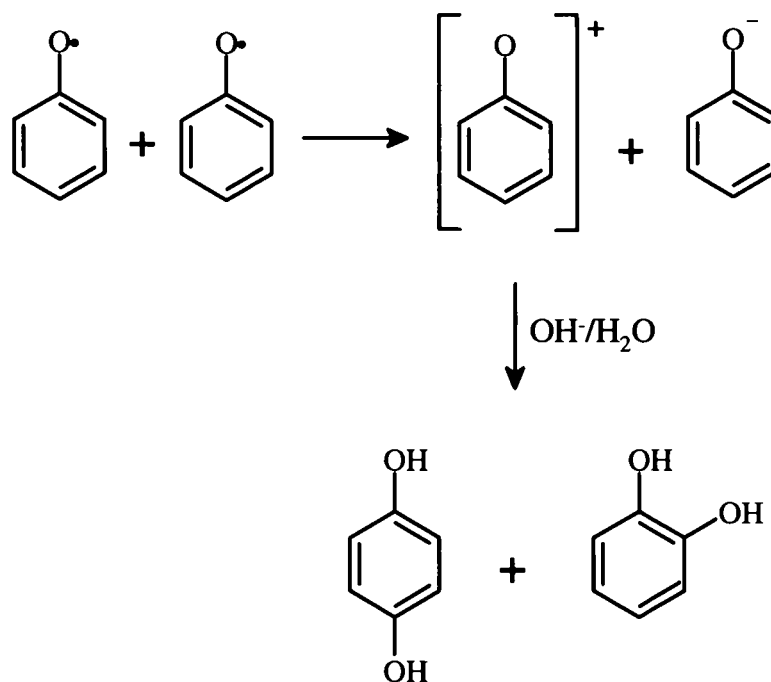
Fig. 3.51. Formation of hydroquinones from phenoxyl radicals (Neta et al., 1974).

A further increase in the kaempferol:NaOH ratio to 3:1 led to the production of two new signals after the quintet disappeared. The first spectrum consisting of 13 peaks was simulated with 6 proton couplings, four equivalent with a smaller value than the other two. The second signal which was detected after the previous one decreased in intensity had 3 inequivalent protons. The structures of these two radicals are most likely products of reactions of breakdown species, since the presence of the quintet at the beginning of the reaction showed an initial degradation of the kaempferol molecule. The higher concentration of kaempferol in this solution than in the previous experiments enhances the probability of dimeric, trimeric and polymeric radical formation. There is, however, not enough information at present to make definite structure suggestions.

134

a

b
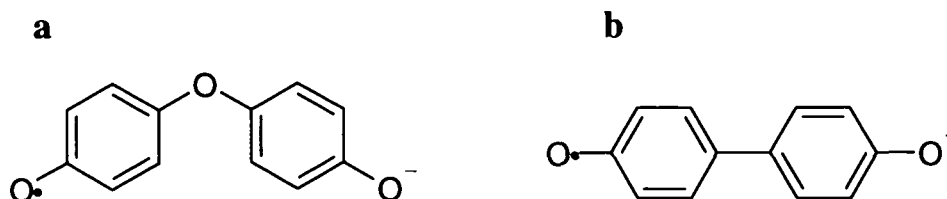
Fig. 3.52. Possible structures of radical dimers produced during autoxidation of kaempferol (the unpaired electron is delocalised over the whole structures but for simplification it is just shown on one oxygen atom).

Oxidation of kaempferol with three different enzymatic systems at physiological pH of 7 resulted in the same spectrum; it consisted of 6 peaks from interaction of the unpaired electron with five ^{1}H nuclei. No other signal was detected before or after the sextet was generated including the quintet which was visible with each experiment at alkaline pH and with potassium superoxide at pH 7. This indicates that the flavonoid structure remained intact. When oxidation of kaempferide by HRP/H_2O_2 was investigated, no radical was detected. Thus the OH-group on ring B must be involved in the oxidation reaction. The generation of a phenoxyl derivative where the OH-group in ring B is oxidised can be excluded because of the small hyperfine splitting constants around 0.1 mT. For para-substituted phenoxyl radicals, hyperfine splittings for the two hydrogens on carbon 3' and 5' would be expected to be in the range 0.4 - 0.7 mT dependent on the substituents (Dixon et al., 1974). The small splittings in the present experiments suggest a dimeric structure where the unpaired electron spin density is delocalised over two aromatic rings and is, therefore, smaller at individual carbon atoms. Loth and Klinge (1964) detected a dimeric structure after oxidation of kaempferol with HRP/H_2O_2. Fig. 3.53.a shows three possibilities for the suggested dimer.

On the basis of the hyperfine splitting constants, the most likely structure consists of an ether bridge from the oxygen on ring B of one kaempferol molecule to carbon 6" in ring A of a second kaempferol molecule (Fig. 3.53.b). The two biggest splittings (a(^{1}H)=0.115 mT) would result from interaction with protons on carbon 3' and 5' and the two smallest splittings (a(^{1}H)=0.087 mT) from coupling with protons on carbon 2' and 6'. The hyperfine splitting constant of a(^{1}H) = 0.103 mT would then be due to the spin density on carbon 8".

135
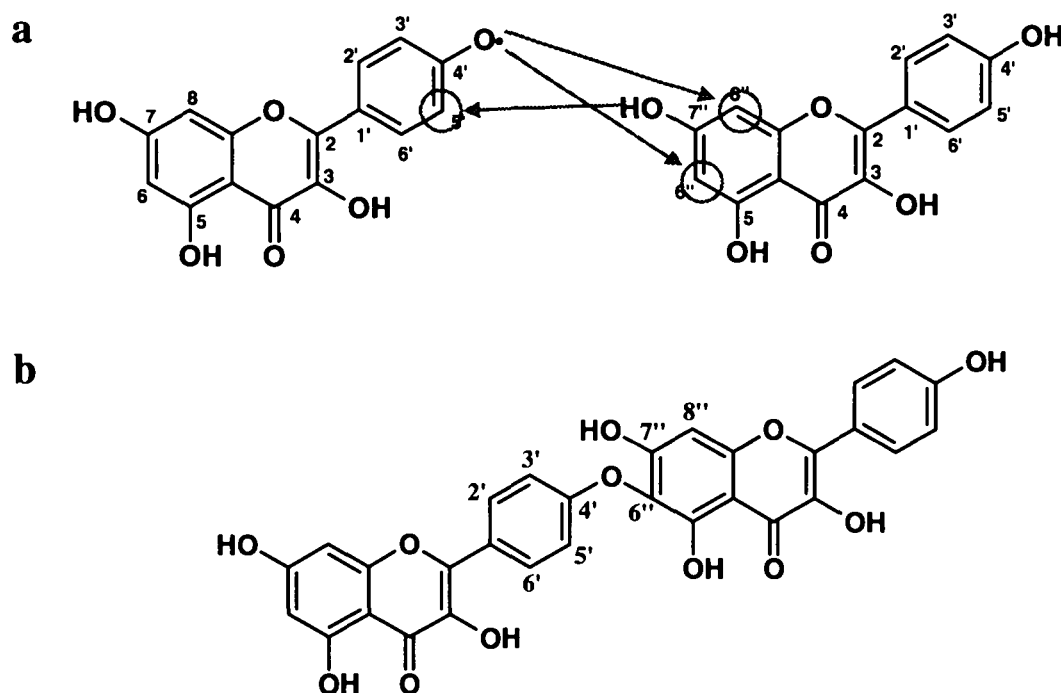
Fig. 3.53. (a) Three possibilities for the dimeric formation from kaempferol after oxidation with HRP/H_2O_2 (Loth and Klinge, 1964), (b) dimeric structure which fits best with the experimental data.

Discussion

Oxidation of kaempferol under different conditions led to the detection of 6 different radicals. One of them, the initial quintet in alkaline solutions, was published by Kuhnle et al. (1969) and assigned to *p*-benzosemiquinone, whereas the other signals are unpublished. Van Acker et al. (1996) also detected a quintet after autoxidation in KOH, but with different hyperfine splitting constants. At pH 7 they recorded a weak triplet when using HRP/H_2O_2 as oxidising agent. This triplet could be part of the six peaks which we detected with HRP/H_2O_2. According to their quantum chemical calculations the spin density of the initial radical produced by kaempferol oxidation is mainly concentrated in ring B on carbon 4'.

The autoxidation experiments showed a dependency of the radical chemistry on the amount of oxygen and on the ratio of kaempferol to NaOH. Yu et al. (1994) reported the formation of dimers from phenoxyl radicals in water after oxidation with HRP/H_2O_2. There is some evidence that most of the detected radicals from our

autoxidation experiments are also based on a dimeric or polymeric structure which follows degradation of kaempferol.

The effect of the HRP/H_2O_2 system on kaempferol has been investigated with various analytical methods. Miller and Schreier (1985) used UV-, IR-spectroscopy, mass spectrometry, ^{1}H-NMR and ^{13}C-NMR to identify products of the reaction such as 4-hydroxybenzoic acid, 2,4,6-trihydroxybenzoic acid, 2,2-dihydroxy-1-(2,4,6-trihydroxyphenyl)-3-(4-hydroxyphenyl)-1,3-propandione and 2-(4-methoxyphenyl)-5,7-dihydroxy-4H-1-benzopyran-4-one(acacetin), but none of these had structures that could be related to the hyperfine structure in our EPR spectra. In the PhD thesis of Miller (1984), there was speculation of a dimeric structure for one reaction product but this was not confirmed. A dimer as product of the reaction of kaempferol-3-glucoside with HRP/H_2O_2 was also suggested by Loth and Klinge (1964) on the basis of results from UV spectroscopy, vapour pressure osmometry (for molecular mass determination) and alkaline degradation. One of the three structural suggestions for this dimeric product (Fig. 3.52.b) could generate a radical that might explain our EPR results.

Takahama (1987) investigated the oxidation of kaempferol by superoxide anion radicals using techniques other than EPR. Two degradation products were detected but neither of them has a structure that correlates with our EPR results. There are some reports about inhibitory effects of kaempferol on the enzyme xanthine oxidase (Cotelle et al., 1996; Selloum et al., 2001; van Hoorn et al., 2002), where it is supposed that OH-groups on carbon 5 and 7 block the position in the enzyme where xanthine should add. Since in our experiments the xanthine/xanthine oxidase reaction commenced before addition of the flavonol, any inhibitory effect will have no consequence for the initial radical generation in the reaction with kaempferol.

Kaempferol has been reported to be able to function as both an antioxidant and a pro-oxidant in Fenton-type reactions (Puppo, 1992). In the presence of Fe^{III}, EDTA and H_2O_2 kaempferol stimulates hydroxyl radical formation by reducing Fe^{III} to Fe^{II}, and therefore helping to redox-cycle the iron. In the presence of ascorbate, there is a competition between the flavonoid and the ascorbate molecule to reduce the iron. Using ATP instead of EDTA which does not allow the redox cycling of iron, kaempferol acts as ·OH scavenger. Both effects were observed to a much lower extent with kaempferol

than with other flavonoids. In our experiments the Fenton system was already generating ·OH-radicals before the flavonol was added on top of it in the flat cell. Thus reaction with ·OH radicals might be the dominant process in the oxidation of kaempferol.

3.5.2. Luteolin

Luteolin is a flavone with a catechol group in ring B. The structure (Fig. 3.54.) is similar to that of kaempferol, but with one additional OH-group on the B ring and no OH group on carbon 3 of the C ring.
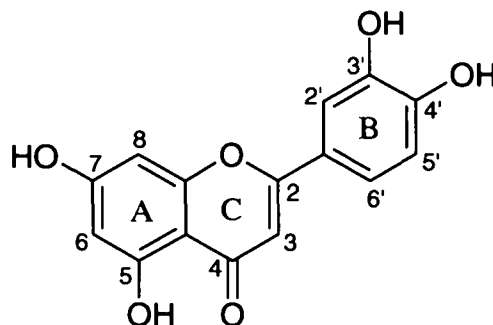
Fig. 3.54. Structure of luteolin.

Autoxidation

Autoxidation of luteolin gave two EPR signals at different times after starting the reaction. The first radical, which was generated using Proc. 1, consists of 6 main peaks (Fig. 3.55.a), but additional structure could be resolved with low modulation amplitude (Fig. 3.55.b) and 2nd derivative recording (Fig. 3.55.d). This spectrum could be simulated with 4 inequivalent proton couplings (Fig. 3.55.c). The hyperfine splitting constants (Table 3.8.) varied slightly depending on the experimental conditions. The EPR spectra obtained from Proc. 2 are shown in Fig. 3.56.

Table 3.8. Hyperfine splitting constants (mT) of the 1st radical of autoxidized luteolin in relation to the experimental setup.

	Proc. 1	Proc. 2 (luteolin:NaOH)		
		1:1	1.67:1	3:1
$a(^1H)$	0.275	0.277	0.275	0.278
$a(^1H)$	0.150	0.150	0.150	0.151
$a(^1H)$	0.125	0.122	0.125	0.132
$a(^1H)$	0.117	0.102	0.117	0.122

This 1st radical was not stable in all experiments and after around 25 minutes the signal in Proc. 1 had changed into an 8 peak spectrum from 3 inequivalent proton splittings (Fig. 3.57.). Similar spectra were also obtained using Proc. 2 (Fig. 3.58.). Again there were slight differences in the hyperfine splittings observed using the different experimental setups (Table 3.9.).

If $ZnCl_2$ was added to the alkali solution in the Eppendorf tube (Proc. 2), the 1st radical was stabilised for more than 1 hour and formation of the 2nd radical was completely prevented.

Table 3.9. Hyperfine splitting constants (mT) of the 2nd radical of autoxidised luteolin in relation to the experimental setup.

	Proc. 1	Proc. 2 (luteolin:NaOH)		
		1:1	1.67:1	3:1
a(^{1}H)	0.465	0.475	0.463	0.450
a(^{1}H)	0.083	0.084	0.082	0.080
a(^{1}H)	0.025	0.026	0.026	0.027

Oxidation of luteolin with the three different enzymatic systems (HRP/H_2O_2, X/XO, Fenton reaction system) and with potassium superoxide at pH 7 resulted in a 6 peak spectrum (Fig. 3.59.) that is similar to the one obtained with autoxidation (Proc. 1). However, with potassium superoxide the spectrum consisted of sharp lines with a good hyperfine splitting resolution whereas with the systems HRP/H_2O_2, X/XO, and the Fenton reaction the resolution of the spectra was poorer than that obtained with autoxidation; with these spectra resolution was not improved either by decreasing the modulation amplitude or flushing the solutions with N_2 gas.

Structural suggestions

Two different EPR spectra from oxidised luteolin were observed under different conditions at pH 7 and pH 13. These spectra are similar to those reported by others (Cotelle et al., 1996; Kuhnle et al., 1969 and van Acker et al., 1996). The oxidation site is most likely the catechol group on ring B, which is known to be the region responsible

for the antioxidant activity in flavonoids (Amić et al., 2003). The probable structure of the radical from oxidised luteolin is shown in Fig. 3.60.

The largest splitting can be assigned to the proton on carbon 6', whereas smaller splittings around 0.1 mT come from interactions with protons in positions 2', 5' and 3 (Cotelle et al., 1996).

The 2nd radical of luteolin, which was detected at pH 13 after the 1st radical decreased in intensity, was also reported from Cotelle et al. (1996). These authors explained the structure as resulting from oxidation at carbon 2' (Fig. 3.61.). With this radical, the largest hyperfine splitting again comes from the proton on carbon 6'.

A comparison of the various hyperfine splitting constants from the present experiments with those in the literature is presented in Table 3.10. There is good agreement between our data and those of Cotelle et al. (1996), but the results are completely different from those published by van Acker et al. (1996).
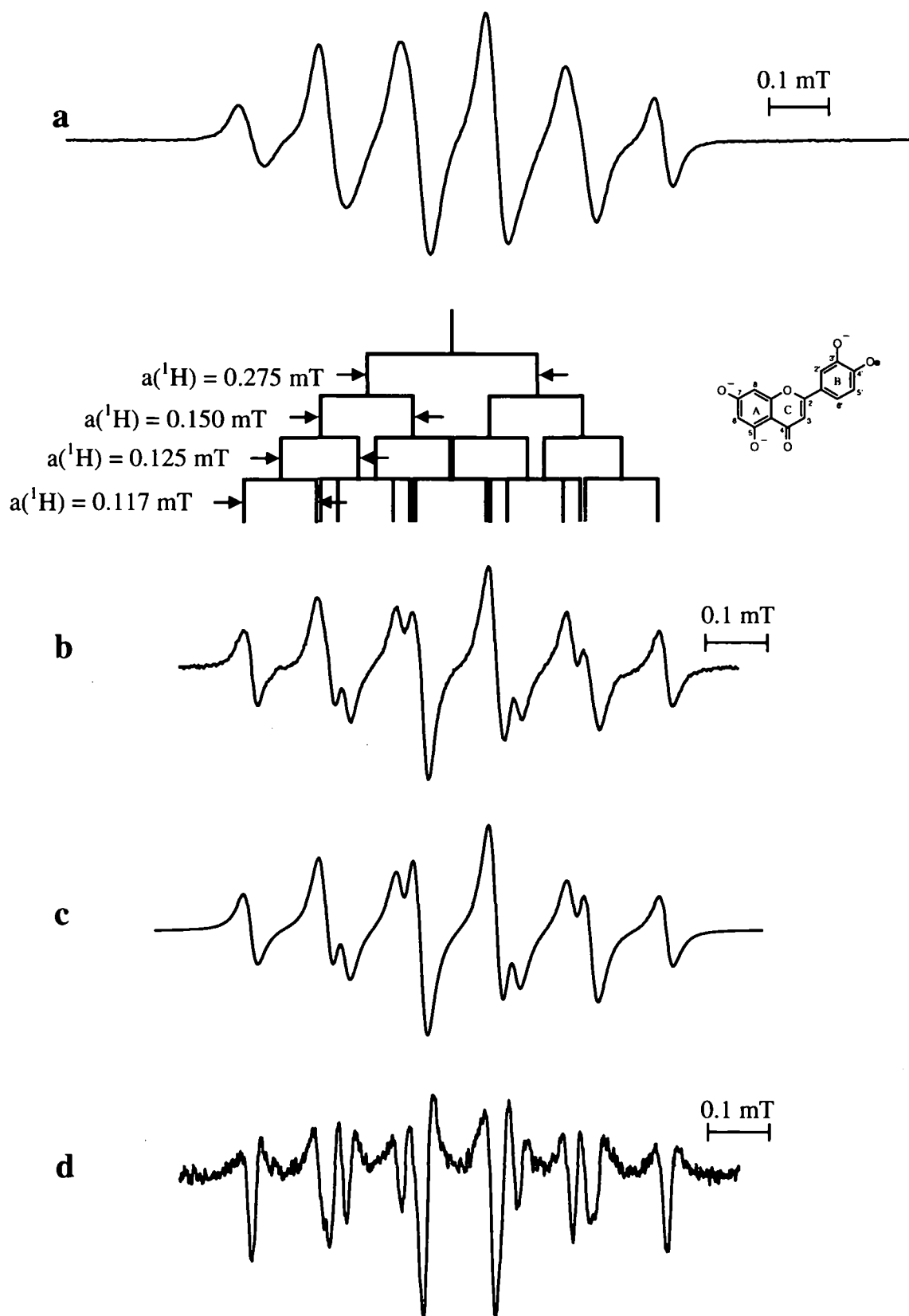
Fig. 3.55. EPR spectra of the 1st radical from luteolin autoxidised using Proc. 1. (a) spectrum recorded in the 1st derivative, MA 0.034 mT, (b) spectrum recorded in the 1st derivative, MA 0.01 mT (c) simulation of (b), (d) spectrum recorded in the 2nd derivative.
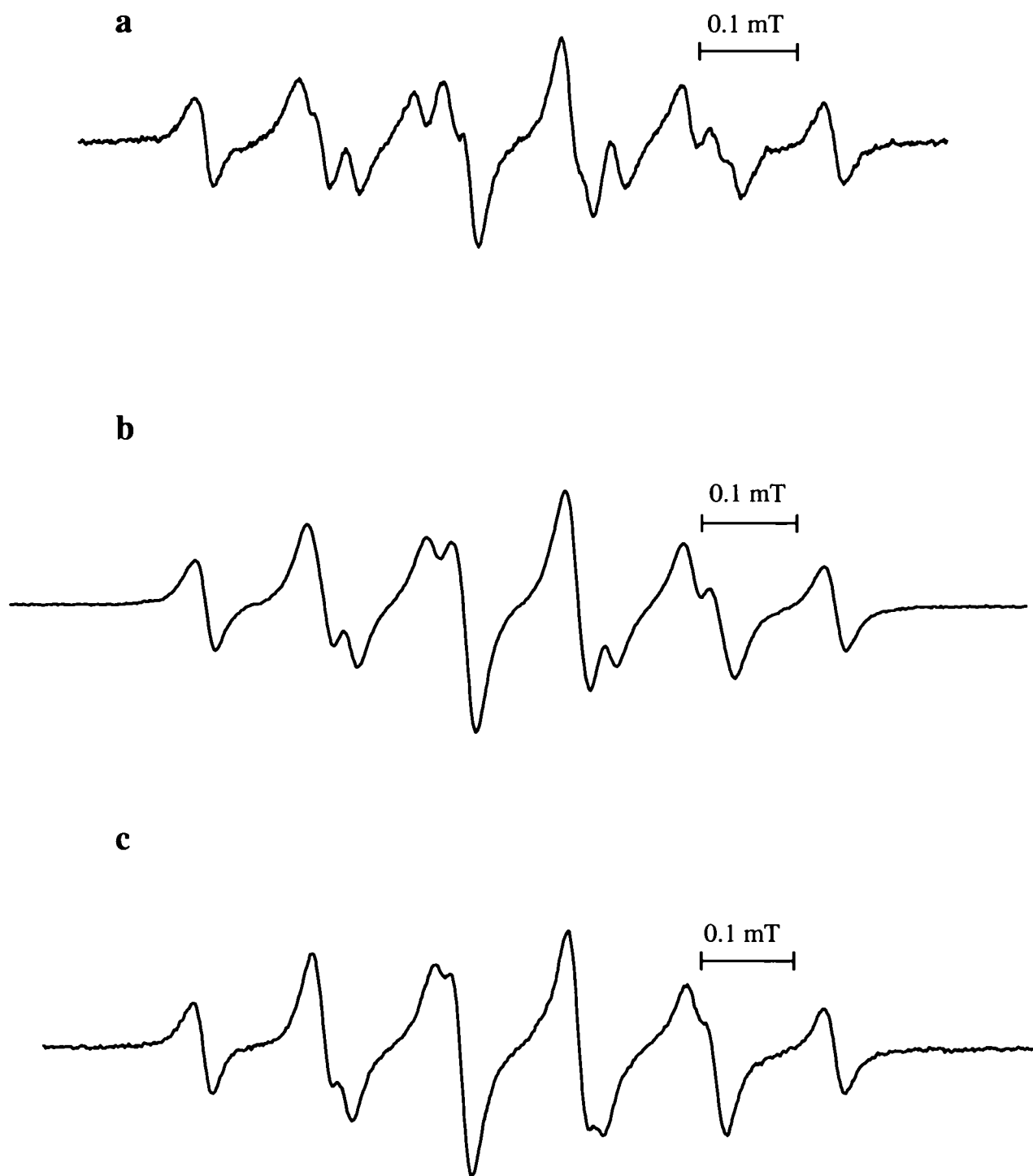
Fig. 3.56. EPR spectra of the 1st radical from luteolin autoxidised using Proc. 2. (a) luteolin:NaOH = 1:1 (MA 0.008 mT, 10 scans) (b) luteolin:NaOH = 1.67:1 (MA 0.01 mT, 9 scans), (c) luteolin:NaOH = 3:1 (MA 0.003 mT, 7 scans).

143

$a(^1H) = 0.465$ mT $\longrightarrow$

$a(^1H) = 0.083$ mT $\longrightarrow$

$a(^1H) = 0.025$ mT $\longrightarrow$

a

0.1 mT

b
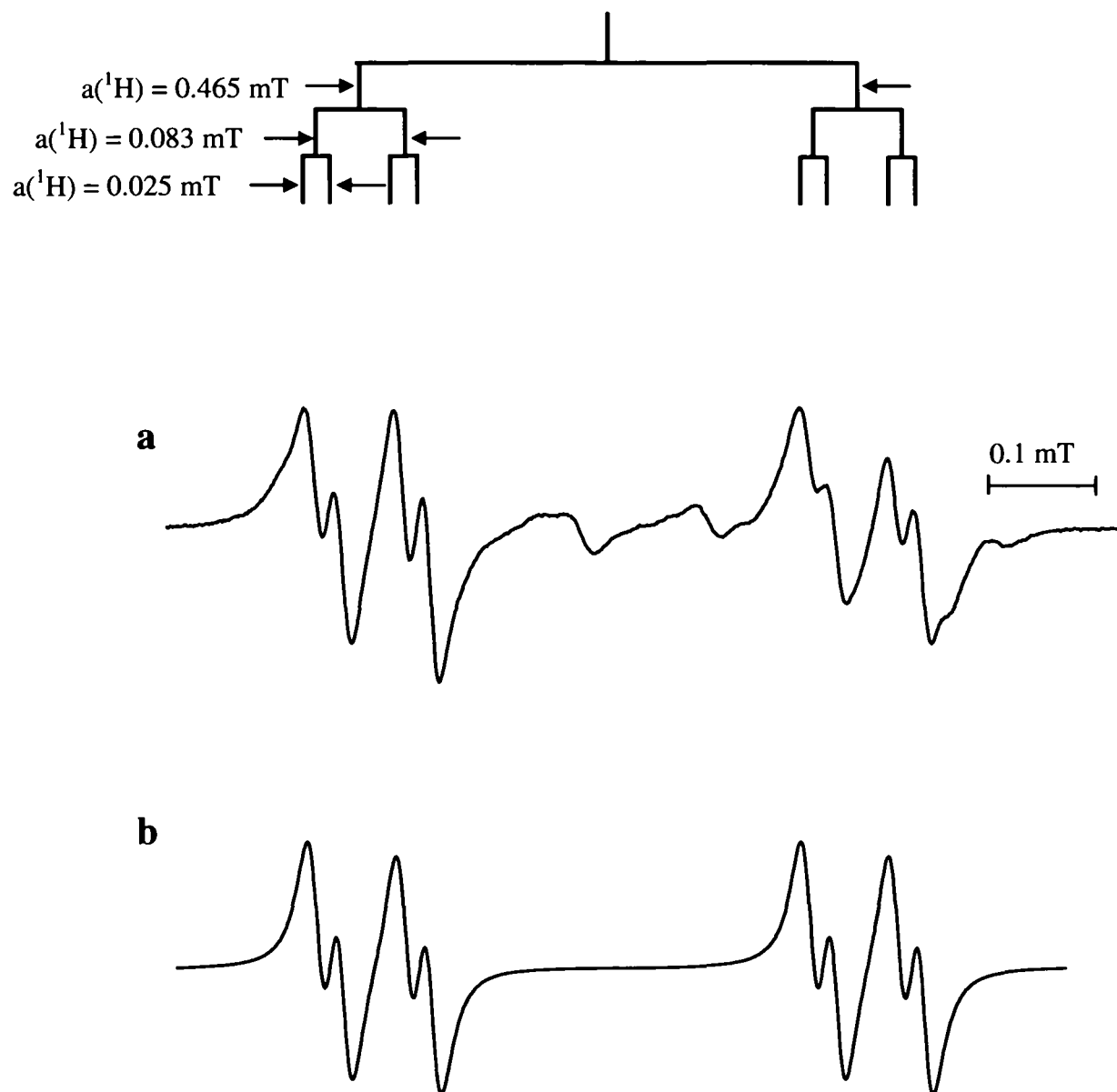
Fig. 3.57. EPR spectrum of the 2nd radical from luteolin autoxidised using Proc. 1. (a) experiment spectrum (MA 0.01 mT, 10 scans), (b) simulation of (a).

144
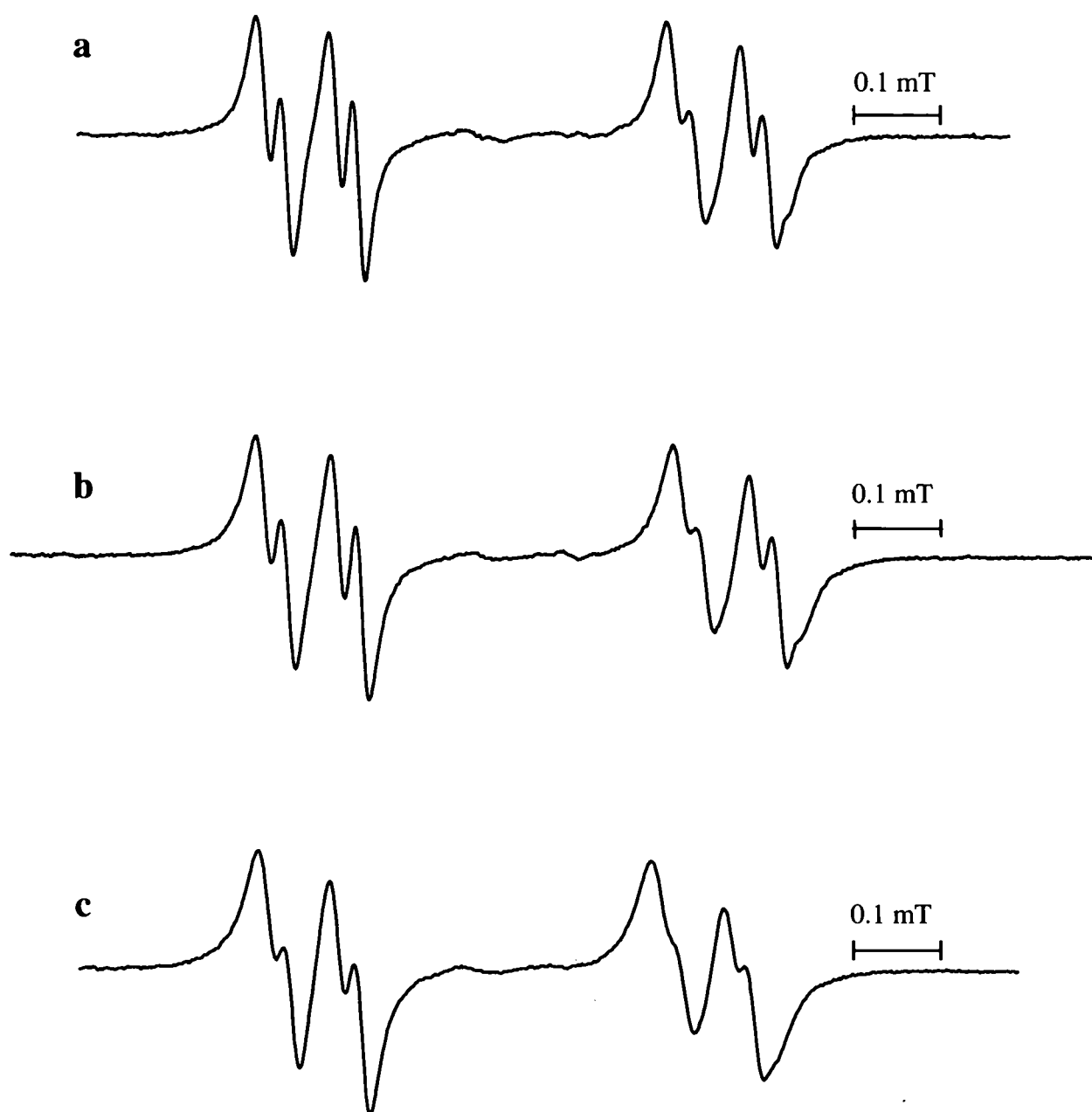
Fig. 3.58. EPR spectrum of the 2nd radical from luteolin autoxidised using Proc. 2. (a) luteolin:NaOH = 1:1 (MA 0.01 mT, 20 scans), (b) luteolin: NaOH = 1.67:1 (MA 0.01 mT, 10 scans), (c) luteolin:NaOH = 3:1 (MA 0.008 mT, 10 scans).
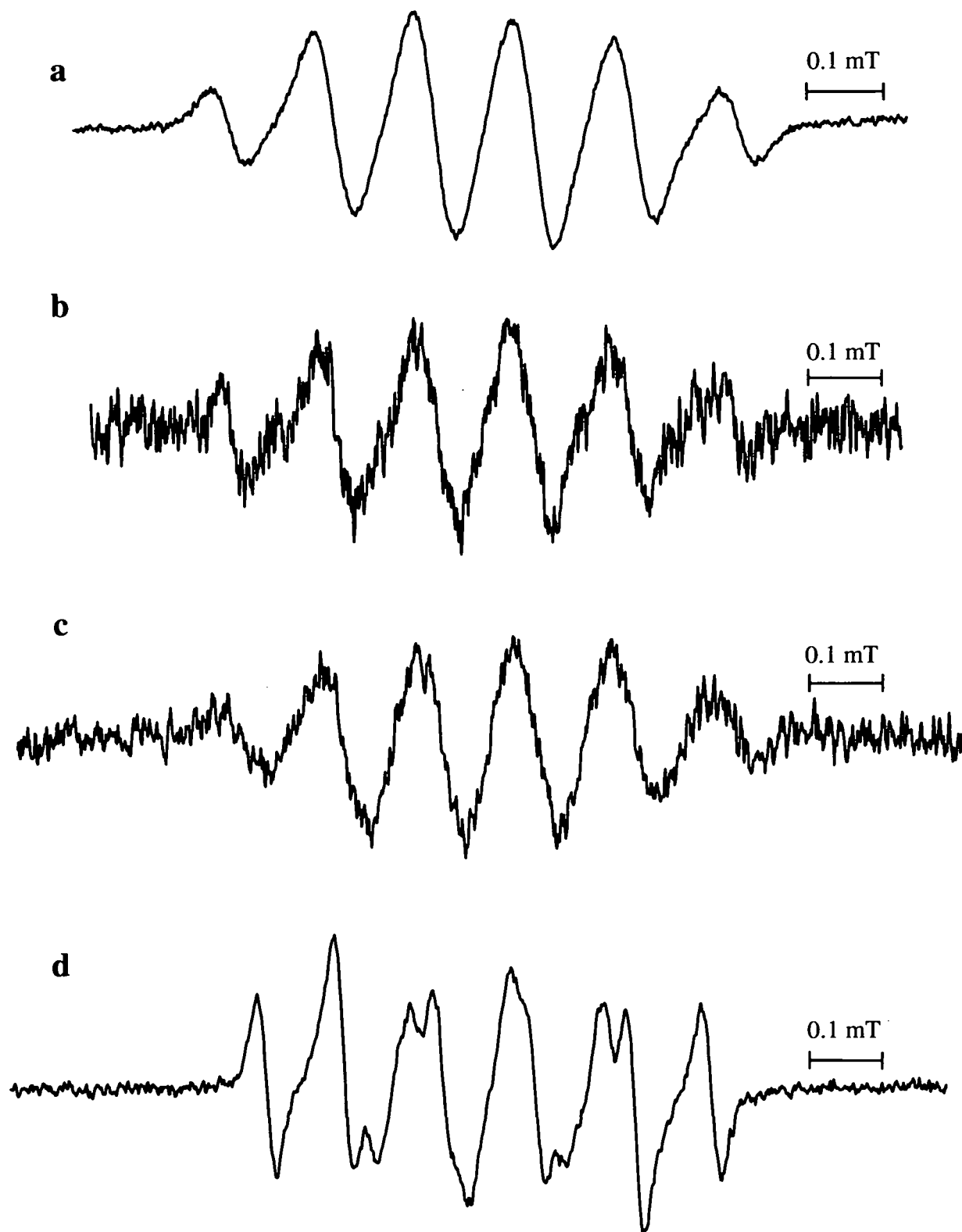
Fig. 3.59. EPR spectra from luteolin oxidised by (a) HRP/H_2O_2 (MA 0.05 mT, 20 scans), (b) X/XO (MA 0.03 mT, 17 scans), (c) Fenton reaction system (MA 0.08 mT, 30 scans), (d) KO_2 (MA 0.04 mT, 10 scans).
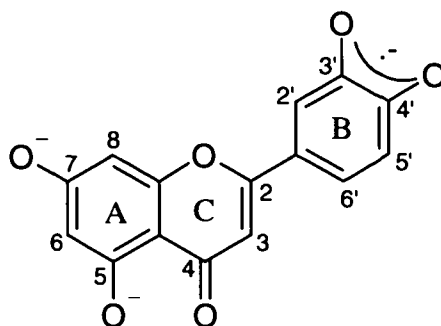
Fig. 3.60. Proposed structure for the 1st radical from luteolin oxidised under alkaline conditions.
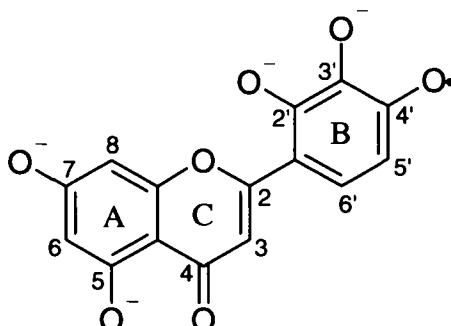
Fig. 3.61. Suggested structure for the 2nd radical from luteolin oxidised under alkaline conditions.

Table 3.10. Hyperfine splitting constants (mT) from our experiments compared with previously reported data.

1st signal   2nd signal
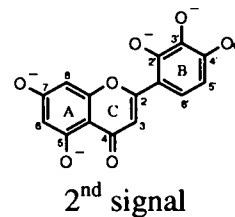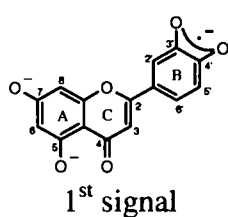
		a(^{1}H=2')	a(^{1}H=5')	a(^{1}H=6')	a(^{1}H=3)
1st signal	Proc. 1	0.117	0.150	0.275	0.125
	Cotelle 1996	0.115	0.140	0.260	0.125
	Kuhnle 1969	0.160	0.140	0.260	0.125
	van Acker 1996	0.184	0.184	0.326	0.099
2nd signal	Proc. 2 (1:1)		0.840	0.475	0.026
	Cotelle		0.850	0.500	0.025

Discussion

Two different EPR signals were detected during the oxidation of luteolin. The present results were in close agreement with those published by Cotelle et al. (1996), who investigated the autoxidation of various flavonols and flavones with catechol and pyrogallol structures in ring B. In contrast to the experiments with kaempferol, where the radicals seen in the EPR spectra correspond to either fragmentation or dimerisation of the oxidised molecule, the flavonoid structure was stable in oxidised luteolin, and radicals are formed by deprotonation and electron abstraction from one of the OH-groups in ring B. A second radical, which was observed at pH 13 but not at pH 7, probably results from hydroxylation at the 2' position on ring B. Cotelle et al. (1996) obtained this spectrum after increasing the pH to 13, whereas our spectrum developed over the time at pH 13.

Formation of the 2nd radical was prevented by $ZnCl_2$ at pH 13, and the 1st radical was stable for more than 1 hour under these conditions. Flavonoids with catechol groups on ring B are able to form complexes with Zn^{2+} ions, which thus prevent the oxidised molecule from dimerisation or solvent attack (Le Nest et al., 2004). Hydroxylation of this complex was, therefore, completely inhibited.

The spectrum of the 1st EPR signal in van Acker et al. (1996) appeared identical to our spectrum, but using their reported hyperfine splitting constants produced a completely different spectrum on simulation. Furthermore, they were not able to detect a signal using HRP and H_2O_2 at pH 7.4, which may be a consequence of the different experimental setup they used. In our case the flavonoid solution had contact with the solution where ·OH-radicals were already generated in the flat cell, whereas van Acker et al. (1996) included the flavonoid from the beginning in the radical generating solution. Recently, Huang et al. (2005) have reported that HRP can be inactivated by phenoxyl radicals generated by reaction of H_2O_2 with phenols. If luteolin has a similar effect on the enzyme, this could explain the failure of van Acker et al (1996) to observe radical formation in their HRP/H_2O_2/luteolin system.

Oxidation of luteolin by KO_2 resulted in a similar spectrum to the initial sextet spectrum obtained from autoxidation.

The spectra obtained using X/XO and the Fenton reaction system were weak, whereas the identical spectrum obtained with HRP/H_2O_2 was stable and sufficiently intense for good signal to noise ratios to be obtained with single scans. However, all were essentially identical.

3.5.3. Rosmarinic Acid

Rosmarinic acid (RA) is a major phenolic component of *Rosemarinus officinalis L.* The structure consists of two aromatic rings both of which have catechol groups (two OH-groups in *o*-position) that are separated by a carboxylic acid, a carbonyl, an ether group, and a double bond (Fig. 3.62.).
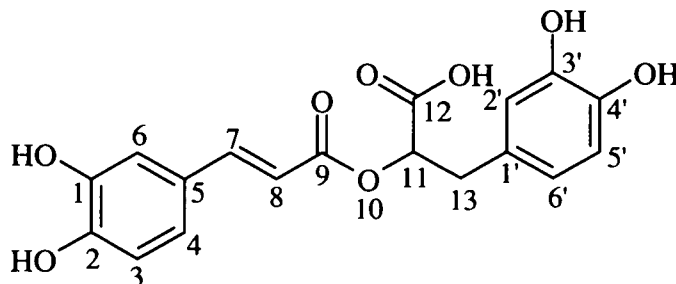
Fig. 3.62. Structure of rosmarinic acid.

Autoxidation

Autoxidation of RA using Proc. 1 gave two radical components, a 19 peak spectrum (Fig. 3.63.) first, followed by a 14 peak spectrum (Fig. 3.64.). If air was flushed through the flat cell, the same two spectra were observed, but with smaller intensities. The spectrum of the 1st radical component was simulated with 5 proton couplings, including two equivalent splittings of 0.36 mT, whereas the spectrum of the 2nd radical component was simulated with 4 inequivalent protons.

Autoxidation of RA using Proc. 2 always resulted in a 14-peak spectrum irrespective of the RA:NaOH ratio, although there were slight differences in the hyperfine splittings (Fig. 3.65.). However, with a RA:NaOH ratio of 3:1, a weak 19 peak spectrum was detected initially, but was then quickly replaced by the 14 peak spectrum, whereas the 14 peak spectrum was observed from the outset with 1:1 and 1.67:1 ratios.

Oxidation with potassium superoxide

Oxidation of RA with KO_2 led first to a spectrum of at least three components, but two of them could not be separated or identified. After c. 25 minutes a single component spectrum of at least 15 peaks was detected (3rd radical component of RA). This radical was already partially visible in the initial spectrum. Fig. 3.66. shows these spectra along with a simulation of the 3rd component with 5 proton couplings.

Enzymatic systems

RA oxidised by the enzymatic systems HRP/H_2O_2, xanthine/xanthine oxidase and the Fenton reaction system, at pH 7, all gave similar spectra consisting of at least two components (Fig. 3.67.). The spectra obtained using HRP/H_2O_2 and the Fenton reaction were recorded with a higher modulation amplitude since their signal intensities were low. Smaller peak splittings can be seen in the spectrum where X/XO was used as oxidising agent because of its higher signal intensity. When the Fenton reaction was performed with ascorbic acid to generate a 'recycling Fenton system' no RA radicals were seen; only the ascorbate radical was visible. The spectrum obtained with X/XO is similar to the later spectrum from RA oxidised with KO_2. The simulation of this 4th radical component (Fig. 3.67.d) which was achieved from Fig. 3.67.c after subtracting the 1st radical component from Fig. 3.63.a, showed that the smallest hyperfine splitting constant has the biggest deviation from the coupling constants of the 3rd radical component. Table 3.11. summarises the hyperfine splitting constants of the radical components of oxidised RA.

Table 3.11. Hyperfine splitting constants (mT) of the three obtained spectra in relation to the experimental setup.

	oxidation type	a(^{1}H)	a(^{1}H)	a(^{1}H)	a(^{1}H)	a(^{1}H)
1st component	Proc. 1 KO$_2$ enzymatic systems	0.360 x 2	0.178	0.108	0.059	
2nd component	Proc. 1	0.305	0.178	0.145	0.038	
	Proc. 2 (RA:NaOH=1:1)	0.302	0.176	0.146	0.037	
	Proc. 2 (RA:NaOH=1.67:1)	0.307	0.176	0.146	0.036	
	Proc. 2 (RA:NaOH=3:1)	0.318	0.175	0.151	0.034	
3rd component	KO$_2$	0.265	0.239	0.118	0.118	0.053
4th component	enzymatic systems	0.257	0.235	0.114	0.110	0.107

Structural suggestions

Four different EPR spectra were detected after oxidising RA under alkaline or neutral conditions. Radical formation of RA can occur at either of the two catechol groups in rings A and B (Cao et al., 2005). Previously reported DFT (density functional theory) calculations from Cao et al. (2005) showed that rings A and B have similar reducing activities. Although ring B is a stronger electron donor than ring A, the radical formed on ring A is more stable. Based on these facts and on publications of hyperfine coupling constants for o-semiquinone radicals substituted in p-positions, the following structures are suggested for the observed radicals.

The 1st radical is most likely generated by oxidation of ring B (Fig. 3.68.a). Similar hyperfine splitting constants were published by Pedersen (1982) for oxidised dihydrocaffeic acid ester in an alkaline ethanol solution (Fig. 3.68.b). The two largest hyperfine splitting constants arise from interaction of the unpaired electron with the proton in position 6' and with one of the two protons in position 13. The other splittings come from the second proton on carbon 13, and the protons in position 5' and 2'. Table 3.12. gives an overview of the hyperfine splitting constants of our spectrum compared to those from Pederson (1982) for dihydrocaffeic acid ester and from Pilar (1970) for p-substituted o-benzosemiquinones.
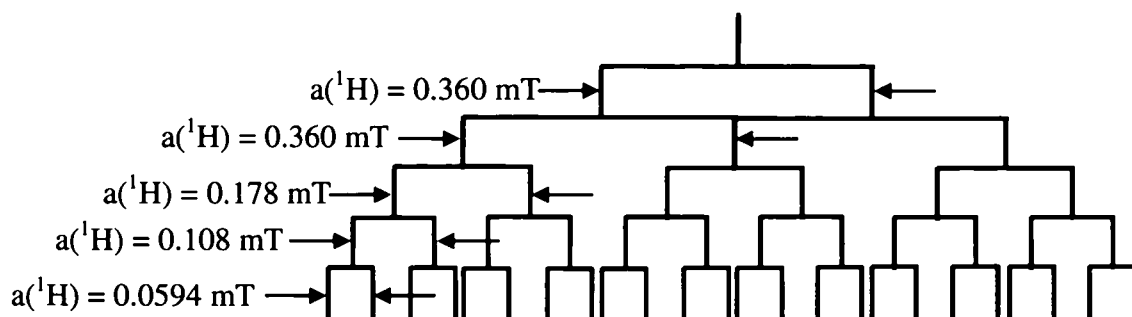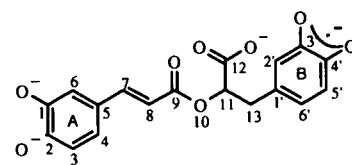
a

b

c
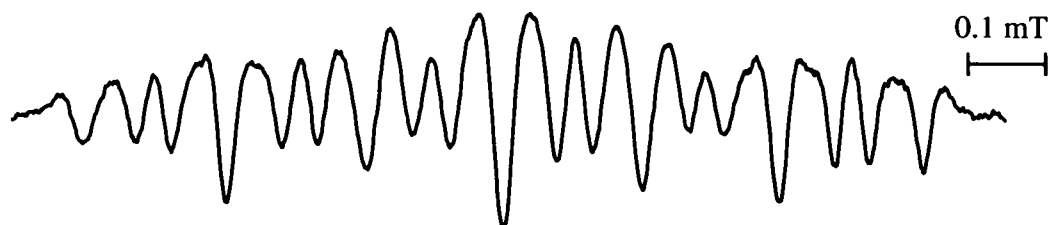
Fig. 3.63. EPR spectra of the 1st radical component of RA oxidised by Proc. 1. (a) experimental spectrum recorded in the 1st derivative (MA 0.01 mT, 1 scan), (b) simulation of (a), (c) experimental spectrum recorded in the 2nd derivative (MA 0.02 mT, 2 scans). Spectral interpretation is shown by the stick diagram.

$a(^1H) = 0.305$ mT

$a(^1H) = 0.178$ mT

$a(^1H) = 0.145$ mT

$a(^1H) = 0.038$ mT

0.1 mT

a

b

0.1 mT

c
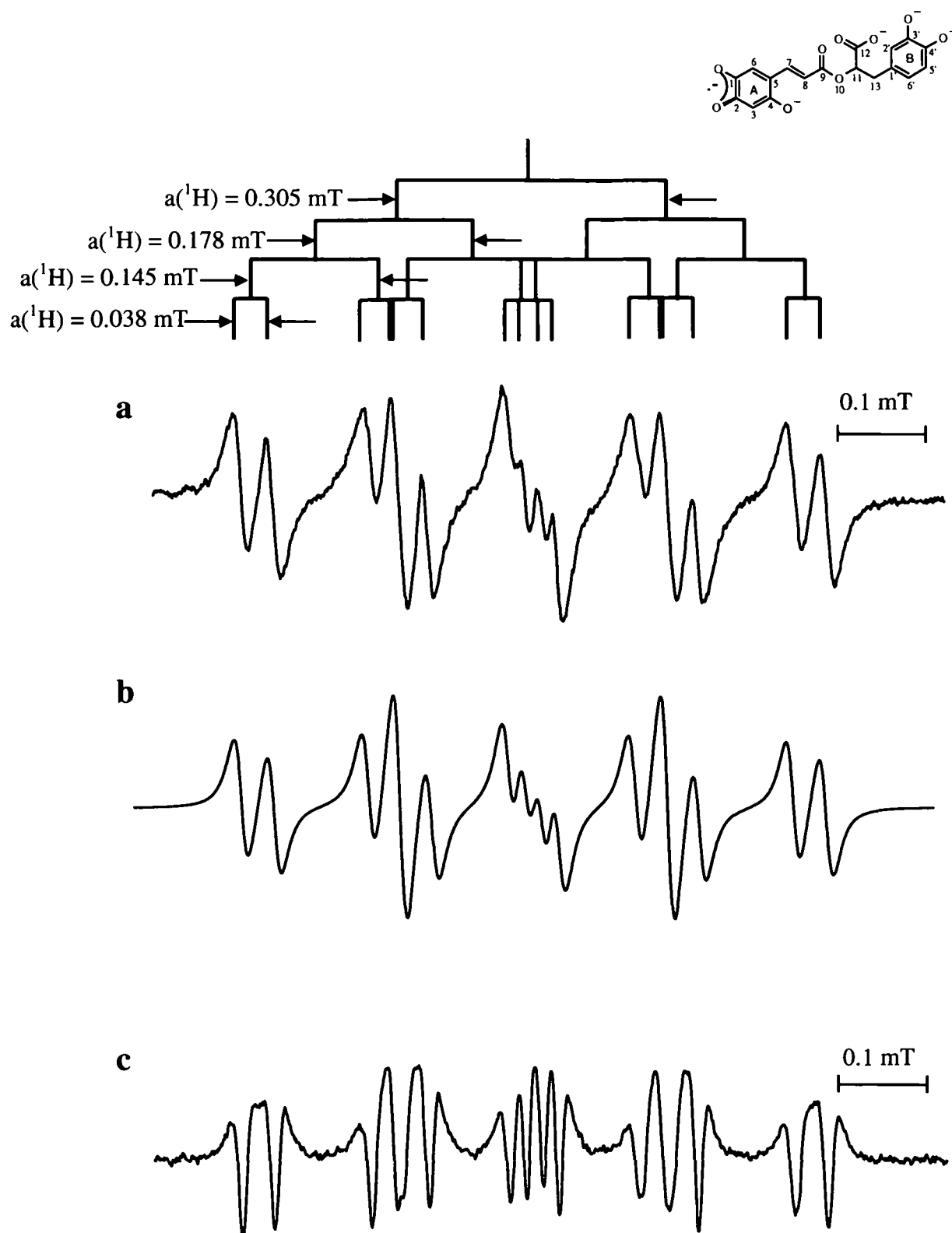
Fig. 3.64. EPR spectra of the 2nd radical component of RA oxidised by Proc. 1. (a) experimental spectrum recorded in the 1st derivative, (b) simulation of (a), (c) experimental spectrum recorded in the 2nd derivative. Spectral interpretation is shown by the stick diagram.

154
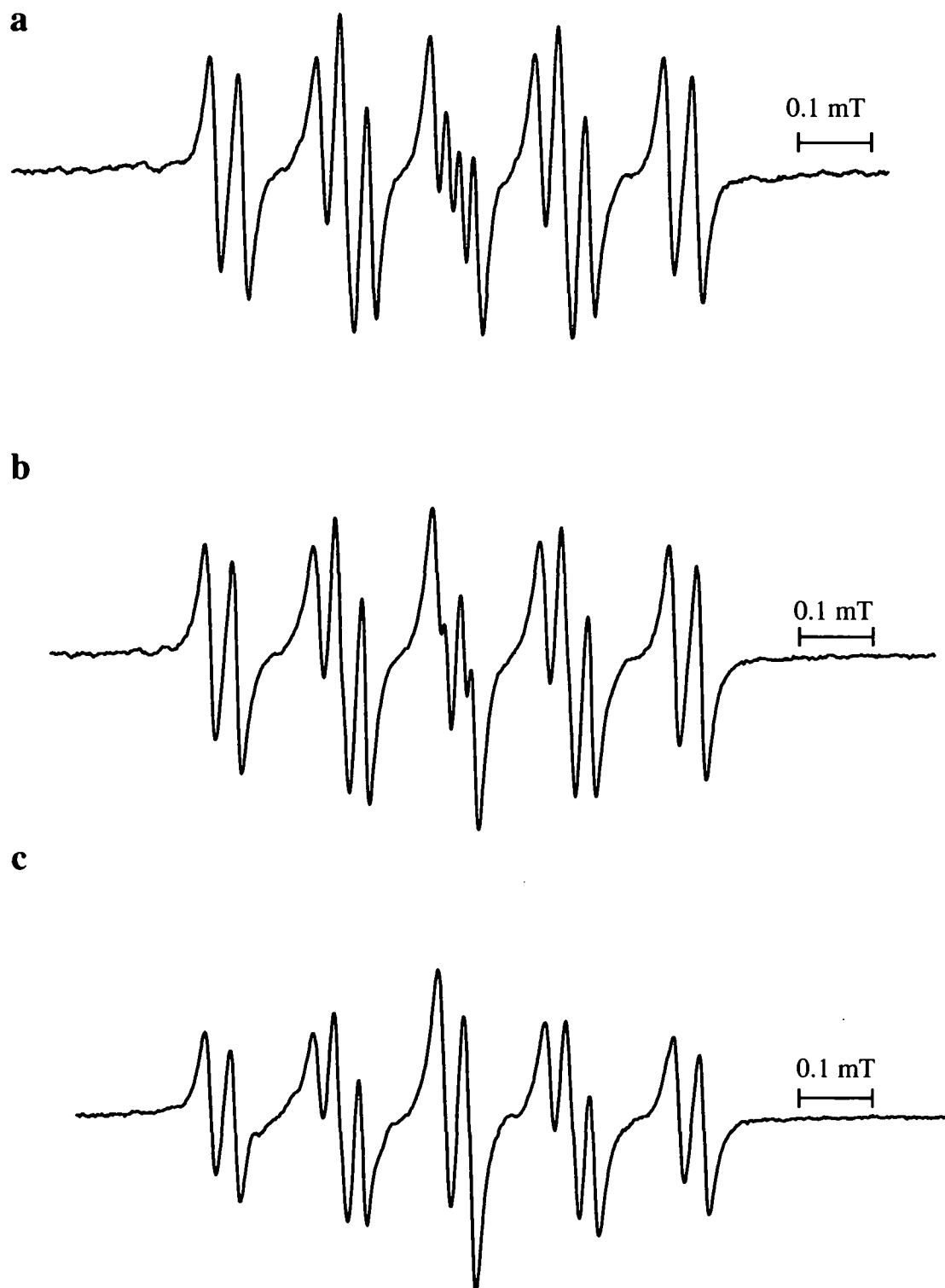
Fig. 3.65. EPR spectra of RA oxidised by Proc. 2. (a) RA:NaOH = 1:1 (MA 0.01 mT, 10 scans), (b) RA:NaOH = 1.67:1 (MA 0.003 mT, 10 scans) (c) RA:NaOH = 3:1 (MA 0.003 mT, 7 scans).

a

$a(^1H) = 0.265$ mT

$a(^1H) = 0.239$ mT

$a(^1H) = 0.118$ mT

$a(^1H) = 0.118$ mT

$a(^1H) = 0.053$ mT

b

0.1 mT

c
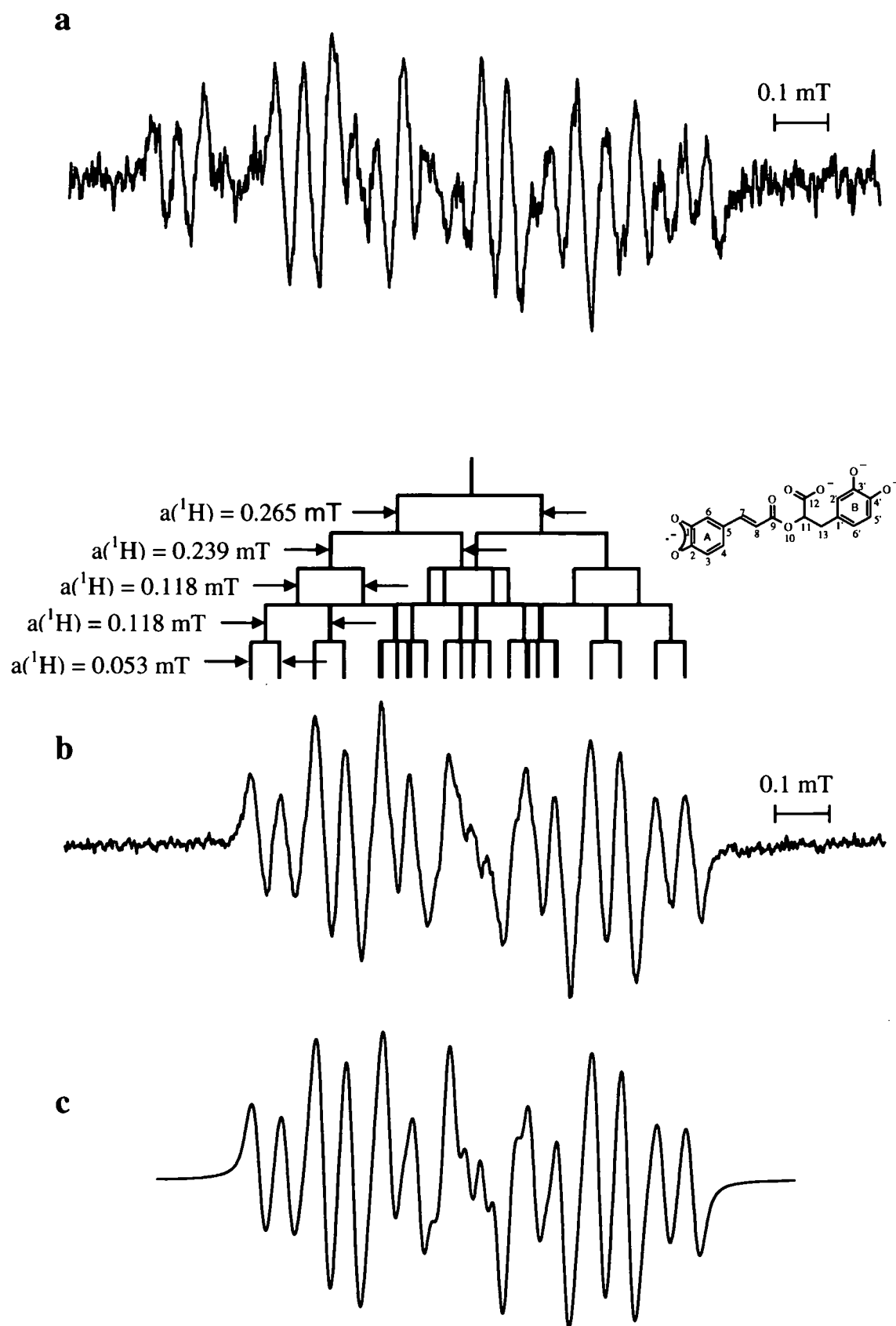
Fig. 3.66. EPR spectra of RA oxidised by KO_2. (a) 1st spectrum (MA 0.03 mT, 5 scans), (b) 3rd radical component (MA 0.02 mT, 30 scans), (c) simulation of (b). Spectral interpretation is shown by the stick diagram.

156
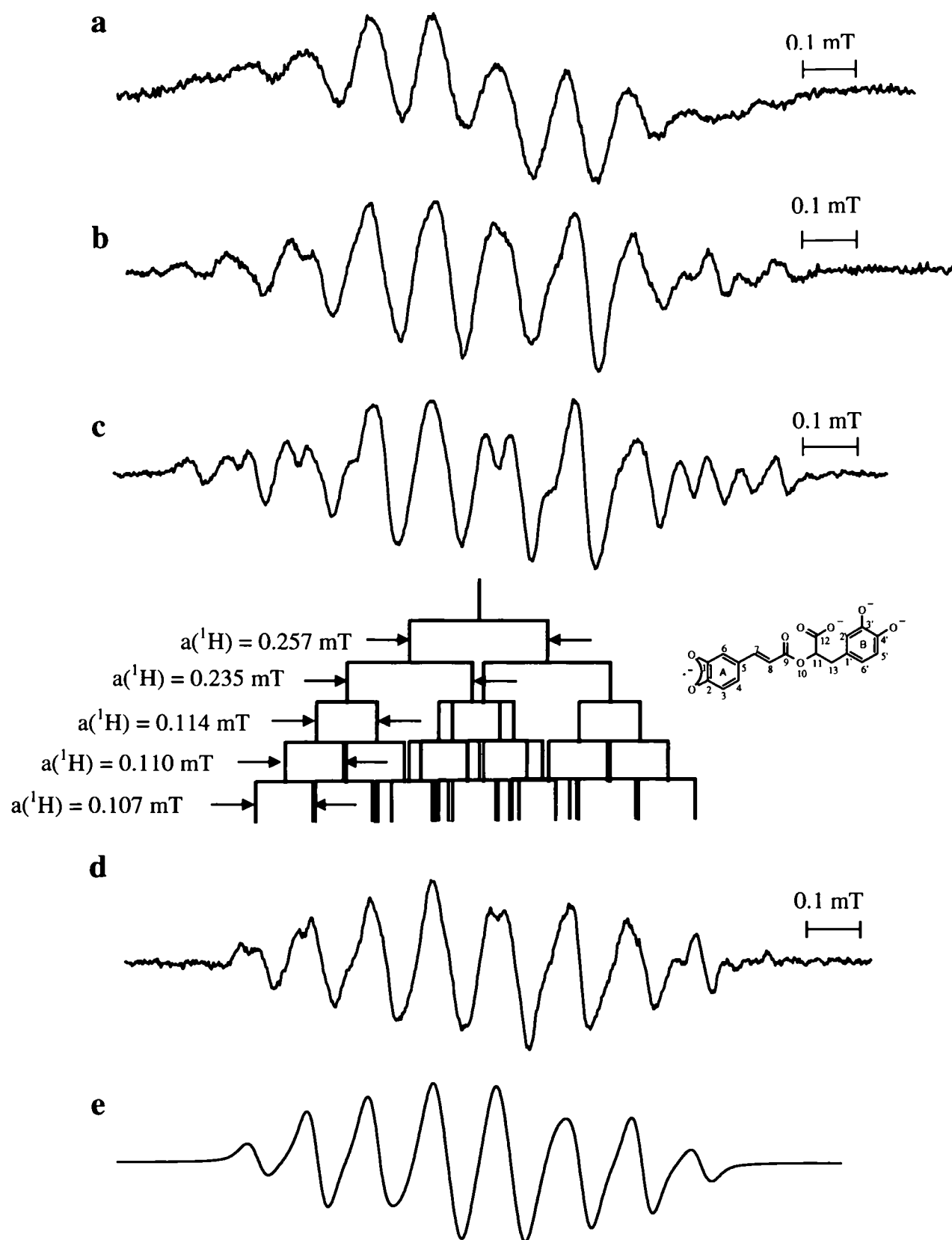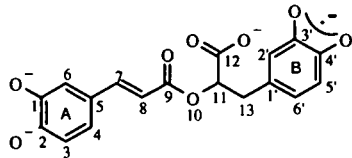
Fig. 3.67. EPR spectra of RA oxidised by (a) HRP/H_2O_2 (MA 0.05 mT, 40 scans), (b) Fenton reaction system (MA 0.03 mT, 10 scans), (c) xanthine/xanthine oxidase (MA 0.01 mT, 20 scans), (d) spectrum of the 4th radical component (c) after subtraction of the 1st radical component, (e) simulation of (d).

Table 3.12. Hyperfine splitting constants (mT) from the 1st radical component compared with those from the literature.

1st radical

	$a_{2'}$	$a_{5'}$	$a_{6'}$	$a_{13}(CH_2)$	$a_{13}(CH_2)$
1st radical	0.059	0.108	0.360	0.360	0.178
Pedersen (1982)[a]	0.046	0.104	0.370	0.330	0.330
Pilar (1970)[b]	0.032	0.100	0.380	0.330	0.330

[a] investigation of a dihydrocaffeic acid ester
[b] investigation of o-benzosemiquinone with 4-propyl as substituent

Fig. 3.68. (a) Proposed structure for the 1st radical component from RA. The coupling constants are assigned to the probable hydrogen atoms, (b) radical structure of dihydrocaffeic acid ester (Pedersen, 1982) (the numbering of the structure is adapted to the one from rosmarinic acid, numbers according to the nomenclature are in brackets and assigned in blue).

The 2nd radical was only observed in alkaline solution and was much more stable than the 1st radical. Following the DFT calculation of Cao et al. (2005), it is likely that this radical is derived from oxidation at the A-ring. However, the spectrum was simulated with 4 protons whereas oxidation of the A-ring would be expected to lead to 5 couplings taking into account the hydrogen atoms in α- and β-position to the aromatic ring on the

double bond. Ashworth (1976) reported that trihydroxycinnamic acids are formed as a result of hydroxylation of dihydroxycinnamic acids during prolonged autoxidation in strongly alkaline solution. If a similar reaction occurs in our solution, carbon 4 would be hydroxylated and the resulting radical would have the structure shown in Fig. 3.69.a. The hyperfine splitting constants are in fairly good agreement with those of Pedersen and Ollgaard (1982) and Ashworth (1976) for the radical from 2,4,5-trihydroxycinnamic acid (Fig. 3.69.b) although Ashworth assigned two values in the opposite way to Pedersen. Table 3.13. shows a comparison of our spectral parameters with those in the literature for radicals from similar structures (e.g. di- and trihydroxycinnamic acids).

Fig. 3.69. (a) Proposed structure for the 2nd radical component from RA, the coupling constants are assigned to the probable hydrogen atoms, (b) radical structure of 6-hydroxycaffeic acid (Pedersen and Ollgaard, 1982) (the numbering of the structure is adapted to the one from rosmarinic acid, numbers according to the nomenclature are in brackets and assigned in blue).

The 3rd and 4th radical components were only detected at pH 7, the 4th radical in combination with the 1st radical. It is probable that oxidation took place on ring A since the hyperfine splitting constants are quite different from that of the 1st radical component in which ring B is oxidised. The parameters obtained from simulation were compared with those reported for oxidised 3,4-dihydroxycinnamic acid in alkaline and acidic medium (Ashworth, 1976; Dixon et al., 1975). The parameters of the 3rd radical

component are in good agreement with those reported by Ashworth (1976), whereas for the 4th radical component the smallest hyperfine splitting is appreciably different. (Table 3.13.). A proposed structure for the 3rd and 4th radicals is shown in Fig. 3.70. together with the structure of 3,4-dihydroxycinnamic acid.

Table 3.13. Hyperfine splitting constants (mT) for the 2nd and 3rd radicals compared with values from the literature.

2nd radical   3rd and 4th radicals
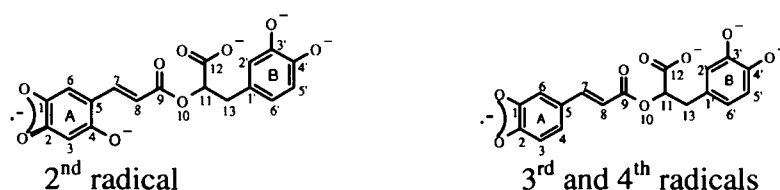
	a_3	a_4	a_6	a_7	a_8
2nd radical component (pH 13)	0.145	-	0.038	0.305	0.178
Pedersen and Ollgaard (1982) (alkaline oxidation)[a]	0.137	-	0.040	0.292	0.180
Ashworth (1976) (alkaline oxidation)[a]	0.044	-	0.132	0.283	0.175
Bors (2003) (HRP/H_2O_2, pH 9.5)	0.258	-	0.126	0.385	-
Bors (2004) (HRP/H_2O_2, pH 9.5)	0.126	-	0.258	-	0.385
Dixon (1975) (alkaline oxidation)[b]	0.135	0.275	0.015	0.245	0.120
Dixon (1975) (Ce[IV] oxidation, 0.5M sulphuric acid)[b]	0.350	0.150	0.175	0.480	0.245
Ashworth (1976) (alkaline oxidation)[b]	0.119	0.282	0.023	0.236	0.130
3rd radical component (KO$_2$, pH 7)	0.118	0.265	0.053	0.239	0.118
4th radical component (enzymatic systems, pH 7)	0.110	0.257	0.107	0.235	0.114

[a] investigation of 2,4,5-tri-OH-cinnamic acid
[b] investigation of 3,4-dihydroxycinnamic acids

Discussion

There are some previous reports of EPR measurements of free radical formation in RA by alkaline oxidation (Pedersen, 1978 and 2000; Mouhajir et al., 2001) and by oxidation with HRP/H_2O_2 at pH 9.5 (Bors et al., 2003 and 2004). The radicals reported by Pedersen and Mouhajir et al. are similar to our 1st radical, but there is no agreement with the results from Bors et al. The 1st radical was probably formed by oxidation of the

catechol group in ring B and was observed at pH 13 and pH 7 whereas the 2nd, 3rd and 4th radicals were most likely generated by oxidation of the catechol group in ring A.
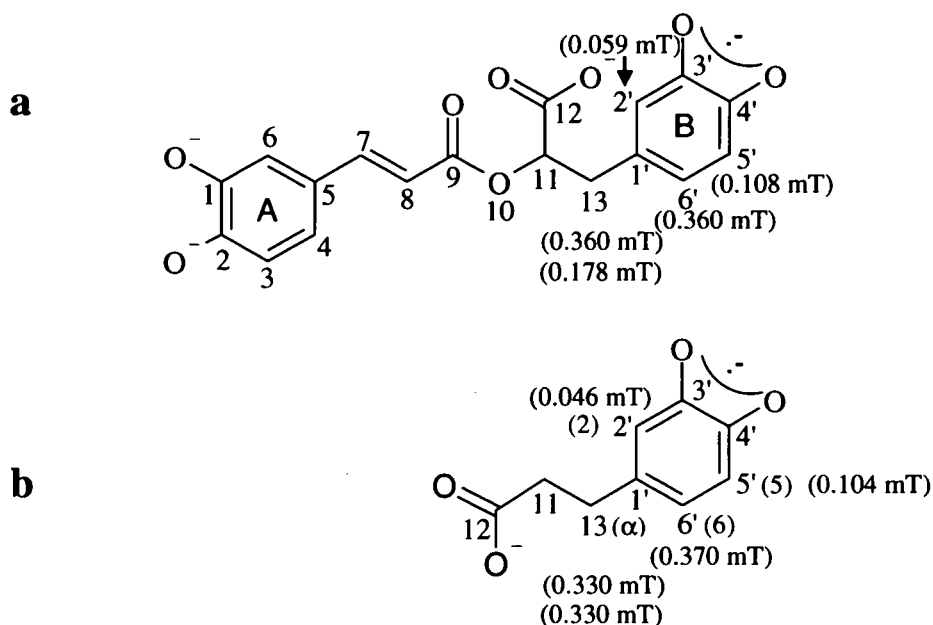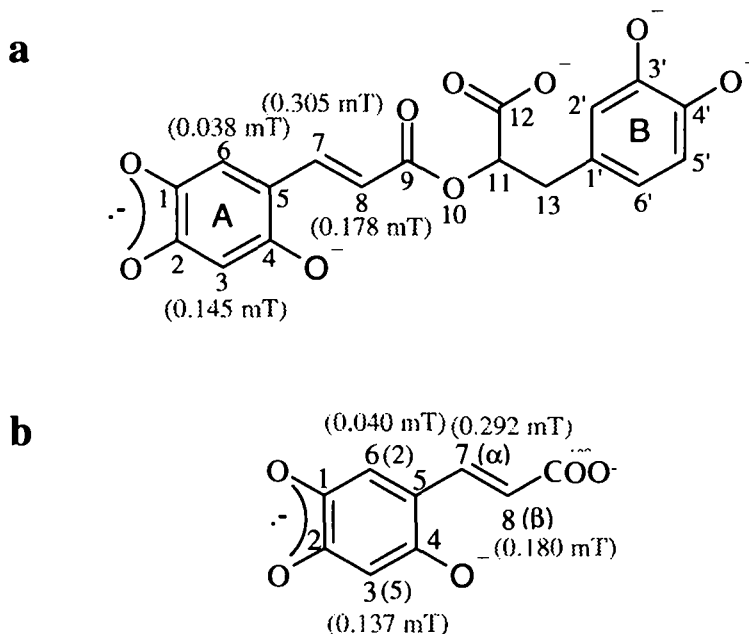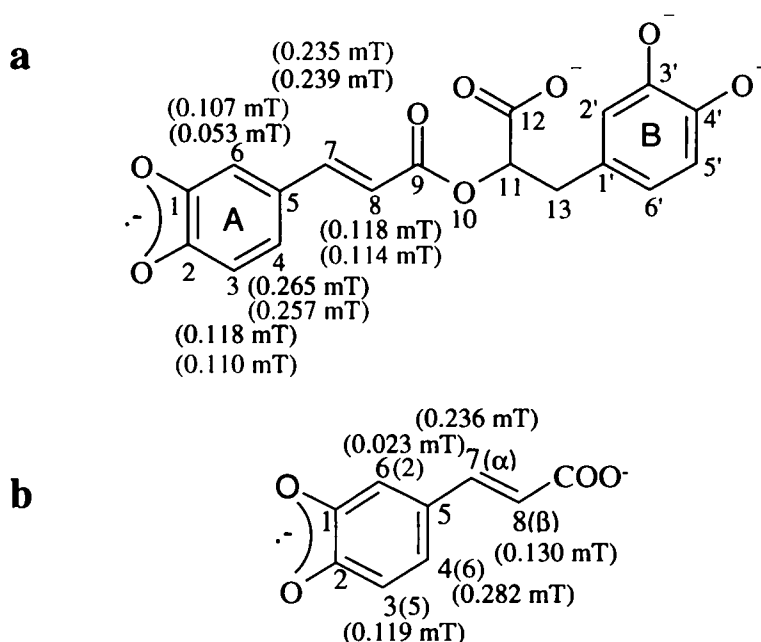

Fig. 3.70. (a) Proposed structure for the 3rd and 4th radical component from RA. The coupling constants are assigned to the probable hydrogen atoms (red for the 3rd and green for the 4th radical), (b) Structure of 3,4-dihydroxycinnamic acid radical (Ashworth, 1976) (the numbering of the structure is adapted to the one from rosmarinic acid, numbers according to the nomenclature are in brackets and assigned in blue).

Formation of free radicals from RA is pH dependent (2nd radical at pH 13, 3rd and 4th radical at pH 7). A good agreement with reported hyperfine splitting constants from oxidised 2,4,5-trihydroxycinnamic acid (Pedersen and Ollgaard, 1982) led to the assumption that the 2nd radical was hydroxylated at carbon 4 under the strong alkaline conditions that we used. A comparison of the 3rd and 4th radicals with that from 3,4-dihydroxycinnamic acid (Ashworth, 1976), which has a similar structure to the A-ring part of the structure from RA, showed a good consistence of the coupling constants. The different values for the smallest hyperfine splitting for the 3rd and 4th radicals may be due to the different DMSO content in the solutions of KO_2 (only 10 %) and the enzymatic systems (50 % DMSO). The fact that RA is larger than hydroxycinnamic acid, and therefore has more restricted motion, could be an explanation for the smaller hyperfine splitting constant of the proton on carbon 8.

Recently Cao et al. (2005) investigated the high antioxidant activity of RA in a DFT study. Similar activity was found for both rings A and B; ring B is a stronger electron donor than ring A, but the radical formed on ring A is more stable than that of ring B. These calculations support the possibility that both rings could be oxidised under the various experimental conditions used in the present work.

3.5.4. Carnosic Acid

Carnosic acid (CA) (Fig. 3.71.) is a diterpene and a major component of rosemary and common sage. The antioxidant effect in CA comes from the catechol structure - two OH-groups on carbon 11 and 12.
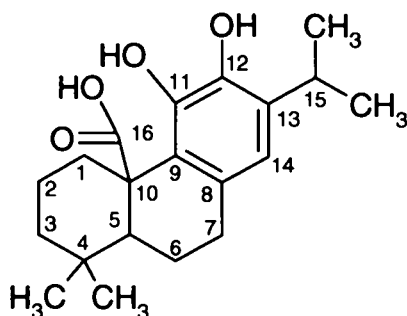
Fig. 3.71. Structure of carnosic acid.

Autoxidation

Equal volumes of CA and NaOH solutions transferred separately into a flat cell (Proc. 1) generated a sextet spectrum, which was stable for more than 40 min. and was not accompanied by any other signal (Fig. 3.72.). Additional splittings were resolved in the 2nd derivative recording (Fig. 3.72.c), and the spectrum could be simulated with 4 proton splittings – one large splitting of 0.7 mT, two around 0.4 mT, and one small splitting of 0.04 mT.

Mixing CA with NaOH in a 1:1 ratio using Proc. 2 resulted first in a spectrum of 8 peaks (Fig. 3.73.a) that was simulated with 3 proton couplings (Fig. 3.73.b). This decreased fairly quickly and was then replaced by a complex spectrum consisting of at least 3 different radical species (Fig. 3.73.c). Changing the CA:NaOH ratio to 1.67:1 gave the same complex spectrum (Fig. 3.74.a) as that in Fig. 3.73.c. Autoxidation of CA with NaOH in the volume ratio of 3:1 produced similar results to the mixture with a 1:1 ratio; an initial 8 peak spectrum followed by a complex spectrum of at least 2 components (Fig. 3.74.b, c). The outermost peaks from Fig. 3.74.a are missing in this spectrum, hence Fig. 3.74.c probably consists of two components. Since the complex spectrum of Fig. 3.74.a was the one with the highest intensity, it was chosen for

deconvolution to obtain the spectra of individual radicals. Two of these components were identified as the 6 peak spectrum of Fig. 3.72.a, and the 8 peak spectrum of Fig. 3.73.a. The spectrum which remained after subtracting the contributions from these components is shown in Fig. 3.75. This spectrum is still complex and has not been simulated. It most likely contains more than one component. Since the spectrum was obtained by accumulation of multiple scans due to its weak intensity, it was not possible to record any time dependent changes and hence to isolate further components.

Additional measurements were carried out with a 10 mM solution of CA (CA:NaOH = 1:1) instead of using a 1 mM solution. The spectrum was dominated by the 6 peak resonance, indicating that the radical reactions are dependent on the concentration of CA.

Enzymatic oxidation

Oxidation of CA with either HRP/H_2O_2 or xanthine/xanthine oxidase at pH 7 gave similar 8-peak spectra (Fig. 3.76.a and b), although there was an additional minor component with the xanthine/xanthine oxidase system (Fig. 3.76.b). No signal was seen with the Fenton reaction system using a CA concentration of 1 mM, but a weak 4 peak spectrum (Fig. 3.76.c) was detected with a 5 mM CA solution using 0.1 mT modulation amplitude. This probably arises from the same radical as Figs. 3.76.a and b, and the small ^1H splitting is not resolved in Fig. 3.76.c because of the large modulation amplitude.

Oxidation by potassium superoxide

Oxidation of CA with KO_2 at pH 7 also produced the 8 peak spectrum (Fig. 3.77.), but the signal intensity was much higher than when the enzymatic systems were used as oxidising agents.

The hyperfine splitting constants obtained by simulation of the two main radical components of CA are given in Table 3.14.

Table 3.14. Hyperfine splitting constants (mT) for the radical species from CA.

	a(^{1}H)	a(^{1}H)	a(^{1}H)	a(^{1}H)
CA autoxidised by Proc. 1	0.728	0.449	0.406	0.043
CA autoxidised by Proc. 2, oxidised by enzymatic systems and KO$_2$		0.466	0.298	0.061
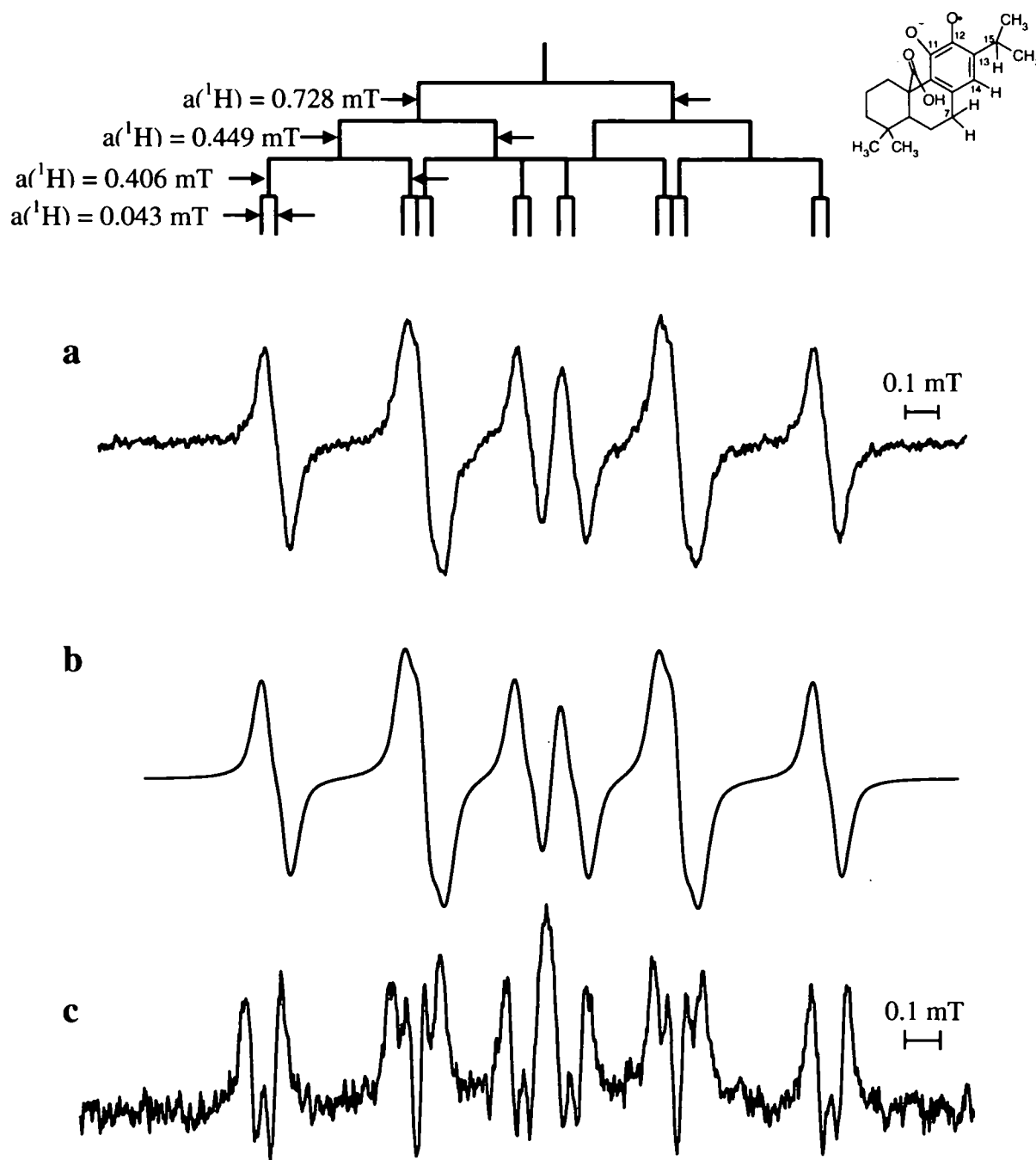
Fig. 3.72. EPR spectrum of carnosic acid autoxidised by Proc. 1. (a) experimental spectrum recorded in the 1st derivative (MA 0.01 mT, 10 scans), (b) simulation of (a), (c) experimental spectrum recorded in the 2nd derivative (0.03 mT, 10 scans). Spectral interpretation is shown by the stick diagram.

$a(^1H) = 0.466$ mT→

$a(^1H) = 0.298$ mT →

$a(^1H) = 0.061$ mT →

a

0.1 mT

b

c

0.1 mT
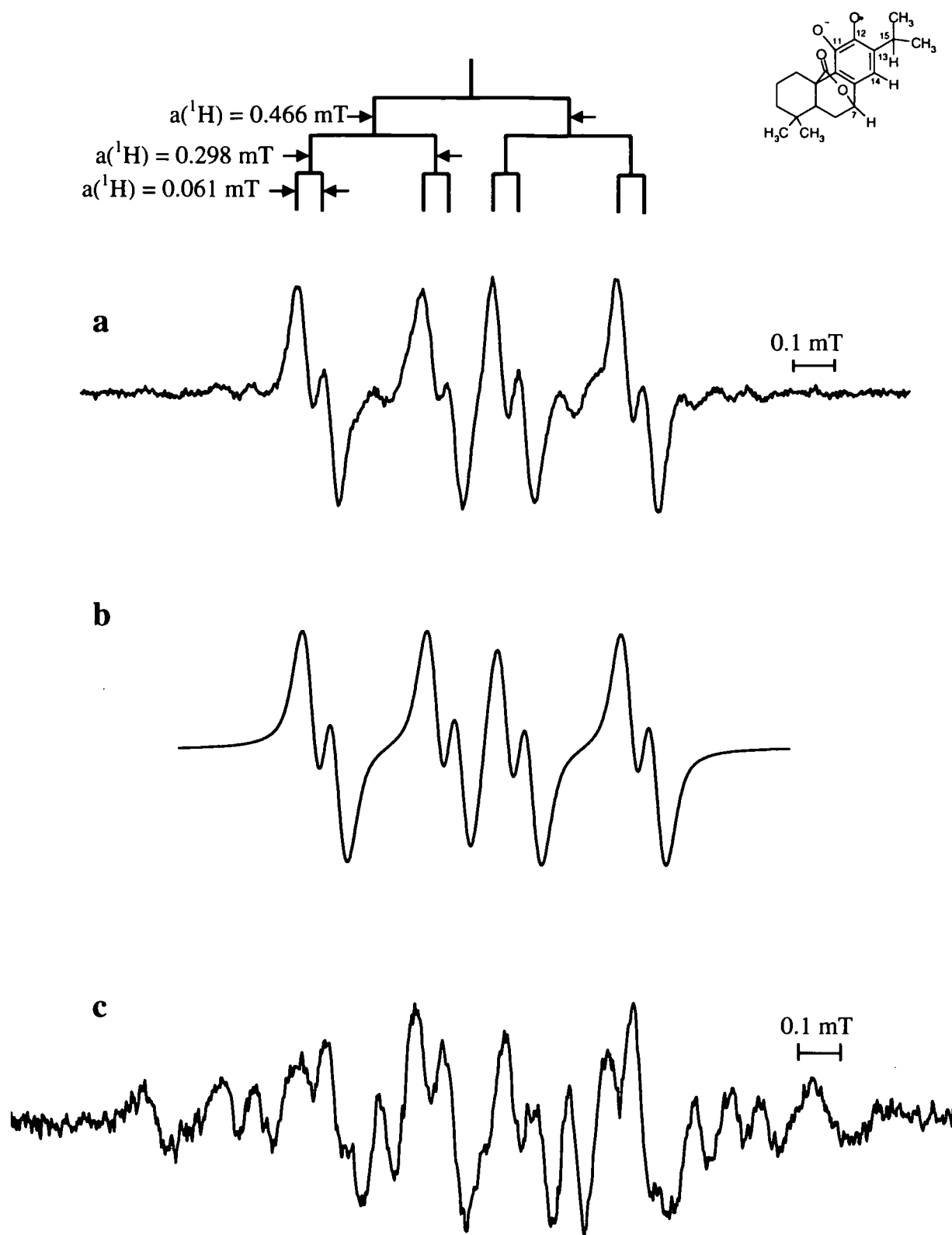
Fig. 3.73. EPR spectrum of carnosic acid autoxidised by Proc. 2. (carnosic acid:NaOH=1:1). (a) experimental spectrum of the 1st component (MA 0.05 mT, 20 scans), (b) simulation of (a), (c) experimental spectrum after the 1st component decreased (MA 0.05 mT, 30 scans). Spectral interpretation of the 1st component is shown by the stick diagram.

a

0.1 mT
⊢—⊣

b

0.1 mT
⊢—⊣

c

0.1 mT
⊢—⊣
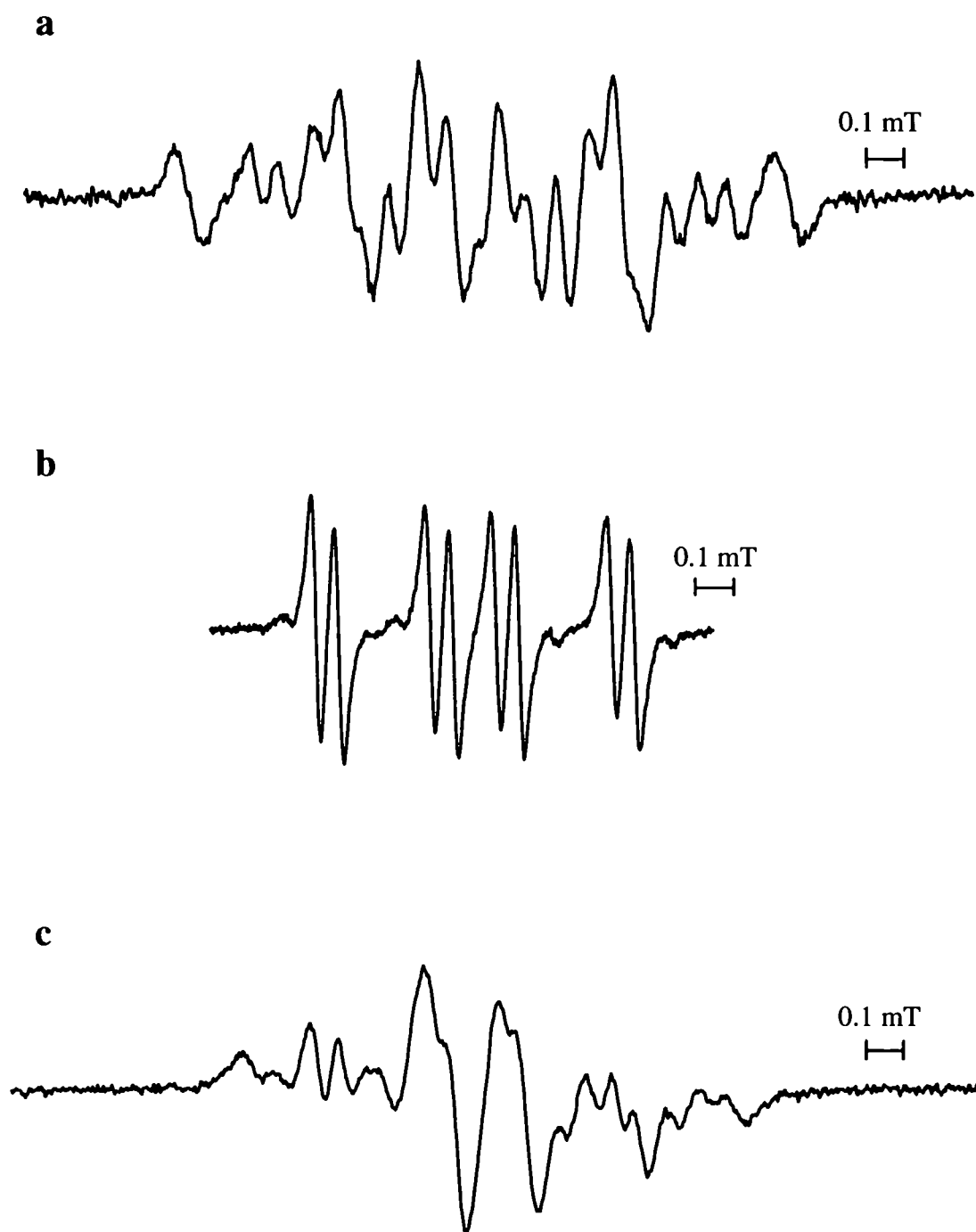
Fig. 3.74. EPR spectra of carnosic acid autoxidised by Proc. 2. (a) carnosic acid:NaOH = 1.67:1 (MA 0.05 mT, 40 scans), (b) carnosic acid:NaOH = 3:1, 1st component (MA 0.03 mT, 9 scans), (c) carnosic acid:NaOH = 3:1, spectrum after the 1st component decreased (MA 0.05 mT, 37 scans).

0.1 mT

Fig. 3.75. EPR spectrum of Fig. 3.74.a after subtracting simulations of the 6- and 8-peak spectra.

a

0.1 mT

b

0.1 mT

c
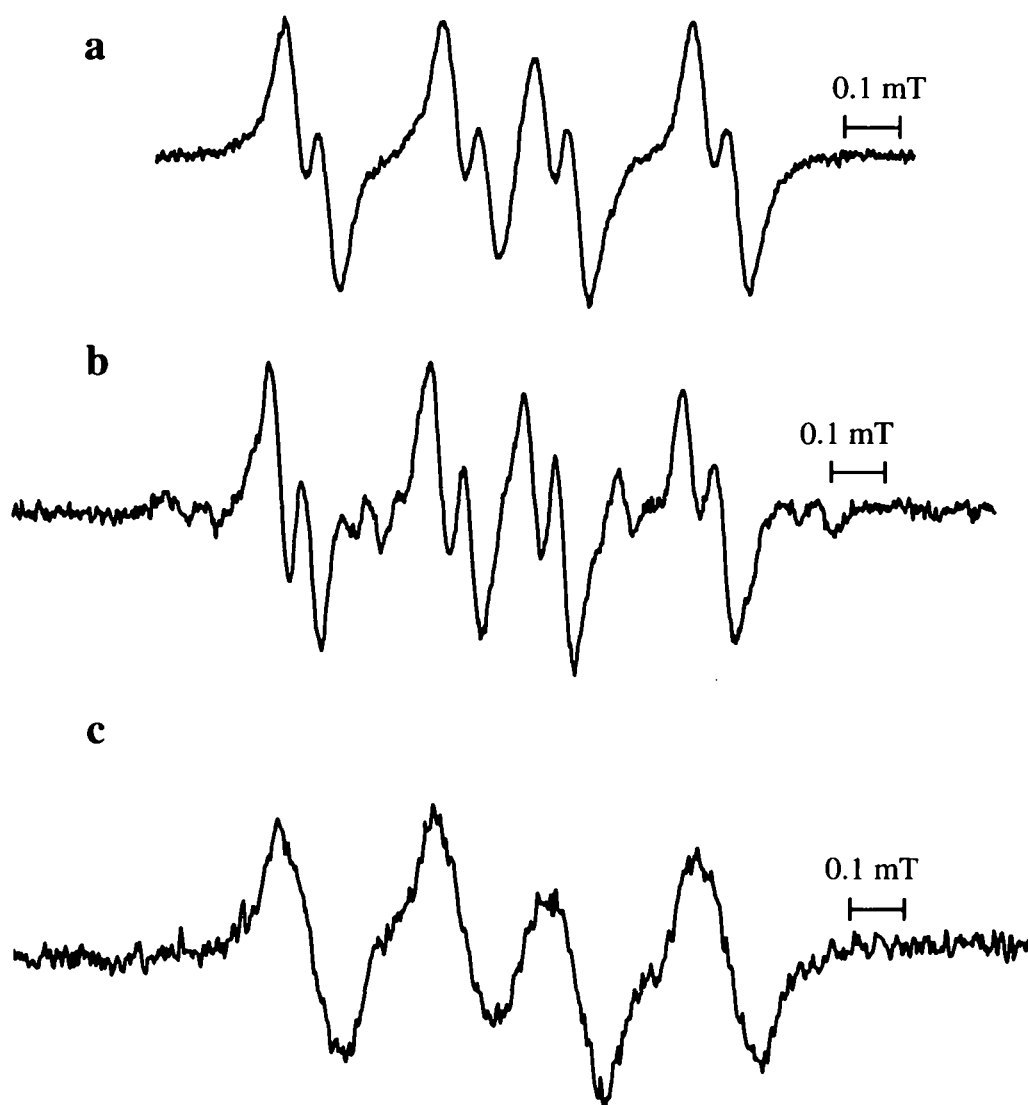
0.1 mT

Fig. 3.76. EPR spectra of carnosic acid oxidized by (a) HRP/H_2O_2 (MA 0.034 mT, 21 scans), (b) xanthine/xanthine oxidase (MA 0.034 mT, 20 scans), (c) Fenton reaction system (MA 0.1 mT, 30 scans).
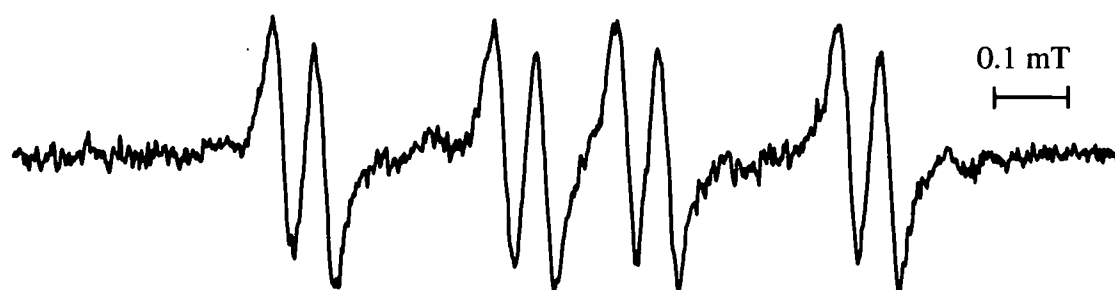
Fig. 3.77. EPR spectrum of carnosic acid oxidised by KO_2 (MA 0.01 mT, 5 scans).

Structural Suggestion

Two different EPR signals could be isolated and simulated with four or three proton couplings respectively for the 1st and 2nd radical components. The structure of the 1st component could be generated by oxidation of one of the OH-groups on carbon 11 or 12. According to Geoffry et al. (1994), the preferred oxidation site is the OH group on carbon 12, leading to the formation of an o-hydroxyphenoxyl radical rather than an o-semiquinone because of an interaction of the near carboxyl group with the proton in position 11. Fig. 3.78. presents a possible structure for the 1st radical component. The largest hyperfine splitting of 0.73 mT would then come from interaction of the unpaired electron with one of the two hydrogen nuclei in position 7 since this is the p-position to the oxidised OH-group and therefore the position with the highest spin density (Dixon et al., 1974). The 0.45 mT splitting is probably due to the proton on carbon 15 representing the o-position. Another 0.4 mT splitting could be detected from the 2nd proton in position 7. Although this coupling is supposed to be very small in methyl oleate (Geoffroy et al., 1994), it may be larger in $DMSO/H_2O$. The smallest coupling of 0.04 mT then very likely arises from the proton in m-position on carbon 14.

There are some reports about the transformation of oxidised CA to carnosol (Hosny et al., 2002; Wenkert, 1965; Schwarz, 1992). Comparing the hyperfine splitting constants of the 2nd radical component with the structure of carnosol, it seems likely that the radical corresponds to oxidised carnosol (Fig. 3.79.). The largest splitting of 0.47 mT probably arises from the proton in position 7 and the 0.3 mT splitting from the proton on carbon 15. The 3rd and smallest coupling of 0.06 mT would then result from the

proton on carbon 14. The formation of carnosol would explain the loss of the largest coupling of 0.7 mT in the 2nd radical component.
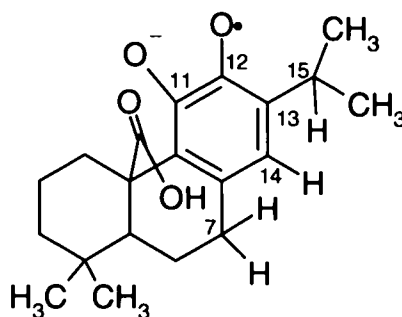
Fig. 3.78. Possible structure of the 1st radical component of carnosic acid in alkaline solution.
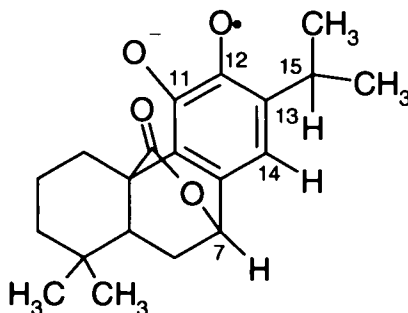
Fig. 3.79. Possible structure of carnosol-derived 2nd radical component of carnosic acid in alkaline solution.

Discussion

Oxidation of CA was detected with all oxidising agents. Two radical species could be identified as 1-electron oxidation products of CA and carnosol. Spectral parameters for a third radical could not be derived and consequently it is not possible to speculate on its structure at present.

The stereochemistry of CA and carnosol was investigated by Narayanan and Linde (1965) who first proposed that the A/B rings were *trans*-fused (Fig. 3.71.), and the potential site of oxidation is the catechol group on carbon 11 or 12, generating an *o*-semiquinone. These are also the positions suggested by Geoffroy et al. (1994), who investigated EPR spectra of CA in oxidised methyl oleate, and by Masuda et al. (2001),

who identified the formation of two oxidation products of CA. The spectra and hyperfine splitting constants reported by Geoffroy et al. (1994) are completely different from our results, even though our discussion of the spectra is based on the same radical structure as their's (i.e. oxidation at the OH-group on carbon 12). An explanation for this difference might be the use of different solvents and oxidation conditions. Masuda et al. suggested the OH-group on carbon 11 as the oxidation site. However, one would expect that the EPR spectrum of such a radical would show only two proton couplings (from C14 and the proton from the OH-group in position 12), since these would be the positions of highest spin density. The most likely structure is a mixture of both oxidised forms generating an o-semiquinone.

The formation of carnosol from carnosic acid under oxidising conditions has been reported previously. Wenkert et al. (1965) found that carnosol was produced in a methanolic solution of CA when standing in the dark at room temperature for 3 weeks. Carnosol was also generated from CA by microbial transformation using *Nocardia* (Hosny et al., 2002). This was suggested to occur via enzymatic oxidation of CA to a quinoid intermediate, followed by an intramolecular Michael addition of the carboxylate anion at position 7. Schwarz and Ternes (1992) found that CA was converted to carnosol in methanol solution if O_2 was present. Hence it is likely that carnosol was generated in our oxidation experiments and that the 2nd radical from CA is in fact an oxidation product of carnosol.

CHAPTER 4

GENERAL DISCUSSION

Carrots, herbs and mushrooms were investigated by grinding a small amount of the material in the presence of a spin trap to detect free radical formation generated by cell disruption. With mushroom, a trapped carbon-centred radical was identified as 4-(hydroxymethyl)phenyl radical, whereas with carrots and herbs the spin adducts were assigned to the ·OH radical and carbon-centred radicals in general but with no specific identification. The 4-(hydroxymethyl)benzene diazonium salt which is the substrate for the 4-(hydroxymethyl)phenyl radical is found in appreciable amounts in mushrooms (Levenberg, 1962; Ross et al., 1982).

Herb samples were examined in a screening experiment using the spin trap 4-POBN. A few spectra of herbs were dominated by the ascorbate radical, some showed a spin adduct similar to a carbon-centred radical, but the majority of the investigated herb extracts were able to oxidise the spin trap. This oxidation product of the spin trap 4-POBN was also seen with carrot samples in addition to *t*-butylhydronitroxide, a breakdown product of the spin traps PBN and 4-POBN. It's possible that this pro-oxidant activity arises from specific plant components which are oxidised by cell disruption under atmospheric condition. The resulting product(s) may be powerful oxidants which are able to oxidise and degrade the spin trap. Carrot samples taken from different positions of the root (top, centre, tip) varied in their pro-oxidative activity showing the highest activity in the tip of the root which may be correlated with a higher generation of ·OH radicals in this growing zone (Liszkay et al., 2004; Schopfer et al., 2002; Schopfer, 2001). Variations in the pro-oxidative behaviour were also observed with different herb leaves of sage which were harvested on different times on a day distinguishing between sunny and shady leaves. However, inconsistencies in the results with the sage leaves made it impossible to relate them to time or sunlight intensity. Different leaves showed randomly either the presence of a carbon-centred radical or oxidised the spin trap 4-POBN.

This pro-oxidative ability of tissue extracts from carrots and herbs was the basis for further investigations of oxidation reactions with specific phenolic compounds

(kaempferol, luteolin, rosmarinic acid (RA) and carnosic acid (CA)) which occur in a significant amount in herbs (kaempferol in lemon balm; luteolin in parsley, thyme, peppermint, basil; RA and CA in rosemary and sage). These reactions were initiated with 5 different systems – autoxidation at ~pH 13, HRP/H_2O_2, X/XO, Fenton reaction system and KO_2 at pH 7.

The ·OH radical which is often the initial radical formed in living systems e.g. by the Fenton reaction, is not stable and reacts with virtually every molecule it contacts. It is often the initiator of lipid peroxidaton by abstracting a hydrogen atom from lipid molecules such as fatty acids. (Halliwell and Gutteridge, 1984) Since it plays an important role in biochemical reactions it was chosen as oxidising agent in a Fenton-like reaction system.

Superoxide anion radicals which are major products of the photosynthetic pathway (Smirnoff, 1993), and therefore are present in any green tissue, were taken as the second oxidation medium. They were generated using the enzyme system xanthine/xanthine oxidase and potassium superoxide, both at pH 7.

Phenolic compounds were also oxidised with a solution containing the enzyme HRP and H_2O_2, which functions by generating compounds with iron in a high (+IV) oxidation state. Compound I is reduced to compound II by oxidising a phenolic compound. This reaction is repeated with compound II and oxidation of another phenolic molecule leads to regeneration of the original enzyme structure. (Chen and Schopfer, 1999)

Plants protect themselves against free radical damage by the production of antioxidant molecules. In herbs this role is often ascribed to phenolic compounds such as flavonoids. (Pietta et al., 2003) The antioxidant activity of such compounds has been investigated extensively (Sichel et al., 1991; Pedrielli et al., 2001; McPhail et al., 2003; Bors and Saran, 1987), although the *in vivo* function of flavonoids is still not clare. There is evidence that flavonoids not only function as antioxidants, but they may modulate proteins and lipid kinase signalling cascades (Williams et al., 2004). They may also act as pro-oxidants or mutagens at high concentrations, where toxicity effects may dominate. Up to now there are no human data on long-term effects of high-dose

supplementation of flavonoids (Skibola and Smith, 2000), and the influence and consequence of the radical formation of flavonoids is not fully understood, even though their chemistry has been studied over many years.

This work presents some new EPR spectra of oxidised phenolic compounds. The stability of the phenolic radicals ranged from ~6 min. (semiquinone radical generated by the oxidation of kaempferol) to >3 hours (hydroxylated structure of RA).

Autoxidation which plays an important role in food storage processes, was used to gain preliminary information about the radical formation of such antioxidants. Some spectra from the autoxidation experiments at pH 13 were also observed with oxidation conditions at pH 7, which are physiologically more relevant.

Although the flavonoids luteolin and kaempferol differ only in the position of one hydroxyl group, they behaved completely differently under the applied oxidation conditions. Whereas kaempferol reacted with the formation of degradation products and dimers, the structure of luteolin was sustained after oxidation. Various measurements of the antioxidant activity did not produce a clear picture as to which of the two compounds has the higher free radical scavenging activity, e.g. peroxyl radicals and azide radicals were better scavenged by kaempferol, but galvinoxyl radicals were scavenged from both flavonoids with equal intensity (Madsen et al., 2000; McPhail et al., 2003; Bors and Saran, 1987). The sustained free radical scavenging activity of luteolin is probably due to its ability to redox cycle, whereas the activity of kaempferol may be related to the chemistry of its metabolites.

RA and CA are main components in rosemary and sage and are thought to be also responsible for some of the positive health effects of these herbs (Munné-Bosch and Alegre, 2001; del Bano et al., 2003). In both structures catechol groups are the sites of oxidation. It seems as if the original structure of RA remains intact after oxidation as is the case with luteolin. EPR spectra of luteolin and RA, recorded after some time in alkaline solution, are most likely based on hydroxylated structures. CA is not regenerated once it is oxidised. Monné-Bosch et al. (2001) made concentration measurements in cell compartments and showed that the location of CA and its oxidation product carnosol is only at their site of generation, in chloroplasts. After

oxidation the concentration of other products such as rosmanol and isorosmanol increased in the cells. The present EPR results indicate free radical formation from both CA and carnosol.

All of the chosen phenolic compounds could be oxidised and free radicals were detected under the various oxidation conditions. The EPR signals were sufficiently stable to produce good quality spectra, most of which could be interpreted, and some structures could be formulated. The concentrations of the phenolic solutions in these measurements were between 0.5 and 1 mM, which may be already in the range for toxicity effects according to some *in vitro* experiments (Spencer et al., 2003), but the results may still serve as basis for further investigations under physiological relevant conditions.

It could be clearly shown that the mechanism of the reaction of antioxidants and free radicals varies with the antioxidant molecule, the type of oxidising reagent and pH. These results indicate the importance of such EPR measurements in addition to biochemical methods for understanding antioxidant behaviour.

CHAPTER 5

SUMMARY AND CONCLUSION

The generation of free radicals by cell disruption in different biological materials was investigated in the presence of spin traps. This is considered to be a simulation of the mechanical destruction of these plant tissues during the preparation and eating of fresh food products. Pro-oxidative activity of carrot and herb samples was observed with the spin traps PBN and 4-POBN. Carbon-centred radicals were detected with DMPO derivatives, TRAZON and PEPO, ·OH radicals were also trapped with DEPMPO and DPPMPO as spin traps. Specific identification of the free radical from mushroom as the N-t-butylhydronitroxide radical was possible with this range of spin traps.

More controlled experiments from the chemical point of view were performed with four specific phenolic compounds which are considered to be important components in several herbs. Oxidation under different conditions resulted in different EPR spectra which were interpreted and various structural suggestions have been formulated. The chosen oxidation conditions were relatively mild but all components could be easily oxidised, consistent with their excellent abilities to scavenge free radicals by donating hydrogen atoms.

The stability of the detected radicals was quite long with at least 6 min. lifetime. Such radicals *in vivo* would probably be able to diffuse in other parts of the cell and away from their site of oxidation.

The structures of kaempferol and CA changed by oxidation and their metabolites may be of relevance in the antioxidant mechanism. In contrast, the structures of RA and luteolin remained intact, and they are likely to be able to be redox-cycled.

Information gained in this work could serve as basis for further investigations of food preparation or even the chewing process. Furthermore the radical formation of relevant phenolic compounds was detected under physiologically relevant conditions at pH 7 and the formation of stable free radicals may be relevant to questions relating to their use as health products or pro-oxidative and toxic substances.

REFERENCES

Achinewhu S.C., Ogbonna C.C., Hart A.D., 1995, Chemical composition of indigenous wild herbs, spices, fruits, nuts and leafy vegetables used as food, *Plant Foods for Human Nutrition*, 48, 341-348.

Alul R.H., Wood M., Longo J., Marcotte A.L., Campione A.L., Moore M.K., Lynch S.M., 2003, Vitamin C protects low-density lipoprotein from homocysteine-mediated oxidation, *Free Radical Biology & Medicine*, 34 (7), 881-891.

Amić D., Davidović-Amić D., Beslo D., Trinajstić N., 2003, Structure-Radical Scavenging Activity Relationships of Flavonoids, *Croatica Chemica Acta*, 76 (1), 55-61.

Anon, 1994, Die Grosse Enzyklopädie der Heilpflanzen; Ihre Anwendung und Ihre natürliche Heilkraft, Neuer Kaiser Verlag, Klagenfurt, Austria.

AOAC Methods, 1980, 43.066.

Aruoma O.I., Halliwell B., Aeschbach R., Löligers J., 1992, Antioxidant and pro-oxidant properties of active rosemary constituents: carnosol and carnosic acid, *Xenobiotica*, 22 (2), 257-268.

Aruoma O.I., Spencer J.P.E., Rossi R., Aeschbach R., Khan A., Mahmood N., Munoz A., Murcia A., Butler J., Halliwell B., 1996, An Evaluation of the Antioxidant and Antiviral Action of Extracts of Rosemary and Provencal Herbs, *Food and Chemical Toxicology*, 34, 449-456.

Ashworth P., 1976, Electron Spin Resonance Studies of Structure and Conformation in Anion Radicals Formed during the Autoxidation of Hydroxylated Coumarins, *Journal of Organic Chemistry*, 41 (17), 2920-2927.

Atamna H., Paler-Martinez A., Ames B.N., 2000, N-t-Butyl Hydroxylamine, a Hydrolysis Product of α-Phenyl-N-t-butyl Nitrone, Is More Potent in Delaying Senescence in Human Lung Fibroblasts, *The Journal of Biological Chemistry*, 275 (10), 6741-6748.

Aviram M., Fuhrman B., 2003, Effects of Flavonoids on the Oxidation of Low-Density Lipoprotein and Atherosclerosis, in C.A. Rice-Evans and L. Packer, *Flavonoids in Health and Disease*, 2nd edition, Marcel Dekker Inc., New York, 165-203.

Barata-Soares A.D., Gomez M.L.P.A., de Mesquita C.H., Lajolo F.M., 2004, Ascorbic acid biosynthesis: a precursor study on plants, *Brazilian Journal of Plant Physiology*, 16 (3), 147-154.

Barrett S., 2005, Antioxidants and Other Phytochemicals: Current Scientific Perspective, http://www.quackwatch.org/03HealthPromotion/antioxidants.html (accessed online September 2005).

Benzie I.F.F., Strain J.J., 1996, The Ferric Reducing Ability of Plasma (FRAP) as a Measure of "Antioxidant Power": The FRAP Assay, *Analytical Biochemistry*, 239, 70-76.

Berger A., 2001, Versuche zur Klonierung der Rosmarinsäuresynthase und anderer Gene der Rosmarinsäure-Biosynthese aus *Coleus blumei*, PhD, Heinrich-Heine-Universität Düsseldorf, Germany.

Bolton J.R., 1972, Electron Spin Resonance Theory, in: H.M. Swartz, J.R. Bolton, D.C. Borg, *Biological Applications of Electron Spin Resonance*, John Wiley & Sons, Inc., New York, London, Sydney, Toronto, pp 24.

Bors W., Michel C., Stettmaier K., Lu Y., Foo L.Y., 2003, Pulse radiolysis, electron paramagnetic resonance spectroscopy and theoretical calculations of caffeic acid oligomer radicals, *Biochimica et Biophysica Acta*, 1620, 97-107.

Bors W., Michel C., Stettmaier K., Lu Y., Foo L.Y., 2004, Antioxidant Mechanisms of Polyphenolic Caffeic Acid Oligomers, Constituents of *Salvia officinalis*, *Biological Research*, 37, 301-311.

Bors W., Saran M., 1987, Radical Scavenging by Flavonoid Antioxidants, *Free Radical Research Communications*, 2 (4-6), 289-294.

Breene W.M., 1990, Nutritional and Medicinal Value of Specialty Mushrooms, *Journal of Food Protection*, 53 (10), 883-894.

Britton G., Liaaen-Jensen S., Pfander H., 1995, *Carotenoids, Volume 1A: Isolation and Analysis*, Birkhäuser, Basel, Switzerland.

Britton G., Liaaen-Jensen S., Pfander H., 1998, *Carotenoids, Volume 3: Biosynthesis and Metabolism*, Birkhäuser, Basel, Switzerland.

Brody T., 1999, Vitamins, in: *Nutritional Biochemistry*, 2nd Edition, Academic Press, San Diego, New York, Boston, London, Sydney, Tokyo, Toronto.

Buettner G.R., 1987, Spin Trapping: ESR Parameters of Spin Adducts, *Free Radical Biology & Medicine*, 3, 259-303.

Buettner G.R., Jurkewicz B.A., 1993, Ascorbate free radical as a marker of oxidative stress – an EPR study. *Free Radical Biology and Medicine*, 14, 49-55.

Cao G., Sofic E., Prior R.L., 1997, Antioxidant and prooxidant behaviour of flavonoids: structure-activity relationships, *Free Radical Biology & Medicine*, 22 (5), 749-760.

Cao H., Cheng W.-X., Li C., Pan X.-L., Xie X.-G., Lie T.-H., 2005, DFT study on the antioxidant activity of rosmarinic acid, *Journal of Molecular Structure: THEOCHEM*, 719, 177-183.

Chen S.-X., Schopfer P., 1999, Hydroxyl-radical production in physiological reactions, *European Journal of Biochemistry*, 260, 726-735.

Cheung L.M., Cheung P.C.K., Ooi V.E.C., 2003, Antioxidant activity and total phenolics of edible mushroom extracts, *Food Chemistry*, 81, 249-255.

Cotelle N., Bernier J.-L., Catteau J.-P., Pommery J., Wallet J.-C., Gaydou E.M., 1996, Antioxidant Properties of Hydroxy-Flavones, *Free Radical Biology & Medicine*, 20 (1), 35-43.

Craig W.J., 1999, Health-promoting properties of common herbs, *American Journal of Clinical Nutrition*, 70, 491S-499S.

Davies M.B., Austin J., Partridge D.A., 1991, *Vitamin C – Its Chemistry and Biochemistry*, The Royal Society of Chemistry, Cambridge; The Bath Press, Bath, UK.

Deighton N., Glidewell S.M., Deans S.D., Goodman B.A., 1993, Identification by EPR spectroscopy of carvacrol and thymol as the major sources of free radicals in the oxidation of plant essential oils, *Journal of the Science of Food and Agriculture*, 63, 221-225.

Deighton N., Glidewell S.M., Goodman B.A. and Deans S.D., 1994, The chemical fate of endogenous plant antioxidants carvacrol and thymol during oxidative stress, Proceedings of the Royal Society of Edinburgh, 102B, 247-252.

del Bano M.J., Lorente J., Castillo J., Benavente-Garcia O., del Rio J.A., Ortuno A., Quirin K.-W., Gerard D., 2003, Phenolic Diterpenes, Flavones, and Rosmarinic Acid Distribution during the Development of Leaves, Flowers, Stems, and Roots of *Rosmarinus officinalis*. Antioxidant Acitvity, *Journal of Agricultural and Food Chemistry*, 51, 4247-4253.

Dixon W.T., Moghimi M., Murphy D., 1974, Substituent Effects in the E.s.r. Spectra of Phenoxyl Radicals, *Journal of the Chemical Society-Faraday Transactions II*, 70, 1713-1720.

Dixon W.T., Moghimi M., Murphy D., 1975, Electron Spin Resonance Study of the Stereochemistry of Radicals related to Cinnamic Acid, *Journal of the Chemical Society-Perkin Transactions 2*, 1189.

Food Standards Agency, 2002, McCance and Widdowson's The Composition of Foods, Sixth Summary Edition, Royal Society of Chemistry, Cambridge, UK.

Foyer C.H., Noctor G., 2001, The molecular biology and metabolism of glutathione, in Grill D., Tausz M., De Kok L.J., *Significance of Glutathione in Plant Adaptation to the Environment*, Kluwer Academic Publisher, Dordrecht, pp 27-56.

Frankel E.N., Meyer A.S., 2000, The problems of using one-dimensional methods to evaluate multifunctional food and biological antioxidants, *Journal of the Science of Food and Agriculture*, 80, 1925-1941.

Fréjaville C., Karoui H., Tuccio B., Le Moigne F., Culcasi M., Pietri S., Lauricella R., Tordo P., 1995, 5-(Diethoxyphosphoryl)-5-methyl-1-pyrroline-*N*-oxide: A new efficient phosphorylated nitrone for the *in vitro* and *in vivo* trapping of oxygen-centred radicals, *Journal of Medicinal Chemistry*, 38, 258-265.

Fuhrman B., Volkova N., Rosenblat M., Aviram M., 2000, Lycopene Synergistically Inhibits LDL Oxidation in Combination with Vitamin E, Glabridin, Rosmarinic Acid, Carnosic Acid, or Garlic, *Antioxidants & Redox Signaling*, 2 (3), 491-506.

Geoffroy M., Lambelet P., Richert P., 1994, Radical Intermediates and Antioxidants: An ESR Study of Radicals Formed on Carnosic Acid in the Presence of oxidized Lipids, *Free Radical Research*, 21(4), 247-258.

George P., 1953, The Chemical Nature of the Second Hydrogen Peroxide Compound Formed by Cytochrome c Peroxidase and Horseradish Peroxidase, *Biochemical Journal*, 54, 267-276.

Gershenzon J., Kreis W., 1999, Biochemistry of terpenoids: monoterpenes, sesquiterpenes, diterpenes, sterols, cardiac glycosides and steroid saponins, in: M. Wink, *Biochemistry of Plant Secondary Metabolism*, Sheffield Academic Press, England, pp 222-299.

Gesundheitsratgeber, http://www.drogistenverband.at/gesundheitsratgeber/Natur/ergaenz/vitamine.htm (accessed online September 2005).

Gigante B., Santos C., Silva A.M., Curto M.J.M., Nascimento M.S.J., Pinto E., Pedro M., Cerqueira F., Pinto M.M., Duarte M.P., Laires A., Rueff J., Goncalves J., Pegado M.I., Valdeira M.L., 2003, Catechols from Abietic Acid: Synthesis and Evaluation as Bioactive Compounds, *Bioorganic & Medicinal Chemistry*, 11, 1631-1638.

Gil M.I., Ferreres F., Tomás-Barberán F.A., 1999, Effect of Postharvest Storage and Processing on the Antioxidant Constituents (Flavonoids and Vitamin C) of Fresh-Cut Spinach, *Journal of Agricultural and Food Chemistry*, 47 (6), 2213-2217.

Giusti M. M., Wrolstad R.E., 2001, Characterization and Measurements of Anthocyanins by UV-Visible Spectroscopy, in: *Current Protocols in Food Analytical Chemistry"*, Unit F1.2.

Glidewell S.M., Goodman B.A. and Skilling J., 1996, in J. Skilling and S. Sibisi, *Maximum Entropy and Bayesian Methods*, Cambridge 1994, Kluwer, Dordrecht, pp 22.

González A.G., Andrés L.S., Aguiar Z.E., Luis J.G., 1995, Diterpenes from *Salvia mellifera* and their biogenetic significance, *Phytochemistry*, 31, 1297-1305.

Goodman B.A., Raynor J.B., 1970, Electron Spin Resonance of Transition Metal Complexes, in: H.J. Emeléus, A.G. Sharpe, *Advances in Inorganic Chemistry and Radiochemistry*, Vol. 13, Academic Press, New York, London, pp 136.

Goodman B.A., Glidewell S.M., Arbuckle C.M., Bernardin S., Cook T.R., Hillman J.R., 2002, An EPR study of free radical generation during maceration of uncooked vegetables, *Journal of the Science of Food and Agriculture*, 82, 1208-1215.

Goodwin T.W., Britton G., 1988, Distribution and Analysis of Carotenoids in: T.W. Goodwin, *Plant Pigments*, Academic Press, London, San Diego, New York, Berkeley, Boston, Sydney, Tokyo, Toronto.

Graf H., 1990, Sauerstoffradikale in biologischen Systemen, *GIT Fachz. Lab.* 8/90, 963-968.

Green M.J., Hill H.A.O., 1984, Chemistry of Dioxygen, *Methods in Enzymology*, 105, 3-22.

Halliwell B., Gutteridge J.M.C., 1984, Oxygen toxicity, oxygen radicals, transition metals and disease, *Biochemical Journal*, 219, 1-14.

Halliwell B., Aeschbach R., Löliger J., Aruoma O.I., 1995, The Characterizatiin of Antioxidants, *Food and Chemical Toxicology*, 33 (7), 601-617.

Haraguchi H., Saito T., Okamura N., Yagi A., 1995, Inhibition of Lipid Peroxidation and Superoxide Generation by Diterpenoids from *Rosmarinus officinalis*, *Planta Medica*, 61, 333-336.

Hart D.J., Scott K.J., 1995, Development and evaluation of an HPLC method for the analysis of carotenoids in foods, and the measurement of the carotenoid content of vegetables and fruits commonly consumed in the UK, *Food Chemistry*, 54, 101-111.

Harvard School of Public Health, 2004, Fruits & Vegetables, http://www.hsph.harvard.edu/nutritionsource/fruits.html (accessed online September 2005).

Higdon J., 2004, http://lpi.oregonstate.edu/infocenter/vitamins/vitaminC (accessed online September 2005).

Hiramoto K., Kaku M., Kato T. and Kikugawa K., 1995, DNA strand breaking by the carbon-centred radical generated from 4-(hydroxymethyl)benzene diazonium salt, a carcinogen in mushroom *Agaricus bisporus*, Chemico-Biological Interactions, 94, 21-36.

Hosny M., Johnson H.A., Ueltschy A.K., Rosazza J.P.N., 2002, Oxidation, Reduction, and Methylation of Carnosic Acid by *Nocardia*, *Journal of Natural Products*, 65, 1266-1269.

Huang Q., Huang Q., Pinto R.A., Griebenow K., Schweitzer-Stenner R., Weber W.J.jr., 2005, Inactivation of Horseradish Peroxidase by Phenoxyl Radical Attack, *Journal of the American Chemical Society*, 127, 1431-1437.

Ito H., Miyazaki T., Ono M., Sakurai H., 1998, Antiallergic Activities of Rabdosiin and its Related Compounds: Chemical and Biochemical Evaluations, *Bioorganic & Medicinal Chemistry*, 6, 1051-1056.

Jakopitsch C., Wanasinghe A., Jantschko W., Furtmüller P.G., Obinger C., 2005, Kinetics of Interconversion of Ferrous Enzymes, Compound II and Compound III, of

Wild-type *Synechocystis* Catalase-peroxidase and Y249F, *The Journal of Biological Chemistry,* 280 (10), 9037-9042.

Janzen E.G., 1984, Spin Trapping of Superoxide and Hydroxyl Radicals, *Methods in Enzymology,* 105, 198-209.

Kellner R., Mermet J.-M., Otto M., Valcárcel M., Widmer H.M., 2004, *Analytical Chemistry,* 2nd edition, Wiley-VCH Verlag GmbH & Co. KGaA, Weinheim.

Koch-Heitzmann I., Shultze W., 1988, 2000 Jahre *Melissa officinalis* von der Bienenpflanze zum Virustatikum, *Zeitschrift für Phytotherapie,* 9, 77-85.

Kosaka K., Yokoi T., 2003, Carnosic Acid, a Component of Rosemary (Rosmarinus officinalis L.), Promotes Synthesis of Nerve Growth Factor in T98G Human Glioblastoma Cells, *Biological and Pharmaceutical Bulletin,* 26 (11), 1620-1622.

Kuhnle J.A., Windle J.J., Waiss A.C. jun., 1969, Electron Paramagnetic Resonance Spectra of Flavonoid Anion-radicals, *Journal of the Chemical Society (B),* 613-616.

Laroff G.P., Fessenden R.W., Schuler R.H., 1972, The electron spin resonance spectra of radical intermediates in the oxidation of ascorbic acid and related substances, *Journal of the American Chemical Society,* 94, 9062-9073.

Le Nest G., Caille O., Woudstra M., Roche S., Burlat B., Belle V., Guigliarelli B., Lexa D., 2004, Zn-polyphenol chelation: complexes with quercetin, (+)-catechin, and derivatives: II Electrochemical and EPR studies, *Inorganica Chimica Acta,* 357, 2027-2037.

Leng-Peschlow E., Strenge-Hesse A., 1991, Die Mariendistel (*Silybum marianum*) und Silymarin als Lebertherapeutikum, *Zeitschrift für Phytotherapie,* 12, 162-174.

Levenberg B., 1962, An aromatic diazonium compound in the mushroom *Agaricus bisporus, Biochimica et Biophysica Acta,* 63, 212-214.

Lichtenthaler H.K., 1999, The 1-deoxy-D-xylulose-5-phosphate pathway of isoprenoid biosynthesis in plants, *Annual Review of Plant Physiology and Plant Molecular Biology,* 50, 47-65.

List P.H., Horhämmer L., 1973, *Hager's Handbuch der Pharmazeutischen,* Praxis, Springer-Verlag, Berlin, Germany.

Liszkay A., van der Zalm E., Schopfer P., 2004, Production of reactive oxygen intermediates (O_2^-, H_2O_2, and $\cdot OH$) by maize roots and their role in wall loosening and elongation growth, *Plant Physiology,* 136, 3114-3123.

Loth H., Klinge D., 1964, Ein dimeres Flavonol als Intermediärprodukt der Oxydation des Kämpferol-3-glucosids durch Peroxydase, *Archiv der Pharmazie,* 297 (3), 165-172.

Madsen H.L., Nielsen B.R., Bertelsen G., Skibsted L.H., 1996, Screening of antioxidative activity of spices. A comparison between assays based on ESR spin

trapping and electrochemical measurement of oxygen consumption, *Food Chemistry*, 57 (2), 331-337.

Madsen H.L., Andersen C.M., Jörgensen L.V., Skibsted L.H., 2000, Radical scavenging by dietary flavonoids. A kinetic study of antioxidant efficiencies, *European Food Research and Technology*, 211, 240-246.

Masuda T., Inaba Y., Takeda Y., 2001, Antioxidant Mechanism of Carnosic Acid: Structural Identification of Two Oxidation Products, *Journal of Agricultural and Food Chemistry*, 49, 5560-5565.

McCord J.M.; Fridovich I., 1969, Superoxide dismutase: an enzymic function for erythrocuprein (hemocuprein), *Journal of Biological Chemistry*, 244, 6049-6055.

McCormick M.L., Buettner G.R., Britigan B.E., 1995, The spin trap α-(4-pyridyl-1-oxide)-*N-t*-butylnitrone stimulates peroxidase-mediated oxidation of desferoxamine – implications for pharmacological use of spin trapping agents, *Journal of Biological Chemistry*, 270, 29265-29269.

McGarvey D.J., Croteau R., 1995, Terpenoid Metabolism, *The Plant Cell*, 7, 1015-1026.

McPhail D.B., Hartley R.C., Gardner P.T., Duthie G.G., 2003, Kinetic and Stoichiometric Assessment of the Antioxidant Activity of Flavonoids by Electron Spin Resonance Spectroscopy, *Journal of Agricultural and Food Chemistry*, 51, 1684-1690.

Milić B.L., Milić N.B., 1998, Protective Effects of Spice Plants on Mutagenesis, *Phytotherapy Research*, 12, S3-S6.

Miller E., 1984, Modellversuche zur Peroxidase (Donor: H_2O_2-oxidoreductase, EC 1.11.1.7)-katalysierten Umsetzung von Flavonolen (Quercetin, Kämpferol) und (E)-4-Hydroxyzimtsäure mit H_2O_2, PhD, Bayerische Julius-Maximilians-Universität, Germany.

Miller E., Schreier P., 1985, Studies on Flavonol Degradation by Peroxidase (Donor: H_2O_2-oxidoreductase, EC 1.11.1.7): Part 1-Kaempferol, *Food Chemistry*, 17, 143-154.

Miura T., Muraoka S., Fujimoto Y., 2003, Inactivation of creatine kinase induced by quercetin with horseradish peroxidase and hydrogen peroxidase: pro-oxidative and anti-oxidative actions of quercetin, *Food and Chemical Toxicology*, 41, 759-765.

Mouhajir F., Pedersen J.A., Rejdali M., Towers G.H.N., 2001, Phenolics in Moroccan Medicinal Plant Species as Studied by Electron Spin Resonance Spectroscopy, *Pharmaceutical Biology*, 39 (5), 391-398.

Muckenschnabel I., Schulze Gronover C., Deighton N., Goodman B.A., Lyon G.D., Stewart D. and Williamson B., 2003, Long range oxidative effects in leaves of bean (*Phaseolus vulgaris*) infected by *Botrytis cinerea*, *Journal of the Science of Food and Agriculture*, 83, 507-514.

Munné-Bosch S., Alegre L., 2003, Drought-Induced Changes in the Redox State of α-Tocopherol, Ascorbate, and the Diterpene Carnosic Acid in Chloroplasts of Labiatae Species Differing in Carnosic Acid Contents, *Plant Physiology*, 131, 1816-1825.

Munné-Bosch S., Alegre L., 2001, Subcellular Compartmentation of the Diterpene Carnosic Acid and Its Derivatives in the Leaves of Rosemary, *Plant Physiology*, 125, 1094-1102.

Munné-Bosch S., Schwarz K., Alegre L., 1999, Enhanced Formation of α-Tocopherol and Highly Oxidized Abietane Diterpenes in Water-Stressed Rosemary Plants, *Plant Physiology*, 121, 1047-1052.

Murkovic M., Gams K., Draxl S., Pfannhauser W., 2000, Development of an Austrian Carotenoid Database, *Journal of Food Composition and Analysis*, 13, 435-440.

N.I.E.H.S. Spin-Trap DataBase, 1998, http://mole.chm.bris.ac.uk/cgi-bin/stdb (accessed online September 2005).

Narayanan C.R., Linde H., 1965, Stereochemistry of Salvin and Picrosalvin, *Tetrahedron Letters*, 41, 3647-3649.

Neta P., Fessenden R.W., 1974, Hydroxyl Radical Reactions with Phenols and Anilines as Studied by Electron Spin Resonance, *The Journal of Physical Chemistry*, 78 (5), 523-529.

Otto M., 2000, *Analytische Chemie*, 2nd edition, Wiley-VCH Verlag GmbH, Weinheim, Germany.

Pachla L.A., Reynolds D.L., Kissinger P.T., 1985, Analytical Methods for Determining Ascorbic Acid in Biological Samples, Food Products, and Pharmaceuticals, *Journal of the Association of Official Analytical Chemists*, 68 (1), 1-12.

Parejo I., Viladomat F., Bastida J., Rosas-Romero A., Flerlage N., Burillo J., Codina C., Comparison between the radical scavenging activity and antioxidant activity of six distilled and nondistilled Mediterranean herbs and aromatic plants, *Journal of Agricultural and Food Chemistry*, 50 (2002) 6882-6890.

Pascual E.C., Goodman B.A. and Yeretzian C., 2002, Characterisation of free radicals in soluble coffee by electron paramagnetic resonance spectroscopy, *Journal of Agricultural and Food Chemistry*, 50, 6114-6122.

Pascual E.C., 2000, Free Radicals and Oxidative Processes in Coffee, PhD, University of Dundee, UK.

Pastore P., Rizzetto T., Curcuruto O., Cin M.D., Zaramella A., Marton D., 2001, Characterization of dehydroascorbic acid solutions by liquid chromatography/mass spectrometry, *Rapid Communications in Mass Spectrometry*, 15, 2051-2057.

Pedersen J.A., 1978, Naturally occurring Quinols and Quinones studied as Semiquinones by Electron Spin Resonance, *Phytochemistry*, 17, 775-778.

Pedersen J.A., 1982, Phenolic Acids in the Genus *Lycopodium*, *Biochemical Systematics and Ecology*, 10, 3-9.

Pedersen J.A., 2000, Distribution and taxonomic implications of some phenolics in the family Lamiaceae determined by ESR spectroscopy, *Biochemical Systematics and Ecology*, 28, 229-253.

Pedrielli P., Pedulli G.F., Skibsted L.H., 2001, Antioxidant Mechanism of Flavonoids. Solvent Effect on Rate Constant for Chain-Breaking Reaction of Quercetin and Epicatechin in Autoxidation of Methyl Linoleate, *Journal of Agricultural and Food Chemistry*, 49, 3034-3040.

Petersen M., Strack D., Matern U., 1999, Biosynthesis of phenylpropanoids and related compounds, in: M. Wink, *Biochemistry of Plant Secondary Metabolism*, Sheffield Academic Press, England, pp 151-221.

Pietta P., Gardana C., Pietta A., 2003, Flavonoids in Herbs, in: C.A. Rice-Evans and L.Packer, *Flavonoids in Health and Disease*, 2nd edition, Marcel Dekker Inc., New York, pp 43-69.

Pilar J., 1970, Electron Paramagnetic Resonance Study of 4-Alkyl-*o*-benzosemiquinones, *The Journal of Physical Chemistry*, 74 (23), 4029-4037.

Pirker K.F., 2002, Free radical content of tomato and strawberry fruits exposed to drought and ozone stress, Master thesis, Vienna, Austria.

Pirker K.F., Goodman B.A., Pascual E.C., Kiefer S., Soja G., Reichenauer T.G., 2002, Free radicals in the fruit of three strawberry cultivars exposed to drought stress in the field, *Plant Physiology and Biochemistry*, 40 (6-8), 709-717.

Pirker K.F., Reichenauer T.G., Goodman B.A., Stolze K., 2004, Identification of oxidative processes during simulated mastication of uncooked foods using electron paramagnetic resonance spectroscopy, *Analytica Chimica Acta*, 520, 69-77.

Poole C.P.jr., 1997, Electron Spin Resonance - A comprehensive treatise of experimental techniques, Dover publication, Mineola, New York.

Puppo A., 1992, Effect of Flavonoids on Hydroxyl Radical Formation by Fenton-Type Reactions; Influence of the Iron Chelator, *Phytochemistry*, 31 (1), 85-88.

Rice-Evans C.A., Miller N.J., Paganga G., 1996, Structure-antioxidant activity relationships of flavonoids and phenolic acids, *Free Radical Biology and Medicine*, 20 (7), 933-956.

Ross A.E., Nagel D.L. and Toth B., 1982, Evidence for the occurrence and formation of diazonium ions in the *Agaricus bisporus* mushroom and its extracts, *Journal of Agricultural and Food Chemistry*, 30, 521-525.

Sánchez-Moreno C., Larrauri J.A., Saura-Calixto F., 1998, A Procedure to Measure the Antiradical Efficiency of Polyphenols, *Journal of the Science of Food and Agriculture*, 76, 270-276.

Sankuratri N., Janzen E.G., 1996, Synthesis and spin trapping chemistry of a novel bicyclic nitrone: 1,3,3-trimethyl-6-azabicyclo[3.2.1]oct-6-ene-*N*-oxide (TRAZON), Tetrahedron Letters, 37, 5313-5316.

Schopfer P., 2001, Hydroxyl radical-induced cell-wall loosening *in vitro* and *in vivo*: implications for the control of elongation growth, *The Plant Journal*, 28 (6), 679-688.

Schopfer P., Liszkay A., Bechtold M., Frahry G., Wagner A., 2002, Evidence that hydroxyl radicals mediate auxin-induced extension growth, *Planta*, 214, 821-828.

Schroeter H., Spencer J.P.E., 2003, Flavonoids: Neuroprotective Agents? Modulation of Oxidative Stress-Induced MAP Kinase Signal Transduction, in: C.A. Rice-Evans and L. Packer, *Flavonoids in Health and Disease*, 2nd edition, Marcel Dekker Inc., New York, 233-272.

Schwarz K., Ternes W., 1992, Antioxidative constituents of *Rosmarinus officinalis* and *Salvia officinalis*, II. Isolation of carnosic acid and formation of other phenolic diterpenes, *Zeitschrift für Lebensmittel-Untersuchung und -Forschung*, 195, 99-103.

Seigler D.S., 1998, Flavonoids in: *Plant Secondary Metabolism*, Kluwer Academic Publishers, AH Dordrecht, The Netherlands, pp 151-192.

Selloum L., Reichl S., Müller M., Sebihi L., Arnhold J., 2001, Effects of Flavonols on the Generation of Superoxide Anion Radicals by Xanthine Oxidase and Stimulated Neutrophils, *Archives of Biochemistry and Biophysics*, 395 (1), 49-56.

Skoog D.A., Leary J.J., 1992, *Principles of Instrumental Analysis*, 4th edition, Saunders College Publishing, Orlando.

Skibola C.F., Smith M.T., 2000, Potential Health Impacts of Excessive Falvonoid Intake, *Free Radical Biology & Medicine*, 29 (3/4), 375-383.

Smirnoff N., 1993, The role of active oxygen in the response of plants to water deficit and desiccation, *New Phytology*, 125, 27-58.

Smirnoff N., 1996, The Function and Metabolism of Ascorbic Acid in Plants, *Annals of Botany*, 78, 661-669.

Spencer J.P.E., Schroeter H., Rice-Evans C.A., 2003, Cytoprotective and Cytotoxic Effects of Flavonoids, in: C.A. Rice-Evans and L. Packer, *Flavonoids in Health and Disease*, 2nd edition, Marcel Dekker Inc., New York, 309-347.

Steer J., 2005, Structure and Reactions of Chlorophyll, http://www.ch.ic.ac.uk/local/projects/steer/chloro.htm (accessed online September 2005).

Stolze K., Udilova N., Nohl H., 2000, Spin trapping of lipid radicals with DEPMPO-derived spin traps: detection of superoxide, alkyl and alkoxyl radicals in aqueous and lipid phase, *Free Radical Biology & Medicine,* 29, 1005-1014.

Stolze K., Udilova N., Nohl H., 2002, ESR analysis of spin adducts of alkoxyl and lipid-derived radicals with the spin trap Trazon. *Biochemical Pharmacology,* 63, 1465-1470.

Stolze K., Udilova N., Rosenau T., Hofinger A., Nohl H., 2003, Synthesis and characterisation of EMPO-derived 5,5-disubstituted 1-pyrroline *N*-oxides as spin traps forming exceptionally stable superoxide spin adducts, *Biological Chemistry,* 384, 493-500.

Suh J., Zhu B.-Z., Frei B., 2003, Ascorbate does not act as a pro-oxidant towards lipids and proteins in human plasma exposed to redox-active transition metal ions and hydrogen peroxide, *Free Radical Biology & Medicine,* 34 (10), 1306-1314.

Takahama U., 1987, Oxidation Products of Kaempferol by Superoxide Anion Radical, *Plant and Cell Physiology,* 28 (5), 953-957.

Terada L.S., Leff J.A., Repine J.E., 1990, Measurement of Xanthine Oxidase in Biological Tissues, *Methods in Enzymology,* 186, 651-656.

Tyler V.E., 1994, Herbs of Choice; The Therapeutic Use of Phytomedicinals, Pharmaceuticals Products Press, New York, USA.

Vamos-Vigyazo L., 1981, Polyphenol oxidase and peroxidase in fruits and vegetables, *Critical Reviews of Food Science and Nutrition,* 15 (1), 49-127.

Van Acker S.A.B.E., De Groot M.J., Van den Berg D.-J., Tromp M.N.J.L., Den Kelder G.D.-O., Van der Vijgh W.J.F., Bast A., 1996, A Quantum Chemical Explanation of the Antioxidant Activity of Flavonoids, *Chemical Research in Toxicology,* 9, 1305-1312.

Van Hoorn D.E.C., Nijveldt R.J., Van Leeuwen P.A.M., Hofman Z., M'Rabet L., De Bont D.B.A., Van Norren K., 2002, Accurate prediction of xanthine oxidase inhibition based on the structure of flavonoids, *European Journal of Pharmacology,* 451, 111-118.

Vana N., lecture of "Magnetische Resonanzspektroskopie", hold 2003 at the Technical University of Vienna.

Visser F.R., 1984, Some Effects of Replacement of Metaphosphoric Acid/Acetic Acid Solvent System with Trichloroacetic Acid in Microfluorometric Determination of Vitamin C, *Journal of the Association of Official Analytical Chemists,* 67 (5), 1020-1022.

Walker A.F., 1996, Of hearts and herbs, Biologist, 43, 177-180.

Wenkert E., Fuchs A., McChesney J.D., 1965, Chemical Artifacts from the Family *Labiatae, Journal of Organic Chemistry,* 36, 2931-2934.

Wheeler G.L., Jones M.A., Smirnoff N., 1998, The biosynthetic pathway of vitamin C in higher plants, *Nature*, 393, 365-369.

Williams R.J., Spencer J.P.E., Rice-Evans C., 2004, Flavonoids: Antioxidants or signalling molecules?, *Free Radical Biology & Medicine*, 36 (7), 838-849.

Wikipedia, 2005, http://de.wikipedia.org/wiki/Flavonoide.

Wink M., Introduction: biochemistry, role and biotechnology of secondary metabolites, in: M. Wink, *Biochemistry of Plant Secondary Metabolism*, Sheffield Academic Press, England, pp 1-16.

Wrolstad R.E., Culbertson J.D., Cornwell C.J., and Mattick L.R. 1982, Detection of adulteration in blackberry juice concentrates and wines, *Journal of the Association of Official Analytical Chemists*, 65, 1417-1423.

Yu J., Taylor K.E., Zou H., Biswas N., Bewtra J.K., 1994, Phenol Conversion and Dimeric Intermediates in Horseradish Peroxidase-Catalyzed Phenol Removal from Water, *Environmental Science and Technology*, 28, 2154-2160.

APPENDICES

A.1. PUBLICATION OF MUSHROOMS AND HERBS

Pirker K.F., Reichenauer T.G., Goodman B.A., Stolze K., 2004, Identification of oxidative processes during simulated mastication of uncooked foods using electron paramagnetic resonance spectroscopy, *Analytica Chimica Acta,* 520, 69-77.

Identification of oxidative processes during simulated mastication of uncooked foods using electron paramagnetic resonance spectroscopy

Katharina F. Pirker[a,*], Thomas G. Reichenauer[a], Bernard A. Goodman[a], Klaus Stolze[b]

[a] ARC Seibersdorf research GmbH, Department of Environmental Research, A-2444 Seibersdorf, Austria
[b] Institute of Applied Botany, Veterinary University of Vienna, Basic Pharmacology and Toxicology, A-1210 Vienna, Austria

Abstract

Electron paramagnetic resonance (EPR) spectroscopy is used to measure directly the generation of free radicals during a simulation of the mastication process. This involves the gentle grinding of the food product in the presence of a spin trap, a molecule which reacts selectively with unstable free radicals to generate (more) stable radical adducts, which can then be characterised. With mushrooms of the *Agaricus* family, adducts consistent with a carbon-centred radical are seen with a wide range of spin traps and this radical has been confirmed as 4-(hydroxymethyl)phenyl. In plant tissues that are rich in ascorbic acid, this molecule competes successfully with spin traps for the free radicals and the (monodehydro)ascorbate radical, formed by the 1-electron oxidation of ascorbic acid, is seen in the EPR spectra. However, with >50% of the plant tissue samples studied in the present experiment, free radicals resulting from oxidation of the spin traps were observed. The formation of such molecules, for which oxygen was found to be necessary, requires the existence of powerful oxidation processes as the plant tissue is broken down. Such pro-oxidant behaviour is contrary to the popular assumption that the beneficial effects of uncooked plant tissues are the result of their high levels of anti-oxidant molecules.
© 2004 Elsevier B.V. All rights reserved.

Keywords: Free radicals; Spin traps; Mushrooms; Herbs; Antioxidant; Pro-oxidant

1. Introduction

There is currently great interest in the relationships between health and eating habits and major efforts are now being made to develop our understanding of what constitutes a healthy diet. Indeed, there is clear evidence that high blood pressure and elevated low-density lipoprotein (LDL) cholesterol, two factors that are associated with the risk of a heart disease and stroke, have strong dietary links [1,2]. Fresh fruits and vegetables are established as essential components of healthy diets, and it is generally assumed that this is because they contain appreciable quantities of molecules with antioxidant properties that can act as scavengers of reactive oxygen species (ROS). ROS is a general name given to oxygen-derived natural products that have higher reactivity than atmospheric oxygen ($^3O_2$), examples of which include diamagnetic molecules, such as hydrogen peroxide (H_2O_2) and singlet oxygen ($^1O_2$), as well as free radicals

such as the hydroxyl radical ($^•OH$), the superoxide radical anion ($O_2^{•-}$), and radical products of lipid peroxidation reactions ($ROO^•$, $RO^•$ and $R^•$).

Herbs and spices have been suggested to play important roles in stabilising blood pressure and cholesterol levels [3]. Since small quantities of herbs in a dish are enough to change its sensory properties, this indicates that herb-derived substances are involved in chemical reactions with other food components. In addition, many herbs are commonly used as medicinal plants [4,5]. The activities of a number of herbal medicines are considered to be derived from their general antioxidant properties (e.g. *Gingko biloba* L.—[4]; *Silybum marianum* L. (milk thistle)—[6]). In other cases activity has been specifically associated with phenolic compounds (e.g. *Melissa officinalis* L.—[7]; *Thymus vulgaris* L.—[8]), which would also be expected to function as antioxidants. However, reaction of an organic molecule with a free radical generally leads to the generation of a new free radical species, and hence the reactions of many antioxidants might be expected to proceed via free radical pathways, as has been shown for the phenols thymol and carvacrol from *T. vulgaris* L. [9,10].

The aim of the present paper is help develop our understanding of free radical reactions in foodstuffs that may be consumed in uncooked forms, and the present work is based on the use of electron paramagnetic resonance (EPR) spectroscopy to detect directly free radicals that are generated during simulated mastication. These measurements have been performed on the liquid phases separated from mushroom and plant tissues that were crushed in the presence of chemical spin traps to stabilise and detect short-lived radicals. Extensive measurements were performed with mushrooms from the *Agaricus* family in order to demonstrate the potential of this experimental approach, since it was shown previously [11] that they give intense and informative EPR signals in the presence of the spin traps phenyl-*N*-*t*-butylnitrone (PBN) and α-(4-pyridyl-1-oxide)-*N*-*t*-butylnitrone (4-POBN). The present work builds on these earlier studies by investigating the radical adducts formed with various derivatives of the spin trap 5,5-dimethyl-1-pyrroline-*N*-oxide (DMPO), and also the role of O_2 in the generation of the radical. The radical responsible for the EPR spectra was identified as a carbon-centred radical which was then confirmed by chemical synthesis. The experimental approaches developed for the study of mushrooms were then applied to a range of culinary herbs and other plant tissues. A variety of responses were obtained and examples are presented of specimens which show antioxidant and pro-oxidant reactions as well as the generation of free radicals that can be stabilised by the formation of adducts with spin traps as was the case with the *Agaricus* mushrooms.

2. Materials and methods

2.1. Mushrooms and herbs

Cultivated mushrooms (*Agaricus bisporus*) were purchased from a local supermarket and stored in a refrigerator at 4 °C until they were studied (1–2 days from purchase). Fresh herb samples were either harvested from the garden of one of the authors, immediately frozen to 77 K and maintained at that temperature until being studied, or purchased from a local vegetable market on the day of study. These latter samples were kept at room temperature. In addition commercial samples of freeze-dried herbs (marketed by Kotanyi, Wolkersdorf, Austria) were purchased pre-packaged from local suppliers. Full details of the specimens studied are presented in Table 1.

2.2. Spin traps

4-POBN was purchased from Sigma (St. Louis, MO, USA) and stored in the solid form in a cold room (at ca. −15 °C) for approximately 2 years prior to use. EPR spectra of solutions of this 4-POBN sample did not show the presence of any signal that could have resulted from reactions of the spin trap during storage. Other spin traps, namely 5-(diethoxyphosphoryl)-5-methyl-1-pyrroline-*N*-oxide (DEPMPO), 5-propoxy-carbonyl-5-ethylpyrroline-1-oxide (PEPO) and 1,3,3-trimethyl-6-azabicyclo[3.2.1]oct-6-ene-*N*-oxide (TRAZON) were synthesised at the Institute of Applied Botany in Vienna according to previously published methods

Table 1
Full details of herb samples investigated

Common name	Latin name	Physical form investigated		
		Fresh	Frozen	Freeze-dried
Basil	*Ocimum basilicum*	×		
Bay	*Laurus nobilis*		×	
Celery	*Apium graveolens*		×	
Chives	*Allium schoenoprasum*	×	×	×
Coriander	*Coriandrum sativum*	×		
Deadnettle (red)	*Lamium maculatum*		×	
Deadnettle (white)	*Lamium album*		×	
Elder	*Sambucus nigra*		×	
Ivy	*Hedera helix*		×	
Lavender	*Lavendula angustifolia*		×	
Lemon balm	*Melissa officinalis*		×	
Lovage	*Levisticum officinalis*		×	×
Marjoram	*Origanum majorana*		×	×
Mint	*Mentha piperita*	×	×	
Oregano	*Origanum vulgare*			×
Parsley	*Petroselinum sativum*	×	×	×
Parsley crimpy	*Petroselinum crispum*	×	×	
Rosemary	*Rosmarinus officinalis*	×	×	×
Sage	*Salvia officinalis*	×	×	
Stinging-nettle	*Urtica dioica*		×	
Tarragon	*Artemisia dracunculus*		×	
Thyme	*Thymus vulgaris*	×	×	×

[12–14]. Solutions of these spin traps were made up in distilled water.

2.3. Sample preparation

The mushroom samples studied with DEPMPO, PEPO or TRAZON spin traps were cut into thin slices (ca. 2 mm) and crushed gently in a mortar together with the spin trap solution (ca. 100 mM). The mixture was then centrifuged for 3 min (13,000 rpm, 4 °C) and 500 μl of the supernatant were transferred into cryo tubes and frozen immediately to 77 K. In an additional experiment with DEPMPO the cryo tubes were allowed to stand at room temperature for 30 min before they were transferred into liquid nitrogen. All of these samples were then stored in liquid nitrogen. Immediately prior to running the EPR spectra, the samples were thawed in a water bath (ca. 40 °C) and transferred rapidly to a flat cell. For measurements with 4-POBN as spin trap, a thin slice of mushroom in a mortar was crushed gently with a small quantity of 4-POBN (ca. 1 mg) and distilled water (500 μl), filtered through a disposable syringe filter holder (Fa. Sartorius, 0.45 μm), and the solution transferred to a flat cell for recording the EPR spectrum. The effects of O_2 were investigated by performing the above operations in a glove bag filled with argon and using distilled water that had been saturated with argon.

All of the measurements with herb specimens were performed with 4-POBN and the sample preparation method was analogous to that described in the previous paragraph. Measurements with a sample of thyme in which the spin trap was added separately to fresh and frozen leaves showed that there were no qualitative differences between the results from the two preparation procedures.

2.4. Synthesis of the 4-(hydroxymethyl)phenyl radical

It had been reported previously that the 4-(hydroxymethyl)phenyl radical is produced from 4-(hydroxymethyl)-benzene diazonium salts that are found at appreciable levels in Agaricus mushroom samples [15]. In order to confirm this, adducts with the spin traps 4-POBN, DEPMPO, PEPO and TRAZON were prepared using the following reaction:

$$Ar–NH_2 + NO_2^- + 2H^+ \rightarrow Ar–N_2^+ + 2H_2O$$

$$Ar–N_2^+ + e^- + ST \rightarrow ST–Ar^\bullet + N_2$$
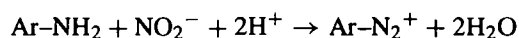
One mole of the primary amine was dissolved in 2.5 mol hydrochloric acid, placed in an ice–salt mixture, and an equivalent amount of a 2.5 mol/l sodium nitrite solution was then added slowly under agitation. Fifty microlitre of this diazo solution were transferred to an Eppendorf tube along with 50 μl of spin trap (ST) solution (0.1 mol/l for 4-POBN, ca. 15 mmol/l for DEPMPO, PEPO and TRAZON). After 30 s, 400 μl phosphate buffer was added and the mixture was transferred to a flat cell for measurement of its EPR spectrum.

The involvement of oxygen in the synthesis of the 4-(hydroxymethyl)phenyl radical was also investigated by performing the above preparation under an inert atmosphere. Two approaches were tried, both using degassed solutions of the amine, $NaNO_2$, spin trap, buffer and water, and differing only in the way the spin trap solution was mixed with the diazonium salt. In the first method the preparation procedure was identical to that for the preparation in air, except that all operations were carried out in a glove bag filled with argon. In the second method the solutions were made up in a test tube bubbled with nitrogen gas, and the final solution was pumped directly into a flow cell located in the EPR spectrometer. This latter method decreased appreciably the time delay between mixing the spin trap and radical solutions and recording the EPR spectrum.

2.5. EPR spectral measurement and processing

All EPR spectra were recorded at X-band frequencies at ambient temperature (ca. 22 °C) on solutions in flat cells (Wilmad-Labglass, Buena, NJ, USA) using a Bruker ESP 300E computer controlled spectrometer (Bruker Biospin, Rheinstetten, Germany) with an ER4103TM microwave cavity. Microwave generation was with a klystron and the frequency was measured with a built-in frequency counter. All spectra were acquired with a microwave power of 20 mW and 100 kHz modulation frequency. A modulation amplitude of 0.1 mT was used for most spectra, but smaller values (≥ 0.03 mT) were used with selected samples to check for the possible presence of small hyperfine splittings. Additionally, larger modulations (≤ 0.16 mT) were used on occasions when the spectra were very weak). DEPMPO adducts were recorded over a 12 mT scan range, PEPO and TRAZON adducts with an 8 mT scan range, whilst all other spectra were recorded over 6 mT. These values are typical of those used for recording spectra of radical adducts of these spin traps.

The accuracy of parameters derived from the spectra was confirmed by simulation using the Bruker Simfonia software. g-values are expressed relative to diphenylpicrylhydroxyl (DPPH) ($g = 2.0036$) which was used as an external standard.

3. Results and discussion

EPR spectra of radical adducts of 4-POBN and PEPO are normally sextets, which result from interaction of the unpaired electron with the ^1H ($I = 1/2$) on the α-carbon of the spin trap and the ^{14}N ($I = 1$) of the nitroxide group. With DEPMPO an additional hyperfine splitting from the interaction of the unpaired electron with ^{31}P ($I = 1/2$) is observed. Spectra from Trazon adducts are more complex. Two inequivalent molecules can be formed by radical addition to the α-C, and each of these can show hyperfine structure
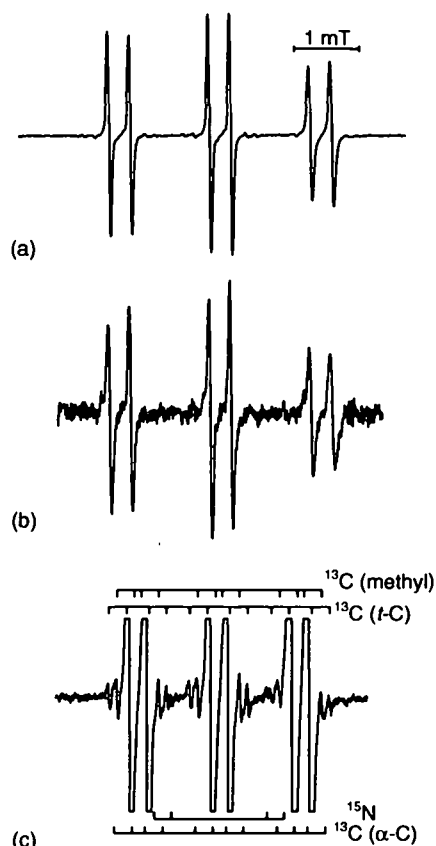
Fig. 1. EPR spectrum of (a) the C-centred radical from mushroom trapped by 4-POBN, (b) 4-(hydroxymethyl) phenyl radical, (c) spectrum from a measured with a high instrumental gain. Spectral interpretation is shown by the "stick" diagram.

from up to five inequivalent protons in addition to the ^{14}N nucleus.

3.1. Agaricus mushroom samples

The main feature in the EPR spectrum from mushroom crushed with 4-POBN (Fig. 1a) is the expected sextet structure and it is essentially identical to that reported for similar samples [11]. As suggested previously, the $a(^{14}N)$ and $a(^{1}H)$ parameters (Table 2) are consistent with the trapping of a carbon-centred radical [16]. In addition, weak satellite peaks were observed at high instrumental gain (Fig. 1c). However, whereas, previous experiments led only to the resolution of features originating from ^{13}C atoms ($I = 1/2$, natural abundance 1.108%) in the t-butyl group [11], Fig. 1b shows clear presence of three different ^{13}C splittings. Furthermore, two additional peaks were observed and these correspond to part of the quartet structure expected for interaction of the unpaired electron with ^{15}N ($I = 1/2$, natural abundance 0.365%), with $a(^{15}N) = 2.19\,mT$. The value of 1.404 for the ratio of the hyperfine splittings $a(^{15}N)/a(^{14}N)$ is that expected from the ratio of their magnetic moments (see e.g. Tables 6 and 7 in Poole and Farach, [17]).
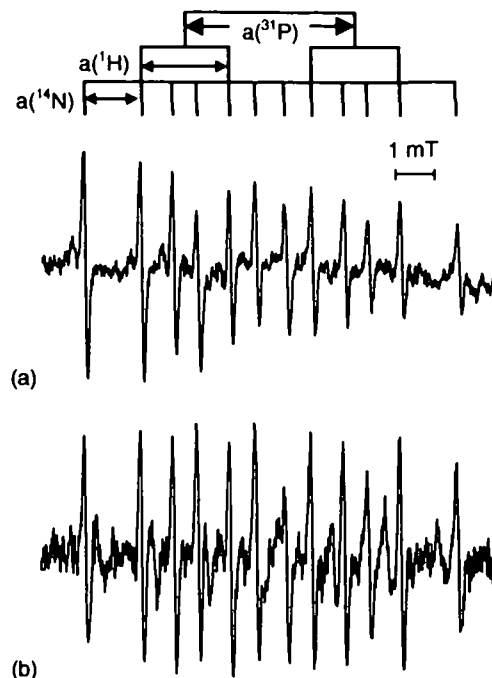

Fig. 2. EPR spectrum of (a) the C-centred radical from mushroom trapped by DEPMPO, (b) 4-(hydroxymethyl) phenyl radical. Spectral interpretation is shown by the "stick" diagram.

When the above reaction was performed in a glove bag under argon an identical spectrum was observed, but its intensity was greatly reduced (to ca. 2% of that observed when the preparation was made in air). Since it is unlikely that the atmosphere in a glove bag could be completely O_2-free, and there would likely have been some air trapped within the mushroom structure, this result strongly suggests that O_2 is required for the generation of the radical.

Spectra from the reaction of mushroom with the spin traps DEPMPO, PEPO and TRAZON (Figs. 2–4) also had parameters (Table 2) that are broadly in line with the values expected for carbon-centred radical adducts. However, with samples from DEPMPO the signals were unstable and decayed with a half life of a few minutes. Interestingly, the intensity of the spectrum from the DEPMPO adduct that was allowed to stand in air for 30 min before freezing was similar to that of the freshly prepared sample. The logical interpretation of this result, therefore, is that O_2 is required for the production of the radical and that on standing in air a steady-state concentration is achieved when the rates of adduct formation and decay are balanced. The EPR signal decayed in the spectrometer, because of the limited air space and/or restricted O_2 diffusion within the flat cell.

3.2. Identity of the free radical formed in mushrooms

In their original work, Hiramoto et al. [15] reported EPR spectral parameters for DMPO, PBN and 3,5-dibromo-4-nitrosobenzene sulfonate (DBNBS) adducts of the 4-(hydroxymethyl)phenyl radical. This radical is readily formed

Table 2
Summary of the hyperfine splittings observed with different spin traps

Spin trap	System	$a(^{31}P)^a$ (mT)	$a(^1H)^a$ (mT)	$a(^{14}N)^a$ (mT)	ΔBpp^b (mT)	g-value[a]
DEPMPO	Mushroom	4.50	2.33	1.48		2.0057
	4-(Hydroxymethyl)phenyl radical	4.50	2.33	1.48	0.1	2.0056
4-POBN	Mushroom		0.33	1.56		2.0058
	4-(Hydroxymethyl)phenyl radical		0.32	1.56	0.05	2.0057
	POBN• radical		0.145, 0.05	1.49, 0.18		
	Coriander, elder, chives		0.26	1.57		
PEPO	Mushroom		2.30	1.50		2.0057
	4-(Hydroxymethyl)phenyl radical		2.30, 0.129	1.52	0.15	2.0056
TRAZON	Mushroom		1.69, 0.97, 0.18, 0.11	1.55		2.0056
	4-(Hydroxymethyl)phenyl radical		1.70, 0.97, 0.18, 0.11	1.55	0.1	2.0055

[a] Hyperfine splittings were confirmed by simulation and are accurate to ca. 0.01 mT. Errors associated with the g-values are ca. ± 0.0003 (estimated by variability in the centre field correction from repeated measurements with DPPH).

[b] ΔBpp is the field separation of the peaks and troughs of the first derivative spectra (from simulations using Gaussian shape).

from the 4-hydroxymethyl benzene diazonium salt, which in turn is formed by enzymatic hydrolysis of agaritine, a major component of *A. bisporus*, [18,19]. Previous experiments [11] showed that the EPR spectral parameters for PBN and 4-POBN adducts from mushrooms were similar to those from the synthetic radical. Our current measurements using the spin traps 4-POBN, DEPMPO, PEPO and TRAZON support this conclusion.

In the spectrum of the DEPMPO adduct of the synthetic 4-(hydroxymethyl)phenyl radical, the hydroxyl-radical adduct of DEPMPO, with the parameters $a(^{31}P) = 4.72$ mT, $a(^1H) \sim a(^{14}N) = 1.38$ mT, was visible at the beginning of the experiment, but its intensity decreased rapidly. The
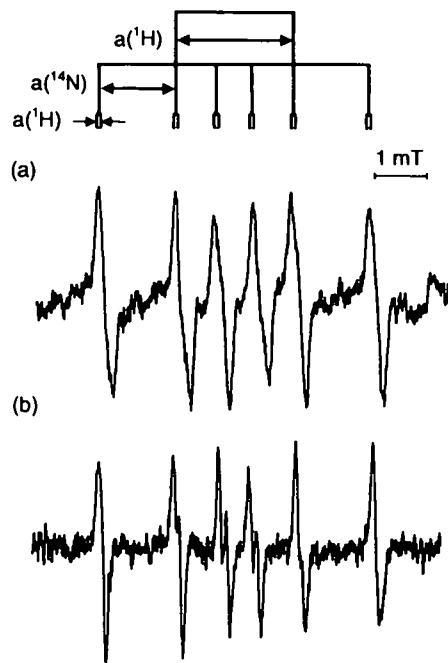

Fig. 3. EPR spectrum of (a) the C-centred radical from mushroom trapped by PEPO, (b) 4-(hydroxymethyl) phenyl radical. Spectral interpretation is shown by the "stick" diagram.
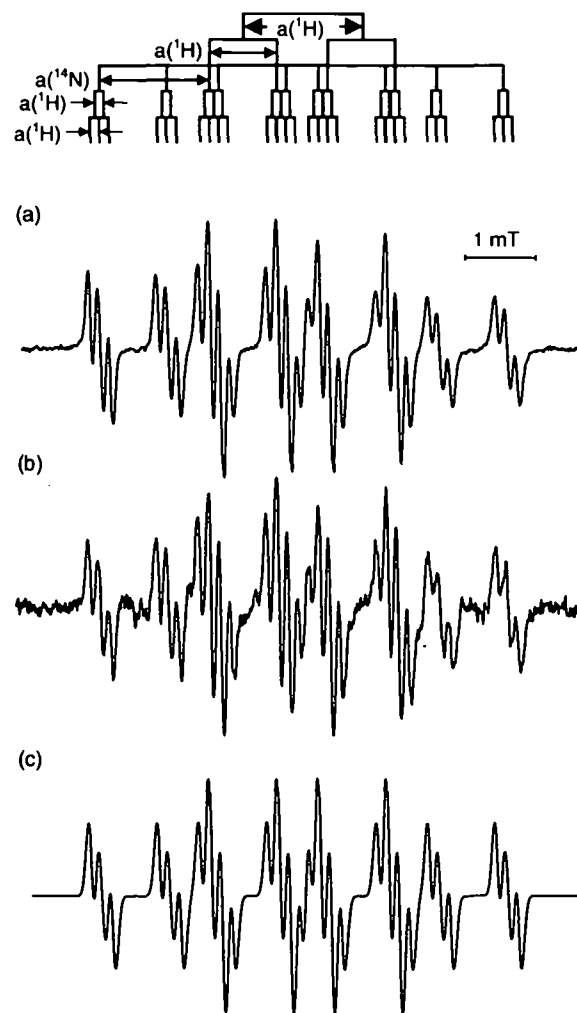

Fig. 4. EPR spectrum of (a) the C-centred radical from mushroom trapped by TRAZON, (b) 4-(hydroxymethyl) phenyl radical, (c) simulation with $a(^1H) = 1.70$ mT, $a(^1H) = 0.97$ mT, $a(^1H) = 0.18$ mT, $a(^1H) = 0.11$ mT, $a(^{14}N) = 1.55$ mT and Gaussian lineshape. Spectral interpretation is shown by the "stick" diagram.

generation of this radical was not observed after preparation under inert atmosphere. In contrast, the carbon-centred radical adduct was stable for at least 20 min. Reaction of the spin traps with the synthesised radical under inert atmospheres (nitrogen or argon) gave the same results as these seen in air. The stability of the 4-(hydroxymethyl)phenyl radical adducts indicates that the instability of the signal in mushroom extracts (Fig. 2) is not the result of an inherent instability of the radical adduct, and may, therefore, be the result of reaction with radical scavengers in the mushroom. Such behaviour has been observed with coffee (instant), which has the ability to rapidly scavenge radical adducts of DEPMPO, but forms stable adducts with 4-POBN [20].

3.3. EPR spectra from herb samples

In the absence of any spin trap the EPR spectra from the herb samples were dominated by a sextet signal from Mn(II). In the presence of 4-POBN three fundamentally different EPR spectra, consisting doublet, sextet or dodecet signals, were obtained from different herb samples. Similar types of signal were observed in a study of macerated vegetables [11], where the doublet had $a(^1H) = 0.18$ mT, the sextet had $a(^{14}N) = 1.59$ mT, $a(^1H) = 0.32$ mT and the dodecet could be fitted with three hyperfine splittings, $a(^{14}N) = 1.493$ mT, $a(^{14}N) = 0.182$ mT, $a(^1H) = 0.145$ mT. These spectra are assigned respectively to the (monodehydro)ascorbate radical [21], a carbon-centred radical adduct of 4-POBN [16] and the 4-POBN adduct of the 4-POBN• radical [22].

In the samples studied, the ascorbate radical was seen with parsley, bay, white dead nettle and lovage, although the spectrum from lovage also contained the sextet component. The ascorbate radical is produced by the (1-electron) oxidation of ascorbic acid. However, the same signal was observed when the sample preparation was carried out in an inert atmosphere, indicating that the oxidation agent was derived exclusively from the plant tissue. Different methods of sample preparation were investigated with parsley, but no qualitative differences in the spectra were observed between fresh, frozen, and freeze-dried samples. The similarity of these results is somewhat surprising since the drying of plant tissues generally leads to a major reduction in their ascorbic acid contents [23], and we have shown previously [24] that the freeze-drying process involves substantial free radical activity. It might have been expected, therefore, that the sextet signal would have been seen in the freeze-dried sample, since the formation of radical adducts of the spin trap becomes more important as ascorbic acid levels drop [25]. However, parsley is generally very rich in ascorbic acid [23] and the present results suggest that appreciable quantities of this antioxidant remain in the freeze-dried sample. Variations in the levels of various antioxidants, including ascorbic acid, as a function of post-harvest treatments will be the subject of a future investigation.

In addition to lovage (see above), the sextet signal was also observed with coriander leaves, elder fruits and freeze-dried

chives. The wide range of tissue types that exhibit this signal suggests that it results from a general reaction of physically damaged tissue. However, the same spectrum was observed when sample preparation was performed under an inert atmosphere, indicating that O_2 was not involved in the reactions leading to the formation of the radical adduct. Indeed, with red dead nettle leaves the sextet spectrum was observed when sample preparation was performed under argon, but the dodecet spectrum (see below) was obtained when the sample was prepared in air. No signal was observed with fresh and frozen samples of chives, but this could be because it was below the detection limit, and does not necessarily indicate that the sextet signal was the consequence of a reaction that occurred during the freeze drying process.

The dodecet spectrum was observed with samples of basil, celery, red deadnettle, ivy, lavender, lemon balm, marjoram, mint, rosemary, sage, stinging nettle, tarragon and thyme; it has been shown by McCormick et al. [22] to correspond to the 4-POBN adduct of the 4-POBN• radical, which is formed by oxidation of the spin trap. The EPR spectrum obtained with stinging nettle (Fig. 5a) can be interpreted in terms of two triplets from interaction of the unpaired electron with two nitrogen nuclei and one doublet from interaction with the hydrogen nucleus. However, at low modulation amplitude, additional hyperfine structure was observed (Fig. 5b), analogous to that reported by Glidewell et al. [26] for lettuce macerated in the presence of 4-POBN. This spectrum can be simulated (Fig. 5c) by two triplets from ^{14}N and two doublets from ^1H. Similar spectra were also observed in previous experiments [11] with samples of carrot hypocotyl rootstock and lettuce leaf, and with >50% of the herb samples studied in the present work. Its generation indicates that the ability to oxidise the spin trap is a property that is common to many plant tissues. This reaction was shown to require O_2, as mentioned in the previous paragraph for red dead nettle leaves, but the fact that the dodecet signal was not universally observed in all aerobically-prepared samples suggests that this is not a direct reaction. Thus it seems likely that specific plant components are oxidised when tissues are broken down in air and that product(s) of this reaction are sufficiently powerful oxidant(s) to oxidize the spin trap.

We also observed in experiments with stinging nettle that the ability to generate the dodecet signal diminished with increased storage time, even at low temperature. Measurements made at the beginning of the experiment (about 3 days after the harvest), produced a strong dodecet signal, whereas a much weaker signal was obtained after the sample had been stored for three weeks in liquid nitrogen (but with a few minutes exposure to ambient temperature). It would appear, therefore, that a component of this oxidation pathway in stinging nettle has limited stability after the sample has been harvested, although the observation of dodecet spectrum from the reaction of 4-POBN with freeze-dried samples of marjoram, thyme and rosemary indicates that this is not a general characteristic.
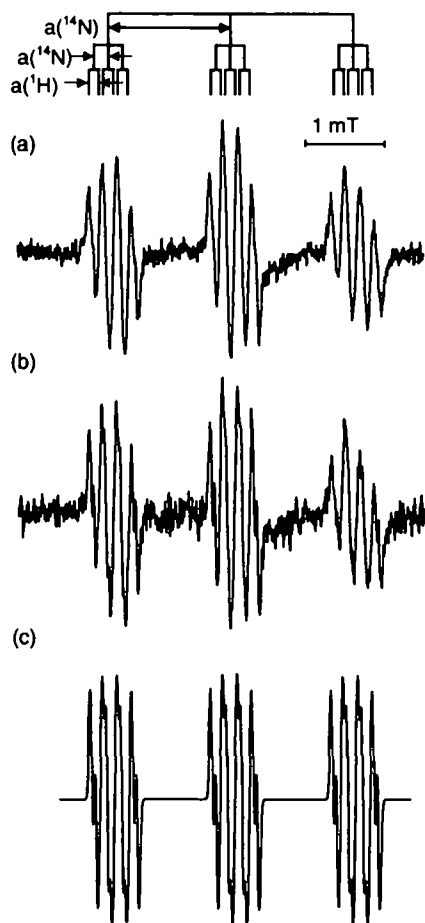
Fig. 5. EPR spectrum of 4-POBN• radical from stinging nettle trapped by 4-POBN, (a) experimental spectrum using 0.1 mT modulation amplitude, (b) experimental spectrum using 0.04 mT modulation amplitude, (c) simulation with $a(^{14}N) = 1.493$ mT, $a(^{14}N) = 0.182$ mT, $a(^{1}H) = 0.145$ mT, $a(^{1}H) = 0.05$ mT and Gaussian lineshape. Spectral interpretation is shown by the "stick" diagram (which does not include the small ^{1}H splitting).

4. General discussion

The present experiments show that extensive free radical generation occurs in plant tissues when they are physically damaged in a simulation of the mastication process. This is presumably largely the consequence of reactions between cellular contents when compartmentalisation is broken down. Thus the reactions which occur on mastication are analogous to the plant defence reactions that are initiated in response to physical damage by a parasite or infection by an incompatible pathogen. Not surprisingly, the nature of these reactions differs between different types of plant tissue. Such radical generation will, therefore, result in a reduction in the levels of free radical scavengers/antioxidants relative to those in the undamaged tissue prior to mastication.

The results from the measurements with *Agaricus* mushrooms indicate the trapping of a carbon-centred radical, which is most likely the 4-(hydroxymethyl)phenyl radical. Our results show conclusively that the 4-POBN radical adduct requires O_2 for its formation, and that the adduct

with DEPMPO is unstable in the absence of O_2. The instability of the DEPMPO adduct is likely to be the consequence of its reaction with components in the mushroom, since this adduct is stable in simple solutions. This result suggests that mushrooms contain compounds that are effective radical scavengers. The apparent stability of the adduct when the sample was allowed to stand in air is then in reality a steady state situation, in which the rates of adduct formation and decomposition are balanced.

For the 4-(hydroxymethyl)phenyl radical adducts of 4-POBN the present experiments measured values for the ^{13}C hyperfine coupling constants from the tertiary- and methyl-carbons of the t-butyl group, as well as from the α-carbon adjacent to the nitroxide group. Such values are potentially informative for the characterisation of adducts formed with unknown radicals, but at present there is no library to show the level of variability of ^{13}C coupling constants for 4-POBN adducts of different types of known radicals. We strongly suggest that such values should be reported whenever there is sufficient spectral sensitivity for their resolution. The present work has also derived spectral parameters for adducts of 4-(hydroxymethyl) phenyl radicals with the spin traps DEPMPO, PEPO and TRAZON, whose adducts with such radicals had not previously been reported.

In contrast to the observations with *Agaricus* mushrooms, there was no influence of atmosphere on the formation of the sextet signal with the coriander samples. There are, therefore, fundamental differences in the processes for carbon-centred radical formation in these two types of food product, and the radical trapped from the plant tissues would appear to be formed directly as a result of physical damage to the tissue. It might be possible that the coriander samples contained sufficient quantities of O_2 for oxidation to occur in the inert atmosphere since they were photosynthetic tissue. However, the experiments with red deadnettle showed that the sextet signal was only observed in an inert atmosphere, thus indicating that O_2 is not required for its formation in these plant tissues.

It is also interesting to compare the EPR spectral behaviour of *Agaricus* mushrooms described above, with that from the herb thyme, which contains large quantities of the phenols thymol and carvacrol. Spectra from thyme were very weak and inconsistent with the formation of a carbon-centred radical adduct of 4-POBN, even though both carvacrol and thymol readily generate radicals in simple chemical systems [9,10]. Indeed, the reaction between 4-POBN and the plant tissue extract resulted in oxidation of the spin trap, again indicating that the chemical processes occurring on physical damage to the plant tissue are distinctly different from those of major potentially-reactive components.

Oxidation of the spin trap also occurred on reaction of 4-POBN with >50% of the various types of herb samples studied in the present work (Table 1), whereas the expected radical adduct spectra were only seen with three plant species (coriander, elder and chives). It appears that

physical damage to the tissues of many herb samples results in the initiation of powerful oxidation reactions. Such reactions may, therefore, be fundamental to the generation of flavour active compounds in foods in which such herbal products are incorporated, and may also have a role in the medicinal properties of these plants. This observation is in contrast to the common assumption that health benefits from plant tissues are due to their high contents of antioxidants which reduce the formation of free radicals and other ROS (e.g. Madsen et al., [27]; Parejo et al., [28]). However, since the ability of tissues to oxidise 4-POBN may be greatly affected by storage (as demonstrated for stinging nettle), there is a case for more extensive studies of the effects of both production and post-harvest storage conditions on the chemical properties of these plant products.

In parsley, which is known to be rich in ascorbic acid [23], no reaction was observed with 4-POBN, and instead the spectrum of the ascorbate radical was generated. Similar spectra have also been reported for cabbage leaf, carrot hypocotyls root stock, celery stalk, cress shoots, cucumber fruit and parsley leaf [11], and for fruits of pepper (*Capsicum annuum*) and leaves of French bean (*Phaseolus vulgaris*) [25,29]. The fact that ascorbate radical formation (investigated in parsley, but there is no reason to suspect that this is not a general effect) was independent of O_2 suggests that the ability of ascorbic acid to inhibit carbon-centred free radical generation exists under anaerobic as well as aerobic conditions, an observation which could at least in part explain the health benefits of Vitamin C rich foods.

In the present experiments, lovage was the only sample which produced simultaneously the signals from the ascorbate radical and the carbon-centred radical adduct of 4-POBN. Although Muckenschnabel et al. [29] observed a gradual transition between the two types of spectrum with distance from the edge of soft rot lesions in leaves of *P. vulgaris* and fruits of *C. annuum*, other investigations [11] showed that it was rare to see signals from both of these radicals in the same food sample. It would appear, therefore, that this happens only in samples with appreciable quantities of ascorbic acid, but insufficient to completely prevent carbon-centred radical generation when the tissue is damaged.

5. Conclusions

Free radical generation as a result of physical damage (in a simulation of the eating process) has been observed in *Agaricus* mushrooms and several species of herbs that are used for culinary or medicinal purposes. With mushrooms, the identity of the free radical as the previously proposed 4-(hydroxymethyl)phenyl species has been confirmed, and it has been demonstrated that it is the product of an oxidative process (involving O_2) in the mushrooms. Adducts with the

spin trap DEPMPO showed limited stability, even though the 4-(hydroxymethyl)phenyl radical adducts of this spin trap were stable, an observation which indicates that mushrooms also contain appreciable quantities of free radical scavengers. EPR spectral parameters have been determined for the first time for adducts of the 4-(hydroxymethyl)phenyl radical with the spin traps DEPMPO, PEPO and TRAZON. In addition, ^{13}C hyperfine splittings for the α-carbon and the tertiary and methyl carbons of the *t*-butyl group have been measured for the 4-POBN adduct.

Oxidative processes were also important in the free radical generation in many of the herbs, and in >50% of the samples product(s) were formed which were able to oxidise the spin trap 4-POBN. This observation of widespread pro-oxidant activity in plant tissues (that are traditionally consumed in uncooked forms) was surprising, since such foods are generally promoted for their anti-oxidant properties. The influence of cooking was not investigated in the present experiments, but it might be expected that the cooking process would change both the levels and bioavailability of many food components. However, the observation of pro-oxidant activity in many plant food products suggests that it may be necessary to rethink our ideas on antioxidants in foods. Nevertheless, a specific role for the antioxidant ascorbic acid was also observed in these experiments, since it inhibited the formation of carbon-centred free radicals. This inhibition was independent of oxygen, consistent with the ability of this molecule to function as a food preservative and beneficial dietary component.

Acknowledgements

References

[1] The Scottish Office, The Scottish Diet, The Scottish Office Home and Health Department, Edinburgh, 1993.
[2] J.M.C. Gutteridge, B. Halliwell, Antioxidants in Nutrition, Health and Disease, Oxford University Press, Oxford, UK, 1994.
[3] A.F. Walker, Biologist 43 (1996) 177.
[4] V.E. Tyler, Herbs of choice, The Therapeutic Use of Phytomedicinals, Pharmaceuticals Products Press, New York, 1994.
[5] W. Wurzer, Die Grosse Enzyklopädie der Heilpflanzen, Ihre Anwendung und Ihre natürliche Heilkraft, Neuer Kaiser Verlag, Klagenfurt, Austria, 1994.
[6] E. Leng-Peschlow, A. Strenge-Hesse, Z. Phytother. 12 (1991) 162.
[7] I. Koch-Heitzmann, W. Shultze, Z. Phytother. 9 (1988) 77.
[8] P.H. List, L. Horhämmer, in: P.H. List, L. Horhämmer (Eds.), Hager's Handbuch der Pharmazeutischen, Praxis, Springer, Berlin, 1973.
[9] N. Deighton, S.M. Glidewell, S.D. Deans, B.A. Goodman, J. Sci. Food Agric. 63 (1993) 221.
[10] N. Deighton, S.M. Glidewell, B.A. Goodman, S.D. Deans, Proc. Roy. Soc. Edinb. 102B (1994) 247.
[11] B.A. Goodman, S.M. Glidewell, C.M. Arbuckle, S. Bernardin, T.R. Cook, J.R. Hillman, J. Sci. Food Agric. 82 (2002) 1208.

[12] N. Sankuratri, E.G. Janzen, Tetrahedron Lett. 37 (1996) 5313.
[13] K. Stolze, N. Udilova, H. Nohl, Free Radic. Biol. Med. 29 (2000) 1005.
[14] K. Stolze, N. Udilova, T. Rosenau, A. Hofinger, H. Nohl, Biol. Chem. 384 (2003) 493.
[15] K. Hiramoto, M. Kaku, T. Kato, K. Kikugawa, Chem. Biol. Interact. 94 (1995) 21.
[16] G.R. Buettner, Free Radic. Biol. Med. 3 (1987) 259.
[17] C.P. Poole, H.A. Farach, Handbook of Electron Spin Resonance, American Institute of Physics, New York, 1994.
[18] B. Levenberg, Biochim. Biophys. Acta 63 (1962) 212.
[19] A.E. Ross, D.L. Nagel, B. Toth, J. Agric. Food Chem. 30 (1982) 521.
[20] E.C. Pascual, B.A. Goodman, C. Yeretzian, J. Agric. Food Chem. 50 (2002) 6114.
[21] G.P. Laroff, R.W. Fessenden, R.H. Schuler, J. Am. Chem. Soc. 94 (1972) 9062.
[22] M.L. McCormick, G.R. Buettner, B.E. Britigan, J. Biol. Chem. 270 (1995) 29265.

[23] Food Standards Agency, McCance and Widdowson's The Composition of Foods, sixth summary ed., Royal Society of Chemistry, Cambridge, UK, 2002.
[24] K.F. Pirker, B.A. Goodman, E.C. Pascual, S. Kiefer, G. Soja, T.G. Reichenauer, Plant Physiol. Biochem. 40 (2002) 709.
[25] I. Muckenschnabel, C. Schulze Gronover, N. Deighton, B.A. Goodman, G.D. Lyon, D. Stewart, B. Williamson, J. Sci. Food Agric. 83 (2003) 507.
[26] S.M. Glidewell, B.A. Goodman, J. Skilling, in: J. Skilling, S. Sibisi, Maximum Entropy and Bayesian Methods, Kluwer, Dordrecht, 1996, p. 23.
[27] H.L. Madsen, B.R. Nielsen, G. Bertelsen, L.H. Skibsted, Food Chem. 57 (1996) 331.
[28] I. Parejo, F. Viladomat, J. Bastida, A. Rosas-Romero, N. Flerlage, J. Burillo, C. Codina, J. Agric. Food Chem. 50 (2002) 6882.
[29] I. Muckenschnabel, B.A. Goodman, N. Deighton, G.D. Lyon, B. Williamson, Protoplasma 218 (2001) 112.

A.2. POSTER OF MUSHROOMS AND HERBS

Pirker K.F., Reichenauer T.G., Goodman B.A., Stolze K., 2003, Does eating plant tissue lead to the initiation of strong oxidation processes?, First International Symposium on Recent Advances in Food Analysis, Prague, Czech Republic, 05th -07th November.

DOES EATING PLANT TISSUE LEAD TO THE INITIATION OF STRONG OXIDATION PROCESSES?

Katharina F. Pirker[1], Thomas G. Reichenauer[1], Bernard A. Goodman[1] & Klaus Stolze[2]

[1]ARC Seibersdorf research GmbH, Dept. of Environmental Research, A-2444 Seibersdorf, Austria; [2]Veterinary University of Vienna, Basic Pharmacology and Toxicology, Institute of Applied Botany, A-1210 Vienna, Austria

Introduction

Fresh fruits and vegetables are now established as essential components of healthy diets, and it is generally assumed that this is because they contain appreciable quantities of molecules with antioxidant properties that can react as scavengers of reactive oxygen species (ROS).

Herbs and spices are important food additions as taste improvement as well as a health benefit. They have been suggested to stabilize blood pressure and the cholesterol levels (Walker, 1996).

The present work is based on investigations about free radical generation in mascinated food using electron paramagnetic resonance (EPR) spectroscopy. Different spin traps were used to detect short lived radicals produced under gentle grinding of the samples.

Materials and Methods

Mushrooms were bought from a local supermarket and stored at room temperature until use. Different herbs were taken from one of the author's garden, frozen in liquid nitrogen and maintained at that temperature until measurement, or bought fresh from a local market resp. freeze-dried from the supermarket, stored at room temperature. Fresh samples were measured on the same day of purchase.

Thin slices of mushroom samples resp. small amounts of herbs were crushed gently in a mortar together with spin trap solutions, filtered through a disposable syringe filter holder and transferred to a flat cell for recording the EPR spectrum. The 4-(hydroxymethyl)phenyl radical was synthesised by reaction of the primary amine, solved in hydrochloric acid, placed on an ice-salt-mixture, with sodium nitrite which was added slowly under agitation. The influence of oxygen was investigated by performing all operations in both air and inert atmospheres.

Mushroom

Mushroom samples were investigated with different spin traps which led to typical spectra of spin trap adducts including carbon-centered radicals (Buettner, 1987). 4-POBN and PEPO gave sextets whereas DEPMPO showed 12 peaks and TRAZON 28 peaks due to additional interactions of the nuclei with the unpaired electron. With 4-POBN weak satellite peaks were observed at high instrumental gain.
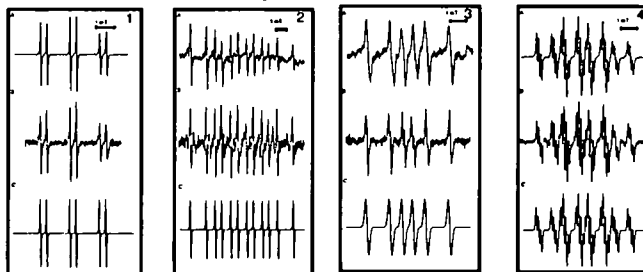
EPR spectra of a C-centred radical from mushroom trapped by 4-POBN (1), DEPMPO (2), PEPO (3) and TRAZON (4); A: experimental spectrum, B: synthesised 4-(hydroxymethyl) phenyl radical, C: simulation.

The synthesised 4-(hydroxymethyl)phenyl radical trapped by the various spin traps gave similar spectra compared with the radical detected in mushroom. According to Ross et al. (1982) the 4-(hydroxymethyl) benzene diazonium ion is produced in fresh mushroom by enzymatic hydrolysis of agaritine and produces hyperfine splitting constants similar to that of carbon-centered radicals (Hiramoto et al., 1995).

Investigations in controlled atmospheres showed that the 4-POBN radical adducts require oxygen (O_2) for their formation and that the adduct with DEPMPO is unstable in the absence of O_2. In contrast the synthesis of the 4-(hydroxymethyl) phenyl radical is independent of the surrounding atmosphere.

Herbs

With coriander the sextet signal was shown in the EPR spectra corresponding to a 4-POBN adduct of a carbon-centred radical. The same spectrum was observed when sample preparation was performed under inert atmosphere, indicating that oxygen was not involved in the reactions leading to the formation of the radical adduct.

In addition to parsley, bay, white dead nettle and lovage also showed the ascorbate radical in the EPR spectra. No qualitative differences were observed in the spectra of parsley with various methods of sample preparation, e.g. between fresh, frozen, and freeze-dried samples resp. between inert and air atmosphere. There was no reaction with the spin trap 4-POBN visible. The absence of any influence of oxygen on the ability of ascorbic acid to inhibit carbon-centred free radical generation could at least in part explain the health benefits of Vitamin C rich foods.

EPR spectrum of POBN· radical from stinging nettle trapped by 4-POBN, A: experimental spectrum, B: simulation.

Stinging nettle was one of the herbs which led to an oxidation of the spin trap 4-POBN producing a dodecet signal in the EPR spectrum corresponding to the 4-POBN adduct of the 4-POBN· radical. Table 1 gives an overview of all the other samples that have the ability to oxidize the spin trap.

The generation of the 4-POBN· radical is dependent on oxygen which could be shown with red dead nettle. The dodecet spectrum was obtained when the samples were prepared under air whereas the sextet signal was seen after preparation under inert atmosphere. There is also a storage effect on the intensity of the signal. Stinging nettle showed a strong dodecet signal a few days after harvest but a very weak signal was observed after a three week storage time in liquid nitrogen which could be related to oxygen consumption in the dewar.

Results	Common name	Frozen	Fresh	Freeze-dried	Results	Common name	Frozen	Fresh	Freeze-dried
ascorbate	bay	x			POBN· adduct	basil		x	
	deadnettle (white)	x				celery	x		
	parsley	x	x	x		deadnettle (red)	x		
	parsley	x	x			ivy	x		
	crimpy					lavender	x		
	lovage	x		x		lemon	x		
no signal	chives	x	x			balm			
	oregano			x		marjoram	x		x
	sage		x			mint	x	x	
	thyme		x			rosemary	x	x	
sextet	coriander		x			sage	x		
	elder	x				stinging-nettle	x		
	chives			x		tarragon	x		
	lovage	x		x		thyme	x		x
						rosemary			x

Conclusion

• The chemical nature of the free radical 4-(hydroxymethyl) phenyl generated from mushroom and most likely the product of an oxidative process has now been positively identified.

• Pro-oxidant activity was found in >50 % of the herb samples where product(s) were formed which were able to oxidise the spin trap 4-POBN.

• The majority of the herb samples which showed the ascorbate radical were free of carbon-centred radicals indicating possible inhibition reactions of the antioxidant ascorbic acid.

A.3. POSTER OF CARROTS

Pirker K.F., Goodman B.A., Naglreiter C., Reichenauer T.G, 2004, Antioxidant molecules and free radical processes in carrot hypercotyl root stock, 3rd International Congress on Pigments in Food, Quimper, France, 14th -17th June.

Antioxidant molecules and free radical processes in carrot hypercotyl root stock

K.F. Pirker[1]*, B.A. Goodman[1], C. Naglreiter[1] and T.G. Reichenauer[1]

[1] ARC Seibersdorf research GmbH, Department of Environmental Research, A-2444 Seibersdorf, Austria (katharina.pirker@arcs.ac.at)

Introduction

Carrots are important horticultural crops grown in central Europe. They make contributions to a healthy diet because of their contents of beneficial antioxidant molecules, especially the carotenoids.

In our investigation levels of carotenoids were determined along with those of free radicals generated when tissues were broken down (as in eating).

One variety of carrot (*Daucus carota cv. Maestro*), grown under stress free conditions, was studied.

The influence of maturity on the composition of pigments and free radical generation was determined with samples harvested at three different growth stages.

Material

Carrots (*cv. Maestro*) were grown in pots fitted with a self-irrigating system. Three harvests (49, 55 and 83 days after sewing) were carried out, representing three different developmental stages of the carrots.

Sample preparation

Thin slices of each carrot sample were taken from the top, the centre, and the tip of the root, immediately frozen to 77 K and stored in liquid nitrogen until analysis.

Analysis

EPR-analysis was carried out using two different spin traps – one more lipophilic, phenyl-*N-t*-butylnitrone (PBN), and one more hydrophilic, α-(4-pyridyl-1-oxide)-*N-t*-butylnitrone (4-POBN), to detect short-lived radicals when cells were disrupted. Samples were ground under liquid nitrogen, the powder was gently merged together with the spin trap solution, then filtered and measured in a flat cell. The first peak, doublet, quartet was taken for quantifying the results.

Carotenoids were analysed by HPLC using the approach described by Hart and Scott (Food Chemistry 54, pp. 101-111, 1995).
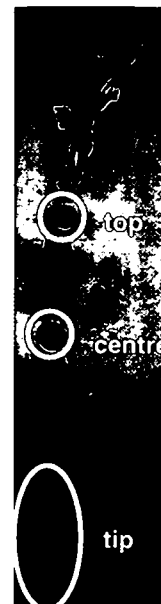
EPR-Results

- C-centred radical could be trapped with PBN ➡ sextet
- 4-POBN was oxidised by the sample ➡ oxidation product
- additionally the spin traps were degraded by the sample activity ➡ breakdown product

PBN

SEXTET SIGNAL coming from a C-centred radical:

- highest signal intensity in the centre of the carrot
- lowest signal intensity in the tip of the carrot
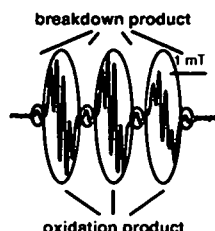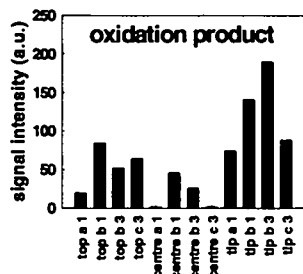
BREAKDOWN PRODUCT of the spin trap:

- lowest signal intensity in the centre of the carrot
- decreasing signal intensity with maturation of the carrot
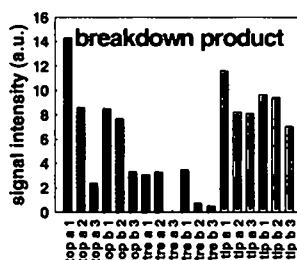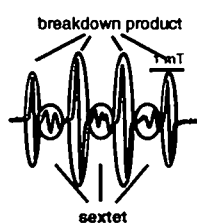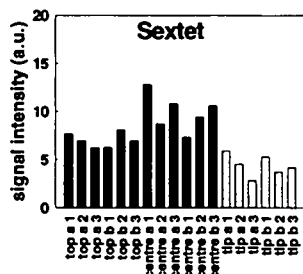
4-POBN

**OXIDATION PRODUCT** of the spin trap:

- highest signal intensity in the tip of the carrot
- lowest signal intensity in the centre of the carrot

a, b, c ... sample replicates
1, 2, 3 ... 1st, 2nd, 3rd harvest

Carotenoids-Results

- amount of α- and β-carotene increased between the 2nd and 3rd harvests in both the top and centre
- slightly lower amounts of α- and β-carotene were found in the centre of the carrot than in the top
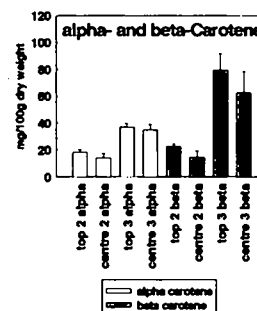
- Lutein levels were highest in the tops and lowest in the tips, shown below normalised to those at the centres. Deviations from the centre values decreased with maturation for the tops, but increased for the tips.
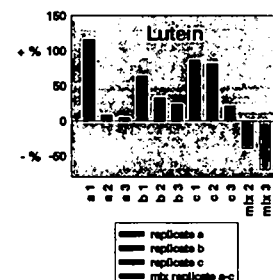
Conclusion

- Carrots showed both pro-oxidative and anti-oxidative capacity and these varied over small distances
- The levels of α- and β-carotene increased with increasing maturity of the tissues, whereas the extent of breakdown of the spin trap PBN decreased
- The pro-oxidant activities seen with the spin trap 4-POBN were highest in the tips

A.4. POSTER OF KAEMPFEROL

Pirker K.F., Stolze K., Reichenauer T.G., Nohl H., Goodman B.A., 2005, The influence of oxidation conditions on free radical formation in kaempferol, "Advanced Techniques & Applications of EPR", The 38th Annual International Meeting, Bath, UK, 20th -24th March.

THE INFLUENCE OF OXIDATION CONDITIONS ON FREE RADICAL FORMATION IN KAEMPFEROL

K.F. Pirker[1], K. Stolze[2], T.G. Reichenauer[1], and B.A. Goodman[1]

[1]ARC Seibersdorf research GmbH, Dept. of Environmental Research, A-2444 Seibersdorf, Austria;
[2]Research Institute for biochemical Pharmacology and Toxicology, A-1210 Vienna, Austria
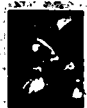
red onions
Lemon balm
red wine
red apples
Gingko leaves
tomatoes

INTRODUCTION

Foods rich in flavonoids have numerous positive effects such as anticancer, antiviral, antiallergic, anti-atherogenesic, antithrombosic, and anti-inflammatory properties. These are often considered to be related to antioxidant activity and there is a growing tendency to use antioxidant assays as indicators of beneficial properties.[1-3] Flavonoids also show inhibitory effects on enzymes such as xanthine oxidase.[4]

Although the free radical chemistry of flavonoids has been studied by EPR spectroscopy over many years, we have recently revisited the subject and are finding many unexpected results. This poster describes the work on the oxidation of kaempferol, a polyphenolic component in various foods (see above).
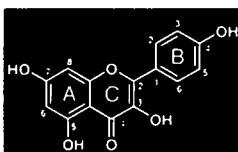
MATERIALS AND METHODS

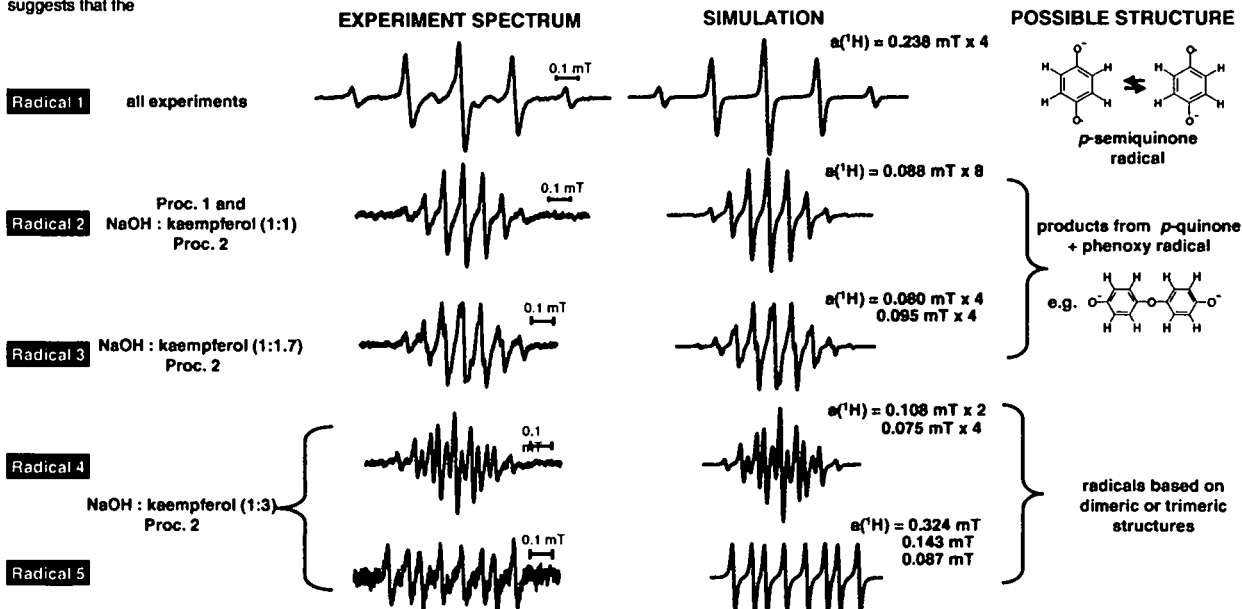Autoxidation of kaempferol was carried out in 0.1 M NaOH using two procedures:

Procedure 1: 200 µl of the NaOH solution was transferred into the flat cell and 200 µl of the flavonoid solution (1 mM in DMSO) were added on top. Mixing of the solutions was diffusion controlled and dissolved O_2 performed the oxidation.

Procedure 2: Similar solutions to those in Proc. 1 were added to an Eppendorf tube, and mixed in a Vortex mixer for a few seconds before transferring into a flat cell. This gave a homogeneous solution with higher O2 concentration.

In both procedures the flat cell was placed in the spectrometer as quickly as possible for recording the spectrum.

The dependence of relative concentrations of NaOH and the flavonoid was tested with the NaOH and kaempferol solutions in ratios of 1:1, 1:1.7 and 1:3.

RESULTS

Five different EPR-spectra were observed during autoxidation of kaempferol. The quintet signal (Radical 1), which was the 1st radical detected in all experiments, is identical to that of the p-semiquinone radical[5]. (Its formation could have been preceded by a short-lived phenoxy radical, but there was no evidence for such a radical in our experiments). A septet signal (Radical 2) was observed after the quintet decreased (Proc. 1) and from the outset with Proc. 2. The intensity distribution of the peaks suggests that they are the inner 7 peaks of a nonet from 8 equivalent protons; this was confirmed by simulation. An identical spectrum was obtained by oxidising a phenol solution with a trace of hydroquinone, which suggests that the radical is based on a dimeric structure, in which the unpaired electron has equal density on each of the unsubstituted aromatic carbons. Radical 3, which was observed at slightly higher flavonoid concentration, has 2 sets of 4 equivalent [1]Hs, with average splittings equal to that of Radical 2. It probably also corresponds to a dimeric structure similar to that proposed for Radical 2. When higher levels of kaempferol were used, two new radicals were observed, Radical 5 appearing after Radical 4. It seems likely that both are formed from small degradation products of kaempferol and are based on structures with 2 or more aromatic rings. At present these have not been identified.

EXPERIMENT SPECTRUM	SIMULATION	POSSIBLE STRUCTURE

Radical 1 — all experiments
$a(^1H) = 0.238$ mT x 4
p-semiquinone radical

Radical 2 — Proc. 1 and NaOH : kaempferol (1:1) Proc. 2
$a(^1H) = 0.088$ mT x 8
products from p-quinone + phenoxy radical

Radical 3 — NaOH : kaempferol (1:1.7) Proc. 2
$a(^1H) = 0.080$ mT x 4
0.095 mT x 4
e.g.

Radical 4 — NaOH : kaempferol (1:3) Proc. 2
$a(^1H) = 0.108$ mT x 2
0.075 mT x 4
radicals based on dimeric or trimeric structures

Radical 5
$a(^1H) = 0.324$ mT
0.143 mT
0.087 mT

0.1 mT

SUMMARY

• The flavonoid molecule is degraded rapidly by O_2 in alkaline solutions.
• The p-semiquinone radical is the 1st signal seen in all the EPR spectra (though its formation could be preceded by a phenoxy radical).
• Subsequent radicals are likely based on reactions of p-semiquinone.
• These radicals probably have di- and/or trimeric structures.
• Radical 2 is also formed by oxidation of a mixture of p-hydroquinone and phenol.

CONCLUSIONS

• The rapid oxidative degradation of kaempferol means that no redox-cycling is observed.
• Some products of kaempferol degradation are reactive radical species.
• The dietary/nutritional relevance of kaempferol is likely to be more complex than a simple antioxidant process. Thus simple determinations of antioxidant capacity may not be a reliable indicator of its biological effect.
• A thorough understanding of the basic chemistry needs to be obtained before using such natural products in concentrated form as dietary supplements.

References
[1]Hibatallah, J. et al., 1999, J. Pharm. Pharmacol., 51, 1435-1440
[2]Madsen, H. L. et al., 2000, Eur. Food Res. Technol., 211, 240-246
[3]Inoue, T. et al., 2002, Biol. Pharm. Bull., 25(2), 256-259
[4]Selloum, L. et al., 2001, Arch. of Biochem. Biophys., 395(1), 49-56
[5]Kuhnle, J. A., et al., 1969, J. Chem. Soc. (B), 6, 613-616

A.5. PUBLICATION OF CARROTS

Pirker K.F., Stolze K., Reichenauer T.G., Nohl H., Goodman B.A., Free radical processes in developing carrot tissue, submitted in *Plant Physiology and Biochemistry*.

Free radical processes in developing carrot tissue

Katharina F. Pirker[1], Klaus Stolze[2], Thomas G. Reichenauer[1], Hans Nohl[2], and Bernard A. Goodman[1,3]

[1]*Department of Environmental Research, ARC Seibersdorf research GmbH, A-2444 Seibersdorf, Austria*

[2]*Research Institute for biochemical Pharmacology and Toxicology,* [2]*Veterinary University of Vienna, A-1210 Vienna, Austria*

[3]*Department of Natural Resources and Environmental Sciences, University of Illinois at Urbana-Champaign, IL 61801, USA*

Corresponding author: Katharina F. Pirker

Department of Environmental Research

ARC Seibersdorf research GmbH

A-2444 Seibersdorf, Austria

Tel. +43 50550 3609; Fax +43 50550 3520

E-mail address: k.pirker@umweltforschung.at

Abstract

Free radical processes in carrot hypocotyl root stock at different positions and developmental stages were investigated by electron paramagnetic resonance (EPR) spectroscopy after reaction with the chemical spin traps phenyl-N-t-butylnitrone (PBN) and α-(4-pyridyl-1-oxide)-N-t-butylnitrone (4-POBN), the former is lipophilic, whereas the latter is hydrophilic. The EPR spectra from the products of reaction with PBN were identified as a carbon-centred radical adduct of the spin trap and the N-(t-butyl)aminoxyl radical (also called N-t-butyl hydronitroxide), which is formed via a radical induced fragmentation of the spin trap. With 4-POBN, the N-(t-butyl)aminoxyl radical was also seen along with an adduct of an oxidation product of the spin trap. With both spin traps, the relative proportions of the EPR signals varied with position from which the tissue was extracted, but not with its age of development. Additional EPR measurements were made with a range of spin traps related to 5,5'-dimethyl-1-pyrroline-N-oxide (DMPO), but with substituents that produced a range of properties varying between hydrophilic and lipophilic in order to obtain additional information on the origin of the free radical species. With the hydrophilic spin trap 5-(diethoxyphosphoryl)-5-methyl-1-pyrroline-N-oxide (DEPMPO), the EPR spectrum was dominated by the signal from the hydroxyl radical adduct, whereas the carbon-centred radical adduct increased in importance with increasing lipophilic character of the spin traps.

List of Abbreviations

DBPMPO 5-(dibutoxyphosphoryl)-5-methyl-1-pyrroline-N-oxide

DEPMPO 5-(diethoxyphosphoryl)-5-methyl-1-pyrroline-N-oxide

DPPMPO 5-(dipropoxyphosphoryl)-5-methyl-1-pyrroline-N-oxide

EDTA ethylenediaminetetraacetic acid

EPR electron paramagnetic resonance

PBN phenyl-*N*-*t*-butylnitrone

PEPO 5-propoxycarbonyl-5-ethylpyrolline-1-oxide

4-POBN α-(4-pyridyl-1-oxide)-*N*-*t*-butylnitrone

1. Introduction

Carrots are important horticultural crops grown in central Europe. They make contributions to a healthy diet because of their contents of beneficial antioxidant molecules, especially the carotenoids. Since a function of these molecules *in planta* is to control free radical reactions which are part of the normal metabolic processes, it is of interest also to investigate these reactions in order to gain an understanding of the processes that influence the levels of these carotenoid molecules.

Previous studies of free radical processes in carrot hypocotyl root stock by Goodman et al. [9] found major differences in behaviour between different specimens with respect to the products of their reaction with the spin trap α-(4-pyridyl-1-oxide)-*N*-*t*-butylnitrone (4-POBN). Those measurements were based on commercially-grown carrot samples of unknown age and origin. It is thus unclear whether these differences were related to the plant genetics, growth history or position in the carrot from which the sample was taken.

The present experiments were designed to address these problems. Effects related to genetic variations were eliminated by using seeds of just one variety from a single seed lot. Plants were grown under carefully controlled conditions using an automated irrigation system to eliminate any effects of water stress. Harvests were made at three distinct developmental stages and samples taken from different positions with the root tissue.

These samples were used in investigations of reactions with two related spin traps; 4-POBN, as in the early experiments of Goodman et al. [9], and the related lipophilic molecule, phenyl-*N*-*t*-butylnitrone (PBN). Also, in order to determine whether the lipophilicity of the spin trap might be a factor influencing the differences observed between measurements with PBN and 4-POBN, additional EPR measurements were performed using another family of spin traps (derived from dimethyl piperidine oxide – DMPO).

4

2. EPR-Results

The EPR spectra obtained with PBN consisted of two components (*figure 1*), a sextet with parameters (*table I*) similar to those of a carbon-centred radical adduct of the spin trap and a quartet, with parameters identical to those reported for the N-(*t*-butyl)aminoxyl radical [1, 2, 5]. The larger linewidth of the high field spectral components are the result of incomplete averaging of the spectral anisotropy.

The intensity of the sextet signal varied according to the position in the carrot root from which the sample was taken (*figure 2*), the highest intensity being obtained with samples from the centre of the root and the lowest with those from the tip. The age/maturity of the tissue did not appear to have much influence on the intensity of this signal.

The intensity of the N-(*t*-butyl)aminoxyl signal was also dependent on the position of the carrot root from which the sample was taken. In this case, however, the lowest signal intensity was obtained from tissue from the centre of the carrot (*figure 3*). The highest intensity of this signal was obtained from the tip of the root. Also, its intensity appeared to decrease with increasing age of the samples.

The EPR spectra obtained with the spin trap 4-POBN also consisted of two signals (*figure 4*) but they were quite different from those obtained with PBN. The N-(*t*-butyl)aminoxyl radical was present as a minor component, but the spectra were dominated by a dodecet signal, which probably corresponds to an adduct involving a radical oxidation product of the spin trap [11] (*table I*). Within individual carrots, there appeared to be a relationship between the intensity of the dodecet signal and the position in the carrot from which the samples were taken, the highest intensity being with samples from the tips and the lowest from the centres (*figure 5*). No correlation with age/maturity of the carrot was observed.

The EPR spectra obtained with carrots and the different DMPO-related spin traps are shown in *figures 6-8* and parameters in *table I*, along with selected values from the literature. The main features in the spectrum with DEPMPO (*figure 6 A*) correspond to a hydroxyl radical adduct of the spin trap. There is an additional peak near the centre of the spectrum which corresponds to one half of a doublet from the monodehydroascorbate radical (a(^{1}H) = 1.8 gauss) [3], with the other half being obscured by the OH-radical adduct signal. There are also broader features in positions characteristic of C-centred radical adducts.

With DPPMPO (*figure 7*) the spectrum contains a mixture of components from the hydroxyl radical and carbon-centred radical adducts. When a simulation consisting of a

5

weighted sum of these two components (*figure 7 B*) is compared with the original spectrum it can be seen that there must also be a third component in the experimental spectrum. The individual simulations of the carbon-centred radical adduct and the hydroxyl radical adduct are given in *figures 7 C* and *D*.

When the experiment with DEPMPO was repeated in the presence of an iron chelator (EDTA) at pH 7, the c-centred radical dominated the spectrum (*figure 6 C*) whereas the contribution from the hydroxyl radical adduct was much lower than in *figure 6 A*, indicating that formation of the hydroxyl radical was inhibited. Since EDTA is frequently used to hold Fe(III) in solution in model Fenton reaction systems, the above result suggests that it interferes with a reactant that is a precursor of the Fenton reaction, and possibly inhibits the formation of H_2O_2 by the superoxide dismutase enzyme.

The spin trap PEPO mixed with carrot juice produced a spectrum which also corresponded to a carbon-centred radical adduct (*figure 8, table I*) whereas no detectable signal could be seen from the reaction of DBPMPO and carrot juice.

3. Discussion

The carrot samples from different positions of the root all showed two distinct EPR signals when mixed with the spin traps PBN and 4-POBN. One of the components, with parameters identical to those reported for the N-(t-butyl)aminoxyl radical, was common to the reactions with both spin traps and must derive either from a fragmentation of the spin traps [1, 2, 5] or from an impurity of the spin trap [6]. The decomposition of PBN was described to form benzaldehyde and N-t-butyl hydroxylamine (*figure 9*), the latter would also be expected to be a fragmentation product of 4-POBN. According to Dikalov et al. [6] the N-(t-butyl)aminoxyl radical is formed by metal catalysed oxidation of N-(t-butyl)hydroxylamine which is an impurity of the Sigma product PBN. The most relevant metal in carrot tissue is in this case iron with ~2.1 mg/100g [4], which catalyses the Fenton reaction. Consequently, OH radicals are formed which then react with N-t-butyl hydroxylamines forming N-(t-butyl)aminoxyl radicals.

The carbon-centred radical that was seen with PBN may not be the primary radical generated during cell disruption. Apart from its implication in the formation of N-(t-butyl)aminoxyl radicals discussed in the previous paragraph, there is more direct evidence for the presence of hydroxyl radicals from measurements with the spin traps DEPMPO and DPPMPO. Hydroxyl radicals can react indiscriminately with a wide range of organic molecules from which they extract a hydrogen atom with the formation of water and a carbon-centred radical.

$$R\text{-}H + HO^{\cdot} \rightarrow R^{\cdot} + H_2O$$
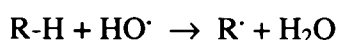
Such a carbon-centred radical could be detected in the reaction with PBN. The differences in adducts seen with PBN and DEPMPO illustrate the differences in the selectivity of different spin traps for different types of radical. As was reported by Goodman et al. [9], the carbon-centred radical adduct with DEPMPO was less stable than the hydroxyl radical adduct. We also observed a signal from a carbon-centred radical adduct when DEPMPO and DPPMPO were used as spin traps.

It may be significant that the spectrum of the hydroxyl radical adduct with DEPMPO was accompanied by a single component (which is probably one half of the spectrum from the monodehydroascorbate radical). This result suggests that ascorbic acid may be reacting with the carbon-centred radical formed from components in the carrot.

7

When 4-POBN was used as spin trap, both of the observed EPR signals correspond to reactions involving the spin trap. In addition to the N-(t-butyl)aminoxyl radical, which is probably a fragmentation product as a result of a similar mechanism to that discussed above for PBN, the dodecet signal almost certainly corresponds to an adduct of a radical formed by oxidation of a 4-POBN molecule. Such a radical has been observed previously with carrots [9] and with a number of different types of leaf tissue [8, 15]. The formation of the 4-POBN· radical is dependent on the presence of oxygen and Pirker et al. [15] suggested that during the disruption of cells some plant components are oxidised and that it is these products that then oxidise 4-POBN.

In some specimens, there was a clear relationship between the intensities of the various EPR signals and the position in the carrot from which the samples were taken. The oxidation product observed with 4-POBN and the N-(t-butyl)aminoxyl radical observed with PBN were highest in the tips and lowest in the central regions, whereas the carbon-centred radical seen with PBN was highest in the samples from the central regions of the roots and lowest in the tips. The hydroxyl radical has been shown to play an important role in root elongation in maize (*Zea mays*) seedlings by facilitating cell wall loosening in the growing zone [10, 12, 13]. These authors did not distinguish between the possibilities of HO· being generated by Fenton chemistry or from peroxidases in the presence of NADH and H_2O_2.

It seems from the current experiments that the hydroxyl radical is also important in the growth zone in carrot hypocotyl root stock, and it may be of general importance in plant root development. The higher level of hydroxyl radical generation at the tips compared to the other tissues in the carrot could also be the explanation for its higher oxidation potential. Furthermore, the fact that the highest levels of carbon-centred radical adduct formation (with PBN) were observed in tissues with the lowest levels of hydroxyl radical generation suggests that formation of (much of) the carbon-centred radicals is independent of hydroxyl radicals. The observation by Goodman et al. [9] of two separate carbon-centred radical adducts with DEPMPO may represent radicals formed by ·OH-dependent and ·OH-independent mechanisms. Similar adducts were also observed in the present experiments when measurements were performed over extended periods of time.

The highest levels of the carbon-centred radical adduct were seen with the spin trap PBN. In contrast, the tissue from the tips produced the highest levels of breakdown of the spin traps PBN and 4-POBN, the former by fragmentation and the latter by oxidation. Since measurements made with the spin traps DEPMPO and DPPMPO demonstrate that the hydroxyl radical is formed in large amounts after tissue disruption, it seems reasonable to

implicate this radical in the damage to the spin traps, either directly or indirectly. The work of Goodman et al. [9] showed that hydroxyl radical production continued in the carrot extracts long after tissue disruption, suggesting that it was the result of an enzymatic process.

4. Conclusions

These experiments show that there is considerable spatial variability in the composition of carrot root tissue and this gives rise to differences in the reactions with spin trap molecules. Carrot tissue reacts with the spin traps PBN and 4-POBN to generate fragmentation and oxidation products respectively to a much greater extent when it is derived from the rapidly growing root tips than with tissue from other parts of the root. This can probably be referred to metal-catalytic generation of hydroxyl radicals maybe indicating either a higher metal-concentration or a higher H_2O_2 concentration in this part of the root. In contrast the levels of carbon-centred radical adducts of PBN were lowest when tissue from the tips was used.

5. Materials and Methods

5.1. Production of carrot tissue

Seeds of carrot (*cv. Maestro*) were sown in two 15-liter pots, which were covered with plastic until the plants were *c.* 2 cm high. During this germination stage, the pots were watered from above only; later a home-made self-irrigating system was used. Each pot was placed on a bucket filled with water, to which it was connected by wicks of glass fibre. Samples were harvested at three different developmental stages 49, 55 and 83 days after sewing. Thin slices of each carrot sample were taken from the top, the centre, and the tip of the root (*figure 10*). They were immediately frozen to 77 K and stored in liquid nitrogen until analysis.

5.2. Chemicals

The spin traps PBN and 4-POBN were purchased from Sigma-Aldrich. 5-(diethoxyphosphoryl)-5-methyl-1-pyrroline-N-oxide (DEPMPO), 5-(dipropoxyphosphoryl)-5-methyl-1-pyrroline-N-oxide (DPPMPO), 5-(dibutoxyphosphoryl)-5-methyl-1-pyrroline-N-oxide (DBPMPO), and 5-propoxycarbonyl-5-ethylpyrolline-1-oxide (PEPO) were synthesised at the Research Institute of Biochemical Pharmacology and Molecular Toxicology at the University of Veterinary Medicine, Vienna. 20 mM phosphate buffer was used and the pH was set to 7.

5.3. Preparation of samples for EPR spectroscopy

In one set of experiments, EPR spectroscopy was carried out using the spin traps PBN and 4-POBN to detect short-lived radicals when cells were disrupted. The 4-POBN solution was made with distilled water, the PBN solution was prepared with a 10% ethanol solution. Frozen carrot samples were ground under liquid nitrogen until a homogenous powder was obtained. A small quantity of the powder was gently mixed with 800μl of the spin trap solution (164 mM) in a second mortar. The suspension was filtered through a disposable syringe filter holder (Fa. Sartorius, 0.45 μm), the filtrate was transferred into the flat cell and the EPR spectrum measured immediately.

10

In a second set of experiments using the spin traps DEPMPO and DPPMPO (~300 mM), thin slices of fresh carrot were crushed in a mortar together with the spin trap. The mixture was then centrifuged for 3 minutes (13000 rpm, 4 °C), after which 500 µl of the supernatant were transferred into cryo tubes and stored in liquid nitrogen. DEPMPO was also diluted with 20 mM phosphate buffer (pH 7) containing a 0.5 mM iron chelator (EDTA). The suspension was filtered through a disposable syringe filter holder (Fa. Sartorius, 0.45 µm), the filtrate was transferred into the flat cell and the EPR spectrum measured immediately.

A third set of experiments were performed with fresh carrot juice, prepared by homogenising a mixture of carrot tissue and distilled water in a food blender. 300 µl of the mixture were transferred in an Eppendorf tube and 300 µl of the spin trap solution (960 mM PEPO and 288 mM DBPMPO) were added. After mixing, the solution was centrifuged for 3 minutes (13000 rpm, 4 °C). 500 µl of the supernatant were transferred into cryo tubes and stored in liquid nitrogen.

Immediately prior to running the EPR spectra, the samples were thawed in a water bath (hot water, ~40 °C) and transferred to a flat cell as quickly as possible.

5.4. EPR spectroscopy

All EPR spectra were recorded using a Bruker ESP300E computer-controlled spectrometer operating at X-band frequencies equipped with an ER4103TM microwave cavity. Microwave generation was by a klystron. Solutions were measured in a flat cell made from Wilmad-Labglass (Buena, NJ, USA).

Spectra from the samples with PBN and 4-POBN spin traps were recorded as the sum of 10 scans, (each taking about 42 s) in 1024 points using 100 kHz modulation frequency. A microwave power of 20 mW, modulation amplitude of 0.16 mT and a sweep width of 6 mT were used.

Spectra with the other spin traps were recorded as single scans, taking about 84 s in 1024 points using 100 kHz modulation frequency. A microwave power of 20 mW, modulation amplitude of 0.068 mT and a sweep width of 12 or 14 mT were used.

All spectra used for quantification were baseline corrected and filtered twice every 15 points using a polynomial filter. The first peak, doublet or quartet of each spectral component was integrated.

In addition, spectral parameters were confirmed by simulation using the Bruker SimFonia software.

Acknowledgements

12

References

[1] Atamna H., Paler-Martinez A., Ames B.N., N-t-Butyl Hydroxylamine, a Hydrolysis Product of α-Phenyl-N-t-butyl Nitrone, Is More Potent in Delaying Senescence in Human Lung Fibroblasts, J. Biol. Chem. 275 (2000) 6741-6748.

[2] Britigan B.E., Pou S., Rosen G.M., Lilleg D.M., Buettner G.R., Hydroxyl Radical Is Not a Product of the Reaction of Xanthine Oxidase and Xanthine, J. Biol. Chem. 265 (1990) 17533-17538.

[3] Buettner G.R., Jurkewicz B.A., Ascorbate free radical as a marker of oxidative stress – an EPR study, Free Radical Biol. Med. 14 (1993) 49-55.

[4] Carlsson S., Die Karotte – Heilkraft aus der Wurzel, Ehrenwirth Verlag GmbH, Munich, 2000.

[5] Chamulitrat W., Jordan S., Mason R.P., Kieko S., Cutler G., Nitric Oxide Formation during Light-induced Decomposition of Phenyl N-tert-Butylnitrone, J. Biol. Chem. 268 (1993) 11520-11527.

[6] Dikalov S.I., Vitek M.P., Maples K.R., Mason R.P., Amyloid β Peptides Do Not Form Peptide-derived Free Radicals Spontaneously, but Can Enhance Metal-catalyzed Oxidation of Hydroxylamines to Nitroxides, J. Biol. Chem. 274 (1999) 9392-9399.

[7] Fréjaville C., Karoui H., Tuccio B., Le Moigne F., Culcasi M., Pietri S., Lauricella R., Tordo P., 5-(Diethoxyphosphoryl)-5-methyl-1-pyrroline-N-oxide: A new efficient phosphorylated nitrone for the in vitro and in vivo trapping of oxygen-centred radicals, J. Med. Chem. 38 (1995) 258-265.

[8] Glidewell S.M., Goodman B.A., Skilling J., Quantified maximum entropy and biological EPR spectra, in: Skilling J., Sibisi S. (Eds.), Maximum Entropy and Bayesian Methods, Kluwer, Dordrecht, 1996, pp. 22-30.

[9] Goodman B.A., Glidewell S.M., Arbuckle C.M., Bernardin S., Cook T.R., Hillman J.R., An EPR study of free radical generation during maceration of uncooked vegetables, J. Sci. Food Agric. 82 (2002) 1208-1215.

[10] Liszkay A., van der Zalm E., Schopfer P., Production of reactive oxygen intermediates (O_2^-, H_2O_2, and ·OH) by maize roots and their role in wall loosening and elongation growth, Plant Physiol. 136 (2004) 3114-3123.

[11] McCormick M.L., Buettner G.R., Britigan B.E., The Spin Trap α-(4-Pyridyl-1-oxide)-*N*-*tert*-butylnitrone Stimulates Peroxidase-mediated Oxidation of Deferoxamine, J. Biol. Chem. 270 (1995) 29265-29269.

[12] Schopfer P., Hydroxyl radical-induced cell-wall loosening *in vitro* and *in vivo*: implications for the control of elongation growth, Plant J. 28 (2001) 679-688.

[13] Schopfer P., Liszkay A., Bechtold M., Frahry G., Wagner A., Evidence that hydroxyl radicals mediate auxin-induced extension growth, Planta 214 (2002) 821-828.

[14] N.I.E.H.S. Spin-Trap DataBase, http://mole.chm.bris.ac.uk/cgi-bin/stdb (1998).

[15] Pirker K.F., Reichenauer T.G., Goodman B.A., Stolze K., Identification of oxidative processes during simulated mastication of uncooked foods using electron paramagnetic resonance spectroscopy, Anal. Chim. Acta 520 (2004) 69-77.

[16] Stolze K., Udilova N., Nohl H., Spin trapping of lipid radicals with DEPMPO-derived spin traps: detection of superoxide, alkyl and alkoxyl radicals in aqueous and lipid phase, Free Radical Biol. Med. 29 (2000) 1005-1014.

[17] Stolze K., Udilova N., Rosenau T., Hofinger A., Nohl H., Synthesis and characterisation of EMPO-derived 5,5-disubstituted 1-pyrroline *N*-oxides as spin traps forming exceptionally stable superoxide spin adducts, Biol. Chem. 384 (2003) 493-500.

table I. Summary of hyperfine splitting parameters compared with literature data.

Adduct	System	$a(^{31}P)$ (mT)	$a(^1H)$ (mT)	$a(^{14}N)$ (mT)
N-(*t*-butyl)aminoxyl	Dikalov et al. [6]		1.393	1.461
4-POBN· radical	McCormick et al. [11]		0.180	1.49, 0.185
	Carrot (present paper)		0.145, 0.050	1.490, 0.180
PBN-COCH₃	NIEHS database [14]		0.330	1.590
PBN-C	Carrot (present paper)		0.328	1.590
DEPMPO-OH	Fréjaville et al [7]	4.780	1.300	1.400
	Carrot (present paper)	4.723	1.384	1.384
DPPMPO-OH	Stolze et al [16]	4.695	1.320	1.400
	Carrot (present paper)	4.680	1.382	1.382
DEPMPO-C	Fréjaville et al [7]	4.810	2.230	1.500
	Carrot (present paper)	4.773	2.185	1.486
DPPMPO-C	Stolze et al [16]	4.848	2.218	1.512
	Carrot (present paper)	4.780	2.223	1.515
PEPO-OH	Stolze et al [17]		1.594, 0.063	1.400
			1.201, 0.078	1.387
PEPO-OOH	Stolze et al [17]		1.160/0.903	1.321/1.321
PEPO-C	carrot juice (present paper)		2.300	1.500
PEPO-C(LOOH)	(unpublished results)		2.349	1.503
PEPO-CH₂OH	(unpublished results)		2.150, 0.087	1.474
PEPO-CH₃	(unpublished results)		2.417	1.508

15

Legends to Figures

figure 1. A typical EPR spectrum of a carrot sample, using the spin trap phenyl-*N*-*t*-butylnitrone. It consists of the sextet (carbon-centred radical) and the quartet (breakdown product of the spin trap).

figure 2. Signal intensity of the C-centred radical trapped with phenyl-*N*-*t*-butylnitrone in relation to the position and the maturation of the carrot. a, b are two replicates of the carrots. top, centre, tip are the position of the carrot where the samples were taken. 1, 2, 3 are the 1st, 2nd and 3rd harvests.

figure 3. Signal intensity of the breakdown product from phenyl-*N*-*t*-butylnitrone in relation to the position and to the maturation of the carrot. a, b are two replicates of the carrots. top, centre, tip are the position of the carrot where the samples were taken. 1, 2, 3 are the 1st, 2nd and 3rd harvests.

figure 4. Typical EPR spectrum of a carrot sample using α-(4-pyridyl-1-oxide)-*N*-*t*-butylnitrone as spin trap. It consists of the oxidation product and the breakdown product.

figure 5. Signal intensity of the oxidation product from α-(4-pyridyl-1-oxide)-*N*-*t*-butylnitrone in relation to the position and to the maturation of the carrot. c, d are two replicates of the carrots. top, centre, tip are the position of the carrot where the samples were taken. 1 and 3 are the 1st and 3rd harvests.

figure 6. EPR spectrum of (A) a hydroxyl radical from carrot trapped by 5-(diethoxyphosphoryl)-5-methyl-1-pyrroline-N-oxide, (B) simulation of spectrum (A), (C) spectrum received from carrot and 5-(diethoxyphosphoryl)-5-methyl-1-pyrroline-N-oxide in the presence of buffer and ethylenediaminetetraacetic acid, (D) simulation of a carbon-centred radical. Spectral interpretation is shown by the "stick" diagram.

figure 7. EPR spectra from carrot and 5-(dipropoxyphosphoryl)-5-methyl-1-pyrroline-N-oxide. (A) experimental spectrum, (B) simulation of a carbon-centred radical combined with a hydroxyl-radical, (C) simulation of the carbon-centred radical adduct, (D) simulation of the hydroxyl-radical adduct. Spectral interpretation is shown by the "stick" diagrams.

16

figure 8. EPR spectrum of (*A*) a radical in carrot trapped by 5-propoxycarbonyl-5-ethylpyrolline-1-oxide, (*B*) simulation of the spectrum (A). Spectral interpretation is shown by the "stick" diagram.

figure 9. Decomposition of the spin trap phenyl-*N*-*t*-butylnitrone.

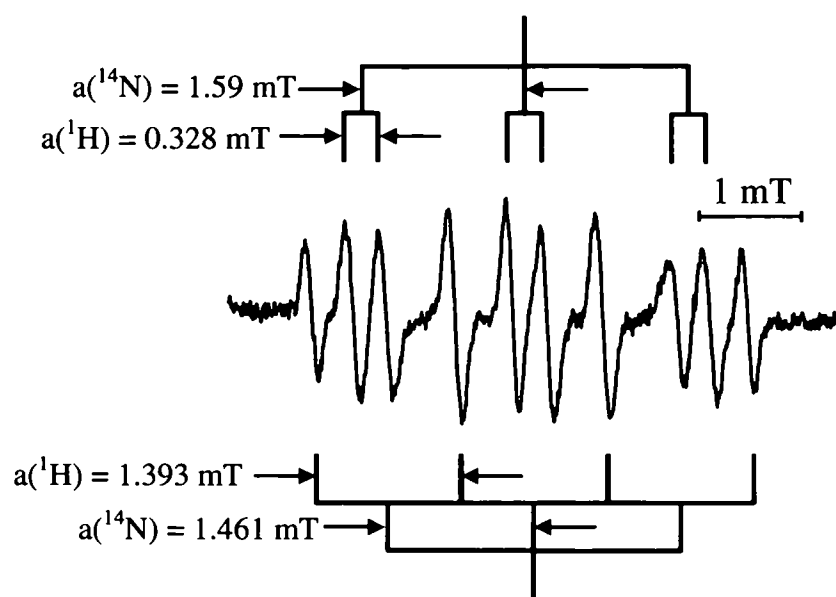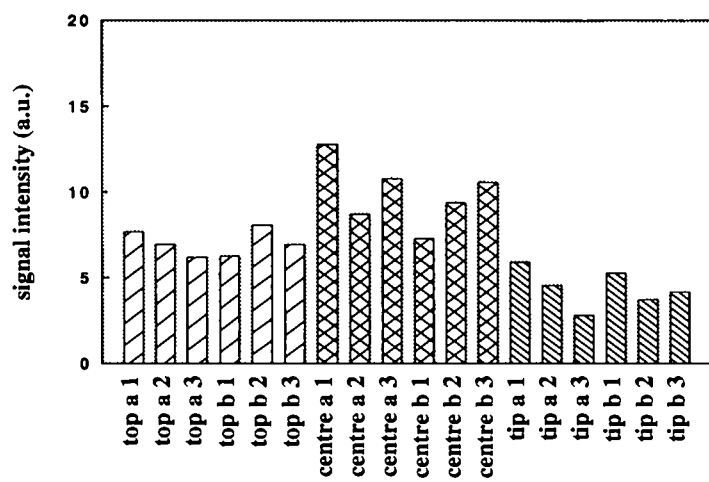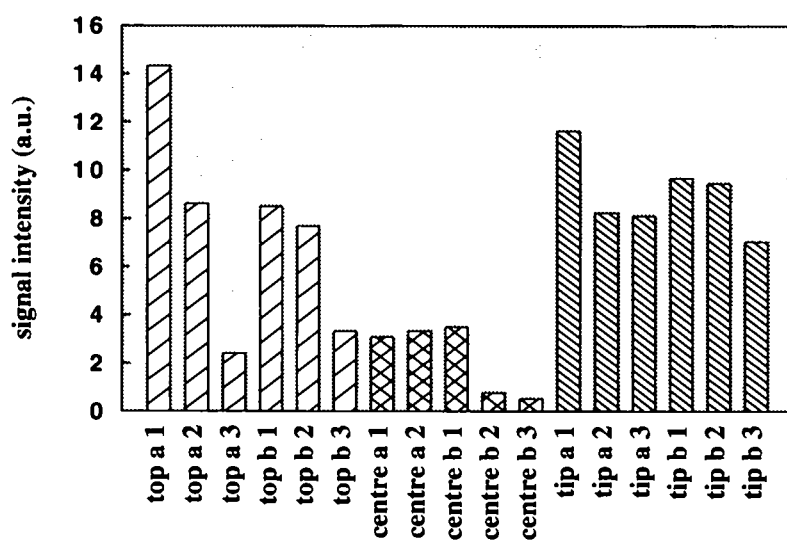*figure 10.* Carrot samples (yellow marked) taken from each root.

$a(^{14}N) = 1.59$ mT

$a(^{1}H) = 0.328$ mT

1 mT

$a(^{1}H) = 1.393$ mT

$a(^{14}N) = 1.461$ mT

figure 1

figure 2

figure 3

$a(^{14}N) = 1.493$ mT

$a(^{14}N) = 0.182$ mT

$a(^1H) = 0.145$ mT

1 mT

$a(^1H) = 1.393$ mT

$a(^{14}N) = 1.461$ mT

figure 4

21

figure 5

$a(^{31}P)=4.723$ mT

$a(^1H)=1.384$ mT

$a(^{14}N)=1.384$ mT

1 mT

A

B

$a(^{31}P)=4.773$ mT

$a(^1H)=2.185$ mT

$a(^{14}N)=1.486$ mT

1 mT

C

D

figure 6

A

B

a(³¹P)=4.78 mT
a(¹H)=22.33 mT
a(¹⁴N)=15.15 mT

C

a(³¹P)=4.68 mT
a(¹H)=13.82 mT
a(¹⁴N)=13.82 mT

D

figure 7

figure 8

PBN   benzaldehyde   N-*t*-butyl hydroxylamine
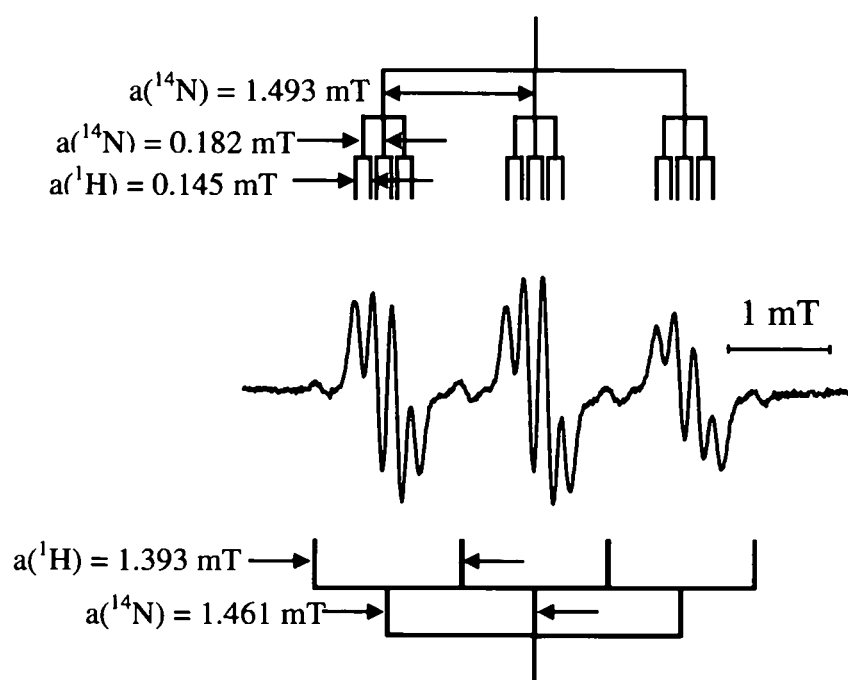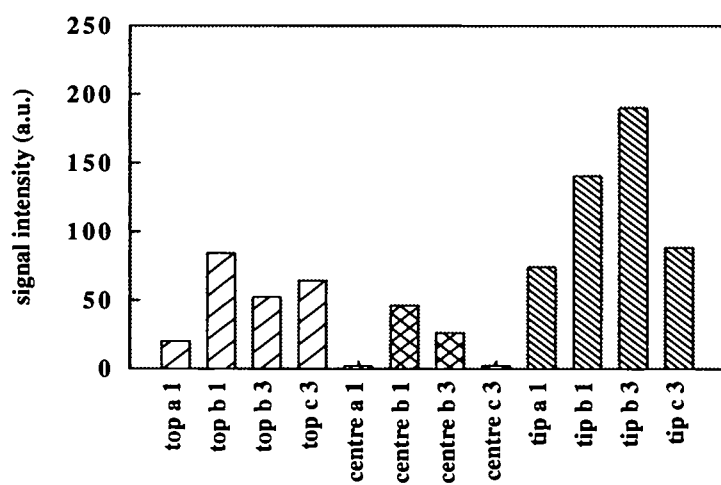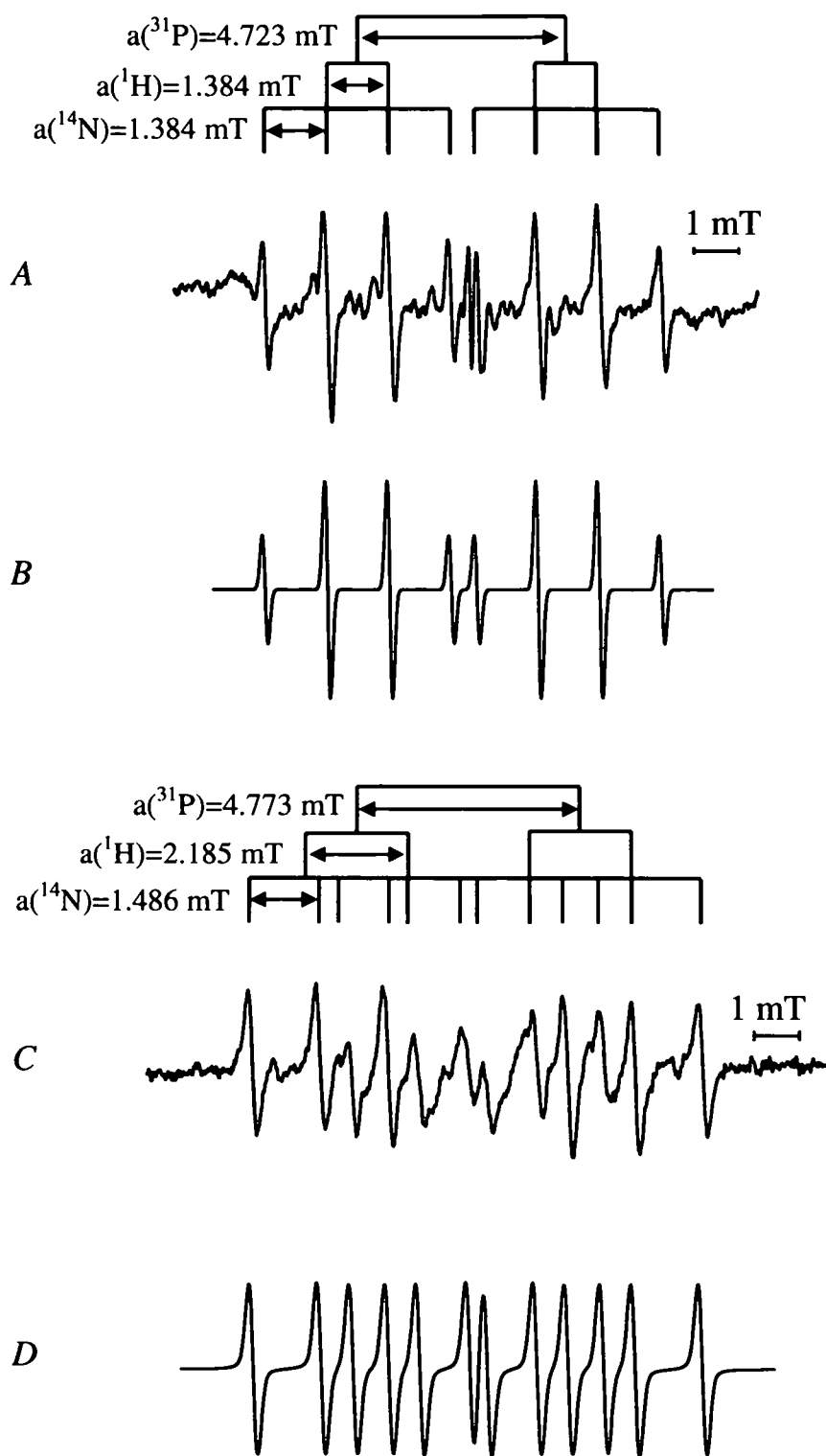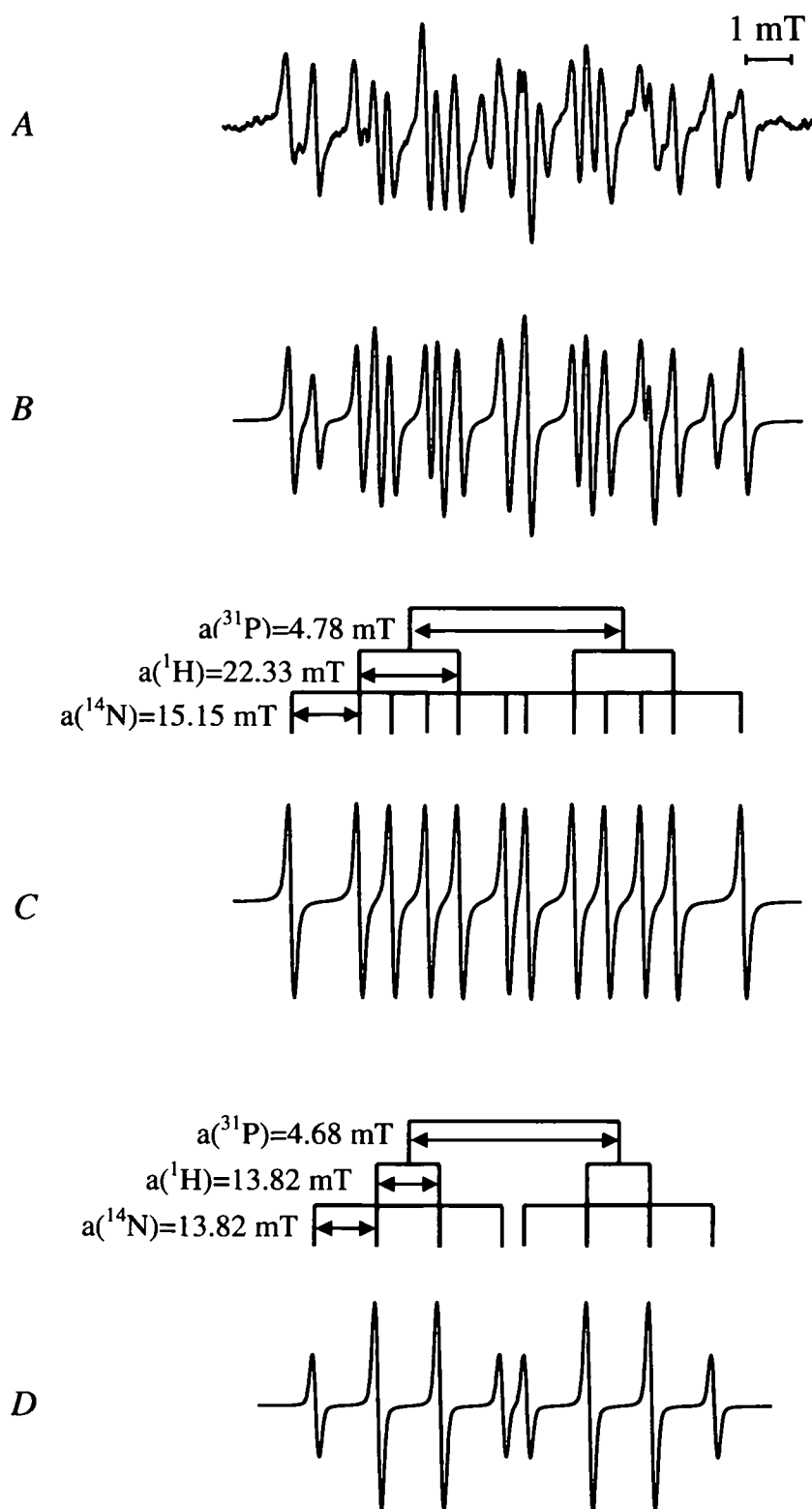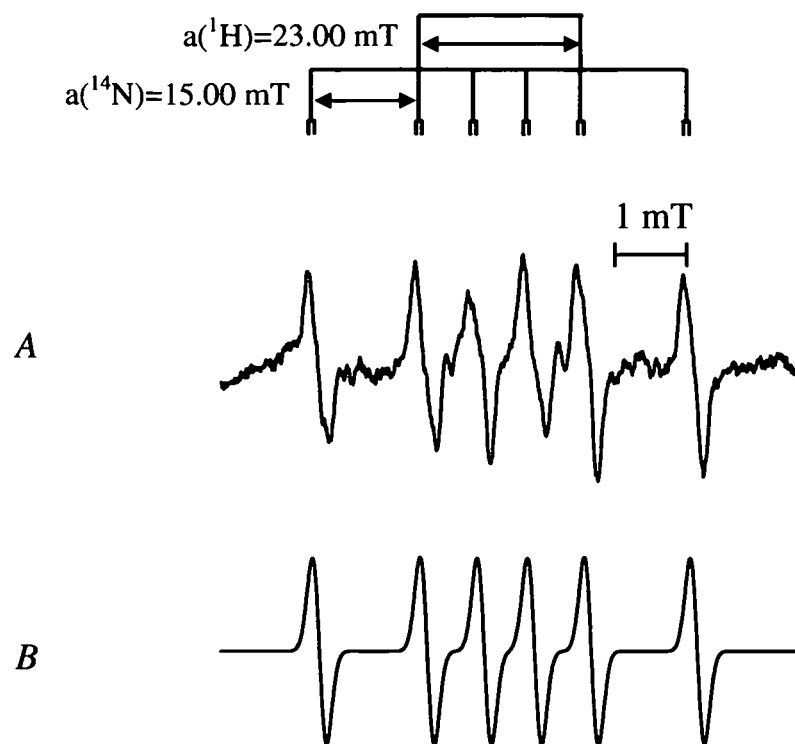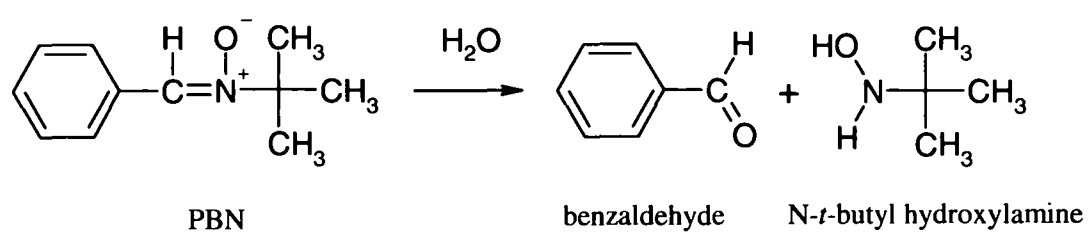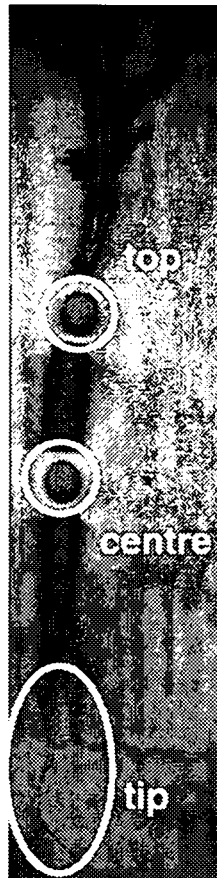
figure 9

figure 10

A.6. PUBLICATION OF KAEMPFEROL

Pirker K.F., Stolze K., Reichenauer T.G., Nohl H., Goodman B.A., Are the biological properties of kaempferol determined by its oxidation products?, submitted in *Free Radical Research.-*

Are the biological properties of kaempferol determined by its oxidation products?

Running title: **EPR of kaempferol oxidation products**

KATHARINA F. PIRKER[1], KLAUS STOLZE[2], THOMAS G. REICHENAUER[1], HANS NOHL[2], AND BERNARD A. GOODMAN[1,3]

[1]ARC Seibersdorf research GmbH, Seibersdorf, Austria, and [2]Research Institute for Biochemical Pharmacology and Toxicology, Veterinary University of Vienna, Vienna, Austria, and [3]University of Illinois, Urbana-Champaign, USA

Abstract

Although the flavonoid molecules have attracted considerable interest in recent years because of their antioxidant properties and their presence in many medicinal plants, there are considerable differences in their chemical properties. The present paper uses electron paramagnetic resonance (EPR) spectroscopy to compare the oxidative free radical chemistry of two such molecules, kaempferol and luteolin, which have the same empirical formula and differ only in the position of one OH group. However, whereas the basic flavonoid structure remains intact in luteolin, structural changes occur in kaempferol when it undergoes 1-electron oxidation. Autoxidation of kaempferol in alkaline solution leads to rapid fragmentation, and the subsequent free radical chemistry derives from these fragments, whereas radicals generated enzymatically at physiological pH have spectral properties that are best described by dimeric structures. The biological properties of kaempferol are likely to be determined to a considerable extent by the chemistry of its oxidation products.

Correspondence: Katharina F. Pirker, Department of Environmental Research, ARC Seibersdorf research GmbH, A-2444 Seibersdorf, Austria. Tel. +43 50550 3609. Fax +43 50550 3520. Email: k.pirker@umweltforschung.at

1. Introduction

Flavonoid molecules have attracted considerable interest in recent years, because of their antioxidant properties, and their occurrence in plants that are used as traditional medicines in many parts of the world. Based on measurements of antioxidant activity and free radical scavenging ability, individual flavonoid molecules are now being used as dietary supplements with claims for anti-aging and disease prevention properties. However, it is by no means clear that such molecules consumed individually will have the same biological effects as when part of a whole food. Nor is it clear whether the biological properties are determined by the individual flavonoid molecules, or by their reaction products.

In plants there are large numbers of flavonoid molecules, and there are likely to be considerable differences in their chemistry depending on the nature and position of substituent groups in the basic flavonoid structure. From a dietary supplement/herbal medicine point of view, it is especially important to understand their behaviour with respect to oxidation, since their use is being promoted on the basis of their antioxidant properties. The present paper compares the oxidative free radical chemistry of luteolin and kaempferol, two molecules which differ only in the position of one OH group. On the basis of these results, it is proposed that the biological activity of kaempferol is likely derived from oxidation products.

The structures of luteolin and kaempferol are shown in Figure 1 (a and b). Each has two aromatic rings, one heterocyclic ring and four substituent hydroxyl groups; Ring C contains also a keto group. Luteolin is a flavone with a catechol group in ring B. Kaempferol, a flavonol, has the OH group at carbon 3' of the B ring replaced by one at carbon 3 of the C ring.

Autoxidation proceeds by deprotonation and electron abstraction to produce ionised radical anions. This was performed using alkaline, aerated solutions to produce initial information on the oxidised components. In addition, reactions with three aqueous oxidation systems were investigated at pH 7. These were (a) horseradish peroxidase and hydrogen peroxide (HRP/H_2O_2), which has been reported to form three complexes with a high oxidation potential [1]; (b) xanthine and xanthine oxidase (X/XO), which is supposed to generate superoxide anion radicals [2, 3] and (c) the Fenton reaction system, which generates hydroxyl radicals [4]. Reactions with O_2^- were also investigated directly using potassium superoxide at pH 6.9.

2. Materials and Methods

The flavonoids kaempferol (≥96% purity) and luteolin (≥99% purity) and the enzyme horseradish peroxidase (~150 units/mg) were purchased from Fluka (Vienna, Austria), catalase (from bovine liver, 2000-5000 units/mg) and superoxide dismutase (SOD) (from bovine erythrocytes, 2500-7000 units/mg) were purchased from Sigma (Vienna, Austria), potassium superoxide from Aldrich (Vienna, Austria), and kaempferide from Extrasynthese S.A. (Lyon, France).

2.1. Autoxidation procedures

Two different experimental setups were used in order to investigate the influence of oxygen levels as well as of the relative concentrations of NaOH and the phenol. In both procedures a 1 mM stock solution of the phenol in DMSO was used.

In the first procedure (Proc. 1), 200 μl of a 0.1 M sodium hydroxide solution were transferred into an EPR flat cell (Wilmad-Labglass, Buena, NJ, USA), then 200 μl of the flavonoid solution were added. The reaction between the flavonoid and the alkali was immediately visible as a strong yellow band at the interface of the two liquid phases. This then spread slowly through the cell as a result of diffusion of the molecules. After addition of the flavonoid, the flat cell was immediately placed in the spectrometer and the spectrum recorded within one minute. In this procedure the amount of oxygen is limited to that dissolved in the solutions. The second procedure (Proc. 2) was carried out in an Eppendorf tube to test the influence of a higher oxygen concentration. 200 μl of the NaOH-solution and 200 μl of the flavonoid solution were transferred into an Eppendorf tube and mixed with a Vortex mixer for a few seconds. The mixed solution had an intensive yellow colour and since the oxidation is an exothermic process the tube walls got warm very quickly. The oxidised solution was transferred into a flat cell as quickly as possible and placed immediately into the spectrometer for recording the spectrum. The oxygen concentration in this experiment (Proc. 2) should have been much higher than in the first set up (Proc. 1).

The dependence of relative concentrations of NaOH and the flavonoid was tested using Proc. 2 by thorough mixing of the two solutions in an Eppendorf tube. The two stock solutions were combined in different amounts; 1:1, 1.67:1 and 3:1 volume ratios of flavonoid:NaOH solutions.

4

2.2. Oxidation with horseradish peroxidase/hydrogen peroxide (HRP/H₂O₂)

Concentrations of solutions for the system HRP/H_2O_2 were similar to those of Miura et al. [5]. 200 µl of a potassium phosphate buffer (pH 7) were mixed in an Eppendorf tube together with 50 µl of $ZnCl_2$ (10 mM), 50 µl HRP (12.5 µM), and 5 µl H_2O_2 (100 µM). All solutions were made with distilled water. 200 µl of the mixed solution were transferred into an EPR flat cell and 200 µl of the flavonoid stock solution were added.

2.3. Oxidation with xanthine/xanthine oxidase(X/XO)

The system X/XO was used to generate superoxide anion radicals. The experiment was carried out with 200 µl of a potassium phosphate buffer (pH 7) mixed for a few seconds together with 20 µl of xanthine solution (657 µM) and 5 µl of xanthine oxidase (8µl/1ml,activity). All individual solutions were prepared with distilled water. 200 µl of the mixed solution were transferred into the flat cell and 200 µl of the flavonoid stock solution were added.

2.4. Oxidation in a Fenton reaction system

Hydroxyl radicals are generated in the Fenton system by the reaction of H_2O_2 with Fe(II). The reagent concentrations were those of Blank et al. [6]. 200 µl of a potassium phosphate buffer (pH 7) were placed in an Eppendorf tube. 5 µl $FeCl_3 \cdot 6H_2O$ (10 mM), 5 µl EDTA (25 mM), and 5 µl H_2O_2 (100 µM) were added and the solution was mixed for a few seconds using a Vortex mixer. Distilled water was used for preparation of the individual solutions. 200 µl of the mixed solution were transferred in the flat cell and 200 µl of the flavonoid stock solution were added.

In each case the flat cell was placed in the spectrometer within 1 minute and the EPR spectrum recorded immediately after tuning the spectrometer.

2.5. Potassium superoxide

The reaction of superoxide radical anions with phenols was investigated using potassium superoxide. For this purpose 40 µl of the flavonoid solution (10mM) were mixed in an Eppendorf tube with 60 µl of distilled H_2O in the case of luteolin and with 160 µl DMSO

in the case of kaempferol. The solution was added to c. 0.5 mg KO_2 and the reaction was stopped after approx. 5 sec. by adding a pH 6.9 buffer solution (300 µl for luteolin, 200 µl for kaempferol) containing 5 µl catalase (1 mg/ml) and 10 µl SOD (2 mg/ml). The resulting solution was then transferred into a flat cell which was placed in the spectrometer and the spectrum was recorded as quickly as possible.

2.6. EPR spectroscopy

All EPR spectra were acquired in 1024 points using a Bruker ESP 300E CW spectrometer operating at X-band frequencies and equipped with a ER4103TM cavity. Microwave generation was by a klystron and the microwave frequency recorded continuously with a frequency counter. 100 kHz modulation frequency and 20mW microwave power were used for all measurements. Magnetic field sweep widths were in the range 0.9 - 2.0 mT, depending on the spectral widths. For most measurements a modulation amplitude of 0.01 mT was used and the spectra accumulated in 10 scans. Where different conditions were used, these are indicated in the relevant figure captions.

After placing the flat cell in the microwave cavity, the spectrometer was tuned manually to minimise the time between commencement of the reaction and recording the spectrum.

All of the parameters derived from the spectra in this work were confirmed by simulation using the Bruker Simfonia software. However, simulations are only shown for the more complex spectra.

3. Results and Interpretation

3.1. Luteolin

Autoxidation of luteolin (Figure 1a) gave two EPR signals at different times after starting the reaction. The spectrum of the first radical (Figure 2a), which is similar to that reported by Kuhnle et al. [7], Cotelle et al. [8] and van Acker et al. [9] can be simulated by 4 inequivalent proton couplings (Figure 2b). This subsequently developed into an 8 peak spectrum from 3 inequivalent proton splittings (Figure 2c), although the first radical was stabilised if $ZnCl_2$ was added to the alkali solution.

Oxidation of luteolin with HRP/H_2O_2, X/XO, the Fenton reaction system or potassium superoxide at pH 7 all resulted in a 6 peak spectrum similar to Figure 2a. However, with potassium superoxide the spectrum consisted of sharp lines, whereas with HRP/H_2O_2, X/XO, and the Fenton reaction the resolution of the spectra was poorer; resolution was not improved either by decreasing the modulation amplitude or flushing the solutions with N_2 gas.

The oxidation site in luteolin is most likely the catechol group on ring B, which is considered to be the region responsible for the antioxidant activity in flavonoids [10]. The probable structure of the radical from oxidised luteolin is shown in Figure 1c. The largest proton splitting can be assigned to the proton on carbon 6', whereas smaller splittings around 0.1 mT come from interactions with protons in positions 2', 5' and 3 [8].

The second radical, which was detected at pH 13 after the 1st radical decreased in intensity, was also reported from Cotelle et al. [8]. These authors explained the structure as resulting from oxidation at carbon 2' (Figure 1d). With this radical, the largest hyperfine splitting again comes from the proton on carbon 6' and the smaller splittings from protons on carbons 5' and 3.

3.2. Kaempferol

Autoxidation of kaempferol led to five distinct EPR signals, along with additional weak peaks from components that could not be fully resolved. Thus the free radical chemistry of kaempferol is considerably more complex than that of luteolin. The initial signal obtained with equal volumes of the kaempferol and NaOH solutions was a five peak spectrum (Figure 3a), consistent with four equivalent ^1H atoms in the radical. When there was

adequate O_2 supply, this changed rapidly to a septet spectrum (Figure 3b), which was best simulated with 8 equivalent ^1H atoms (the two outermost peaks being too weak to observe in the EPR spectrum). Changing the kaempferol:NaOH ratios resulted in different signals. With a 1.67:1 ratio, additional structure was observed on the septet signal after the quintet had decreased (Figure 3c); this spectrum was simulated with two sets of four equivalent ^1H atoms (Figure 3d). A 3:1 ratio kaempferol:NaOH gave a spectrum with at least three components (Figure 4). The first spectrum (Figure 4a) contained the quintet and a signal with 13 peaks (compound 2). Approximately 5 minutes later the quintet had disappeared and a mixture of two signals was visible, including the 13 peak spectrum (Figure 4b). After another c. 21 minutes compound 2 had almost disappeared and a spectrum of 8 peaks (compound 3) with nearly equal intensity (Figure 4d) was observed. In order to produce the simulation of compound 2 (Figure 4c), a small amount of the simulation of compound 3 was first subtracted from Figure 4b, since this component was already present in the spectrum.

When kaempferide, which has a similar composition to kaempferol except that the hydroxyl group on ring B is replaced by a methoxy-group (Figure 1e), was used for the autoxidation experiment, no spectrum was observed, thus supporting the assumption that the oxidation site in kaempferol is the hydroxyl group on ring B.

Oxidation of kaempferol at pH 7 with HRP/ H_2O_2, X/XO, or the Fenton reaction system gave the same EPR spectrum in each case (Figure 5); this could be simulated with five proton couplings around 0.1 mT. In contrast, oxidation with potassium superoxide at pH 6.9 resulted in a quintet spectrum that is similar to Figure 3a.

The EPR spectral parameters for the initial free radical signal seen on autoxidation of kaempferol are identical to those of p-benzosemiquinone (Figure 1f) [7]. It appears, therefore, that there is rapid fragmentation of the flavonoid structure. According to the spin distribution calculations of van Acker et al. [9], the unpaired electron density in the kaempferol radical is mainly in ring B and is largely associated with the oxygen atom from which the proton was removed. These authors also measured the half peak oxidation potential of kaempferol in the pH range 2 to 13 and showed that no release of protons occurred at pH > 9.

The "7 peak spectrum" (Figure 3b) was best simulated by 8 equivalent protons, and thus most likely corresponds to a dimeric structure in which the unpaired electron interacts equally with 8 protons. It seems probable that short-lived phenoxyl radicals react with the quinone or semiquinone generating either a radical, or a non-radical dimer (which is then

8

oxidised to a radical). A possible structure is based on two aromatic rings connected with either an ether bridge (Figure 1g) or a simple carbon-carbon bond.

To test this interpretation, a solution of phenol with a trace of hydroquinone was oxidised in alkaline solution in a method analogous to Proc. 2. Its spectrum was identical to that in Figure 3b. The same signal was also observed after oxidation of a pure phenol solution but the intensity was much lower than from the solution containing a trace of hydroquinone, thus suggesting that hydroquinone participates in the radical reaction.

Hydroquinone and quinone may form a charge-transfer complex called quinhydrone. Although this complex seems to be more stable in an alkaline solution of pH 8.0 [11], it is most likely not the substrate for the detected radical forming the 7-peak spectrum. Quinhydrone has a purple colour whereas the oxidised kaempferol solution at pH 13 had an intensive yellow colour indicating the formation of benzoquinone.

The EPR spectrum obtained with a kaempferol to NaOH ratio of 1.67:1 (Figure 3c) could be fitted to 2 sets of 4 equivalent protons (Figure 3d) with an average hyperfine splitting the same as that in Figure 3b. It is probable, therefore, that this signal is also derived from a dimeric radical.

The two additional signals that were seen with a kaempferol:NaOH ratio to 3:1 are probably also radicals with two or more aromatic rings, because of the higher concentration of kaempferol in this solution than in the previous experiments. The first of these (Figure 4b) was simulated with 6 proton couplings (Figure 4c), four equivalent with a smaller value than the other two. The second signal (Figure 4d), which was detected after the previous one decreased in intensity, had 3 inequivalent protons. There is, however, not enough information at present to make definite structure suggestions for these radicals.

Oxidation of kaempferol with HRP/H_2O_2, X/XO, or the Fenton reaction system at physiological pH of 7 resulted in a spectrum with a sextet structure from interaction of the unpaired electron with five ^1H nuclei. No other signal was detected, indicating that the flavonoid structure remained intact. No radical was detected when oxidation of kaempferide (Figure 1e) by HRP/H_2O_2 was attempted, thus indicating that the OH-group on ring B is involved in the oxidation of kaempferol. The generation of a phenoxyl derivative where the OH-group in ring B is oxidised can be excluded because of the small hyperfine splitting constants around 0.1 mT. For para-substituted phenoxyl radicals, hyperfine splittings for the two hydrogens on carbon 3' and 5' would be expected to be in the range 0.4 - 0.7 mT dependent on the substituents [12]. The small splittings in the present experiments suggest a dimeric structure, in which the unpaired electron spin

density is delocalised over two aromatic rings and is, therefore, smaller at individual carbon atoms. Loth and Klinge [13] detected a dimeric structure after oxidation of kaempferol with HRP/H_2O_2, and Figure 6a shows three possibilities which they suggested for the formation of the dimer.

On the basis of the hyperfine splitting constants, the most likely structure consists of an ether bridge from the oxygen on ring B of one kaempferol molecule to carbon 6" in ring A of a second kaempferol molecule (Figure 6b). The two biggest splittings (a(^{1}H)=0.115 mT) would result from interaction with protons on carbon 3' and 5' and the two smallest splittings (a(^{1}H)=0.087 mT) from coupling with protons on carbon 2' and 6'. The hyperfine splitting constant of a(^{1}H) = 0.103 mT would then be due to the spin density on carbon 8".

4. Discussion

Oxidation of kaempferol under different conditions led to the detection of 6 different radicals. One of them, the initial quintet in alkaline solutions, was published by Kuhnle et al. [7] and assigned to p-benzosemiquinone, whereas the other signals have not been published previously. Van Acker et al. [9] also detected a quintet after autoxidation in KOH, but reported different hyperfine splitting constants to those we obtained here. Additionally they reported a weak triplet when HRP/H_2O_2 at pH 7 was used as the oxidising agent; this could be part of the sextet spectrum which we detected with HRP/H_2O_2.

The autoxidation experiments showed a strong dependency of the radical chemistry on the amount of oxygen and on the ratio of kaempferol to NaOH. This could be because the radical chemistry is based on dimeric or polymeric structures of degradation products of kaempferol. Yu et al. [14] reported the formation of dimers from phenoxyl radicals in water after oxidation of phenol with HRP/H_2O_2, and the spectra of four of the radicals produced by kaempferol autoxidation are best interpreted in terms of di- or polymeric structures from the phenol that is generated by fragmentation of the flavonoid molecule.

If the formation of a phenoxyl derivative on ring B is the initial product of autoxidation, as suggested by van Acker et al [9], and of the reaction with KO_2 at pH 6.9, the rapid appearance of the EPR signal from p-benzosemiquinone indicates that this radical is unstable and fragmentation occurs at the 2-1' bond. A plausible mechanism for the early stages of the oxidation is presented in Figure 7. Water addition to the double

10

bond is a likely first step after oxidation of ring B. This 2,3-dihydroxyflavanon has been reported by Frey-Schröder and Barz [15]. 2,2-dihydroxy-1-(2,4,6-trihydroxyphenyl)-3-(4-hydroxyphenyl)-1,3-propandion, which is formed when ring A is opened, has been detected by Miller and Schreier [16]. These authors also detected the formation of 4-hydroxybenzoic acid and 2,4,6-trihydroxybenzoic acid from the oxidation of kaempferol. 4-hydroxybenzoic acid is not stable in alkaline solution and probably degrades to phenol and CO_2. This phenoxyl radical is also unstable and Neta et al. [17] reported the formation of p-hydroquinone from phenoxyl radicals. In the presence of hydroxyl ions or water, addition of OH groups to the phenol structure is possible at both the *ortho* or *para* positions to the oxygen. Since the reaction takes place in an alkaline aerated solution, oxidation of hydroquinone should occur readily with the formation of *ortho*-and *para*-benzosemiquinone radicals. However, although we observe extensive formation of *p*-benzosemiquinone, we have not seen any *o*-benzosemiquinone in any of our current measurements.

In the reaction of HRP with H_2O_2, three complexes with high oxidation potentials are formed [1]. Two of these (complexes II and III) can be reduced directly to the ferric form of the enzyme, whereas complex I is first transformed into complex II. There are previous reports of products of the reaction of the HRP/H_2O_2 system with kaempferol, but it is difficult to relate the results of these investigations to the present results. For example, Miller and Schreier [16] identified several products using UV-, IR-spectroscopy, mass spectrometry, ^{1}H-NMR and ^{13}C-NMR, but none of these had structures that could be related to the hyperfine structure in our EPR spectra, even though three of the products may be included in the degradation process of kaempferol and formation of phenoxy radicals. In the PhD thesis of Miller [18], there was speculation of a dimeric structure for one reaction product but this was not confirmed. Formation of a dimer as a product of the reaction of kaempferol-3-glucoside with HRP/H_2O_2 was also suggested by Loth and Klinge [13] on the basis of results from UV spectroscopy, vapour pressure osmometry (for molecular mass determination) and alkaline degradation. One of the three structural suggestions they made for this dimeric product could generate a radical that might explain our EPR results.

Takahama [19] detected two degradation products from the oxidation of kaempferol by superoxide anion radicals, but neither had a structure that correlates with our EPR results. There are some reports about inhibitory effects of kaempferol on the enzyme xanthine oxidase [8, 20, 21], where it is supposed that OH-groups on carbon 5 and

7 block the position in the enzyme where xanthine should add. Since in our experiments the xanthine/xanthine oxidase reaction is commenced before addition of the flavonol, any inhibitory effect will have no consequence for the initial radical generation in the reaction with kaempferol.

Puppo [22] has reported that kaempferol can function as either an antioxidant or a prooxidant in the Fenton reaction depending on the experimental conditions. In the presence of Fe(III), EDTA and H_2O_2, kaempferol stimulates OH-formation by helping redox-cycling the iron. When ascorbate is present, it can also reduce the Fe(III). If ATP is used instead of EDTA, redox cycling of iron does not occur and kaempferol acts as an OH scavenger. In our experiments the Fenton reaction system was already generating OH-radicals before the flavonol was added, suggesting that reaction with OH radicals might be the dominant process in the oxidation of kaempferol.

The spectrum of the 1st EPR signal reported by van Acker et al. [9] for the autoxidation of luteolin appeared identical to our spectrum (Figure 2a), but their reported hyperfine splitting constants produced a completely different spectrum on simulation. Furthermore, they were not able to detect a signal using HRP and H_2O_2 at pH 7.4, which may be a consequence of the different experimental setup they used. In our case the flavonoid had contact with the solution where OH-radicals were already generated, whereas van Acker et al. [9] included the flavonoid in the radical generating system. Recently, Huang et al. [23] have reported that HRP can be inactivated by phenoxyl radicals generated by reaction of H_2O_2 with phenols. If luteolin has a similar effect on the enzyme, this could explain the failure of van Acker et al [9] to observe radical formation in their HRP/H_2O_2/luteolin system.

5. Conclusions

Although the structures of luteolin and kaempferol differ only in the position of one OH-group, the behaviour of these molecules under oxidative conditions are completely different. The catechol group of luteolin stabilizes the radical anion and hence prevents degradation. In contrast, the initial phenoxyl radical formed by oxidation of kaempferol is unstable, and depending on the pH, it either fragments or forms dimers. Thus, whereas luteolin could be redox cycled, the biological activity of kaempferol is probably related to its degradation and dimeric products.

Acknowledgements

13

References

[1]   George P. The chemical nature of the second hydrogen peroxide compound formed by cytochrome c peroxidase and horseradish peroxidase. Biochemical Journal 1953;54:267-276.

[2]   McCord JM, Fridovich I. Superoxide dismutase: an enzymic function for erythrocuprein (hemocuprein). Journal of Biological Chemistry 1969;244:6049-6055.

[3]   Terada LS, Leff JA, Repine JE. Measurement of xanthine oxidase in biological tissues. Methods in Enzymology 1990;186:651-656.

[4]   Halliwell B, Gutteridge JMC. Oxygen toxicity, oxygen radicals, transition metals and disease. Biochemical Journal 1984;219:1-14.

[5]   Miura T, Muraoka S, Fujimoto Y. Inactivation of creatine kinase induced by quercetin with horseradish peroxidase and hydrogen peroxidase: pro-oxidative and anti-oxidative actions of quercetin. Food and Chemical Toxicology 2003;41:759-765.

[6]   Blank I, Pascual EC, Devaud S, Fay LB, Stadler RH, Yeretzian C, Goodman BA. Degradation of the coffee flavor compound furfuryl mercaptan in model *Fenton*-type reaction systems. Journal of Agricultural and Food Chemistry 2002;50:2356-2364.

[7]   Kuhnle JA, Windle JJ, Waiss AC jun. Electron paramagnetic resonance spectra of flavonoid anion-radicals. Journal of the Chemical Society (B) 1969;613-616.

[8]   Cotelle N, Bernier J-L, Catteau J-P, Pommery J, Wallet J-C, Gaydou EM. Antioxidant properties of hydroxy-flavones. Free Radical Biology and Medicine 1996;20:35-43.

[9]   Van Acker SABE, De Groot MJ, Van den Berg D-J, Tromp MNJL, Den Kelder GD-O, Van der Vijgh WJF, Bast A. A quantum chemical explanation of the antioxidant activity of flavonoids. Chemical Research in Toxicology 1996;9:1305-1312.

[10]   Amić D, Davidović-Amić D, Beslo D, Trinajstić N. Structure-radical scavenging activity relationships of flavonoids. Croatica Chemica Acta 2003;76:55-61.

[11]   Regeimbal J, Gleiter S, Trumpower BL, Yu C-A, Diwakar M, Ballou DP, Bardwell CA. Disulfide bond formation involves a quinhydrone-type charge-transfer complex. Biochemistry 2003;100:13779-13784.

[12]   Dixon WT, Moghimi M, Murphy D. Substituent effects in the e.s.r. spectra of phenoxyl radicals. Journal of the Chemical Society-Faraday Transactions II 1974;70:1713-1720.

[13]   Loth H, Klinge D. Ein dimeres Flavonol als Intermediärprodukt der Oxydation des Kämpferol-3-glucosids durch Peroxydase. Archiv der Pharmazie 1964;297:165-172.

[14]   Yu J, Taylor KE, Zou H, Biswas N, Bewtra JK. Phenol conversion and dimeric intermediates in horseradish peroxidase-catalyzed phenol removal from water. Environmental Science and Technology 1994;28:2154-2160.

[15]   Frey-Schröder G, Barz W. Isolation and characterization of flavonol converting enzymes from Mentha piperita plants and from Mentha arvensis cell suspension cultures. Zeitschrift für Naturforschung C-A Journal of Biosciences 1979;34: 200-209.

[16]   Miller E, Schreier P. Studies on flavonol degradation by peroxidase (donor: H_2O_2-oxidoreductase, EC 1.11.1.7): Part 1-Kaempferol. Food Chemistry 1985;17:143-154.

[17]   Neta P, Fessenden RW. Hydroxyl radical reactions with phenols and anilines as studied by electron spin resonance. The Journal of Physical Chemistry 1974;78:523-529.

[18]   Miller E. Modellversuche zur Peroxidase (Donor:H_2O_2-oxidoreductase, EC I.II.I.7)-katalysierten Umsetzung von Flavonolen (Quercetin, Kämpferol) und (E)-4-Hydroxyzimtsäure mit H_2O_2 [dissertation]. Würzburg (D): Bayerische Julius-Maximilians-Universität; 1984.

[19]   Takahama U. Oxidation products of kaempferol by superoxide anion radical. Plant and Cell Physiology 1987;28:953-957.

[20]   Selloum L, Reichl S, Müller M, Sebihi L, Arnhold J. Effects of flavonols on the generation of superoxide anion radicals by xanthine oxidase and stimulated neutrophils. Archives of Biochemistry and Biophysics 2001;395:49-56.

[21]   Van Hoorn DEC, Nijveldt RJ, Van Leeuwen PAM, Hofman Z, M'Rabet L, De Bont DBA, Van Norren K. Accurate prediction of xanthine oxidase inhibition based on the structure of flavonoids. European Journal of Pharmacology 2002;451:111-118.

[22]   Puppo A. Effect of flavonoids on hydroxyl radical formation by Fenton-type reactions; influence of the iron chelator. Phytochemistry 1992;31:85-88.

[23]   Huang Q, Huang Q, Pinto RA, Griebenow K, Schweitzer-Stenner R, Weber WJ jr. Inactivation of horseradish peroxidase by phenoxyl radical attack. Journal of the American Chemical Society 2005;127:1431-1437.

Captions for Figures

Figure 1. Chemical structures of (a) luteolin, (b) kaempferol, (c) the initial radical from the oxidation of (a), (d) possible second radical from the oxidation of (a), (e) kaempferide, (f) p-benzosemiquinone, and (g) possible structure for the radical dimmer formed after (f).

Figure 2. EPR spectra of (a) the 1st radical from autoxidised luteolin (3 scans), (b) its simulation ($a(^1H)$ = 0.275 mT, 0.150 mT, 0.125 mT, 0.117 mT), and (c) the 2nd radical from autoxidised luteolin.

Figure 3. EPR spectra of autoxidised kaempferol (a) the initial radical (observed under conditions of limited O_2) and 1:1 ratio kaempferol:NaOH solutions (MA 0.05 mT, 1 scan), (b) the 2nd radical (obtained under O_2-rich conditions, or after a time delay when O_2 was limited and 1:1 ratios kaempferol:NaOH solutions), (c) using a kaempferol:NaOH=1.67:1 ratio, and (d) a simulation of (c) ($a(^1H)$ = 0.08 mT x 4, 0.095 mT x 4).

Figure 4. EPR spectra obtained from autoxidation of kaempferol using a 3:1 kaempferol:NaOH ratio. (a) the initial spectrum (3 scans), (b) the spectrum obtained 5 minutes after (a), (c) a simulation of (b) ($a(^1H)$ = 0.108 mT x 2, 0.075 mT x 4) after subtracting a small contribution from (d) which was obtained 21 min. after (a).

Figure 5. EPR spectra from kaempferol after reaction with (a) xanthine/xanthine oxidase (MA 0.08 mT), (b) HRP/H_2O_2 (MA 0.05 mT, 20 scans), (c) the Fenton reaction system (MA 0.1 mT, 20 scans), and (d) their simulation ($a(^1H)$ = 0.115 mT x 2, 0.103 mT, 0.087 mT x 2).

Figure 6. (a) Possible routes for the dimer formation from kaempferol after oxidation with HRP/H_2O_2 (after Loth and Klinge, 1964), (b) the structure which fits best with the EPR data.
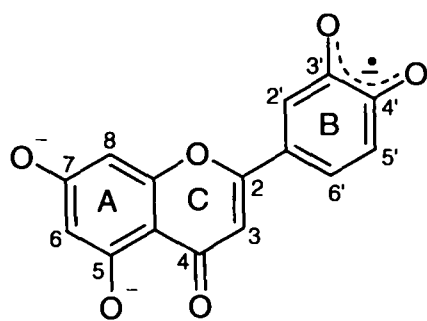
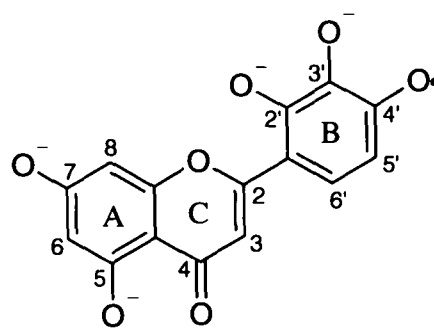Figure 7. Proposed reaction pathway for the oxidation and disproportionation of kaempferol.

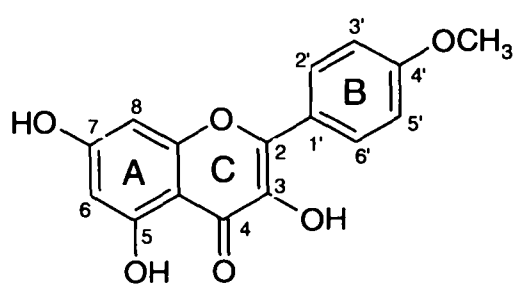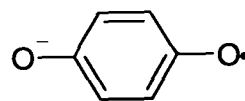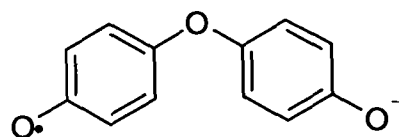Fig. 1

a

0.1 mT

b

c

Fig. 2

18

a

0.1 mT

b

0.1 mT

c

0.1 mT

d

Fig. 3

a   0.1 mT

b   0.1 mT

c

d   0.1 mT

Fig. 4

a

0.1 mT

b

0.1 mT

0.1 mT

c

d

Fig. 5

a

b

Fig. 6